



Mathematical modeling of pest invasion and application to the fight against pest-borne diseases in the Philippines

Cheryl G. Quindao-Mentuda

► To cite this version:

Cheryl G. Quindao-Mentuda. Mathematical modeling of pest invasion and application to the fight against pest-borne diseases in the Philippines. Modeling and Simulation. Université de Picardie Jules Verne, 2022. English. NNT : 2022AMIE0080 . tel-04118650

HAL Id: tel-04118650

<https://theses.hal.science/tel-04118650>

Submitted on 6 Jun 2023

HAL is a multi-disciplinary open access archive for the deposit and dissemination of scientific research documents, whether they are published or not. The documents may come from teaching and research institutions in France or abroad, or from public or private research centers.

L'archive ouverte pluridisciplinaire **HAL**, est destinée au dépôt et à la diffusion de documents scientifiques de niveau recherche, publiés ou non, émanant des établissements d'enseignement et de recherche français ou étrangers, des laboratoires publics ou privés.



Thèse de Doctorat

Mention: Mathématiques

présentée à l'Ecole Doctorale en Sciences, Technologie, Santé (ED 585)

de l'Université de Picardie Jules Verne

par

Cheryl G. Quindao-Mentuda

pour obtenir le grade de Docteur de l'Université de Picardie Jules Verne

***Modélisation mathématique de l'invasion des ravageurs
et application à la lutte contre les maladies transmises
par les ravageurs aux Philippines***

Soutenue le 15 Novembre 2022, après avis des rapporteurs, devant le jury d'examen

M. Yves Dumont	Directeur de Recherche, CIRAD	Rapporteur
M. Yannick Privat	Professeur, Université de Strasbourg	Rapporteur
M ^{me} Nuning Nuraini	Associate Professor, ITB	Examinatrice
M. Hervé Le Meur	Chargé de Recherche, UPJV	Examineur
M. Nicolas Parisey	Ingénieur de Recherche HDR, INRAe	Examineur
M ^{me} Geneviève Prévost	Professeure, UPJV	Président du Jury
M. Jayrold P. Arcede	Professor, Caraga State University	Co-directeur de thèse
M. Youcef Mammeri	Maître de conférences HDR, UPJV	Directeur de thèse



philfrance
scholarships



LAMFA



Acknowledgement

My doctorate journey was not an easy one. The uneasy feeling of leaving my little ones behind, of being in a new place with new people with a foreign language and culture, plus a DELAYED allowance and perk with the COVID-19 pandemic, are just a few of the challenges I faced. The trip was indeed not easy, and there were a lot of ups and downs, crying and laughing. But I made it out alive, and I have these people there to support and guide me along the way, those who, of varying degrees, provided assistance, encouragement, and guidance, and without whom, I would not have succeeded. There are so many people to thank, and I am so grateful for the time and energy these people have given me to produce this thesis and finish my doctorate.

Firstly, I would like to express my deepest gratitude to my thesis adviser Prof. Youcef MAMMERI, who not only shared his genius mind in Mathematics but also extended his knowledge and big heart in guiding me in life. I would never survive in UPJV without you, Professor Youcef. Your unwavering guidance, timely advice, extensive knowledge, scholarly advice, and scientific approach were solely and mainly responsible for completing my work. I am deeply indebted to you (both literally and figuratively), Professor Youcef, for pushing me to my limits, believing in my work, and for always caring for my well-being. You have no idea how many times you saved me during this trip, especially during the quarantine period. Thank you very much for your unrelenting support and long patience. I am glad I made the right choice of choosing you as my adviser. You are THE BEST ADVISER (I cannot think of another word much superior to that) anyone can have.

I would also like to extend my appreciation to my thesis co-adviser and colleague, Professor Jayrold Arcede, for his knowledge, support, and guidance throughout my Ph.D. journey. Thank you so much, Professor Jayrold, for being so supportive when I applied for Ph.D. and for always encouraging me and believing in my work and in me. Thank you for introducing me to the world of applied mathematics and to SEAMS school. You were actually the reason why I ventured into applied mathematics and met Professor Youcef. Thank you very much.

I want to extend my gratitude to the reviewer of this thesis, Dr. Yves Dumont and Prof. Yannick Privat. Thank you very much, Dr. Dumont and Prof. Privat, for sharing your expertise and giving your valuable time in reading and writing a detailed review and helpful remarks on my thesis.

I am also grateful to Dr. Hervé Le Meur, Dr. Nicolas Parisey, Dr. Geneviève Prévost, and Dr. Nuning Nuraini for accepting the invitation to be part of my thesis jury. My most profound appreciation to Dr. Marion Darbas for agreeing to be a

member of my comité de suivi de thèse. Special thanks to Prof. Nabil Bedjaoui for constantly checking up on my well-being and reminding me to unwind and travel in France more.

I am grateful beyond words to all the members of LAMFA, especially in Analyse Appliquée (A3) unit, for the weekly sharing of knowledge in mathematics. It opened my mind to the different problems applied mathematics addressed, making me more in love with the field. Many thanks to Isabelle, Christelle Calimez, and Mylène Gaudissart for being very helpful with me in my administrative papers. Special thanks to Christelle for being so considerate of me in speaking English. You have no idea how much you have helped me, especially when I have a conference or when I am in the Philippines.

Since childhood, I have had difficulty understanding other languages. Thus, living alone in a foreign country where I do not speak the language is extremely difficult. But my stay in France has been bearable and genuinely enjoyable because of my fellow doctoral students, who have become my friends and support system here. My most profound appreciation to these fantastic people, Yohan, Jihade, Henry, Jérémy, Gauthier, Clément, Marouan, Valérie, Sebastian Cea, Ismail, and Owen. To Alice, thank you so much for all your help, especially during the time at La Grand Motte. I truly enjoyed our conversation and the time we spent together. To my Chilean friends, Christopher, Felipe, Bastian, and Josefa, thank you very much for your friendship and all the extra help I received. To my Lao friends, Boausy, Gnorm, and Khankham, thank you so much for always cooking for me and allowing me to be the baby in the group. You had no idea how happy I was when you arrived; I have found a constant companion from Thil to UPJV. Thank you for the late-night talks on mathematics, python, and life. To Mariem, for being a supportive, loving, and thoughtful friend, thank you so much. To Afaf, for being a friend I know I can count on; you have a special place in my heart. I am genuinely comfortable talking and spending time with you. Thank you for assuring me that our friendship is still secure even though I know I do not talk that much and I rarely communicate. Thank you for being my "Ate." To my first Filipino friend in Amiens, Arrianne, you made my first year in Amiens so bearable and passable. Thank you for helping me settle in Amiens and for the constant tips on how to live in France. To my colleague and friend, Ma'am Sheila, and Ma'am Karen, thank you for always cooking Filipino food and being patient with me. You have no idea how happy I am to spend time with you and be able to talk in our language. I am forever grateful to GOD for sending you to France.

I would also like to thank my Filipino friends here in France, whom I constantly annoy with many questions and favors, Sir Juls and Sir Lhords. Thank you so much for always helping me, even though I only communicate when I need something. hehehe... Thank you very much.

Of course, I cannot forget my university back in the Philippines. I am grateful to all my colleagues in Caraga State University, especially to Ma'am Amie Paluga and

Sir Rolando Paluga, for their never-ending support in my studies.

With a big smile, I am immensely thankful to my family for the unwavering support and immeasurable love they have given from the application to my flight to the quarantine period until my defense. To Mentuda and Quindao Family, a ginormous THANK YOU, and I LOVE YOU all. To my siblings, Nickychie and Yolecher II, for your messages of encouragement and love. To my mother-in-law, Mama Abet, thank you for accepting me and loving me like your own. To my sisters-in-law, Caselyn and Princess, for always finding time to do video calls with me so I can talk to my kids. Thank you very much from the bottom of my heart for taking care of my boys on my behalf and treating them like your own. You do not know how thankful I am that you are always there for them.

To my mother, Mama Chirly Garay Quindao, for all your sacrifices, support, and bottomless love for me, for always finding ways to check on me; thank you very much, Ma. You have been my constant source of strength and will always be my reason to keep going regardless of my challenges. In my next life, if the Lord will let me choose a mother, I will always choose you. MA, THIS PAPER IS DEDICATED TO YOU! I hope I made you proud.

To my husband, Elycar Mentuda, thank you for your love even though most of the time I failed to express mine, unwavering support of all my selfish dreams, and behemoth understanding of all my unreasonable requests. You did a good job taking good care of the kids. Thank you very much, and I love you.

To my kids, Elleryl Carl "Todong" and Cycryll Elyce "Today" you have been mommy's source of strength and eternal inspiration. I love you both, and you are forever Mommy's Baby Boy.

And above all, to my brother, father, savior, mentor, and great provider, our LORD GOD ALMIGHTY, thank you so much for all the blessings You've bestowed upon me. Lord, I am nothing without you. If not for You, my dream of studying in Europe would never have been realized. Please always let Your will be done in my life. Praised, glory, honor, and thanks be unto you, oh Lord, forever and ever.

Contents

1	Résumé de la thèse	1
2	General Introduction	25
2.1	Mosquitoes	25
2.1.1	Life Cycle	26
2.1.2	Feeding Habits by Adult Mosquitoes	27
2.1.3	Breeding Sites	28
2.2	Dengue	29
2.2.1	Transmission	30
2.2.2	Vaccination	31
2.2.3	Vector Control	32
2.3	Mathematical Models of Dengue Fever	33
2.4	Outline of Study	35
3	Preliminary study of dengue model	47
3.1	Description of the Model with Vaccination	47
3.2	Study of the Model with Logistic Growth	49
3.2.1	Well-posedness and Positivity of the Solution	49
3.2.2	Stability of the Equilibrium	52
3.2.3	Phase Portrait Analysis	58
3.3	Comparison against Growth Functions	64
3.3.1	Constant Human and Mosquito Population	64
3.3.2	Gompertz Human Population Growth and an Exponential Mosquito Population Growth	73
3.4	Choice of Control Strategies	80
3.4.1	Vaccination	80
3.4.2	Vector Control	82
3.4.3	Combination of Vaccination and Vector Control	84
3.4.4	Summary of the Effective Reproduction Number of Different Control Strategies	86
3.5	Optimal Control strategy	87
3.5.1	Minimizing Infected Humans by Optimal Vaccination	87
3.5.2	Minimizing Infected Humans by Optimal Vector Control	96
3.5.3	Minimizing Infected Humans by both Optimal Vaccination and Vector Control	101

3.5.4	Numerical Simulation of the Optimal Control Problem	104
4	A Dengue-Dengvaxia Model	111
4.1	Description of the Model with Vaccination	111
4.2	Study of the Model with Entomological Growth	112
4.3	Choice of Control Strategies	123
4.3.1	Vaccination	123
4.3.2	Vector Control	125
4.3.3	Combination of Vaccination and Vector Control	127
4.4	Optimal Control strategy	129
4.4.1	Numerical Simulation of Optimal Control	132
5	A Model of Dengue accounting for the Life Cycle	139
5.1	Life Cycle of Mosquitoes	139
5.2	Description of the model	141
5.3	Qualitative Study of the Model	142
5.3.1	Well-posedness and Positivity of the Solution	143
5.3.2	Equilibrium of the Model	145
5.3.3	Next Generation Matrix and Basic Reproduction Number . . .	147
5.3.4	Jacobian Matrix	149
5.3.5	Parameter Identifiability	151
5.4	Optimal Control strategies : Copepods and Pesticides	152
5.4.1	Numerical Simulation of Optimal Control Strategies: Cope- pods vs Pesticides	156
5.4.2	Influence of the starting date of control	170
5.5	Comparison with larval and pupal competition	171
6	A Model of Dengue accounting for the Space	175
6.1	Adult Mosquitoes Habits	175
6.1.1	Feeding Habits	175
6.1.2	Breeding Sites	176
6.2	Summary of Random Walk Modelling	177
6.2.1	Reaction-Diffusion Equation	178
6.2.2	Advection-Diffusion Equation	184
6.2.3	Fokker-Plank Equation	185
6.3	Dengue Model with Spatial Distribution	186
6.4	Well-posedness of the Model	187
6.5	Optimal Control strategies : Copepods, Pesticides & Vaccination . . .	199
6.5.1	Derivation of the Optimal Control	200
6.5.2	Numerical Simulation of the Model with one laying site	211
6.5.3	Numerical Simulation of the Model with Spatial Distribution having Two Laying Sites	216
6.6	Behavior with respect to capacity and diffusion parameters	220

6.6.1	Influence of the Carrying Capacity of pupae	220
6.6.2	Influence of the Laying Sites Capacity	221
6.6.3	Sensitivity Analysis with respect to the diffusion	222
Bibliography		224
A	Symptomatic and Asymptomatic in a SEIR model of COVID-19	233
A.1	Introduction	233
A.2	Materials and methods	235
A.2.1	Confirmed and death data	235
A.2.2	Mathematical model	235
A.2.3	Parameters estimation	236
A.3	Results	237
A.3.1	Basic and effective reproduction numbers	237
A.3.2	Model resolution	239
A.3.3	Strategy to reduce disease to a given threshold	241
A.4	Discussion	246

List of Figures

1.1	Photo d'un moustique adulte femelle <i>Aedes aegypti</i> (gauche) et <i>Aedes albopictus</i> (droite) pendant un repas sanguin [17].	1
1.2	Stades de vie des moustiques femelles <i>Ae. aegypti</i> et <i>Ae. albopictus</i> [19].	2
1.3	Vue dorsale de la femelle adulte <i>Ae. Aegypti</i> adulte [58].	4
1.4	Coupe transversale d'un virus de la dengue montrant ses composants structurels similaires à ceux du virus Zika [40].	6
1.5	Vaccin tétravalent contre la dengue fabriqué par Sanofi Pasteur.	8
1.6	Comparaison de la réponse du compartiment humain infecté dans les 4 stratégies de contrôle : vaccination (vert), contrôle vectoriel (orange), vaccination et contrôle vectoriel (bleu), et sans contrôle (rouge).	15
1.7	Evolution du nombre d'humains infectés sous contrôle optimal.	17
1.8	Comparaison entre le nombre d'humains infectés I_h , le nombre de moustiques infectieux I_m , et le nombre de larves L , avec trois entrées de contrôle optimal (bleu) et sans contrôle (orange).	19
1.9	Comparaison entre le nombre d'humains infectés I_h , le nombre de moustiques infectieux I_m , et le nombre de larves L , avec trois entrées de contrôle (bleu) et sans contrôle (orange).	20
1.10	Evolution spatio-temporelle de la variable de contrôle optimale w_Y liée à l'utilisation des copépodes (en haut) et à sa somme dans l'espace (en bas).	21
2.1	Photo of an adult female <i>Aedes aegypti</i> (left) and <i>Aedes albopictus</i> (right) mosquito during a blood meal [17].	25
2.2	Life stages of female <i>Ae. aegypti</i> and <i>Ae. albopictus</i> mosquitoes. [19]	26
2.3	Dorsal view of the adult female <i>Ae. Aegypti</i> mosquito. [58]	27
2.4	Cross section of a dengue virus showing its structural components [40] similar to the Zika Virus.	30
2.5	Dengue tetravalent vaccine manufactured by Sanofi Pasteur.	31
2.6	Behaviour of infected humans I_h with respect to time without control (red), for the optimal control related to the vaccination only (green), related to the vector only (orange), and with both control (blue). Cyan curve corresponds to optimal control of vaccination of secondary humans only.	38
2.7	Optimal solutions of the infected human in the model.	40

2.8	Comparison between the number of infected humans I_h , number of infectious mosquitoes I_m , and number of larvae L , with three control inputs (blue) and without control (orange).	43
2.9	Spatiotemporal evolution of the optimal control variable w_Y related to the copepods use (top) and its sum in space (down).	44
3.1	Compartmental representation of the model with vaccination considering individuals who have previous dengue infections.	47
3.2	Behaviour of the solution of each variables in the model with dengvaxia versus time using logarithmic and exponential growth functions for human and mosquito population, respectively.	60
3.3	Phase portrait of the model with dengvaxia showing primary susceptible S_h and secondary susceptible \tilde{S}_h versus infected humans I_h in blue color, and susceptible mosquitoes S_m and infected humans I_h versus infected mosquitoes I_m in cyan color. Square and circle indicates the first and last solution of the variables.	62
3.4	Three dimensional phase portrait of the primary susceptible human S_h , secondary susceptible \tilde{S}_h , and the infected I_h human population in the model with dengvaxia.	63
3.5	Behaviour of the solution of each variables in the model 3.19 with dengvaxia versus time using constant growth functions for human and mosquito population. S_h is the red colour figure, I_h is the green, \tilde{S}_h is the blue, R_h is the yellow, S_m is the cyan and I_m is the magenta.	70
3.6	Phase portrait of the model with dengvaxia using constant growth function showing primary S_h and secondary susceptible \tilde{S}_h versus infected humans I_h in blue color, and susceptible mosquitoes S_m and infected humans I_h versus infected mosquitoes I_m in cyan color. Square and circle indicates the first and last solution of the variables.	71
3.7	Phase portrait of the Model	72
3.8	Behaviour of the solution of each variables in the model 3.19 with dengvaxia versus time using Gompertz growth functions for human population and exponential growth function for mosquito population. S_h is the red colour figure, I_h is the green, \tilde{S}_h is the blue, R_h is the yellow, S_m is the cyan and I_m is the magenta.	77
3.9	Phase portrait of the model with dengvaxia using constant growth function showing primary S_h and secondary susceptible \tilde{S}_h versus infected humans I_h in blue color, and susceptible mosquitoes S_m and infected humans I_h versus infected mosquitoes I_m in cyan color. Square and circle indicates the first and last solution of the variables.	78

3.10	Behaviour of the solution of infected and secondary susceptible humans (top) and primary susceptible, recovered and totally immune humans (bottom) in optimal vaccination using constant growth function for human and mosquito population.	93
3.11	Behaviour of the solution of susceptible and infected mosquito in optimal vaccination using constant growth function for human and mosquito population.	94
3.12	Behaviour of the solution of healthy humans in optimal vaccination using constant growth function for human and mosquito population.	94
3.13	Behaviour of the solution of optimal control in primary susceptible (top) and secondary susceptible (bottom) humans in optimal vaccination using constant growth function for human and mosquito population.	95
3.14	Behaviour of the solution of the variables in the human compartments in optimal vector control using constant growth function for human and mosquito population.	99
3.15	Behaviour of the solution of susceptible, infected and total controlled mosquito in optimal vector control using constant growth function for human and mosquito population.	100
3.16	Behaviour of the solution of healthy humans in optimal vector control using constant growth function for human and mosquito population.	100
3.17	Behaviour of the solution of optimal control of mosquitoes in optimal vector control using constant growth function for human and mosquito population.	101
3.18	Response comparison of the infected human compartment in the 4 control strategies: vaccination only (green), vector control only (orange), vaccination and vector control (blue), and without control (red).	105
3.19	Response comparison of each variables in the model with 4 control strategies: vaccination (green), vector control (orange), the combination of vaccination and vector control (blue), and without control (red).	106
3.20	Optimal control of the (A) primary susceptible and (B) secondary susceptible human compartment using vaccination only versus the combination of both control strategies. Optimal control of (C) mosquitoes compartment using vector control only versus the combination of both control strategies. Cyan curve represents optimal control of vaccination of secondary humans only	109
3.21	Convergence of the Error in each control strategies	110
4.1	Compartmental representation of the model with vaccination considering individuals who have previous dengue infections.	111

4.2	Behaviour of the solution of each variables in the model ?? with dengvaxia versus time using constant growth functions for human population and entomological growth function for mosquito population. S_h is the red colour figure, I_h is the green, \tilde{S}_h is the blue, R_h is the yellow, S_m is the cyan and I_m is the magenta.	121
4.3	Phase portrait of the model with dengvaxia using constant growth function showing primary S_h and secondary susceptible \tilde{S}_h versus infected humans I_h in blue color, and susceptible mosquitoes S_m and infected humans I_h versus infected mosquitoes I_m in cyan color. Square and circle indicates the first and last solution of the variables.	122
4.4	Behaviour of infected humans I_h with respect to time without control (red), for the optimal control related to the vaccination only (green), related to the vector only (orange), and with both control (blue). Cyan curve corresponds to optimal control of vaccination of secondary humans only.	133
4.5	Behaviour of (A) human compartment and (B) mosquito compartment with respect to time without control (red), for the optimal control related to the vaccination only (green), related to the vector only (orange), and with both control (blue).	135
4.6	Optimal control of the (A) primary susceptible and (B) secondary susceptible human compartment using vaccination only versus the combination of both control strategies. Optimal control of (C) mosquitoes compartment using vector control only versus the combination of both control strategies. Cyan curve represents optimal control of vaccination of secondary humans only	137
5.1	Life cycle of Aedes mosquitoes.	139
5.2	Compartmental representation	141
5.3	Optimal solutions of the infected human compartment in the model (5.34) with $w_{Y,max} = 23.96, w_{A,max} = 1$	157
5.4	Optimal solutions of each compartments in model (5.34) with $w_{Y,max} = 23.96, w_{A,max} = 1$	158
5.5	Optimal solutions of control variables in model (5.34) with $w_{Y,max} = 23.96, w_{A,max} = 1$	159
5.6	Optimal solutions of the control variables for different maximum number of copepod.	160
5.7	Optimal solutions of the infected human in the model with different control strategies.	165
5.8	Optimal solutions of the infected mosquito in the model with different control strategies.	167
5.9	Optimal solution of the control variables in the model with Copepod, Pesticide and Vaccination control.	168

5.10	Optimal solution of the control variables in the model using the different combination of the control strategies.	169
5.11	Optimal solution of the control variables starting control at day 40, 64 and 150.	170
5.12	P control at day 40, 64 and 150.	171
5.13	Comparison of the solution considering competition induced by larvae and pupae (left), and by pupae only (right).	173
5.14	Comparison of the optimal solution considering competition induced by larvae and pupae (left), and by pupae only (right).	174
6.1	Mosquito can move left or right.	178
6.2	Initial configuration made of one laying site.	212
6.3	Behavior of each variables in the model with spatial distribution with three control inputs (left) and without control inputs (right).	213
6.4	Spatiotemporal evolution of the infected human I_h and infectious mosquitoes I_m without control (top) and with optimal control (down).	215
6.5	Spatiotemporal evolution of the optimal control variables w_Y, w_A, w_H of the model (top) and its sum in space (down).	216
6.6	Initial configuration made of two laying sites.	217
6.7	Behavior of each variables in the model with spatial distribution with three control inputs (left) and without control inputs (right).	217
6.8	Spatiotemporal evolution of the infected human I_h and infectious mosquitoes I_m without control (top) and with optimal control (down).	218
6.9	Spatiotemporal evolution of the optimal control variables w_Y, w_A, w_H of the model (top) and its sum in space (down).	219
6.10	Behavior of eggs, larvae, and pupae in different capacities of pupae.	220
6.11	Duration of the upper bound in the optimal control w_Y with respect to the carrying capacity of pupae.	220
6.12	Behavior of eggs, larvae, and pupae in different capacities of the laying sites.	221
6.13	Duration of the upper bound in the optimal control w_y with respect to the laying capacity.	222
6.14	Effect on the maximum of infected humans I_h from the variations of D_{min}	222
6.15	Maximum value of an infected human in varying parameter values involved in diffusion coefficients.	223
A.1	Compartmental representation of the $SEI_a I_s UR$ —model. Blue arrows represent the infection flow. Green arrows denote for the treatments. Purple arrow is the death.	235

A.2	A. Parameters calibrated according to data from France, Philippines, Italy, Spain, United Kingdom, Hubei, and New York. B. and C. Calibrated solution (straight line) and data (dots) with respect to day for France, Philippines, Italy, Spain, United Kingdom, Hubei and New York. First is the infected I_s (B.), and the second one is the death D (C.). D. Effective reproduction number with respect to day.	240
A.3	A. Boxplot of the posterior distribution computed from France data. B. Effective reproduction number in grey of the posterior distribution, median (= 3.096738) in blue straight line, mean (= 3.474858) is dotted line. C. Fitted symptomatic infected in grey of the posterior distribution, median in red straight line, mean is dotted line. D. Fitted death in grey of the posterior distribution, median in black straight line, mean is dotted line.	241
A.4	Comparison of solutions S, E, I_s, I_a, R, D without control in blue, full containment in green, full treatment of symptomatic in red, and full treatment of exposed in cyan for France. Ordinate axis is expressed in log.	243
A.5	Comparison of solutions S, E, I_s, I_a, R, D without control in blue, full containment in green, full treatment of symptomatic in red, and full treatment of exposed in cyan for the Philippines. Ordinate axis is expressed in log.	244
A.6	A. Comparison of the maximum number of dead. B. Comparison of the maximum number of symptomatic infected. C. Comparison of the intervention duration to reach $\mathcal{T}_c = 1000$ with respect to percentage of containment (green), treatment of symptomatic (red), and treatment of exposed (cyan) for France and Philippines.	245

Chapter 1

Résumé de la thèse

Les moustiques sont un vecteur important pour la transmission de nombreux agents pathogènes et parasites classés, notamment les virus, les bactéries, les champignons, les protozoaires et les nématodes. Cela est principalement dû à leurs habitudes de consommation de sang, pour lesquelles ils se nourrissent d'hôtes vertébrés. Les moustiques infectés transportent ces organismes d'une personne à l'autre sans présenter eux-mêmes de symptômes. Selon [36], d'ici 2050, la moitié de la population mondiale pourrait être exposée à des maladies transmises par les moustiques, comme la dengue ou le virus Zika, le paludisme, et bien d'autres encore. En transmettant ces maladies, les moustiques causent la mort de plus de personnes que tout autre taxon animal. Grâce à un processus d'évolution de plus de 100 millions d'années, les moustiques ont développé des mécanismes d'adaptation capables de prospérer dans divers environnements. À l'exception des endroits gelés en permanence, on trouve ces moustiques dans toutes les régions terrestres du monde. Ils occupent les régions tropicales et subtropicales où le climat semble favorable et efficace pour leur développement, ce qui en fait presque l'animal universel du monde.



FIGURE 1.1: Photo d'un moustique adulte femelle *Aedes aegypti* (gauche) et *Aedes albopictus* (droite) pendant un repas sanguin [17].

Parmi les quelques 3 600 espèces de moustiques qui peuplent la planète, celles qui appartiennent à l'ordre des *Diptera* sont connues pour jouer un rôle crucial en tant que vecteurs de transmission des arbovirus [48]. Au sein de cette famille *Cuculicidae*, le genre *Aedes* est impliqué dans la transmission des maladies. Les deux espèces les plus importantes de ce genre sont *Aedes aegypti* et *Aedes albopictus*. Ils sont les principaux vecteurs de la dengue, de la fièvre jaune, de la fièvre du Nil occidental, du chikungunya, de l'encéphalite équine de l'Est, du virus Zika et de nombreuses autres maladies moins importantes.

Dans cette thèse, nous visons à développer des modèles mathématiques de la dengue prenant en compte la vaccination et le contrôle des vecteurs. Nous nous concentrons donc sur la biologie des moustiques *Ae. aegypti* et *Ae. albopictus* en tant que vecteurs primaires de la dengue.

Cycle de vie

Les moustiques ont un cycle de vie compliqué. Néanmoins, ils ont tous besoin d'eau pour accomplir leur cycle de vie. Ils changent de forme et d'habitat au cours de leur développement. Comme tous les autres moustiques, *Ae. aegypti* et *Ae. albopictus* ont quatre stades distincts : œuf, larve, nymphe et adulte (Fig. 1.2).

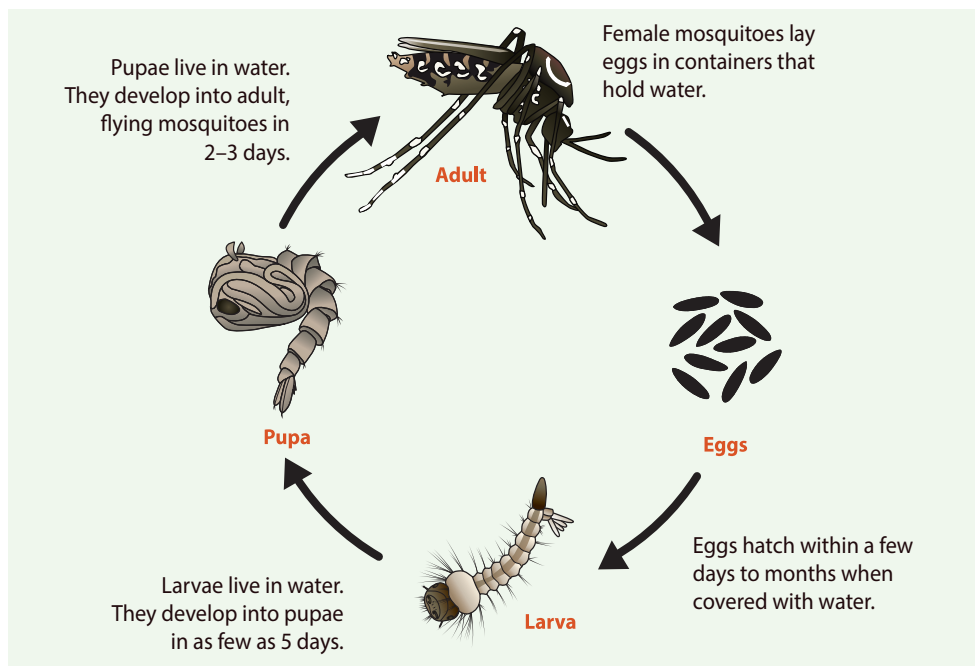


FIGURE 1.2: Stades de vie des moustiques femelles *Ae. aegypti* et *Ae. albopictus* [19].

Seuls les moustiques adultes femelles pondent des œufs quelques jours après avoir pris un repas de sang. Les moustiques pondent généralement 100 œufs à la fois. Ils pondent leurs œufs isolément [31] sur les parois intérieures des récipients juste au-dessus de la ligne de flottaison qui sont ou seront remplis d'eau. Ce site de ponte comprend une paroi de cavité telle qu'une souche creuse ou un récipient tel qu'un seau ou un pneu de véhicule mis au rebut. Seule une infime quantité d'eau est nécessaire pour pondre des œufs. Cependant, les œufs de moustiques peuvent survivre au dessèchement pendant 8 mois ou même en hiver. Dans ce cas, ils doivent supporter une dessiccation considérable avant d'éclore [59]. Une fois qu'ils ont atteint un niveau de dessiccation approprié, ils peuvent entrer en diapause

pendant plusieurs mois. Les œufs d'*Aedes* en diapause ont tendance à éclore de manière irrégulière sur une période prolongée.

Ils éclosent ensuite en larves lorsque de l'eau inonde les œufs, par exemple à la suite de pluies ou du remplissage d'eau par des personnes. Après l'immersion dans l'eau, les œufs éclosent par lots. Étant donné que certains œufs doivent être immergés plusieurs fois dans l'eau avant d'éclore, ce processus peut durer des jours ou des semaines [69].

Les larves vivent dans l'eau et se nourrissent de micro-organismes hétérotrophes tels que des bactéries, des champignons et des protozoaires. Elles se développent en quatre stades, ou instars. Du premier au quatrième stade, les larves muent et perdent leur peau pour poursuivre leur croissance. Au quatrième stade, lorsque la larve est complètement développée, elle se métamorphose en une nouvelle forme appelée pupa. La pupa vit toujours dans l'eau, mais elle ne se nourrit pas. Au bout de deux jours, elles se développent complètement en forme de moustique adulte et percent la peau de la nymphe. Le moustique adulte n'est plus aquatique ; il a un habitat terrestre et peut voler. L'ensemble du cycle de vie des moustiques dure de huit à dix jours à température ambiante, en fonction du niveau d'alimentation.

Habitudes alimentaires des moustiques adultes

Comme tous les autres animaux, les moustiques ont besoin d'énergie et de nutriments pour survivre et se reproduire. Les matières végétales et le sang en sont des sources précieuses.

Seules les femelles moustiques piquent. Elles sont attirées par la lumière infrarouge, la lumière, la transpiration, l'odeur corporelle, l'acide lactique et le dioxyde de carbone. La partie buccale de nombreux moustiques femelles est adaptée pour percer la peau des animaux hôtes et sucer leur sang en tant qu'ectoparasites. Les moustiques femelles se posent sur la peau de l'hôte pendant le repas sanguin et y plantent leur trompe. Leur salive contient des protéines anticoagulantes qui empêchent la coagulation du sang. Elles aspirent ensuite le sang de l'hôte dans leur abdomen. Les moustiques de l'espèce *Ae. Aegypti* ont besoin de $5\mu L$ par portion. Chez de nombreuses espèces de moustiques femelles, les nutriments obtenus à partir des repas sanguins sont essentiels à la production d'œufs, tandis que chez de nombreuses autres espèces, l'obtention de nutriments à partir d'un repas sanguin permet au moustique de pondre davantage d'œufs. Parmi les humains, les moustiques préféreraient se nourrir de ceux qui ont un sang de type O [61], les gros respirateurs, une abondance de bactéries cutanées, une chaleur corporelle élevée et les femmes enceintes [21]. L'attrait des individus pour les moustiques a également une composante héréditaire, contrôlée par les gènes [29].

Les espèces de moustiques hématophages sont des mangeurs sélectifs qui préfèrent une espèce hôte particulière. Néanmoins, ils relâchent cette sélectivité lorsqu'ils sont confrontés à une concurrence sévère, à une pénurie de nourriture et à une activité défensive de la part des hôtes.

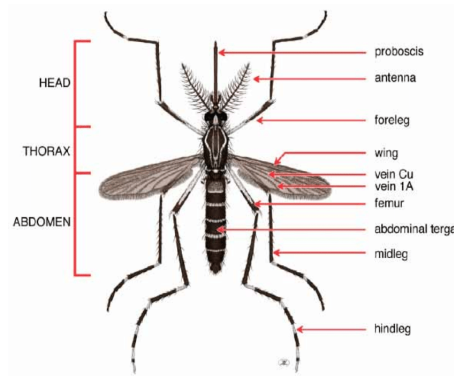


FIGURE 1.3: Vue dorsale de la femelle adulte *Ae. Aegypti* adulte [58].

Si les humains sont rares, les moustiques se nourrissent de singes, tandis que d'autres préfèrent les équidés, les rongeurs, les oiseaux, les chauves-souris et les porcs, d'où proviennent un grand nombre de nos craintes de maladies inter-espèces [41]. Certains moustiques ignorent complètement les humains et se nourrissent exclusivement d'oiseaux, tandis que la plupart mangent tout ce qui est disponible. Les amphibiens, les serpents, les reptiles, les écureuils, les lapins et d'autres petits mammifères comptent parmi les autres repas les plus populaires des moustiques. Les moustiques s'attaquent également à des animaux plus grands, comme les chevaux, les vaches, les primates, les kangourous et les wallabies. Certaines espèces de moustiques peuvent même s'attaquer aux poissons s'ils s'exposent au-dessus du niveau de l'eau. De même, les moustiques peuvent parfois se nourrir d'insectes dans la nature. *Ae. Aegypti* et *Culex tarsalis* sont attirés et se nourrissent de larves d'insectes, et ils vivent pour produire des œufs viables [60]. Alors que *Anopheles Stephensi* est attiré par les larves d'espèces de papillons de nuit comme *Manduca sexta* et *Heliothis subflexa* et peut s'en nourrir avec succès [34].

Le nectar des plantes est une source d'énergie commune pour l'alimentation de toutes les espèces de moustiques, en particulier les moustiques mâles, exclusivement dépendants du nectar des plantes ou de sources alternatives de sucre. La conception de pièges efficaces appâtés au sucre pour les moustiques serait grandement bénéfique pour la prévention des maladies à transmission vectorielle. La préférence pour les plantes est probablement due à une attraction innée qui peut être renforcée par l'expérience, les moustiques reconnaissant les récompenses en sucre disponibles [70]. Elle varie selon les espèces de moustiques, les habitats géographiques et la disponibilité saisonnière. La recherche de nectar implique l'intégration d'au moins trois systèmes sensoriels : l'olfaction, la vision et le goût.

Néanmoins, tous les moustiques sont capables de faire la distinction entre les sources de sucre riches et pauvres pour choisir les plantes ayant une teneur plus élevée en glycogène, en lipides et en protéines [73]. Voici les plantes préférées de différentes espèces de moustiques d'après l'article de Barredo et DeGennaro [7].

Espèces de moustiques	Source du nectar
<i>Aedes aegypti</i>	<i>Asclepias syriaca</i> (asclépiade) Extrait végétal <i>Impatiens walleriana</i> Plantes vivantes
<i>Anopheles gambiae</i>	<i>Mangifera indica</i> <i>Delonix regia</i> Plantes vivantes <i>Parthenium hysterophorus</i> Plantes vivantes <i>Acacia macrostachya</i> <i>Acacia albida</i>
<i>Culex pipiens</i>	<i>A. syriaca</i> (asclépiade) Fleur vivante, extrait et mélange synthétique <i>I. walleriana</i>
<i>Culex pipiens pallens</i>	<i>Ligustrum quihoui</i> (troène à feuilles de cire) <i>Broussonetia papyrifera</i> (mûre en papier) <i>L. quihoui</i> <i>Abelia chinensis</i> <i>Nerium indicum</i>

TABLE 1.1: Les plantes préférées des différentes espèces de moustiques comme source d'énergie d'après [7].

Sites de reproduction

Les moustiques *Aedes* se reproduisent dans tous les réceptacles imaginables. On peut classer les récipients humides artificiels et naturels, de préférence avec des surfaces de couleur sombre et contenant de l'eau claire non polluée [46]. Voici une liste non exhaustive des différents types de sites de reproduction des moustiques *Aedes* [32] :

- Conteneur naturel
 - Trous d'arbres
 - Axilles des feuilles
 - Trous dans la roche.
- Conteneur artificiel
 - Conteneurs jetés
 - * Pneus pour automobiles
 - * Boîtes de conserve
 - * Bouteilles
 - * Vases
 - * Gouttières de toit
 - * Plateaux d'eau pour animaux
 - * Chasses d'eau.
 - Conteneurs de stockage d'eau
 - * Cuves
 - * Fûts
 - * Bidons d'eau

Dengue

La dengue est l'infection virale transmise par les moustiques la plus courante. On la trouve dans les régions tropicales et subtropicales du monde entier, avec un pic de transmission pendant la saison des pluies. En 2019, l'Organisation mondiale de la santé [68] a signalé 5,2 millions de cas de dengue dans le monde. Rien qu'aux Philippines, 271 480 cas avec 1 107 décès sont signalés du 1er janvier au 31 août 2019, en raison de la dengue [28].

La dengue est causée par quatre sérotypes de virus relevant de la famille des Flaviviridae. Il s'agit de sérotypes de virus distincts mais étroitement liés, appelés DENV-1, DENV-2, DENV-3 et DENV-4. Environ une personne sur quatre infectée par la dengue tombera malade [15]. La maladie commence généralement 5 à 7 jours après la piqure infectante des moustiques femelles *Ae. aegypti* et *Ae. albopictus* [8].

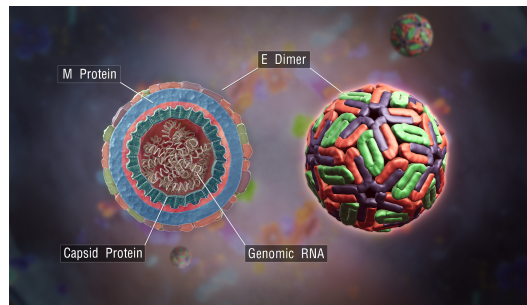


FIGURE 1.4: Coupe transversale d'un virus de la dengue montrant ses composants structurels similaires à ceux du virus Zika [40].

Dans la plupart des cas, la dengue est une maladie autolimitée mais peut nécessiter une hospitalisation, où des soins de soutien peuvent modifier l'évolution de la maladie. Les symptômes peuvent être légers ou graves et durent généralement de 2 à 7 jours. Le symptôme le plus courant de la dengue est la fièvre accompagnée de nausées, de vomissements, d'une éruption cutanée, de courbatures et de douleurs musculaires ou articulaires. L'infection par un type de virus confère une immunité à vie contre cette souche virale et confère temporairement une protection partielle contre les autres types. Une deuxième infection par un autre type de virus entraîne une maladie plus grave, appelée fièvre hémorragique de la dengue (DHF). Aux Philippines, 1 107 décès sont signalés du 1er janvier au 31 août 2019, dus à la dengue [28].

Transmission

Les virus de la dengue se transmettent aux personnes par les piqûres de moustiques infectés de l'espèce *Aedes* [18]. Il peut être transmis par une transmission d'homme à moustique, de moustique à homme et par d'autres transmissions comme la transmission d'homme à homme et de moustique à moustique.

La transmission verticale se produit lorsque des moustiques parents infectés transmettent l'arbovirus à une partie de leur progéniture dans l'ovaire ou pendant

la ponte [30]. Plusieurs articles confirment ces résultats. Une étude de Shroyer DA. [24] est l'un des articles qui confirme la présence de la transmission verticale naturelle du DENV chez *Ae. aegypti* et *Ae. albopictus*. Il indique que le virus DENV peut être transféré du parent à la progéniture dans sept générations consécutives d'*Ae. aegypti* et *Ae. albopictus*, dans des conditions de laboratoire. Cette transmission peut contribuer à la pérennité des moustiques infectés, mais elle n'est pas suffisante pour favoriser la propagation de la dengue.

Une forme de transmission plus courante est connue sous le nom de transmission horizontale. Le virus est transmis à l'homme par les piqûres de moustiques *Ae. aegypti* infectés. Après s'être nourri d'une personne infectée par la dengue, le virus se réplique dans l'intestin moyen du moustique avant de se disséminer dans les tissus secondaires, notamment les glandes salivaires. La période d'incubation extrinsèque (PIE) est le temps qui s'écoule entre l'ingestion du virus et la transmission effective à un nouvel hôte. Elle dure environ 8 à 12 jours lorsque la température ambiante est comprise entre 25 et 28°C. Les variations de la PIE sont également influencées par des facteurs tels que l'ampleur des fluctuations quotidiennes de température, le génotype du virus et la concentration virale initiale [68].

Bien que la possibilité soit faible, il existe des preuves que la dengue peut également se propager par transmission maternelle ou être transmise par une transfusion sanguine infectée. Une femme enceinte qui a une infection par le DENV peut transmettre le virus à son fœtus. Les bébés porteurs du DENV peuvent souffrir d'une naissance prématurée, d'un faible poids à la naissance et d'une détresse fœtale [68].

Vaccination

Il n'existe pas de traitement spécifique pour la dengue. Cependant, des efforts pour développer un vaccin sont en cours depuis des décennies.

Le premier vaccin contre la dengue utilisé commercialement est le CYD-TDV, commercialisé sous le nom de Dengvaxia par Sanofi Pasteur. Il a été homologué en décembre 2015 et approuvé par les autorités réglementaires dans 20 pays. L'un de ces pays est les Philippines. En décembre 2015, la Food and Drugs Administration (FDA) philippine a donné son feu vert au vaccin, faisant des Philippines le premier pays asiatique à le commercialiser [65]. En avril 2016, le ministère de la Santé (DOH) a lancé la campagne de vaccination contre la dengue dans les régions philippines de Central Luzon, Calabarzon et Metro Manila. Plus de 800 000 écoliers ont reçu au moins une dose du vaccin.

Dengvaxia est un vaccin chimérique tétravalent vivant atténué. Il est fabriqué à l'aide de la technologie de l'ADN recombinant en remplaçant les gènes structurels PrM (prémembrane) et E (enveloppe) du vaccin atténué de la souche 17D de la fièvre jaune par ceux des quatre sérotypes de la dengue. Il doit être administré en trois doses de 0,5 ml par voie sous-cutanée (SC) à six mois d'intervalle. Sanofi Pasteur a recommandé que le vaccin ne soit utilisé que chez les personnes âgées de 9 à 45



FIGURE 1.5: Vaccin tétravalent contre la dengue fabriqué par Sanofi Pasteur.

ans et chez les personnes déjà infectées par un type de virus [3]. En effet, les résultats peuvent être moins bons chez les personnes qui n'ont pas encore été infectées auparavant.

Contrôle des vecteurs

Un vecteur de maladie est tout agent vivant portant et transmettant un agent pathogène infectieux à un autre organisme vivant. Le contrôle de ces vecteurs est une méthode essentielle pour limiter ou éradiquer la transmission de ces maladies. Dans le cas de la dengue, il est essentiel de lutter contre les moustiques en s'appuyant sur de bonnes connaissances scientifiques de l'écologie des moustiques et des modes de transmission de la maladie.

L'Organisation mondiale de la santé a considéré les catégories suivantes pour contrôler ou prévenir la propagation du virus de la dengue [33].

- Gestion de l'environnement
 - Un facteur de risque important pour la transmission du virus de la dengue est la proximité des sites de reproduction des moustiques vecteurs avec les habitations humaines. Un système efficace de gestion de l'environnement constitue donc une stratégie efficace de lutte contre les vecteurs. Il comprend la gestion des conteneurs, l'élimination de l'altération des sites de reproduction et la prévention de la reproduction dans les conteneurs de stockage de l'eau.
- Méthodes chimiques et biologiques
 - La larvicide chimique est efficace contre les moustiques *Aedes* qui se reproduisent dans des conteneurs d'eau propre. Elle utilise des insecticides synthétiques organiques tels que le téméphos (Abate) et des régulateurs de croissance des insectes (RCI) tels que le méthoprène (Altosid, imitateur d'hormone juvénile), dont l'impact sur l'environnement est minime s'ils sont utilisés de manière appropriée dans les locaux humains.

- Wolbachia est un type de bactérie que l'on trouve couramment chez les insectes mais qui est inoffensif pour les humains ou les animaux. On ne la trouve pas chez les moustiques *Ae. aegypti*. Lorsque des moustiques *Ae. aegypti* mâles porteurs de Wolbachia s'accouplent avec des moustiques femelles sauvages qui n'en sont pas porteurs, les œufs n'éclosent pas, ce qui entraîne une diminution de la population de moustiques *Ae. aegypti* [14].
- Les copépodes sont un groupe de petits crustacés que l'on trouve dans presque tous les habitats d'eau douce et d'eau salée. L'utilisation de *cyclopoïde copepoda* dans la lutte contre les moustiques s'est avérée plus efficace que les prédateurs invertébrés [44]. Seuls les copépodes dont la longueur du corps est supérieure à 1,4 mm sont utiles dans la lutte contre les moustiques. Ils tuent les moustiques de premier stade avec 40 larves d'*Aedes* par copépode par jour. Ils réduisent généralement la production d'*Aedes* de 99 à 100%.
- Protection personnelle
 - Éviter de se faire piquer par un autre moustique lorsqu'une personne est en état de virémie est un excellent moyen de prévenir la propagation du virus de la dengue. Pendant cette période, le DENV circule dans le sang de la personne et peut donc transmettre le virus à de nouveaux moustiques non infectés, qui peuvent à leur tour infecter d'autres personnes. Par conséquent, la protection individuelle à l'aide de serpentins et d'aérosols, de rideaux et de moustiquaires imprégnés d'insecticide et de répulsifs pour moustiques sont des méthodes essentielles pour la lutte antivectorielle.
- Vaporisation spatiale
 - La pulvérisation spatiale est une stratégie efficace pour tuer rapidement les moustiques *Aedes* adultes dans les zones d'épidémie de dengue. Elle utilise des brouillards thermiques et des aérosols à très faible volume.

Une autre méthode de lutte antivectorielle qui s'est avérée efficace dans le cadre d'essais sur le terrain a démontré que l'incidence de la dengue peut être considérablement réduite en introduisant des souches de la bactérie endosymbiotique appelée Wolbachia dans les populations de moustiques *Aedes aegypti* [66]. Wolbachia est une bactérie ubiquitaire qui se trouve naturellement chez les insectes et qui est sans danger pour les humains. Elle vit à l'intérieur des cellules des insectes et est transmise d'une génération à l'autre par les œufs de l'insecte. Des analyses de risque indépendantes indiquent que la libération de moustiques infectés par Wolbachia présente un risque négligeable pour les humains et l'environnement. Les moustiques porteurs de Wolbachia ont réduit leur capacité à transmettre les arbovirus

[66]. La bactérie entre en compétition avec le virus, ce qui rend plus difficile la reproduction des virus à l'intérieur des moustiques. En effet, les moustiques sont beaucoup moins susceptibles de transmettre les virus d'une personne à l'autre.

Modèles mathématiques de la dengue

La modélisation mathématique a été utilisée pour tester et déterminer l'efficacité de différentes stratégies d'intervention pour contrôler ou éliminer la dengue. Ces différents modèles mathématiques aident les mathématiciens à tester les différentes hypothèses de la dynamique de transmission de la dengue afin de mieux comprendre leur importance.

Les modèles compartimentaux SEIRS tenant compte de la susceptibilité, de l'exposition, de l'infection et de l'élimination pour la population humaine et de la susceptibilité et de l'infection pour la population de moustiques ont été largement promus. Syafruddin et Noorani [62] a étudié un système d'équations différentielles qui modélise la dynamique de la population d'un vecteur SEIR de transmission de la dengue. Il s'agit d'un modèle mathématique qui analyse la propagation d'un sérotype du virus de la dengue entre l'hôte et le vecteur. Ils ont montré qu'il pouvait modéliser la dengue en utilisant des données réelles.

D'autre part, Nuraini et al. [51] ont dérivé et analysé le modèle en tenant compte du compartiment de la dengue hémorragique sévère (DHF) dans le modèle de transmission. Ils considèrent un modèle SIR pour la transmission de la dengue. Ils supposent que deux virus, la souche 1 et la souche 2, sont à l'origine de la maladie. Une immunité durable contre une infection causée par un virus peut ne pas être valable en cas d'infection secondaire par l'autre virus. Ils trouvent une mesure de contrôle pour réduire le nombre de patients atteints de la DHF dans la population ou le maintenir à un niveau acceptable. Ils discutent également du rapport entre le nombre total de compartiments de DHF sévère, le nombre total de compartiments de première infection et le nombre total de compartiments d'infection secondaire, respectivement. En outre, ils ont découvert que ce rapport est nécessaire pour les mesures de contrôle pratiques afin de prédire l'intensité " réelle " des phénomènes endémiques, puisque seules les données sur les compartiments de la DHF sévère sont disponibles.

De plus, Derouich et al. [27] a proposé un modèle avec deux virus différents agissant à des intervalles de temps séparés. Ils étudient la dynamique de la dengue en se concentrant sur sa progression vers la forme hémorragique pour comprendre le phénomène épidémique et proposer des stratégies de contrôle de la maladie. Leur modèle a montré que la stratégie basée sur la prévention de l'épidémie de dengue par la lutte antivectorielle, par la gestion de l'environnement ou par des méthodes chimiques, reste insuffisante. par la gestion de l'environnement ou par des méthodes chimiques reste insuffisante car elle ne permet que de retarder l'apparition de l'épidémie. De plus, la réduction des susceptibilités par la vaccination a peu de

chance d'être applicable à court terme car elle se heurte à des obstacles puisqu'un vaccin doit protéger simultanément contre les quatre sérotypes simultanément.

Par ailleurs, Aguiar et Stollenwerk [2] ont analysé un cadre de modélisation et les hypothèses utilisées par Aguiar et al. [1] (modèle de dengue à 2 et 4 souches) et ont évalué l'impact du vaccin contre la dengue récemment homologué. Ils discutent du rôle de plusieurs infections ultérieures par rapport à un nombre exact de sérotypes de dengue inclus dans le cadre du modèle et des aspects immunologiques humains associés à la gravité de la maladie, en identifiant les implications pour la dynamique du modèle et leur impact sur la mise en œuvre du vaccin. Leurs résultats suggèrent que le fait de réserver les vaccins aux individus séropositifs devrait fournir un niveau élevé de protection, alors que la vaccination sans discernement pourrait augmenter le nombre d'hospitalisations également au niveau de la population.

La détermination du contrôle optimal pour minimiser la propagation de la dengue a également été étudiée. Yang et Ferreira [72] ont décrit la dynamique de la dengue dans le modèle à compartiments, en tenant compte des contrôles chimiques et du contrôle mécanique appliqués aux moustiques. En permettant à certains paramètres du modèle de dépendre du temps, ils ont pu imiter les variations saisonnières et diviser l'année civile en périodes favorables et défavorables pour le développement de la population de vecteurs. Leurs simulations ont montré des flambées épidémiques "imprévisibles" lorsque les variations abiotiques sont prises en compte. Si les mécanismes de contrôle sont introduits régulièrement chaque année, ils observent le déclin de l'indice d'efficacité avec le temps écoulé.

D'autre part, une stratégie essentielle pour contrôler l'épidémie de dengue consiste à contrôler la population de vecteurs. Parmi les nombreux types de recherche, Almeida et al. [4] considèrent deux techniques ; elle consiste à relâcher des moustiques pour réduire la taille de la population (technique de l'insecte stérile) ou à remplacer la population sauvage par une population porteuse d'une bactérie *Wolbachia* (une bactérie responsable du blocage de la transmission des virus du moustique à l'homme). Leur article présente une stratégie optimale dans le protocole de lâcher de ces deux stratégies dans laquelle ils recherchent une fonction de contrôle qui minimise la distance à l'équilibre souhaité (remplacement ou extinction de la population sauvage) au moment du traitement final.

De plus, Puntani et al. [54] ont présenté un mécanisme de contrôle basé sur un modèle de dengue avec transmission verticale considérant les deux politiques, à savoir la vaccination et l'administration d'insecticide. Carvalho et al. [12] a évalué une stratégie de contrôle, qui vise à éliminer le moustique *Aedes aegypti*, ainsi que des propositions pour la campagne de vaccination. Leurs résultats montrent que l'éradication de la dengue se fait à l'aide d'un vaccin immunisant car les mesures de contrôle contre son vecteur sont insuffisantes pour stopper la propagation de la maladie. En outre, Iboi et Gumel [38] a conçu un nouveau modèle mathématique pour évaluer l'impact du nouveau vaccin Dengvaxia sur la dynamique de transmission

de deux souches de dengue co-circulantes.

Plan de la thèse

Cet thèse est la première étude à prendre en compte la proposition de Sanofi Pasteur. Nous présentons ici un nouveau modèle mathématique de la dengvaxia. Comme le recommande l'Organisation Mondiale de la Santé [71], la vaccination doit être administrée aux personnes qui ont déjà été infectées par une souche du virus. Dans ce document, nous divisons le compartiment des humains sensibles en humains sensibles primaires ou secondaires, c'est-à-dire les individus qui n'ont pas été infectés et les individus qui ont été infectés par une ou plusieurs souches du virus de la dengue.

Ce travail de thèse vise à introduire un nouveau modèle mathématique de la dengue. Il a la objectifs suivants:

1. étudier le dengvaxia et montrer si la recommandation de Sanofi est suffisante,
2. déterminer un contrôle efficace de la dengue, et
3. générer un modèle mathématique de la dengue tenant compte de son cycle de vie et de sa distribution spatiale.

Le manuscrit est organisé comme suit.

Le chapitre 3 commence par la présentation d'une modèle de type Ross de la dengue qui considère la vaccination des individus ayant déjà été infectés par la dengue. Dans ce chapitre, on teste des fonctions logistiques, exponentielles et Gompertzienne pour décrire la croissance des populations humaines et de moustiques. Nous montrons le caractère bien posé et la positivité de la solution du modèle. Nous avons obtenu que l'équilibre sans maladie est localement asymptotiquement stable alors que l'équilibre endémique est instable. Le chapitre 4 se concentre sur un nouveau modèle mathématique de la dengvaxia. Ici la population humaine est constante, et une fonction de croissance entomologique est considéré pour la population de moustiques.

Trois types de croissance sont comparés:

- Pop_1 : population humaine et population de moustiques constantes,
- Pop_2 : fonction de croissance de Gompertz pour la population humaine et une fonction de croissance exponentielle pour la population de moustiques,
- Pop_3 : une fonction de croissance entomologique pour le moustique et une fonction de croissance constante pour la population humaine.

Dans le modèle Pop_1 , nous avons montré que le modèle ne possède que l'équilibre sans maladie et nous avons pu prouver qu'il est localement asymptotiquement stable. De même, le modèle Pop_2 ne possède que l'équilibre sans maladie qui est localement stable dès que le taux de croissance α_m est plus petit que le taux de mortalité

μ_m . D'autre part, le modèle Pop_3 possède à la fois un équilibre endémique et un équilibre sans maladie. Nous avons pu définir le nombre de reproduction de base

$$\mathcal{R}_0 = \sqrt{\frac{a^2 b_m u_5^* (\tilde{b}_h u_3^* + b_h u_1^*)}{H_0^2 \mu_m (\gamma_h + \delta_h)}},$$

puis montrer que l'équilibre sans maladie du modèle Pop_3 est localement asymptotiquement stable si $\alpha_m < \mu_m$ et que l'équilibre endémique est stable seulement si $\alpha_m > \mu_m$ et $\mathcal{R}_0 > 1$. Plus largement, nous avons prouvé le théorème ci-dessous pour le modèle Pop_3 .

Théorème 1.0.1. 1. Si $\alpha_m < \mu_m$, alors l'équilibre sans maladie trivial est globalement asymptotiquement stable.
2. Si $\alpha_m > \mu_m$ et $\mathcal{R}_0 > 1$, alors l'équilibre sans maladie non trivial est globalement asymptotiquement stable.

Nous déterminons ensuite la stratégie de contrôle optimale pour minimiser les humains infectés de chacune de ces trois stratégies de contrôle. Nous attribuons trois entrées de contrôle, w_1, w_3 , et w_m , pour les populations humaines primaires, secondaires susceptibles, et les moustiques. Ici, l'action de $w_1(t)$ est le pourcentage de personnes susceptibles primaires, et $w_3(t)$ est le pourcentage de personnes susceptibles secondaires vaccinées par unité de temps. Tandis que $w_5(t), w_6(t)$ est le pourcentage de moustiques éliminés par l'administration d'insecticide dans l'environnement par unité de temps. En considérant la fonction coût

$$\mathcal{J}(w_1, w_3, w_m) = \int_0^T \left(u_2(t) + \frac{1}{2} A_1 w_1^2(t) + \frac{1}{2} A_3 w_3^2(t) + \frac{1}{2} A_m w_5^2(t) + \frac{1}{2} A_m w_6^2(t) \right) dt$$

sous la contrainte

$$\begin{aligned} u_1'(t) &= -\frac{a b_h u_6(t) u_1(t)}{H_0} - w_1(t) u_1(t) \\ u_2'(t) &= \frac{a u_6(t) (b_h u_1(t) + \tilde{b}_h u_3(t))}{H_0} - \gamma_h u_2(t) - \delta_h u_2(t) \\ u_3'(t) &= \gamma_h u_2(t) - \frac{\tilde{a} \tilde{b}_h u_3(t) u_6(t)}{H_0} - w_3(t) u_3(t) \\ u_4'(t) &= \delta_h u_2(t) \\ u_5'(t) &= -\frac{a b_m u_2(t) u_5(t)}{H_0} - \mu_m u_5(t) + g(M(t)) - w_5(t) u_5(t) \\ u_6'(t) &= \frac{a b_m u_2(t) u_5(t)}{H_0} - \mu_m u_6(t) - w_6(t) u_6(t) \end{aligned} \tag{1.1}$$

pour $t \in [0, T]$, avec $0 \leq w_1, w_3 \leq w_H$ et $0 \leq w_5, w_6 \leq w_M$, nous utilisons le principe du maximum de Pontryagin pour déterminer la commande optimale.

Théorème 1.0.2. *Il existe les variables adjointes $\lambda_i, i = 1, 2, \dots, 6$ du système (4.13) qui satisfont le système d'équation différentielle ordinaire à rebours dans le temps suivant :*

$$\begin{aligned} -\frac{d\lambda_1}{dt} &= \lambda_1 \left(\frac{-ab_h u_6}{H_0} - w_1 \right) + \lambda_2 \frac{ab_h u_6}{H_0} \\ -\frac{d\lambda_2}{dt} &= 1 + \lambda_2 (-\gamma_h - \delta_h) + \lambda_3 \gamma_h + \lambda_4 \delta_h - \lambda_5 \frac{ab_m u_5}{H_0} + \lambda_6 \frac{ab_m u_5}{H_0} \\ -\frac{d\lambda_3}{dt} &= \lambda_2 \frac{\tilde{a}b_h u_6}{H_0} + \lambda_3 \left(\frac{-\tilde{a}b_h u_6}{H_0} - w_3 \right) \\ -\frac{d\lambda_4}{dt} &= 0 \\ -\frac{d\lambda_5}{dt} &= \lambda_5 \left(\frac{-ab_m u_2}{H_0} + \frac{\partial g}{\partial u_5} \right) - \lambda_5 (\mu_m + w_5) + \lambda_6 \frac{ab_m u_2}{H_0} \\ -\frac{d\lambda_6}{dt} &= -\lambda_1 \frac{ab_h u_1}{H_0} + \lambda_2 \frac{ab_h u_1 + \tilde{a}b_h u_3}{H_0} - \lambda_3 \frac{\tilde{a}b_h u_3}{H_0} + \lambda_5 \frac{\partial g}{\partial u_6} - \lambda_6 (\mu_m + w_6) \end{aligned}$$

avec la condition de transversalité $\lambda(T) = 0$. De plus, les variables de contrôle optimales, pour $j = 1, 3, 5, 6$, sont données par

$$w_j^*(t) = \max \left(0, \min \left(\frac{\lambda_j u_j}{A_j}, w_H, w_M \right) \right).$$

L'optimalité des modèles est résolue numériquement en utilisant un algorithme de gradient programmé Python. La figure obtenue montre que la vaccination des seuls humains susceptibles secondaires n'est pas idéale. Cela demande un effort constant et prend beaucoup de temps pour les vacciner. Il est donc préférable de vacciner les humains sensibles primaires. Cependant, comme il n'existe pas encore de vaccins sûrs pour les humains sensibles primaires, l'application de la lutte antivectorielle pour minimiser les humains infectés est une meilleure contre-stratégie.

Le chapitre 5 présente un nouveau modèle mathématique de la dengue qui tient compte du cycle de vie des moustiques. Suivant la dynamique de la métamorphose de la population de moustiques, ainsi que la compétition larvaire, les stades aquatiques : œuf E , larve L , et pupe P , sont ajoutés au modèle. Nous montrons que notre nouveau modèle est bien posé et a des solutions positives. Le nombre de reproduction de base est défini comme

$$\begin{aligned} \mathcal{R}_0 &:= \sqrt{\frac{a^2 b_h b_m S_m^* S_h^*}{\mu_A \sigma_h}} \\ &= \sqrt{\frac{a^2 b_h b_m H (\gamma_{E,L} + \mu_E) (\gamma_{L,P} + \mu_L) (\gamma_{P,S_m} + \mu_P) \ln \mathcal{N}_Y}{\mu_A \sigma_h \alpha_m \beta_m \gamma_{E,L} \gamma_{L,P}}}, \end{aligned}$$

avec

$$\mathcal{N}_Y = \left(\frac{\alpha_m \gamma_{E,L} \gamma_{L,P} \gamma_{P,S_m}}{\mu_A (\gamma_{E,L} + \mu_E) (\gamma_{L,P} + \mu_L) (\gamma_{P,S_m} + \mu_P)} \right).$$

Les copépodes sont les ennemis naturels du premier et du deuxième stade larves

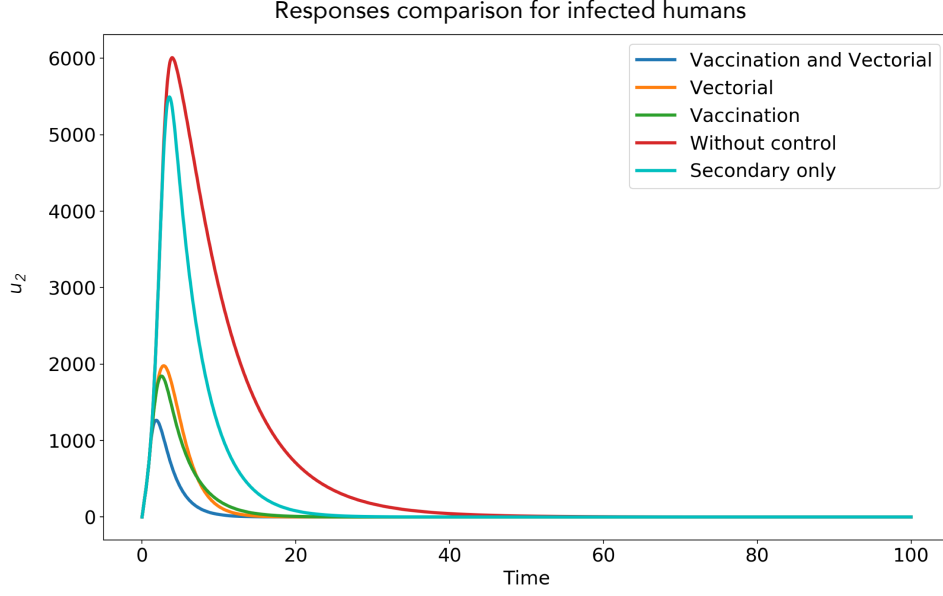


FIGURE 1.6: Comparaison de la réponse du compartiment humain infecté dans les 4 stratégies de contrôle : vaccination (vert), contrôle vectoriel (orange), vaccination et contrôle vectoriel (bleu), et sans contrôle (rouge).

de moustiques. Les copépodes cyclopoïdes de grande taille, dont la taille du corps est supérieur à $1mm$, agissent comme prédateurs des larves de moustiques, ce qui influence fortement la population de larves de moustiques. Avec cela, les copépodes constituent une nouvelle stratégie de contrôle. En appliquant la vaccination et le contrôle des vecteurs au modèle, nous déterminons la stratégie de contrôle optimale pour minimiser les humains infectés. Nous attribuons trois entrées de contrôle, w_Y pour le pourcentage de jeunes moustiques exposés aux copépodes, w_A pour le pourcentage de moustiques adultes exposés aux pesticides et w_H pour le pourcentage d'humains sensibles vaccinés. Nous considérons donc la fonction coût

$$\mathcal{J}(w_Y, w_A, w_H) = \int_0^T \left(I_h(t) + \frac{1}{2} A_Y w_Y^2(t) + \frac{1}{2} A_A w_A^2(t) + \frac{1}{2} A_H w_H^2(t) \right) dt$$

sous la contrainte

$$\begin{aligned} E'(t) &= \alpha_m(S_m(t) + I_m(t)) - \gamma_{E,L}E(t) - \mu_E E(t) \\ L'(t) &= \gamma_{E,L}E(t) - \gamma_{L,P}L(t) - \mu_L L(t) - w_Y L(t) \\ P'(t) &= \gamma_{L,P}L(t) - \gamma_{P,S_m}P(t) - \mu_P P(t) \\ S'_m(t) &= \gamma_{P,S_m}P(t)e^{-\beta_m P} - \mu_A S_m(t) - ab_m I_h(t)S_m(t) - w_A S_m(t) \\ I'_m(t) &= ab_m I_h(t)S_m(t) - \mu_A I_m(t) - w_A I_m(t) \\ S'_h(t) &= \gamma_h R_h(t) - ab_h I_m(t)S_h(t) - w_H S_h(t) \\ I'_h(t) &= ab_h I_m(t)S_h(t) - \sigma_h I_h(t) \\ R'_h(t) &= \sigma_h I_h(t) - \gamma_h R_h(t) \end{aligned} \tag{1.2}$$

pour obtenir la meilleure stratégie de contrôle. Le principe du maximum de Pontryagin est appliqué pour ce faire.

Théorème 1.0.3. *Il existe les variables adjointes $\lambda_i, i = 1, 2, \dots, 6$ du système (5.37) qui satisfont le système d'équation différentielle ordinaire à rebours dans le temps suivant :*

$$\begin{aligned}
 -\frac{\partial \lambda_1(t)}{\partial t} &= -\lambda_1 \mu_E + (\lambda_2 - \lambda_1) \gamma_{E,L} \\
 -\frac{\partial \lambda_2(t)}{\partial t} &= -\lambda_2 (\mu_L + w_Y) + (\lambda_3 - \lambda_2) \gamma_{L,P} \\
 -\frac{\partial \lambda_3(t)}{\partial t} &= -\lambda_3 \mu_P + (\lambda_4 (1 - \beta_m P) e^{-\beta_m P} - \lambda_3) \gamma_{P,S_m} \\
 -\frac{\partial \lambda_4(t)}{\partial t} &= \lambda_1 \alpha_m - \lambda_4 (\mu_A + w_A) + (\lambda_5 - \lambda_4) ab_m I_h(t) \\
 -\frac{\partial \lambda_5(t)}{\partial t} &= \lambda_1 \alpha_m - \lambda_5 (\mu_A + w_A) + (\lambda_7 - \lambda_6) ab_h S_h(t) \\
 -\frac{\partial \lambda_6(t)}{\partial t} &= -\lambda_6 w_H + (\lambda_7 - \lambda_6) ab_h I_m(t) \\
 -\frac{\partial \lambda_7(t)}{\partial t} &= 1 + (\lambda_5 - \lambda_4) ab_m S_m(t) - \lambda_7 \sigma_h \\
 -\frac{\partial \lambda_8(t)}{\partial t} &= (\lambda_6 - \lambda_8) \gamma_h
 \end{aligned}$$

avec la condition de transversalité $\lambda(T) = 0$. De plus, les variables de contrôle optimales, pour $j = Y, A$, sont données par

$$\begin{aligned}
 w_Y^* &= \max \left(0, \min \left(\frac{\lambda_2 L}{A_Y}, w_M \right) \right) \\
 w_A^* &= \max \left(0, \min \left(\frac{\lambda_4 S_m + \lambda_5 I_m}{A_A}, w_M \right) \right) \\
 w_H^* &= \max \left(0, \min \left(\frac{\lambda_6 S_h}{A_H}, w_H \right) \right).
 \end{aligned}$$

Nos résultats montrent que la combinaison des copépodes et des pesticides est une bonne stratégie pour éliminer les humains infectés et la population de moustiques. Cependant, l'élimination des humains infectés est lente. La combinaison de pesticides et de vaccination semble moins efficace que la combinaison de copépodes et de pesticides. Il faut un temps plus court pour réduire le nombre de moustiques avec une durée réduite de l'application de contrôle.

Le dernier chapitre de cette étude rend compte de la distribution spatiale des moustiques adultes. Nous supposons que seul les moustiques adultes se déplacent, et donc, seuls S_m et I_m ont des dimensions spatiales. La propension des moustiques adultes à quitter le point focal peut être définie par le coefficient de diffusion, pour $(x, y) \in \Omega$

$$D(x, y) = D_{min} + \alpha \mathcal{F}_l(x, y) + \beta \mathcal{F}_f(x, y) \quad (1.3)$$

où D_{min} est la valeur minimale de diffusion en l'absence de perception des ressources, $\mathcal{F}_l(x, y)$ et $\mathcal{F}_f(x, y)$ sont les noyaux de perception qui couvrent l'ensemble du paysage

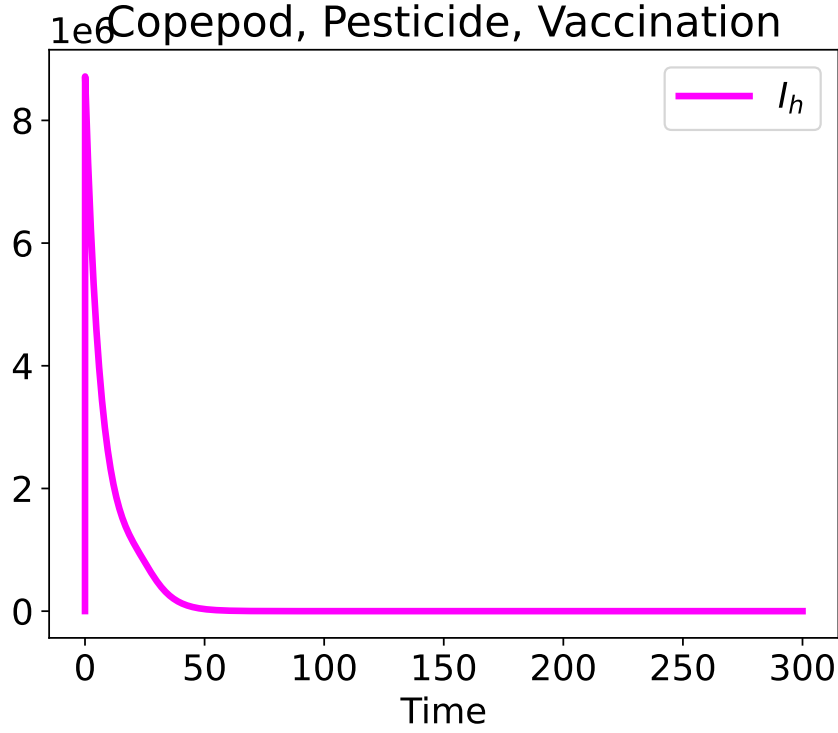


FIGURE 1.7: Evolution du nombre d'humains infectés sous contrôle optimal.

des ressources de ponte (laying) et de nourriture (food) respectivement. Dans cette étude, nous considérons que les moustiques préféreront toujours les sites de ponte les plus proches d'eux. Ainsi, en considérant la densité de population de moustiques adultes pour chaque $(x, y) \in \Omega$, nous avons défini un nouveau modèle qui implique la distribution spatiale des moustiques comme suit

$$\begin{aligned} \frac{\partial S_m(t, x, y)}{\partial t} = & \gamma_{P, S_m} P(t, x, y) e^{-\beta_m P(t, x, y)} - \mu_A S_m(t, x, y) \\ & - ab_m I_h(t, x, y) S_m(t, x, y) + \frac{\partial}{\partial x} \left(D(x, y) \frac{\partial S_m}{\partial x} \right) \\ & + \frac{\partial}{\partial y} \left(D(x, y) \frac{\partial S_m}{\partial y} \right) \end{aligned} \quad (1.4)$$

$$\begin{aligned} \frac{\partial I_m(t, x, y)}{\partial t} = & ab_m I_h(t, x, y) S_m(t, x, y) - \mu_A I_m(t, x, y) \\ & + \frac{\partial}{\partial x} \left(D(x, y) \frac{\partial I_m}{\partial x} \right) + \frac{\partial}{\partial y} \left(D(x, y) \frac{\partial I_m}{\partial y} \right). \end{aligned} \quad (1.5)$$

Le système est complété par des conditions aux bords de type Neumann.

Théorème 1.0.4. Soient $0 \leq S_{h,0}, I_{h,0}, R_{h,0} \leq H_0$, $0 \leq E_0, L_0, P_0 \leq M_{Y,0}$, et $0 \leq S_{m,0}, I_{m,0} \leq M_{A,0}$ où $H_0, M_{Y,0}$ et $M_{A,0}$ sont la densité initiale de la population humaine, des jeunes moustiques et des moustiques adultes, respectivement. Il existe alors une unique solution faible globale en temps $(E, L, P, S_m, I_m, S_h, I_h, R_h) \in L^\infty(\mathbb{R}_+, L^\infty(\Omega))^8$, du problème

aux valeurs initiale. De plus, la solution est non négative, $S_h + I_h \leq H_0$, $E + L + P \leq M_{Y,0}$ et $S_m + I_m \leq M_{A,0}$.

Nous avons montré ce résultat en appliquant le théorème du point fixe de Picard dans la boule

$$B_T = \left\{ Y \in L^\infty(\mathbb{R}_+, L^\infty(\Omega))^8 : \sup_{t \in [0, T]} \|Y(t, \cdot) - Y_0\|_{L^\infty(\Omega)} \leq r \right\} \quad (1.6)$$

à partir de la formulation intégrale

$$\begin{aligned} E &= e^{-(\gamma_{E,L} + \mu_E)t} E_0 + \alpha_m \int_0^t e^{-(\gamma_{E,L} + \mu_E)(t-s)} (S_m + I_m) \\ L &= e^{-(\gamma_{L,P} + \mu_L)t} L_0 + \gamma_{E,L} \int_0^t e^{-(\gamma_{L,P} + \mu_L)(t-s)} E ds \\ P &= e^{-(\gamma_{P,S_m} + \mu_P)t} P_0 + \gamma_{L,P} \int_0^t e^{-(\gamma_{P,S_m} + \mu_P)(t-s)} L ds \\ S_m &= K \star S_{m,0} + \int_0^t K \star (\gamma_{P,S_m} P e^{-\beta_m P} - ab_m I_h S_m) ds \\ I_m &= K \star I_{m,0} + ab_m \int_0^t K \star I_h S_m ds \\ S_h &= S_{h,0} + \int_0^t (\gamma_h R_h - ab_h I_m S_h) ds \\ I_h &= e^{-\sigma_h t} I_{h,0} + ab_h \int_0^t e^{-\sigma_h(t-s)} I_m S_h ds \\ R_h &= e^{-\gamma_h t} R_{h,0} + \sigma_h \int_0^t e^{-\gamma_h(t-s)} I_h ds \end{aligned} \quad (1.7)$$

où K est le noyau de la chaleur.

Dans la dernière section du chapitre quatre, nous déterminons la stratégie de contrôle optimale en appliquant trois contrôles : l'exposition au copépode w_Y pour les jeunes moustiques dans les zones de ponte, le pesticide w_A pour les moustiques adultes, et l'application de la vaccination w_H pour les humains. Ici les contrôles dépendent du temps et de l'espace. Nous considérons le problème, pour $X = (x, y)$

$$\mathcal{J}(w) = \int_\Omega \int_0^T (I_h(X, t) + \frac{1}{2} A_Y w_Y^2(X, t) + \frac{1}{2} A_A w_A^2(X, t) + \frac{1}{2} A_H w_H^2(X, t)) dt dX.$$

Nous utilisons la méthode de l'état adjoint pour déterminer les variables de contrôle optimales.

Théorème 1.0.5. *Il existe les variables adjointes $\lambda_i, i = 1, 2, \dots, 6$ qui satisfont le système d'équations différentielles partielles à rebours dans le temps suivant :*

$$\begin{aligned}
-\frac{\partial \lambda_1(x, t)}{\partial t} &= \lambda_1(x, t)\mu_E + (\lambda_1(x, t) - \lambda_2(x, t))\gamma_{E,L} \\
-\frac{\partial \lambda_2(x, t)}{\partial t} &= \lambda_2(x, t)(\mu_L + w_Y) + (\lambda_2(x, t) - \lambda_3(x, t))\gamma_{L,P} \\
-\frac{\partial \lambda_3(x, t)}{\partial t} &= \lambda_3(x, t)\mu_P + (\lambda_3(x, t) - \lambda_4(x, t)(1 - \beta_m P(x, t)e^{-\beta_m P(x, t)}))\gamma_{P,S_m} \\
-\frac{\partial \lambda_4(x, t)}{\partial t} - D\Delta\lambda_4 &= -\lambda_1(x, t)\alpha_m + \lambda_4(x, t)(\mu_A + w_A) + (\lambda_4(x, t) - \lambda_5(x, t))ab_m I_h(x, t) \\
-\frac{\partial \lambda_5(x, t)}{\partial t} - D\Delta\lambda_5 &= -\lambda_1(x, t)\alpha_m + \lambda_5(x, t)(\mu_A + w_A) + (\lambda_6(x, t) - \lambda_7(x, t))ab_h S_h(x, t) \\
-\frac{\partial \lambda_6(x, t)}{\partial t} &= \lambda_6(x, t)w_H + (\lambda_6(x, t) - \lambda_7(x, t))ab_h I_m(x, t) \\
-\frac{\partial \lambda_7(x, t)}{\partial t} &= 1 + (\lambda_7(x, t) - \lambda_8(x, t))\sigma_h + (\lambda_4(x, t) - \lambda_5(x, t))ab_m S_m(x, t) \\
-\frac{\partial \lambda_8(x, t)}{\partial t} &= (\lambda_8(x, t) - \lambda_6(x, t))\gamma_h
\end{aligned} \tag{1.8}$$

avec la condition de transversalité $\lambda^T(x, T) = 0$ et les conditions aux limites $\mu^T = \frac{\lambda^T(x, 0)h(U(x, 0))}{g(U(x, 0), w)}$ et $\left. \frac{\partial \lambda(x, t)}{\partial x} \right|_{\partial\Omega} = \left. \frac{\partial U(x, t)}{\partial x} \right|_{\partial\Omega} = 0$. En outre, la variable de contrôle optimale w^* est définie comme suit

$$\begin{aligned}
w_Y^*(t) &= \max\left(0, \min\left(\frac{\lambda_2 L}{-A_Y}, w_M\right)\right) \\
w_A^*(t) &= \max\left(0, \min\left(\frac{(\lambda_4 I_h + \lambda_5 S_h)}{-A_A}, w_M\right)\right) \\
w_H^*(t) &= \max\left(0, \min\left(\frac{\lambda_6 S_h}{-A_H}, w_H\right)\right).
\end{aligned}$$

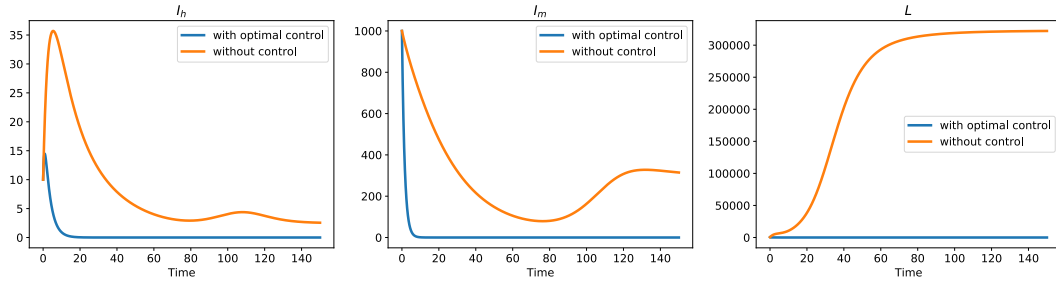
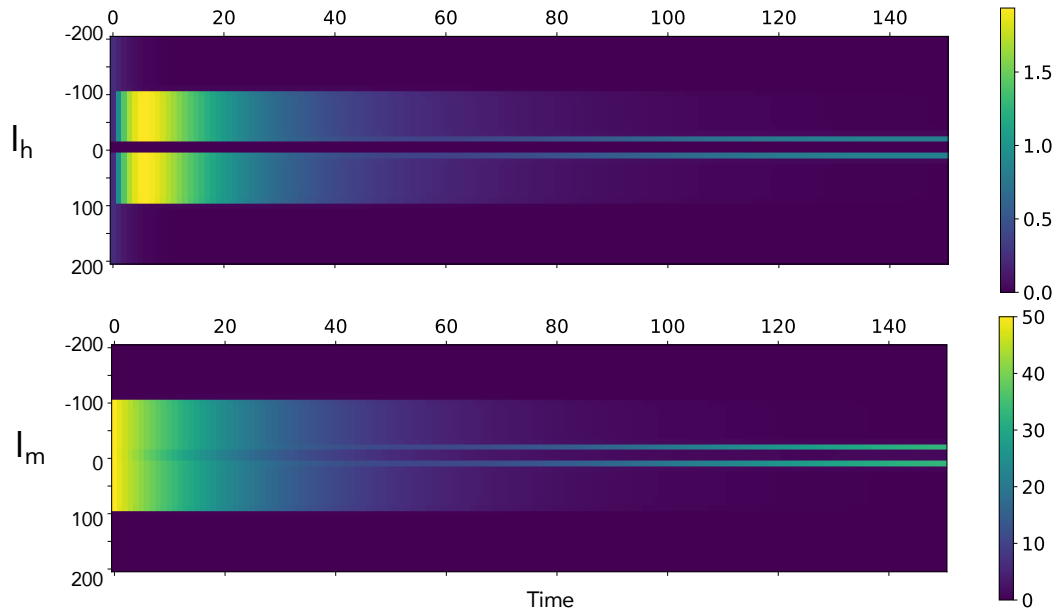


FIGURE 1.8: Comparaison entre le nombre d'humains infectés I_h , le nombre de moustiques infectieux I_m , et le nombre de larves L , avec trois entrées de contrôle optimal (bleu) et sans contrôle (orange).

La figure montre une différence significative entre le graphique avec trois entrées de contrôle et sans stratégie de contrôle. Elle montre que l'application de la stratégie de contrôle minimise efficacement la population de larves, les humains infectés et la population de moustiques. Il faut peu de temps pour minimiser chaque population.

La figure montre l'évolution spatio-temporelle des humains et des moustiques infectieux avec et sans contrôle. La figure montre qu'en l'absence de contrôle, nous

without control



with optimal control

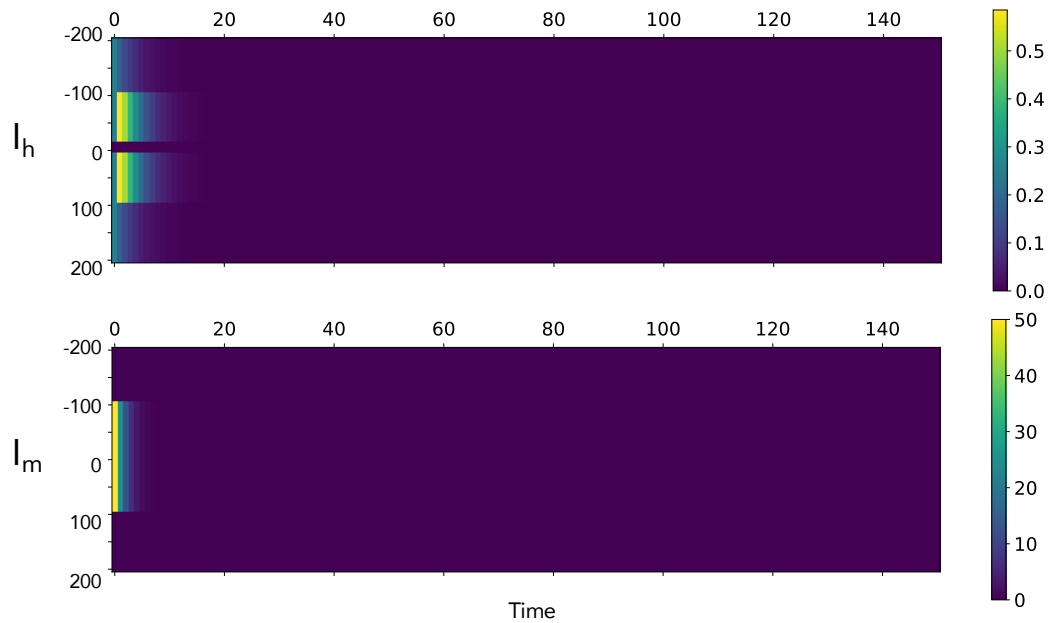


FIGURE 1.9: Comparaison entre le nombre d'humains infectés I_h , le nombre de moustiques infectieux I_m , et le nombre de larves L , avec trois entrées de contrôle (bleu) et sans contrôle (orange).

devons appliquer la stratégie de contrôle pendant une longue période, puis la diminuer. Cependant, diminuer les efforts de contrôle ne signifie pas arrêter son application. La figure montre que nous devons continuellement appliquer la stratégie de contrôle à proximité des sites de ponte.

La figure montre l'évolution spatio-temporelle de chaque variable de contrôle

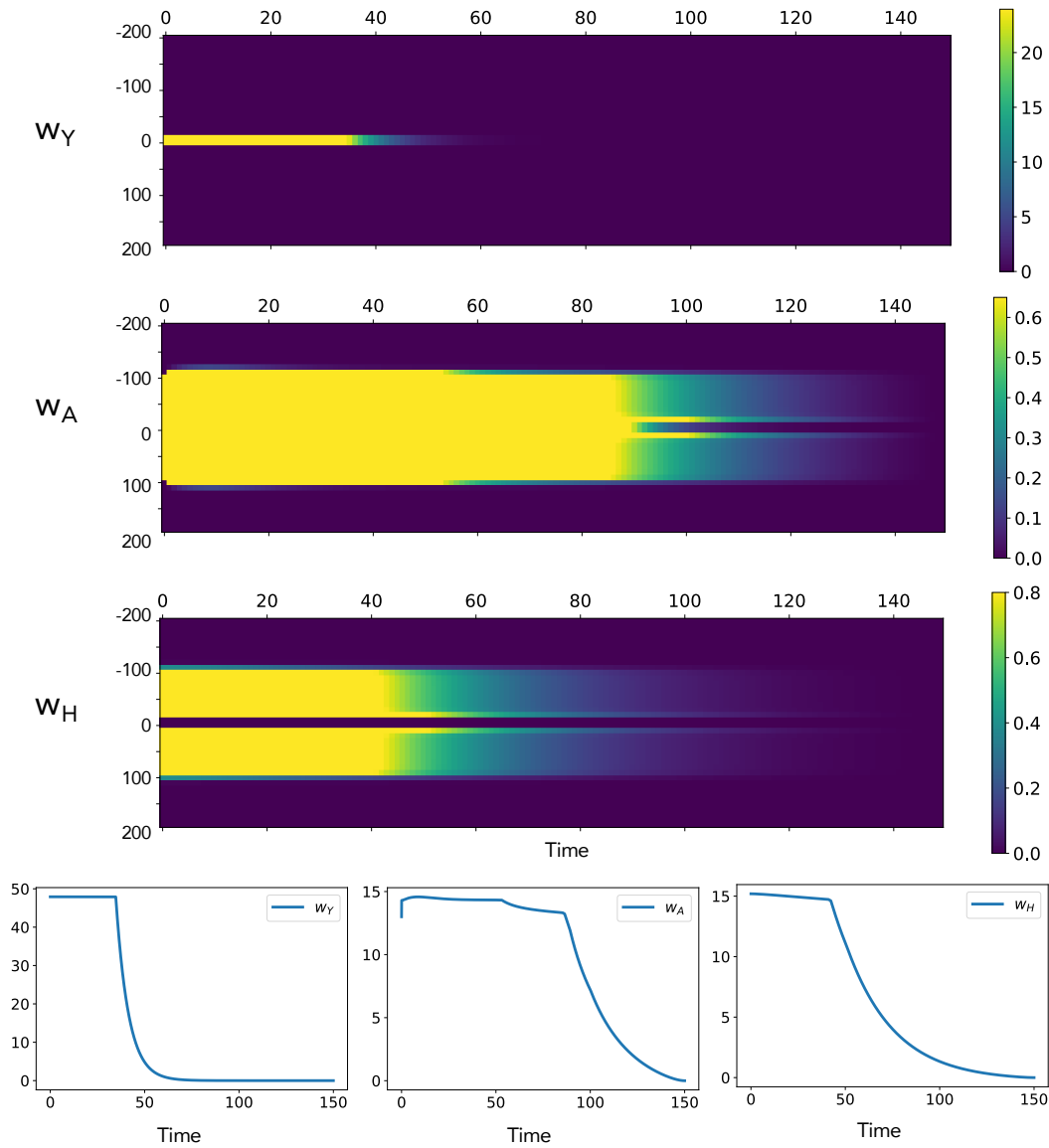


FIGURE 1.10: Evolution spatio-temporelle de la variable de contrôle optimale w_Y liée à l'utilisation des copépodes (en haut) et à sa somme dans l'espace (en bas).

optimale du modèle avec trois entrées de contrôle. Elle montre que nous devons administrer le copépode en continu pendant 100 jours tout en diminuant l'application du pesticide et la vaccination au fil du temps. Cependant, la figure montre que nous devons appliquer le pesticide et la vaccination en continu à proximité des sites de ponte de manière progressive.

La section annexe contient l'article publié sur le covid intitulé "Accounting for Symptomatic and Asymptomatic in a SEIR-type model of COVID-19".

Perspectives de l'étude

La modélisation mathématique de la dengue est un sujet vaste qui traite de diverses inconnues. Il est quelque peu impossible de couvrir une grande partie du sujet en trois ans. Voici donc une liste de perspectives de recherche possibles que nous prévoyons d'étudier.

Une perspective de l'étude est de considérer la structure d'âge de la population humaine. Compte tenu de la recommandation de Sanofi Pasteur sur l'application de Dengvaxia, il est intéressant de créer un modèle avec une structure d'âge dans la population humaine pour décrire la transmission de la dengue avec différents taux d'infection parmi les différents groupes d'âge.

Une autre solution consiste à développer un modèle complet de dengue-dengvaxia intégrant le cycle de vie des moustiques, les quatre souches de virus de la dengue de la population humaine, et l'efficacité de Dengvaxia sur les différentes souches de virus. L'ajout de la structure d'âge et de l'effet du climat sur la dengue dans ce modèle en ferait un modèle robuste de la dengue.

Une perspective supplémentaire de l'étude est de considérer les habitudes de reproduction et d'alimentation des moustiques. On peut incorporer le sexe des moustiques dans le modèle et appliquer une stratégie de contrôle pour minimiser les moustiques infectés. Puisque les moustiques mâles se nourrissent du nectar des plantes et que certaines plantes mangent les moustiques, en concevant une position stratégique des plantes dans l'environnement, on peut déterminer la stratégie de contrôle optimale pour minimiser les moustiques infectés dans la population.

En lien, on peut aussi considérer les besoins énergétiques des moustiques. Les sites d'alimentation et de ponte affectent directement l'approvisionnement en énergie des moustiques. L'énergie des moustiques augmente lorsqu'ils se nourrissent et diminue pendant la période de ponte. Dans cette optique, nous définissons la quatrième dimension U qui rend compte de l'approvisionnement en énergie du moustique, appelée dimension énergétique. Nous pouvons supposer que seuls les moustiques adultes se déplacent et donc que seuls S_m et I_m ont une dimension énergétique. Cette dimension énergétique utilise un budget énergétique dynamique simplifié par des termes d'advection dans la dimension énergétique supplémentaire U . Cela repose sur un paysage énergétique après discrétisation de l'espace. Les couvertures terrestres ont été regroupées en fonction de leurs effets présumés sur la fourniture d'énergie. Les nouveaux moustiques adultes émergents ont un niveau d'énergie U où $U = 1$ est la limite énergétique supérieure et $U = 0$ est la limite énergétique inférieure, c'est-à-dire que $S_m, I_m(t, x, y, U = 0) = 0$ simule la mort par

famine des moustiques adultes sensibles et infectés. On peut donc définir la dynamique du moustique adulte comme suit :

$$\begin{aligned} \frac{\partial S_m(t, x, y)}{\partial t} = & \gamma_{P, S_m} P(t, x, y) e^{-\beta_m P(t, x, y)} - \mu_A S_m(t, x, y) \\ & - ab_m I_h(t, x, y) S_m(t, x, y) + \frac{\partial}{\partial x} \left(D(x, y) \frac{\partial S_m}{\partial x} \right) \\ & + \frac{\partial}{\partial y} \left(D(x, y) \frac{\partial S_m}{\partial y} \right) - C(x, y) \frac{\partial S_m}{\partial U} \end{aligned} \quad (1.9)$$

$$\begin{aligned} \frac{\partial I_m(t, x, y)}{\partial t} = & ab_m I_h(t, x, y) S_m(t, x, y) - \mu_A I_m(t, x, y) \\ & + \frac{\partial}{\partial x} \left(D(x, y) \frac{\partial I_m}{\partial x} \right) + \frac{\partial}{\partial y} \left(D(x, y) \frac{\partial I_m}{\partial y} \right) - C(x, y) \frac{\partial I_m}{\partial U}. \end{aligned} \quad (1.10)$$

Une autre perspective intéressante de l'étude est de considérer la co-infection de la dengue et du Covid-19. En raison du chevauchement des caractéristiques cliniques et de laboratoire de ces maladies, la pandémie de Covid-19 dans les zones où la dengue est endémique représente un défi majeur. On peut donc concevoir un bon modèle mathématique montrant la co-infection de ces maladies et appliquer une stratégie de contrôle optimal pour minimiser les humains infectés.

Chapter 2

General Introduction

2.1 Mosquitoes

Mosquitoes are an important vector for disease transmission of many of the classified pathogens and parasites, including viruses, bacteria, fungi, protozoa, and nematodes. It is mainly due to their blood-feeding habits, for which they feed on vertebrate hosts. Infected mosquitoes carry these organisms from person to person without exhibiting symptoms themselves. According to [36], by 2050, half the world's population could be at risk of mosquito-borne diseases like dengue fever or the Zika virus, malaria, and many more. By transmitting these diseases, mosquitoes cause the deaths of more people than any other animal taxon. With more than 100 million years of an evolutionary process, mosquitoes developed adaptation mechanisms capable of thriving in various environments. Except for permanently frozen places, these mosquitoes are found in every land region globally. They occupy the tropics and sub-tropics where the climate seems favorable and efficient for their development—making them nearly the universal animal in the world.



FIGURE 2.1: Photo of an adult female *Aedes aegypti* (left) and *Aedes albopictus* (right) mosquito during a blood meal [17].

Of almost 3,600 species of mosquitoes inhabiting the planet, the ones belonging to the family *Cuculicidae* of order *Diptera* are known to play a crucial role as vectors of arbovirus transmission [48]. Within this family, the genus *Aedes* is involved in the transmission of diseases. The two most prominent species within this genus are *Aedes aegypti* and *Aedes albopictus*. They are the primary vector for dengue, yellow fever, West Nile fever, chikungunya, eastern equine encephalitis, Zika virus [32], and many other less notable diseases.

In this thesis, we aim to develop a mathematical model of dengue taking into account vaccination and vector control. Thus, we focus on the biology of *Ae. aegypti* and *Ae. albopictus* mosquitoes as the primary vector of dengue.

2.1.1 Life Cycle

Mosquitoes have a complex life cycle. Nevertheless, all of them require water to complete their life cycle. They change their shape and habitat as they develop. Like all other mosquitoes, *Ae. aegypti* and *Ae. albopictus* have four distinct stages: egg, larva, pupa, and adult (Fig. 2.2).

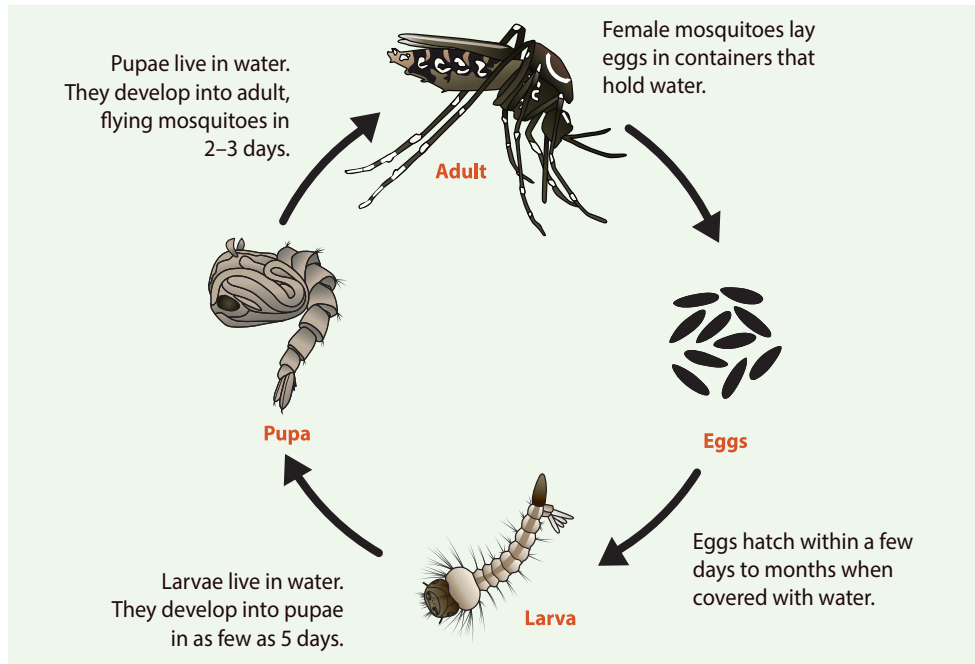


FIGURE 2.2: Life stages of female *Ae. aegypti* and *Ae. albopictus* mosquitoes. [19]

Female adult mosquitoes lay eggs a few days after acquiring a blood meal. Mosquitoes generally lay up to 100 eggs at a time. They lay their eggs singly [31] on the inner walls of containers just above the water line that is or will be filled with water. It sticks like glue. This oviposition site includes a cavity wall such as a hollow stump or a container such as a bucket or a discarded vehicle tire. Only a tiny amount of water is needed to lay eggs. However, mosquito eggs can survive drying out for up to 8 months or even in winter in the southern United States [20]. When that happens, they have to resist a considerable desiccation before they hatch [59]. Once they achieve a suitable desiccation level, they can enter diapause for several months. *Aedes* eggs in diapause tend to hatch irregularly over an extended period.

It then hatches to larvae when water inundates the eggs, such as rains or filling water by people. Following water immersion, eggs hatch in batches. Since some

eggs require multiple soakings in water before hatching, this process may last days or weeks [69].

Larvae live in water, and they feed on heterotrophic microorganisms such as bacteria, fungi, and protozoans. They develop through four stages, or instars. The larvae molt in the first to fourth-instar, shedding their skins to grow further. On the fourth instar, when the larva is fully grown, they metamorphose into a new form called pupae. Pupa still lives in water, but they do not feed. After two days, they fully develop into adult mosquito forms and break through the pupa's skin. The adult mosquito is no longer aquatic; it has a terrestrial habitat and can fly. This entire life cycle of mosquitoes lasts for eight to ten days at room temperature, depending on the feeding level.

2.1.2 Feeding Habits by Adult Mosquitoes

Like all other living animals, Mosquitoes need energy and nutrients for survival and reproduction. Plant materials and blood are valuable sources of this.

Only female mosquitoes bite. They are attracted by infrared light, light, perspiration, body odor, lactic acid, and carbon dioxide. The mouth part of many female mosquitoes is adapted for piercing animal hosts' skin and sucking their blood as ectoparasites. The female mosquitoes land on the host skin during the blood meal and stick their proboscis. Their saliva contains anticoagulant proteins that prevent blood clotting. They then suck the host blood into their abdomen. *Ae. Aegypti* mosquitoes need 5 μL per serving [23]. In many female mosquito species, nutrients obtained from blood meals are essential for the production of eggs, whereas in many other species, obtaining nutrients from a blood meal enables the mosquito to lay more eggs. Among humans, mosquitoes preferred feeding those with type O blood[61], heavy breathers, an abundance of skin bacteria, high body heat, and pregnant women [21]. Individuals' attractiveness to mosquitoes also has a heritable, genetically-controlled component [29].

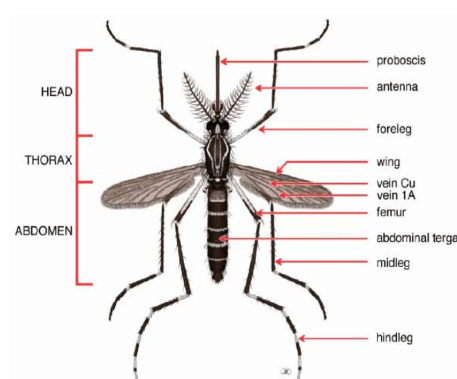


FIGURE 2.3: Dorsal view of the adult female *Ae. Aegypti* mosquito.
[58]

Blood-sucking species of mosquitoes are selective feeders that prefer a particular host species. Nevertheless, they relax this selectivity when they experience severe competition and scarcity of food and defensive activity on the part of the hosts.

If humans are scarce, mosquitoes resort to feeding on monkeys, while others prefer on equines, rodents, birds, bats, and pigs, which is where so many of our cross-species disease fears originate from [41]. Some mosquitoes ignore humans altogether and feed exclusively on birds, while most eat whatever is available. Some of the other most popular dining options for mosquitoes include amphibians, snakes, reptiles, squirrels, rabbits, and other small mammals. Mosquitoes also target larger animals, such as horses, cows, primates, kangaroos, and wallabies [39]. Some mosquito species may attack even fish if they expose themselves above water level, as mud-skippers do [63]... Comparably, mosquitoes may sometimes feed on insects in nature. *Ae. Aegypti* and *Culextarsalis* are attracted and feed on insect larvae, and they live to produce viable eggs [60]. While *Anopheles Stephensi* is attracted to and can feed successfully on larvae of moth species known as *Manduca sexta* and *Heliothis subflexa* [34].

Plant nectar is a common energy source for diet across mosquito species, particularly male mosquitoes, exclusively dependent on plant nectar or alternative sugar sources. The design of efficient sugar-baited traps for mosquitoes would greatly benefit the prevention of vector-borne illness. Plant preference is likely driven by an innate attraction that may be enhanced by experience, as mosquitoes recognize available sugar rewards [70]. It varies among mosquito species, geographical habitats, and seasonal availability. Nectar-seeking involves integrating at least three sensory systems: olfaction, vision, and taste.

Nevertheless, altogether mosquitoes can discriminate between rich and poor sugar sources to choose plants with higher glycogen, lipid, and protein content [73]. Below are the preferred plant of different mosquito species from the paper of Barredo and DeGennaro [7].

2.1.3 Breeding Sites

The *Aedes* mosquitoes breed in all imaginable receptacles. It can be classified as artificial and natural wet containers, preferably with dark-colored surfaces and holding clear unpolluted water [46]. Below is roughly the list of different kinds of breeding sites of *Aedes* mosquitoes [32]:

- Natural Container
 - Tree Holes
 - Leaf Axils
 - Rock Holes.
- Artificial Container

Mosquito Species	Nectar Source
<i>Aedes aegypti</i>	<i>Asclepias syriaca</i> (milkweed) Plant extract <i>Impatiens walleriana</i> Live plants
<i>Anopheles gambiae</i>	<i>Mangifera indica</i> <i>Delonix regia</i> Live plants <i>Parthenium hysterophorus</i> Live plants <i>Acacia macrostachya</i> <i>Acacia albida</i>
<i>Culex pipiens</i>	<i>A. syriaca</i> (milkweed) Live Flower, extract, and synthetic blend <i>I. walleriana</i>
<i>Culex pipiens pallens</i>	<i>Ligustrum quihoui</i> (waxyleaf privet) <i>Broussonetia papyrifera</i> (paper mulberry) <i>L. quihoui</i> <i>Abelia chinensis</i> <i>Nerium indicum</i>

TABLE 2.1: Preferred plants of different mosquito species as energy source.

– Discarded Containers

- * Automobile Tires
- * Tin Cans
- * Bottles
- * Vases
- * Roof Gutters
- * Animal Water Dishes
- * Water Closets.

– Water Storage Containers

- * Tanks
- * Drums
- * Water Jars

2.2 Dengue

Dengue is the most common mosquito-borne viral infection. It can be found in tropical and subtropical regions worldwide, with peak transmission during the rainy season. In 2019, World Health Organization [68] reported 5.2 million dengue cases worldwide. In the Philippines alone, 271,480 cases with 1,107 deaths are reported from January 1 to August 31, 2019, due to dengue fever [28].

Dengue is caused by four serotypes of viruses under the Flaviviridae family. They are distinct but closely related serotypes of viruses called DENV-1, DENV-2, DENV-3, and DENV-4. About one in four people that are infected with dengue will get sick [15]. The illness usually begins 5–7 days after the infective bite of *Ae. aegypti* and *Ae. albopictus* female mosquitoes [8].

In most cases, dengue is a self-limiting illness but may require hospital admission, where supportive care can modify the course of the illness. Symptoms can be mild or severe and typically last 2–7 days. The most common symptom of dengue

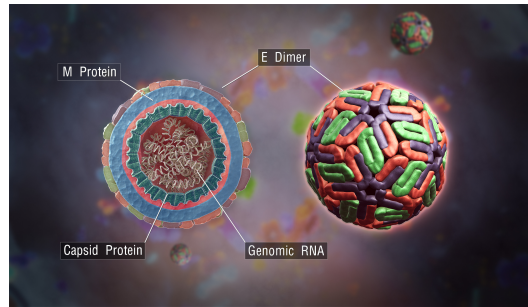


FIGURE 2.4: Cross section of a dengue virus showing its structural components [40] similar to the Zika Virus.

is fever accompanied by nausea, vomiting, rash, aches, and pains in the muscles or joints. Infection from one type grants life-long immunity to that virus strain and temporarily grants partial protection against the other types. When infected with a different type of virus for a second time, a more severe disease will occur, known as Dengue Hemorrhagic Fever (DHF). In the Philippines, 1,107 deaths are reported from January 1 to August 31, 2019, due to dengue fever [28].

2.2.1 Transmission

Dengue viruses are spread to people through the bites of infected *Aedes* species mosquitoes [18]. It can be transmitted by human-to-mosquito, mosquito-to-human, and other transmissions such as human-to-human and mosquito-to-mosquito transmission.

Vertical transmission is when infected parent mosquitoes transmit the arbovirus to some part of their offspring within the ovary or during oviposition [30]. Several articles confirm these findings. A study of Shroyer DA.[24] is one of the articles that confirms the presence of the natural vertical transmission of DENV in *Ae. aegypti* and *Ae. albopictus*. It says that the DENV virus can be transferred from parent to offspring in seven consecutive generations of *Ae. aegypti* and *Ae. albopictus*, under laboratory conditions. This transmission can contribute to the continuation of infected mosquitoes; however, this is not enough to support the dengue spread.

A more common form of transmission is known as horizontal transmission. The virus is transmitted to humans through the bites of infected *Ae. aegypti* mosquitoes. After feeding on a dengue-infected person, the virus replicates in the mosquito midgut before disseminating to secondary tissues, including the salivary glands. The Extrinsic Incubation Period (EIP) is the time it takes from ingesting the virus to actual transmission to a new host. It takes about 8-12 days when the ambient temperature is between 25-28°C. Variations in the EIP are also influenced by factors such as the magnitude of daily temperature fluctuations, virus genotype, and initial viral concentration [68]. Once infectious, the mosquito can transmit the virus for the rest of its life.

Mosquitoes can become infected by someone who is viremic with DENV. Viremia is a condition in which there is a high level of the dengue virus in the person's blood. It occurs four days after an infected *Ae. aegypti* mosquito bites an individual. Most people are viremic for about 4-5 days, but viremia can last as long as 12 days [68].

Though the possibility is low, there is evidence that dengue can also spread through maternal transmission or be transmitted through infected blood transfusion. A pregnant woman who has a DENV infection can pass the virus to her fetus. Babies who carry DENV may suffer from pre-term birth, low birth weight, and fetal distress [68].

2.2.2 Vaccination

There is no specific treatment for dengue fever. However, efforts to develop a vaccine have been ongoing for decades.

The first dengue vaccine used commercially is CYD-TDV, marketed as Dengvaxia by Sanofi Pasteur. It was licensed in December 2015 and approved by regulatory authorities in 20 countries. One such country is the Philippines. In December 2015, the Philippine Food and Drugs Administration (FDA) greenlighted the vaccine making the Philippines the first Asian country to commercialize it [65]. In April 2016, the Department of Health (DOH) launched the dengue vaccination campaign in the Philippine regions of Central Luzon, Calabarzon, and Metro Manila. More than 800,000 school children received at least one dose of the vaccine.



FIGURE 2.5: Dengue tetraivalent vaccine manufactured by Sanofi Pasteur.

Dengvaxia is a live attenuated tetraivalent chimeric vaccine. It is made using recombinant DNA technology by replacing the PrM (pre-membrane) and E (envelope) structural genes of yellow fever attenuated 17D strain vaccine with those from the four dengue serotypes. It should be administered in three doses of 0.5 mL subcutaneous (SC) six months apart. Sanofi Pasteur recommended that the vaccine only be used in people between the age of 9 to 45 and people already infected by one type of virus [3]. It is because outcomes may be worse in those who have not yet been previously infected.

2.2.3 Vector Control

A disease vector is any living agent carrying and transmitting an infectious pathogen to another living organism. Controlling such vectors is an essential method of limiting or eradicating the transmission of such diseases. For dengue fever, mosquito control with good scientific insights into mosquito ecology and disease transmission patterns is essential to combat dengue fever.

The World Health Organization considered the following categories to control or prevent the spread of the dengue virus [33].

- Environmental management
 - A significant risk factor for dengue virus transmission is the proximity of mosquito vector breeding sites to human habitation. Thus an efficient environmental management system is an effective strategy for vector control. It includes container management, eliminating breeding sites' alteration, and preventing breeding in the water storage container.
- Chemical and biological methods
 - Chemical larviciding is effective against container breeders of *Aedes* mosquitoes in clean water. It uses organic synthetic insecticides such as temephos (Abate) and insect growth regulators (IGRs) such as methoprene (Altosid, juvenile hormone mimic), where environmental impact is minimal if appropriately used on human premises.
 - Wolbachia is a common type of bacteria found in insects but is harmless to people or animals. It is not found in *Aedes aegypti* mosquitoes. When male *Ae. aegypti* mosquitoes with Wolbachia mate with wild female mosquitoes that do not have Wolbachia; the eggs will not hatch, resulting in a decrease population of *Ae. aegypti* mosquitoes [14].
 - Copepods are a group of small crustaceans found in nearly every freshwater and saltwater habitat. The use of *cyclopoida copepoda* as mosquito control has proven to be more effective than invertebrate predators [44]. Only copepod with a body length greater than 1.4 mm is of practical use as mosquito control. They kill the first instar mosquitoes with 40 *Aedes* larvae/copepod/day. They typically reduce *Aedes* production by 99-100%.
- Personal protection
 - Avoiding getting further mosquito bites when a person is in a viremic state is an excellent way to prevent the spread of the dengue virus. During this time, DENV is circulating in the person's blood and therefore may transmit the virus to new uninfected mosquitoes, who may, in turn, infect other people. Therefore, personal protection using mosquito coils and aerosols, insecticide-impregnated curtains and mosquito nets, and mosquito repellents are essential methods for vector control.

- Space spray application
 - Space spray is an effective strategy for rapidly killing adult *Aedes* mosquitoes in dengue epidemic areas. It uses thermal fogs and ultra-low volume aerosol sprays.

Another vector control that is proven effective under field trials has demonstrated that dengue incidence can be substantially reduced by introgressing strains of the endosymbiotic bacterium called *Wolbachia* into *Aedes aegypti* mosquito populations [66]. *Wolbachia* is a ubiquitous bacteria that occurs naturally in insects and is safe for humans. They live inside insect cells and are passed from one generation to the next through an insect's eggs. Independent risk analyses indicate that the release of *Wolbachia*-infected mosquitoes poses negligible risk to humans and the environment. *Wolbachia*-carrying mosquitoes reduced their ability to transmit arboviruses [55]. The bacteria compete with the virus, making it harder for viruses to reproduce inside the mosquitoes. In effect, mosquitoes are much less likely to spread viruses from person to person.

2.3 Mathematical Models of Dengue Fever

Mathematical modeling has been used to test and determine the effectiveness of different intervention strategies in controlling or eliminating dengue. These various mathematical models aid mathematicians in testing the different hypotheses in the dengue transmission dynamic to understand their importance better.

SEIRS compartmental models accounting for susceptible, exposed, infected, and removed for the human population and susceptible and infected for mosquito population were widely promoted. Syafruddin and Noorani [62] studied a system of differential equations that models the population dynamics of an SEIR vector transmission of dengue fever. It is a mathematical model that analyses the spread of one serotype of dengue virus between host and vector. They have shown that it can model dengue fever using actual data.

On the other hand, Nuraini et al. [51] derived and analyzed the model taking into account the severe Dengue Hemorrhagic Fever (DHF) compartment in the transmission model. They consider a SIR model for dengue disease transmission. It is assumed that two viruses, strain one and strain 2, cause the disease. Long-lasting immunity from infection caused by one virus may not be valid concerning a secondary infection by the other virus. They find a control measure to reduce the DHF patients in the population or keep them at an acceptable level. They also discuss the ratio between the total number of severe DHF compartments, the total number of first infection compartments, and the total number of secondary infection compartments, respectively. Furthermore, they found out that this ratio is needed for practical control measures to predict the “real” intensity of the endemic phenomena since only data on severe DHF compartment is available.

Furthermore, Derouich et al. [27] proposed a model with two different viruses acting at separated intervals of time. They study the dynamics of dengue fever while concentrating on its progression to the hemorrhagic form to understand the epidemic phenomenon and suggest strategies for controlling the disease. Their model showed that the strategy based on preventing the dengue epidemic using vector control through environmental management or chemical methods remains insufficient since it only permits delaying the outbreak of the epidemic. Moreover, the reduction of susceptibles via vaccination is unlikely to be applicable in the short term because it faces some hurdles since a vaccine must protect against the four serotypes simultaneously.

Also, Aguiar and Stollenwerk [2] analyzed a modeling framework and assumptions used by Aguiar et al. [1] (2 and 4 strain dengue model) and assessed the impact of the newly licensed dengue vaccine. They discuss the role of several subsequent infections versus an exact number of dengue serotypes included in the model framework and the human immunological aspects associated with disease severity, identifying the implications for model dynamics and their impact on vaccine implementation. Their results suggested that reserving vaccines for seropositive individuals should provide a high level of protection, whereas indiscriminate vaccination could increase the number of hospitalizations also on the population level.

Determining the optimal control in minimizing the spread of dengue fever has also been studied. Yang and Ferreira [72] described the dynamics of dengue disease in the compartment model, taking into account chemical controls and mechanical control applied to the mosquitoes. Allowing some model parameters to depend on time, they were able to mimic seasonal variations and divide the calendar year into favorable and unfavorable periods regarding the vector population's development. Their simulations showed 'unpredictable' epidemic outbreaks when abiotic variations are taken into account. If controlling mechanisms are introduced regularly every year, they observe the decline of the efficiency index with the elapsed time.

On the other hand, an essential strategy in controlling the dengue epidemic is controlling the vector population. Among the many kinds of research, Almeida et al. [4] considers two techniques; it consists in releasing mosquitoes to reduce the size of the population (Sterile Insect Technique) or in replacing the wild population with a population carrying a *Wolbachia* bacteria (a bacteria responsible for blocking the transmission of viruses from mosquitoes to human). Their paper presents an optimal strategy in the release protocol of these two strategies wherein they look for a control function that minimizes the distance to the desired equilibrium (replacement or extinction of the wild population) at the final treatment time.

Moreover, Puntani et al. [54] presented a control mechanism based on a dengue model with vertical transmission considering the two policies, namely vaccination and insecticide administration. Carvalho et al. [12] evaluated a control strategy, which aims to eliminate the *Aedes aegypti* mosquito, as well as proposals for the

vaccination campaign. Their results show that eradicating dengue fever is done using an immunizing vaccine since control measures against its vector are insufficient to stop the disease from spreading. Additionally, Iboi and Gumel [38] designed a new mathematical model to assess the impact of the newly- released Dengvaxia vaccine on the transmission dynamics of two co-circulating dengue strains.

2.4 Outline of Study

This thesis is the first study to consider the proposal of Sanofi Pasteur. Herein we introduce a new mathematical model of dengvaxia. As recommended by the World Health Organization [71], vaccination should be given to individuals who have been already infected by one strain virus. In this paper, we split the susceptible human compartment into primary or secondary susceptible humans, that is, individuals who have not been infected and individuals who have been infected by one or more strains of the dengue virus.

This thesis paper aims to introduce a new mathematical model of dengue. It has the following objective:

1. to study dengvaxia and show if the recommendation of Sanofi is enough,
2. to determine an effective control of dengue, and
3. to generate a mathematical model of dengue accounting for its life cycle and spatial distribution.

The manuscript is organized as follows.

The third chapter started with the presentation of the Ross-type model of dengue that considers vaccinating individuals who have previous dengue infections. Using the logistic and exponential functions for human and mosquito populations, respectively, we have shown the well-posedness and positivity of the solution of the model. We obtained that the diseases free equilibrium is locally asymptotically stable while the endemic equilibrium is unstable. In this chapter, we compare the model using three growth functions:

- Pop_1 : constant human and mosquitoes population,
- Pop_2 : Gompertz growth function for the human population and an exponential growth function for mosquitoes population,
- Pop_3 : an entomological growth function for mosquito and a constant growth function for the human population.

In the Pop_1 model, we showed that the model has only the disease-free equilibrium and we were able to prove that it is locally asymptotically stable. Similarly, the Pop_2 model has only the disease-free equilibrium which is locally asymptotically stable as soon as the growth rate α_m is smaller than the mortality rate μ_m . On the other hand,

the Pop_3 model has both an endemic and a disease-free equilibrium. We were able to define the basic reproduction number

$$\mathcal{R}_0 = \sqrt{\frac{a^2 b_m u_5^* (\tilde{b}_h u_3^* + b_h u_1^*)}{H_0^2 \mu_m (\gamma_h + \delta_h)}},$$

then show that the disease-free equilibrium of model Pop_3 is locally asymptotically stable if $\alpha_m < \mu_m$ and that the endemic equilibrium is stable only if $\alpha_m > \mu_m$ and $\mathcal{R}_0 > 1$. More widely, we have proved the theorem below for the Pop_3 model.

Theorem 2.4.1. 1. If $\alpha_m < \mu_m$, the the trivial disease-free equilibrium is globally asymptotically stable.

2. If $\alpha_m > \mu_m$ and $\mathcal{R}_0 > 1$, then the non-trivial disease-free equilibrium is globally asymptotically stable.

We then determine the optimal control strategy for minimizing infected humans of each of these three control strategies. We attribute three control inputs, w_1 , w_3 , and w_m , for the primary, secondary human, and mosquito populations. Here, the action of $w_1(t)$ is the percentage of primary susceptible, and $w_3(t)$ is the percentage of a secondary susceptible individual being vaccinated per unit of time. While $w_5(t)$, $w_6(t)$ is the percentage of removed mosquitoes due to insecticide administration to the environment per unit of time. Considering the objective function

$$\mathcal{J}(w_1, w_3, w_m) = \int_0^T \left(u_2(t) + \frac{1}{2} A_1 w_1^2(t) + \frac{1}{2} A_3 w_3^2(t) + \frac{1}{2} A_m w_5^2(t) + \frac{1}{2} A_m w_6^2(t) \right) dt$$

subject to

$$\begin{aligned} u_1'(t) &= -\frac{ab_h u_6(t) u_1(t)}{H_0} - w_1(t) u_1(t) \\ u_2'(t) &= \frac{au_6(t) (b_h u_1(t) + \tilde{b}_h u_3(t))}{H_0} - \gamma_h u_2(t) - \delta_h u_2(t) \\ u_3'(t) &= \gamma_h u_2(t) - \frac{a\tilde{b}_h u_3(t) u_6(t)}{H_0} - w_3(t) u_3(t) \\ u_4'(t) &= \delta_h u_2(t) \\ u_5'(t) &= -\frac{ab_m u_2(t) u_5(t)}{H_0} - \mu_m u_5(t) + g(M(t)) - w_5(t) u_5(t) \\ u_6'(t) &= \frac{ab_m u_2(t) u_5(t)}{H_0} - \mu_m u_6(t) - w_6(t) u_6(t) \end{aligned} \tag{2.1}$$

for $t \in [0, T]$, with $0 \leq w_1, w_3 \leq w_H$ and $0 \leq w_m \leq w_M$, we use the Pontryagin's maximum principle to determine the optimal control.

Theorem 2.4.2. *There exists the adjoint variables $\lambda_i, i = 1, 2, \dots, 6$ of the system (4.13) that satisfy the following backward in time system of ordinary differential equation.*

$$\begin{aligned}
-\frac{d\lambda_1}{dt} &= \lambda_1 \left(\frac{-ab_h u_6}{H_0} - w_1 \right) + \lambda_2 \frac{ab_h u_6}{H_0} \\
-\frac{d\lambda_2}{dt} &= 1 + \lambda_2 (-\gamma_h - \delta_h) + \lambda_3 \gamma_h + \lambda_4 \delta_h - \lambda_5 \frac{ab_m u_5}{H_0} + \lambda_6 \frac{ab_m u_5}{H_0} \\
-\frac{d\lambda_3}{dt} &= \lambda_2 \frac{a\tilde{b}_h u_6}{H_0} + \lambda_3 \left(\frac{-a\tilde{b}_h u_6}{H_0} - w_3 \right) \\
-\frac{d\lambda_4}{dt} &= 0 \\
-\frac{d\lambda_5}{dt} &= \lambda_5 \left(\frac{-ab_m u_2}{H_0} + \frac{\partial g}{\partial u_5} \right) - \lambda_5 (\mu_m + w_5) + \lambda_6 \frac{ab_m u_2}{H_0} \\
-\frac{d\lambda_6}{dt} &= -\lambda_1 \frac{ab_h u_1}{H_0} + \lambda_2 \frac{ab_h u_1 + a\tilde{b}_h u_3}{H_0} - \lambda_3 \frac{a\tilde{b}_h u_3}{H_0} + \lambda_5 \frac{\partial g}{\partial u_6} - \lambda_6 (\mu_m + w_6)
\end{aligned}$$

with the transversality condition $\lambda(T) = 0$. Furthermore, the optimal control variables, for $j = 1, 3, 5, 6$, are given by

$$w_j^*(t) = \max \left(0, \min \left(\frac{\lambda_j u_j}{A_j}, w_H, w_M \right) \right).$$

The optimality of the models is numerically solved using a gradient method written in Python. The figure obtained showed that vaccinating only the secondary susceptible humans is not ideal. It requires constant effort and takes a long time to vaccinate them. Instead, it is better to vaccinate the primary susceptible humans. However, since safe vaccines for primary susceptible humans do not exist to date, the application of vector control to minimize infected humans is a better counter-strategy.

The fifth chapter introduced a new mathematical model of dengue that accounts for the mosquitoes' life cycle. Following the dynamics of the metamorphosis of the mosquito population, the aquatic stage: egg E , larvae L , and pupae P , are added to the model. We show that our new model is well-posed and has positive solutions. The basic reproduction number is defined as

$$\begin{aligned}
\mathcal{R}_0 &:= \sqrt{\frac{a^2 b_h b_m S_m^* S_h^*}{\mu_A \sigma_h}} \\
&= \sqrt{\frac{a^2 b_h b_m H (\gamma_{E,L} + \mu_E) (\gamma_{L,P} + \mu_L) (\gamma_{P,S_m} + \mu_P) \ln \mathcal{N}_Y}{\mu_A \sigma_h \alpha_m \beta_m \gamma_{E,L} \gamma_{L,P}}},
\end{aligned}$$

with

$$\mathcal{N}_Y = \left(\frac{\alpha_m \gamma_{E,L} \gamma_{L,P} \gamma_{P,S_m}}{\mu_A (\gamma_{E,L} + \mu_E) (\gamma_{L,P} + \mu_L) (\gamma_{P,S_m} + \mu_P)} \right).$$

Copepod are natural enemies of the first and second instar of mosquito larvae. A

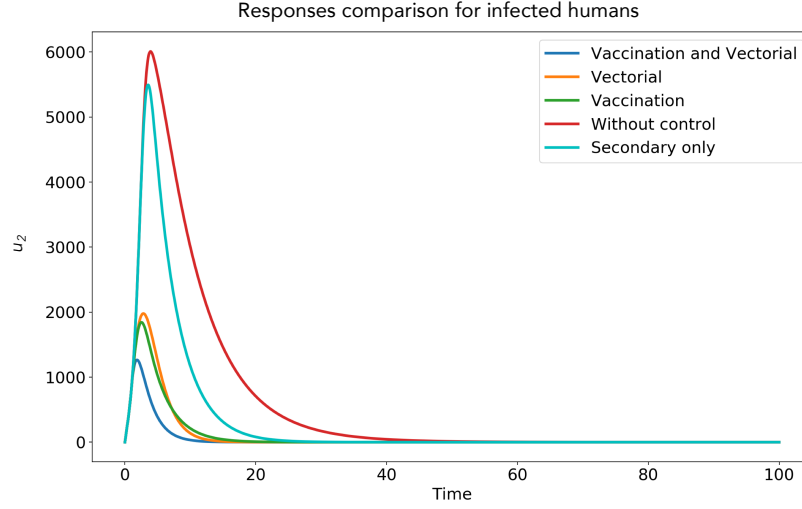


FIGURE 2.6: Behaviour of infected humans I_h with respect to time without control (red), for the optimal control related to the vaccination only (green), related to the vector only (orange), and with both control (blue). Cyan curve corresponds to optimal control of vaccination of secondary humans only.

large sized cyclopoid copepods, having body size greater than $1mm$, acts as predators of mosquito larvae which strongly influence the mosquito larval population. With this, copepod as a new control strategy is applied in Section 5.4. By applying vaccination and vector control to the model, we determine the optimal control strategy in minimizing infected humans. We attribute three control inputs, w_Y for the percentage of young mosquitoes exposed to copepods, w_A for the percentage of adult mosquitoes exposed to pesticides and w_H for the percentage of susceptible humans being vaccinated. Thus we consider the objective function

$$\mathcal{J}(w_Y, w_A, w_H) = \int_0^T \left(I_h(t) + \frac{1}{2} A_Y w_Y^2(t) + \frac{1}{2} A_A w_A^2(t) + \frac{1}{2} A_H w_H^2(t) \right) dt$$

subject to

$$\begin{aligned} E'(t) &= \alpha_m(S_m(t) + I_m(t)) - \gamma_{E,L}E(t) - \mu_E E(t) \\ L'(t) &= \gamma_{E,L}E(t) - \gamma_{L,P}L(t) - \mu_L L(t) - w_Y L(t) \\ P'(t) &= \gamma_{L,P}L(t) - \gamma_{P,S_m}P(t) - \mu_P P(t) \\ S'_m(t) &= \gamma_{P,S_m}P(t)e^{-\beta_m P(t)} - \mu_A S_m(t) - ab_m I_h(t)S_m(t) - w_A S_m(t) \\ I'_m(t) &= ab_m I_h(t)S_m(t) - \mu_A I_m(t) - w_A I_m(t) \\ S'_h(t) &= \gamma_h R_h(t) - ab_h I_m(t)S_h(t) - w_H S_h(t) \\ I'_h(t) &= ab_h I_m(t)S_h(t) - \sigma_h I_h(t) \\ R'_h(t) &= \sigma_h I_h(t) - \gamma_h R_h(t) \end{aligned} \tag{2.2}$$

in obtaining the best control strategy. The Pontryagin's maximum principle is applied in doing so.

Theorem 2.4.3. *There exists the adjoint variables $\lambda_i, i = 1, 2, \dots, 6$ of the system (5.37) that satisfy the following backward in time system of ordinary differential equation.*

$$\begin{aligned}
-\frac{\partial \lambda_1(t)}{\partial t} &= -\lambda_1 \mu_E + (\lambda_2 - \lambda_1) \gamma_{E,L} \\
-\frac{\partial \lambda_2(t)}{\partial t} &= -\lambda_2 (\mu_L + w_Y) + (\lambda_3 - \lambda_2) \gamma_{L,P} \\
-\frac{\partial \lambda_3(t)}{\partial t} &= -\lambda_3 \mu_P + (\lambda_4 (1 - \beta_m P(t)) e^{-\beta_m P(t)} - \lambda_3) \gamma_{P,S_m} \\
-\frac{\partial \lambda_4(t)}{\partial t} &= \lambda_1 \alpha_m - \lambda_4 (\mu_A + w_A) + (\lambda_5 - \lambda_4) a b_m I_h(t) \\
-\frac{\partial \lambda_5(t)}{\partial t} &= \lambda_1 \alpha_m - \lambda_5 (\mu_A + w_A) + (\lambda_7 - \lambda_6) a b_h S_h(t) \\
-\frac{\partial \lambda_6(t)}{\partial t} &= -\lambda_6 w_H + (\lambda_7 - \lambda_6) a b_h I_m(t) \\
-\frac{\partial \lambda_7(t)}{\partial t} &= 1 + (\lambda_5 - \lambda_4) a b_m S_m(t) - \lambda_7 \sigma_h \\
-\frac{\partial \lambda_8(t)}{\partial t} &= (\lambda_6 - \lambda_8) \gamma_h
\end{aligned}$$

with the transversality condition $\lambda(T) = 0$. Moreover, the optimal control variables, for $j = Y, A$, are given by

$$\begin{aligned}
w_Y^* &= \max \left(0, \min \left(\frac{\lambda_2 L}{A_Y}, w_M \right) \right) \\
w_A^* &= \max \left(0, \min \left(\frac{\lambda_4 S_m + \lambda_5 I_m}{A_A}, w_M \right) \right) \\
w_H^* &= \max \left(0, \min \left(\frac{\lambda_6 S_h}{A_H}, w_H \right) \right).
\end{aligned}$$

Our results show that the combination of copepods and pesticides is a good strategy for eliminating infected humans and the mosquito population. However, the elimination of infected humans is slow. The combination of pesticide and vaccination seems less efficient than the combination of copepods and pesticides. It takes a shorter time to reduce the number of mosquitoes with a reduced duration of the control application.

The last chapter of this study accounts for the spatial distribution of mosquitoes. In this study, we assume that only the adult mosquito is moving, and thus, only S_m and I_m have spatial dimension. The propensity of adult mosquitoes to leave the determined focal point (x, y) can be defined by the diffusion coefficient

$$D(x, y) = D_{min} + \alpha \mathcal{F}_l(x, y) + \beta \mathcal{F}_f(x, y) \quad (2.3)$$

where D_{min} is the minimal diffusion value in the absence of resources perception, $\mathcal{F}_l(x, y)$ and $\mathcal{F}_f(x, y)$ are the dispersion kernels that covered the entire landscape of the laying and food resources respectively. In this study, we consider that mosquitoes will always prefer the nearest laying sites to them. Thus, considering the population

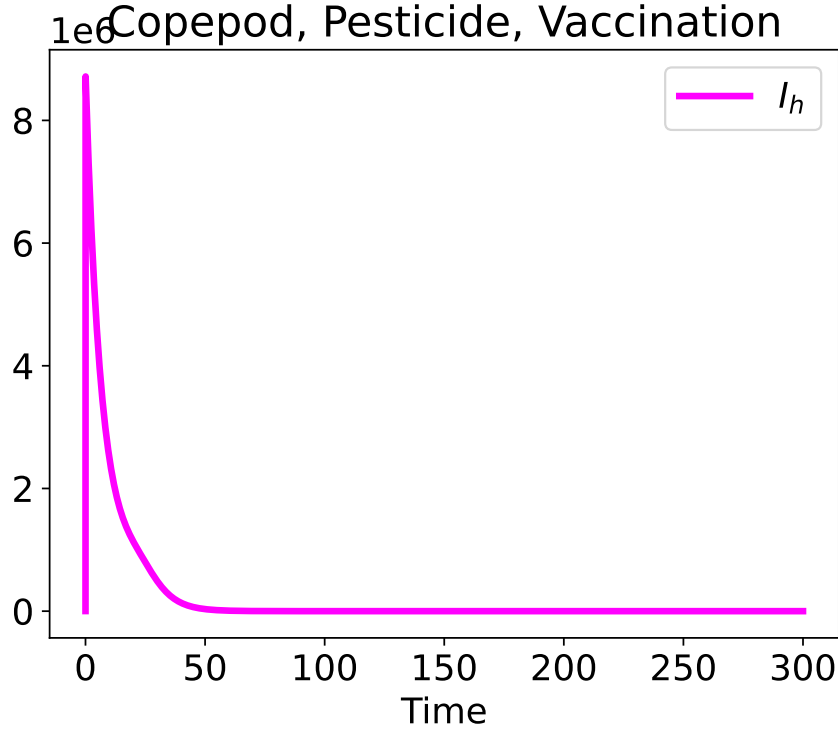


FIGURE 2.7: Optimal solutions of the infected human in the model.

density of adults mosquito for every $(x, y) \in \Omega$, we defined a new model that involved mosquitoes spatial distribution as follows

$$\begin{aligned} \frac{\partial S_m(t, x, y)}{\partial t} = & \gamma_{P, S_m} P(t, x, y) e^{-\beta_m P(t, x, y)} - \mu_A S_m(t, x, y) \\ & - ab_m I_h(t, x, y) S_m(t, x, y) + \frac{\partial}{\partial x} \left(D(x, y) \frac{\partial S_m}{\partial x} \right) \\ & + \frac{\partial}{\partial y} \left(D(x, y) \frac{\partial S_m}{\partial y} \right) \end{aligned} \quad (2.4)$$

$$\begin{aligned} \frac{\partial I_m(t, x, y)}{\partial t} = & ab_m I_h(t, x, y) S_m(t, x, y) - \mu_A I_m(t, x, y, U) \\ & + \frac{\partial}{\partial x} \left(D(x, y) \frac{\partial I_m}{\partial x} \right) + \frac{\partial}{\partial y} \left(D(x, y) \frac{\partial I_m}{\partial y} \right). \end{aligned} \quad (2.5)$$

Neumann boundary conditions are considered.

Theorem 2.4.4. *Let $0 \leq S_{h,0}, I_{h,0}, R_{h,0} \leq H_0$, $0 \leq E_0, L_0, P_0 \leq M_{Y,0}$, and $0 \leq S_{m,0}, I_{m,0} \leq M_{A,0}$ where $H_0, M_{Y,0}$ and $M_{A,0}$ are the initial population density for human, young mosquito and adult mosquito population, respectively. Then there exists a unique global in time weak solution $(E, L, P, S_m, I_m, S_h, I_h, R_h) \in L^\infty(\mathbb{R}_+, L^\infty(\Omega))^8$, of the initial boundary value problem. Moreover, the solution is nonnegative, $S_h + I_h \leq H_0$, $E + L + P \leq M_{Y,0}$ and $S_m + I_m \leq M_{A,0}$.*

This result is proved by applying Picard's fixed point theorem in the closed ball

$$B_T = \left\{ Y \in L^\infty(\mathbb{R}_+, L^\infty(\Omega))^8 : \sup_{t \in [0, T]} \|Y(t, \cdot) - Y_0\|_{L^\infty(\Omega)} \leq r \right\}, \quad (2.6)$$

of the integral formulation

$$\begin{aligned} E &= e^{-(\gamma_{E,L} + \mu_E)t} E_0 + \alpha_m \int_0^t e^{-(\gamma_{E,L} + \mu_E)(t-s)} (S_m + I_m) \\ L &= e^{-(\gamma_{L,P} + \mu_L)t} L_0 + \gamma_{E,L} \int_0^t e^{-(\gamma_{L,P} + \mu_L)(t-s)} E ds \\ P &= e^{-(\gamma_{P,S_m} + \mu_P)t} P_0 + \gamma_{L,P} \int_0^t e^{-(\gamma_{P,S_m} + \mu_P)(t-s)} L ds \\ S_m &= K \star S_{m,0} + \int_0^t K \star (\gamma_{P,S_m} P e^{-\beta_m P} - ab_m I_h S_m) ds \\ I_m &= K \star I_{m,0} + ab_m \int_0^t K \star I_h S_m ds \\ S_h &= S_{h,0} + \int_0^t (\gamma_h R_h - ab_h I_m S_h) ds \\ I_h &= e^{-\sigma_h t} I_{h,0} + ab_h \int_0^t e^{-\sigma_h(t-s)} I_m S_h ds \\ R_h &= e^{-\gamma_h t} R_{h,0} + \sigma_h \int_0^t e^{-\gamma_h(t-s)} I_h ds \end{aligned} \quad (2.7)$$

where K is the heat kernel.

In the last section of chapter four, we determine the optimal control strategy by applying three controls: exposure to copepodes w_Y for the young mosquitoes in the laying areas, pesticide w_A for the adult mosquitoes, and application of vaccination w_H for the humans. Here controls are time and space dependent. We consider the problem

$$\mathcal{J}(w) = \int_{\Omega} \int_0^T (I_h(x, t) + \frac{1}{2} A_Y w_Y^2(x, t) + \frac{1}{2} A_A w_A^2(x, t) + \frac{1}{2} A_H w_H^2(x, t)) dt dX.$$

We use the adjoint state method to determine the optimal control variables.

Theorem 2.4.5. *There exists the adjoint variables $\lambda_i, i = 1, 2, \dots, 6$ that satisfy the following backward in time system of partial differential equations*

$$\begin{aligned}
-\frac{\partial \lambda_1(x, t)}{\partial t} &= \lambda_1(x, t)\mu_E + (\lambda_1(x, t) - \lambda_2(x, t))\gamma_{E,L} \\
-\frac{\partial \lambda_2(x, t)}{\partial t} &= \lambda_2(x, t)(\mu_L + w_Y) + (\lambda_2(x, t) - \lambda_3(x, t))\gamma_{L,P} \\
-\frac{\partial \lambda_3(x, t)}{\partial t} &= \lambda_3(x, t)\mu_P + (\lambda_3(x, t) - \lambda_4(x, t)(1 - \beta_m P(x, t))e^{-\beta_m P(x, t)})\gamma_{P,S_m} \\
-\frac{\partial \lambda_4(x, t)}{\partial t} - D\Delta \lambda_4 &= -\lambda_1(x, t)\alpha_m + \lambda_4(x, t)(\mu_A + w_A) + (\lambda_4(x, t) - \lambda_5(x, t))ab_m I_h(x, t) \\
-\frac{\partial \lambda_5(x, t)}{\partial t} - D\Delta \lambda_5 &= -\lambda_1(x, t)\alpha_m + \lambda_5(x, t)(\mu_A + w_A) + (\lambda_6(x, t) - \lambda_7(x, t))ab_h S_h(x, t) \\
-\frac{\partial \lambda_6(x, t)}{\partial t} &= \lambda_6(x, t)w_H + (\lambda_6(x, t) - \lambda_7(x, t))ab_h I_m(x, t) \\
-\frac{\partial \lambda_7(x, t)}{\partial t} &= 1 + (\lambda_7(x, t) - \lambda_8(x, t))\sigma_h + (\lambda_4(x, t) - \lambda_5(x, t))ab_m S_m(x, t) \\
-\frac{\partial \lambda_8(x, t)}{\partial t} &= (\lambda_8(x, t) - \lambda_6(x, t))\gamma_h
\end{aligned} \tag{2.8}$$

with the transversality condition $\lambda^T(x, T) = 0$ and boundary conditions $\mu^T = \frac{\lambda^T(x, 0)h(U(x, 0))}{g(U(x, 0), w)}$

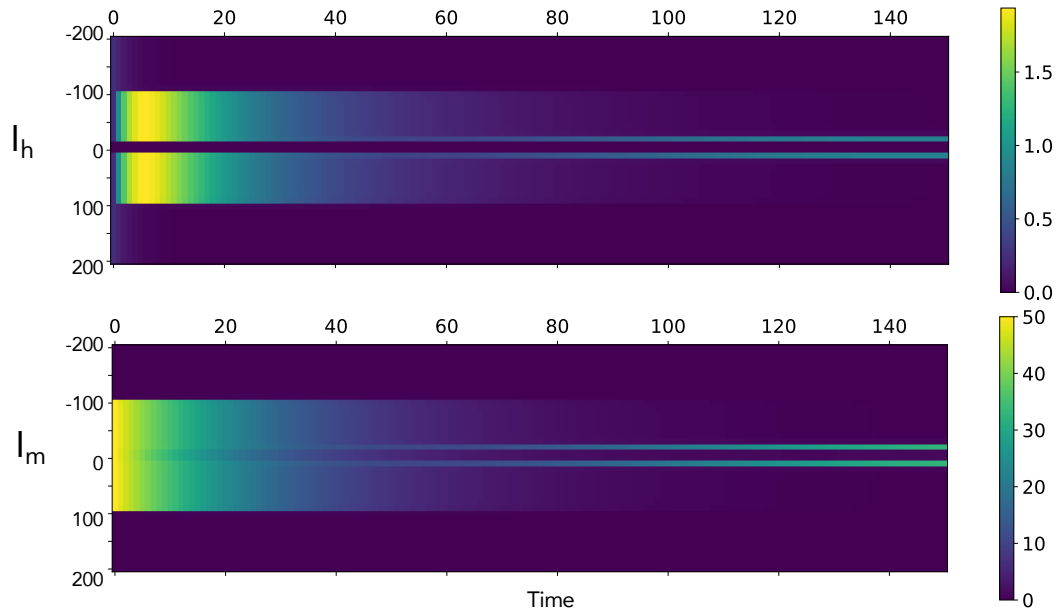
and $\left. \frac{\partial \lambda(x, t)}{\partial x} \right|_{\partial \Omega} = \left. \frac{\partial U(x, t)}{\partial x} \right|_{\partial \Omega} = 0$.

Furthermore, the optimal control variable w^* is defined as

$$\begin{aligned}
w_Y^*(t) &= \max \left(0, \min \left(\frac{\lambda_2 L}{-A_Y}, w_M \right) \right) \\
w_A^*(t) &= \max \left(0, \min \left(\frac{(\lambda_4 I_h + \lambda_5 S_h)}{-A_A}, w_M \right) \right) \\
w_H^*(t) &= \max \left(0, \min \left(\frac{\lambda_6 S_h}{-A_H}, w_H \right) \right).
\end{aligned}$$

Using the gradient method written in Python, we numerically solved the optimality of the model and obtained the following figures.

without control



with optimal control

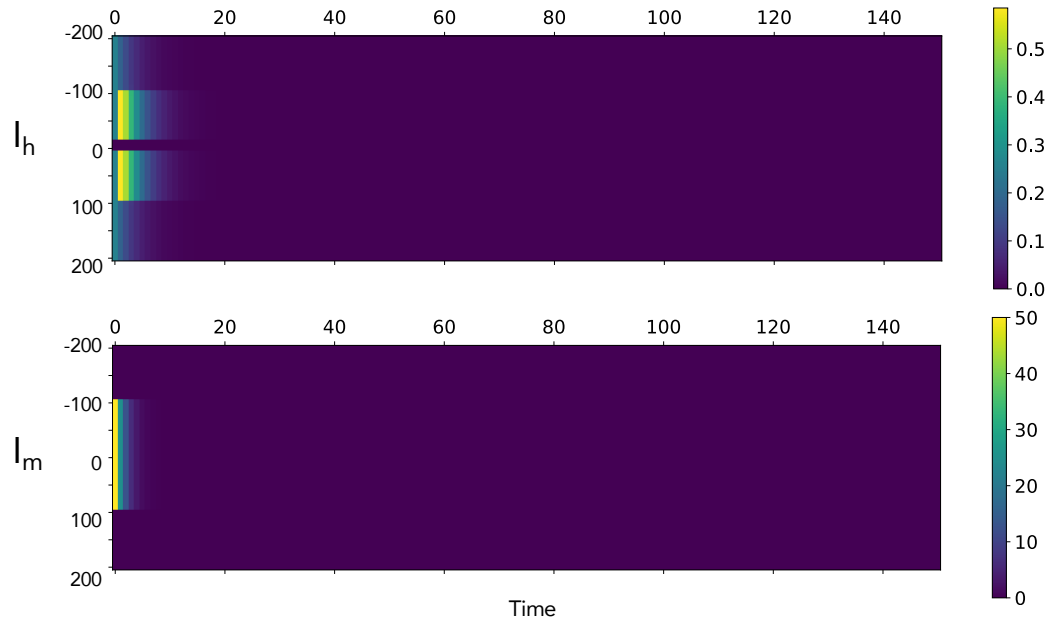


FIGURE 2.8: Comparison between the number of infected humans I_h , number of infectious mosquitoes I_m , and number of larvae L , with three control inputs (blue) and without control (orange).

Figure shows the spatiotemporal evolution of infectious humans and mosquitoes with and without control. The figure shows that without control inputs, we need to apply the control strategy for a long time and then decrease it. However, decreasing the control strategy's efforts does not mean stopping its application. The figure shows that we must continuously apply the control strategy near the laying sites.

Consequently, with the three control inputs, we only need to apply the control strategy for a short period and eventually stop it in more or less 20 days.

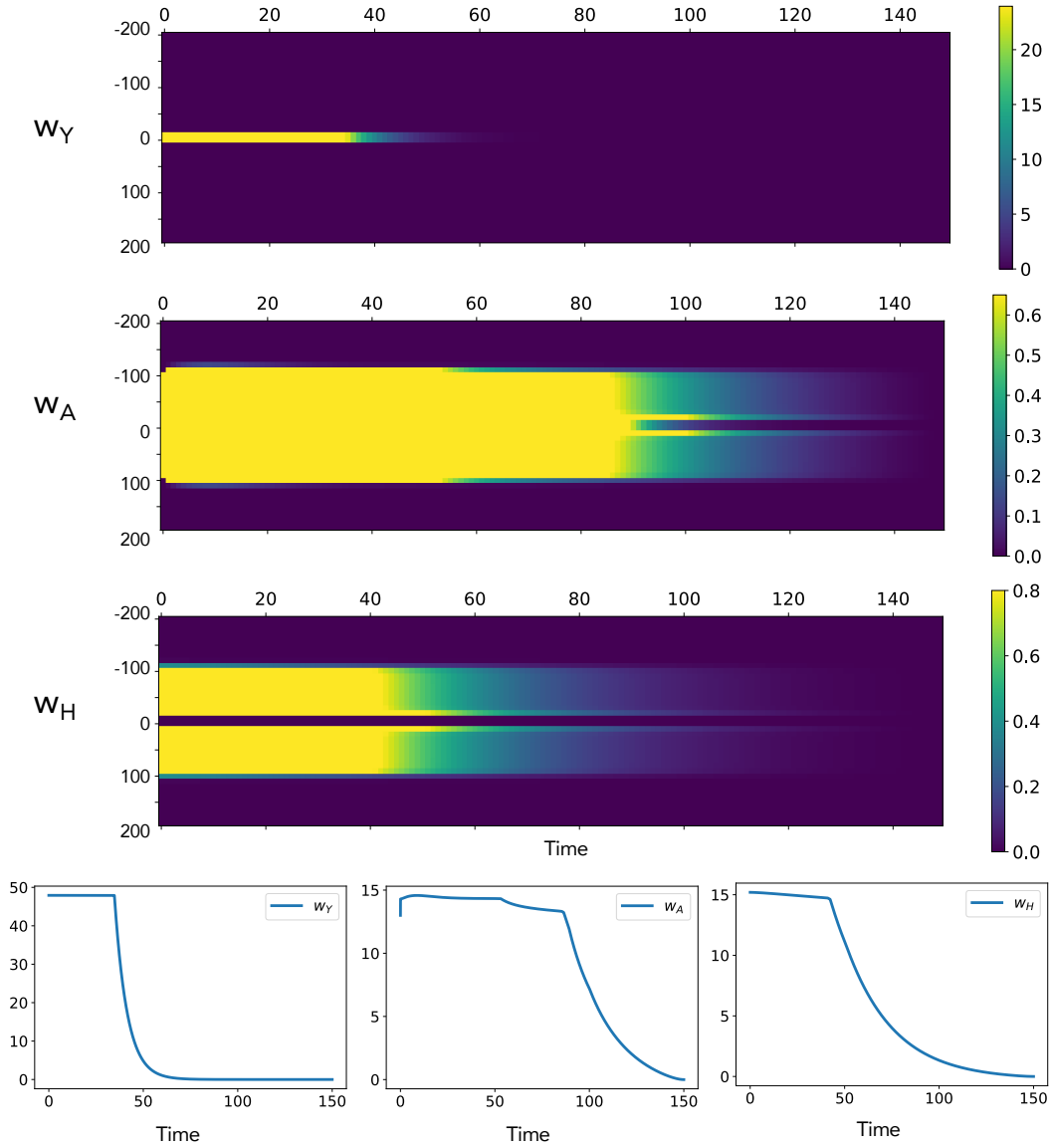


FIGURE 2.9: Spatiotemporal evolution of the optimal control variable w_Y related to the copepods use (top) and its sum in space (down).

Figure shows the spatiotemporal evolution of each optimal control variable of the model with three control inputs. It shows that we need to administer copepod continuously for 100 days while lowering pesticide application and vaccination over time. However, the figure shows that we need to continuously apply the pesticide and vaccination near the laying sites unfadingly.

The appendix section contains the published article about covid entitled "Accounting for Symptomatic and Asymptomatic in a SEIR-type model of COVID-19".

Perspectives of the Study

Mathematical modelling of dengue fever is a wide topic that deals with various unknowns. Covering a good deal of scope for three years is somehow impossible. Thus, here are the list of possible research perspectives we plan to study in the future.

One perspective of the study is to consider the age structure of the human population. Considering the recommendation of Sanofi Pasteur on the application of Dengvaxia, it is interesting to create a model with age structure in the human population to describe dengue transmission with different infection rates among different age groups.

Another is to develop a complete dengue-dengvaxia model incorporating the mosquitoes' life cycle, the human population's four dengue strain viruses, and the efficacy of Dengvaxia in different virus strains. Adding the age structure and climate effect on dengue in this model would make this a robust dengue model.

An additional perspective of the study is to consider the mosquitoes' reproduction and feeding habits. One can incorporate the mosquitoes' gender in the model and apply a control strategy to minimize infected mosquitoes. Since male mosquitoes feed on plant nectar and some plants eat mosquitoes, by devising a strategic position of plants in the environment, one can determine the optimal control strategy for minimizing infected mosquitoes in the population.

In connection, one can also consider the energy mosquito needs. Feeding and laying sites directly affect the energy supply of mosquitoes. Mosquito energy increases when they are feeding and decreases during the laying period. With this in mind, we define the fourth dimension U which account the energy supply of mosquito, called the energetic dimension. We can assume that only the adult mosquito are moving and thus only S_m and I_m have energetic dimension. This energetic dimension uses a simplified dynamic energy budget through advection terms in the additional energy dimension U . This relies on an energetic landscape after space discretisation. Land-covers were grouped depending on their presumed effects on energy supply. New emerging adult mosquitoes have energy level U wherein $U = 1$ is the upper energetic boundary and $U = 0$ is the lower energetic boundary, that is, $S_m, I_m(t, x, y, U = 0) = 0$ simulates the death by starvation of adult susceptible and infected mosquitoes. Thus one can define the dynamics of adult mosquito as follows:

$$\begin{aligned} \frac{\partial S_m(t, x, y)}{\partial t} = & \gamma_{P, S_m} P(t, x, y) e^{-\beta_m P(t, x, y)} - \mu_A S_m(t, x, y) \\ & - ab_m I_h(t, x, y) S_m(t, x, y) + \frac{\partial}{\partial x} \left(D(x, y) \frac{\partial S_m}{\partial x} \right) \\ & + \frac{\partial}{\partial y} \left(D(x, y) \frac{\partial S_m}{\partial y} \right) - C(x, y) \frac{\partial S_m}{\partial U} \end{aligned} \quad (2.9)$$

$$\begin{aligned}
\frac{\partial I_m(t, x, y)}{\partial t} = & ab_m I_h(t, x, y) S_m(t, x, y) - \mu_A I_m(t, x, y) \\
& + \frac{\partial}{\partial x} \left(D(x, y) \frac{\partial I_m}{\partial x} \right) + \frac{\partial}{\partial y} \left(D(x, y) \frac{\partial I_m}{\partial y} \right) - C(x, y) \frac{\partial I_m}{\partial U}.
\end{aligned} \tag{2.10}$$

Another interesting perspective of the study is to consider the co-infection of dengue and Covid-19. Because of the overlapping clinical and laboratory features of these diseases, Covid-19 pandemic in a dengue-endemic areas causes a major challenge. Thus one can design a good mathematical model showing the co-infection of these disease and apply optimal control strategy to minimize infected humans.

Chapter 3

A preliminary study of Dengue models accounting for the Vaccination

In this chapter, we introduce some mathematical models of dengue that consider a vaccine that should be given to people who have previous dengue infections. We compare various growth functions.

3.1 Description of the Model with Vaccination

Based on the Ross-type model, we assumed that dengue viruses are virulent with no other microorganism attacking the human body.

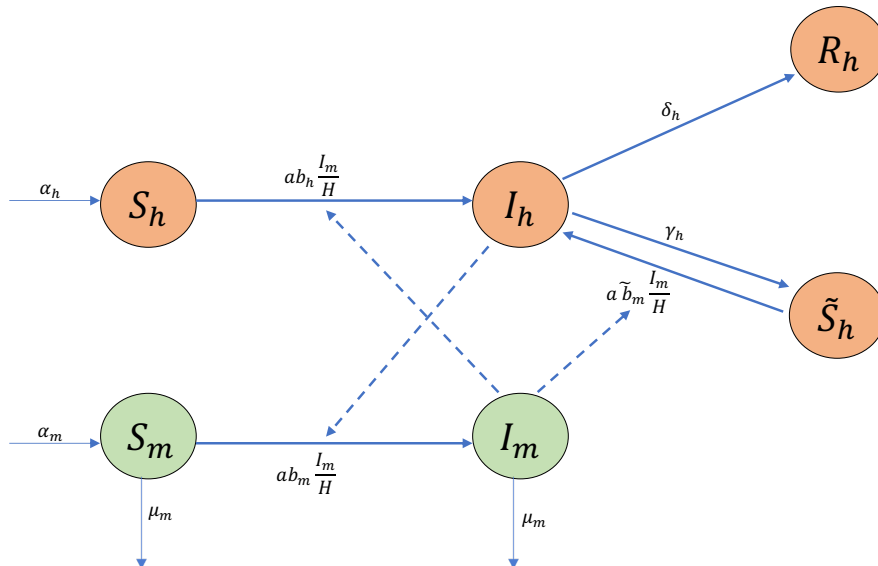


FIGURE 3.1: Compartmental representation of the model with vaccination considering individuals who have previous dengue infections.

Let H be the human population subdivided into primary susceptible S_h , secondary susceptible \tilde{S}_h , infected I_h and removed R_h . Primary susceptible humans are

individuals who have not yet been infected by dengue, while secondary susceptibles humans are individuals who previously had dengue infection.

Let M be the population of female mosquitoes split into two groups of susceptible S_m and infectious I_m mosquitoes. Figure 3.1 describes the flow of dengue disease. In this chapter, we introduce a mathematical model of dengue that considers the vaccine that should be given to people who are already infected by one type of virus.

Since humans have a meager mortality rate compared to mosquitoes, we neglect the natural death of humans but still consider their growth. The following system of ordinary equations governed the dynamics of humans.

$$S'_h(t) = -\frac{ab_h I_m(t)}{H(t)} S_h(t) + f(H(t)) \quad (3.1)$$

$$I'_h(t) = \frac{a I_m(t)}{H(t)} (b_h S_h(t) + \tilde{b}_h \tilde{S}_h(t)) - \gamma_h I_h(t) - \delta_h I_h(t) \quad (3.2)$$

$$\tilde{S}'_h(t) = \gamma_h I_h(t) - \frac{a \tilde{b}_h I_m(t)}{H(t)} \tilde{S}_h(t) \quad (3.3)$$

$$R'_h(t) = \delta_h I_h(t). \quad (3.4)$$

While the dynamics of mosquitoes are as follows

$$S'_m(t) = -\frac{ab_m I_h(t)}{H(t)} S_m(t) - \mu_m S_m(t) + g(M(t)) \quad (3.5)$$

$$I'_m(t) = \frac{ab_m I_h(t)}{H(t)} S_m(t) - \mu_m I_m(t). \quad (3.6)$$

Note that the total human population is given by $H = S_h + I_h + \tilde{S}_h + R_h$ and the total mosquito population is given by $M = S_m + I_m$. The function $f(H(t))$ is the change in the total human population, while $g(M(t))$ is the change in the total mosquito population. In this study, we will consider different growth model for human and mosquito population. Since human have a meager mortality rate compared to mosquitoes, we neglect the natural death of the humans.

The parameters $\frac{ab_h I_m(t)}{H(t)}$ is the probability of a primary susceptible individual to be infected with dengue virus, where b_h is the probability of transmission of the virus from an infected mosquito to primary susceptible human, and a represents a mosquito's average bites. Whereas, $\frac{a \tilde{b}_h I_m(t)}{H(t)}$ is the probability of susceptible individuals who had been previously infected with dengue to become infectious again with different serotypes. That is, \tilde{b}_h is the probability of transmission of the virus from an infected mosquito to a secondary susceptible human. Furthermore, the rate of secondary susceptible people who recovered from infection from one, two, or three serotypes is represented by $\gamma_h I_h(t)$ and δ_h denotes the recovery rate from the four serotypes.

For the mosquito compartment, $\frac{ab_m I_h(t)}{H(t)}$ is the probability of susceptible mosquito to be infectious once it bites a ratio of the infected human population. The parameter

b_m is the transmission probability from an infected human to a susceptible mosquito and μ_m is the mosquitoes' death rate.

The parameters are summed up in the table below.

Symbol	Description
a	number of human beaten per mosquito
b_h	probability of becoming infected
\tilde{b}_h	probability of becoming infected again
γ_h	recovery rate of human from one, two or three serotypes
δ_h	recovery rate of human from four serotypes
b_m	probability of becoming infectious
μ_m	death rate of mosquito

TABLE 3.1: Description of the parameters used in the model.

3.2 Study of the Model with Logistic Growth

In this section, let us consider the logistic growth functions for human population, which is $H'(t) = f(H(t)) = \alpha_h \left(1 - \frac{H(t)}{K}\right) H(t)$, where K is the carrying capacity of human population. And an exponential growth function for mosquito population, which is $M'(t) = g(M(t)) - \mu_m M(t) = \alpha_m M(t) - \mu_m M(t)$, where α_m and μ_m are the mosquitoes growth and death rate, respectively. In this study, we assume that $\alpha_m \leq \mu_m$.

3.2.1 Well-posedness and Positivity of the Solution

To simplify the reading, the system of ordinary differential equation above is rewritten as

$$U'(t) = F(t, u(t)) \quad (3.7)$$

with

$$U(t) = \left(u_1 = S_h, u_2 = I_h, u_3 = \tilde{S}_h, u_4 = R_h, u_5 = S_m, u_6 = I_m \right)^t$$

and

$$F(U(t), t) = \left(-\frac{ab_h u_6 u_1}{H} + f(H), \frac{au_6 (b_h u_1 + \tilde{b}_h u_3)}{H} - \gamma_h u_2 - \delta_h u_2, \right. \\ \left. \gamma_h u_2 - \frac{\tilde{a}\tilde{b}_h u_6 u_3}{H}, \delta_h u_2, -\frac{ab_m u_2 u_5}{H} - \mu_m u_5 + g(M), \frac{ab_m u_2 u_5}{H} - \mu_m u_6 \right)^t.$$

Lemma 3.2.1. *Let $(S_h(0), I_h(0), \tilde{S}_h(0), R_h(0), S_m(0), I_m(0))$ be a nonnegative initial datum with $H(0) = S_h(0) + I_h(0) + \tilde{S}_h(0) + R_h(0) > 0$ and $M(0) = S_m(0) + I_m(0) > 0$. Then there exist a time $T > 0$ and a unique solution $(S_h, I_h, \tilde{S}_h, R_h, S_m, I_m)$ in $\mathcal{C}([0, T], \mathbb{R})^6$.*

Proof. Consider the initial value problem

$$U'(t) = F(t, U(t)) \quad \text{where} \quad U(0) = U_0.$$

Note that F is continuous and has continuous derivative on $I \times U$. Thus, F satisfies the local Lipschitz condition. Therefore, by Cauchy-Lipschitz theorem, there exist $T > 0$ and a unique solution to equation (3.7) in $\mathcal{C}([0, T], \mathbb{R})^6$. \square

Lemma 3.2.2. *The region Ω defined by*

$$\Omega_{log} = \{(u_1, u_2, u_3, u_4, u_5, u_6) \in \mathbb{R}_+^6 : u_1 + u_2 + u_3 + u_4 \leq K, u_5 + u_6 \leq M_0\}$$

is invariant for the flow given by (3.7).

Proof. Let $(u_1, u_2, u_3, u_4, u_5, u_6) \in \Omega_{log}$ be the solution of the system of equation (3.7). Since the total human population is given by the logistic growth model

$$H'(t) = f(H(t)) = \alpha_h \left(1 - \frac{H}{K}\right) H$$

we have,

$$\frac{\frac{1}{K}dH}{\alpha_h - \frac{\alpha_h H}{K}} + \frac{\frac{1}{\alpha_h}dH}{H} = dt.$$

And, integrating both sides of the equation gives us

$$-\frac{1}{\alpha_h} \ln \left| \alpha_h - \frac{\alpha_h H}{K} \right| + \frac{1}{\alpha_h} \ln |H| = t + c.$$

Combining the logarithmic function, we get

$$\ln \left| \frac{H}{\alpha_h - \frac{\alpha_h H}{K}} \right| = \alpha_h t + c_1 \quad \text{where} \quad c_1 = c\alpha_h.$$

Thus, exponentiating both sides, we have

$$\frac{H}{\alpha_h - \frac{\alpha_h H}{K}} = e^{\alpha_h t + c_1} = Ce^{\alpha_h t} \quad \text{where} \quad C = e^{c_1} = e^{c\alpha_h}$$

$$H = \left(\alpha_h - \frac{\alpha_h H}{K} \right) Ce^{\alpha_h t}.$$

Solving for H , we get

$$H = \frac{\alpha_h K C e^{\alpha_h t}}{K + \alpha_h C e^{\alpha_h t}}.$$

Taking the initial condition, when $t = 0$, $H(0) = H_0$

$$H_0 = \frac{\alpha_h K C}{K + \alpha_h C}.$$

Thus, $C = \frac{H_0 K}{H_0 \alpha_h - K \alpha_h}$. Therefore, the solution of the differential equation becomes

$$H(t) = \frac{KH_0}{Ke^{-\alpha_h t} - H_0(e^{-\alpha_h t} - 1)}.$$

Since $\alpha_h \geq 0$, $H(t) \leq K$ for all time $t \geq 0$.

For the total mosquito population, we consider an exponential growth model $M'(t) = \alpha_m M - \mu_m M = (\alpha_m - \mu_m)M$. Let $\sigma_m = \alpha_m - \mu_m \leq 0$. Then

$$M = Ce^{\sigma_m t}.$$

Now, taking the initial condition, i.e. when $t = 0$, $M(0) = M_0$, we get $M_0 = C$. Hence, the solution to our differential equation becomes

$$M(t) = M_0 e^{\sigma_m t}.$$

Consequently, since $\sigma_m \leq 0$,

$$M(t) \leq M_0 \quad \forall t \geq 0.$$

Therefore, all feasible solution of the population of the system (3.7) satisfies

$$u_1 + u_2 + u_3 + u_4 \leq K, u_5 + u_6 \leq M_0.$$

In proving the positivity, we assume that the parameters are positive.

- For u_1 in equation (3.1), we have for all $u_2, u_3, u_4, u_5, u_6 \geq 0$,

$$\begin{aligned} f_1(u_1 = 0, u_2, u_3, u_4, u_5, u_6) &= -\frac{ab_h u_6(0)}{H} + f(H) \\ &= f(H) \end{aligned}$$

Since we take a logistic growth function for human population, we have $f(H) > 0$. Therefore, $f_1 \geq 0$.

- For u_2 in equation (4.2), we have for all $u_1, u_3, u_4, u_5, u_6 \geq 0$,

$$\begin{aligned} f_2(u_1, u_2 = 0, u_3, u_4, u_5, u_6) &= \frac{au_6}{H}(b_h u_1 + \tilde{b}_h u_3) - \gamma_h(0) - \delta_h(0) \\ &= \frac{au_6}{H}(b_h u_1 + \tilde{b}_h u_3) \end{aligned}$$

Thus $f_2 \geq 0$, since the parameters a, b_h and \tilde{b}_h are positive, and $u_1, u_3, u_4, u_5, u_6 \geq 0$. Therefore, $f_2 \geq 0$.

- For u_3 in equation (4.3), we have for all $u_1, u_2, u_4, u_5, u_6 \geq 0$,

$$\begin{aligned} f_3(u_1, u_2, u_3 = 0, u_4, u_5, u_6) &= \gamma_h u_2 - \frac{a\tilde{b}_h u_6(t)(0)}{H(t)} \\ &= \gamma_h u_2 \end{aligned}$$

Since $u_2 \geq 0$, then $f_3 \geq 0$.

- For u_4 in equation (4.4), we have for all $u_1, u_2, u_3, u_5, u_6 \geq 0$,

$$f_4(u_1, u_2, u_3, u_4 = 0, u_5, u_6) = \delta_h u_3$$

Since $u_3 \geq 0$ and $\delta > 0$, therefore, $f_4 \geq 0$.

- For u_5 in equation (4.5), we have for all $u_1, u_2, u_3, u_4, u_6 \geq 0$,

$$\begin{aligned} f_5(u_1, u_2, u_3, u_4, u_5 = 0, u_6) &= -\frac{ab_m u_2(0)}{H} - \mu_m(0) + g(M) \\ &= g(M) \end{aligned}$$

Since we consider an exponential growth function for the mosquito population, $g(M) \geq 0$. Therefore, $f_5 \geq 0$.

- For u_6 in equation (4.6), we have for all $u_1, u_2, u_3, u_4, u_5 \geq 0$,

$$\begin{aligned} f_6(u_1, u_2, u_3, u_4, u_5, u_6 = 0) &= \frac{ab_m u_2 u_5}{u_1 + u_2 + u_3 + u_4 + u_5 + 0} - \mu_m(0) \\ &= \frac{ab_m u_2 u_5}{u_1 + u_2 + u_3 + u_4 + u_5} \end{aligned}$$

Since $u_1, u_2, u_3, u_4, u_5 \geq 0$ and $a, b_m > 0$,

$$\frac{ab_m u_2(t) u_5(t)}{u_1 + u_2 + u_3 + u_4 + u_5} \geq 0.$$

Therefore, $f_6 \geq 0$.

□

From the two lemmas above, we can deduce the following global well-posedness theorem.

Theorem 3.2.3. *Let $(u_1(0), u_2(0), u_3(0), u_4(0), u_5(0), u_6(0))$ be in Ω_{log} . Then there exists a unique global in time solution $(u_1, u_2, u_3, u_4, u_5, u_6)$ in $\mathcal{C}(\mathbb{R}_+, \Omega_{log})$.*

3.2.2 Stability of the Equilibrium

In this section, we will try to determine the possible equilibrium point of the system of an ordinary differential equation (3.7) and assess their stability.

Equilibrium

Let $(u_1^*, u_2^*, u_3^*, u_4^*, u_5^*, u_6^*)$ be an equilibrium point of the system of equation (3.7). Then we have

$$-\frac{ab_h u_6 u_1}{u_1 + u_2 + u_3 + u_4} + \alpha_h(u_1 + u_2 + u_3 + u_4) - \frac{\alpha_h(u_1 + u_2 + u_3 + u_4)^2}{K} = 0 \quad (3.8)$$

$$\frac{au_6(b_h u_1 + \tilde{b}_h u_3)}{u_1 + u_2 + u_3 + u_4} - \gamma_h u_2 - \delta_h u_2 = 0 \quad (3.9)$$

$$\gamma_h u_2 - \frac{a\tilde{b}_h u_3 u_6}{u_1 + u_2 + u_3 + u_4} = 0 \quad (3.10)$$

$$\delta_h u_2 = 0 \quad (3.11)$$

$$-\frac{ab_m u_2 u_5}{u_1 + u_2 + u_3 + u_4} - \mu_m u_5 + \alpha_m u_5 + \alpha_m u_6 = 0 \quad (3.12)$$

$$\frac{ab_m u_2 u_5}{u_1 + u_2 + u_3 + u_4} - \mu_m u_6 = 0 \quad (3.13)$$

Solving the system of equation above, we get $(u_1^*, 0, u_3^*, -u_1^* - u_3^*, u_5^*, 0)$, $(u_1^*, 0, u_3^*, K - u_1^* - u_3^*, 0, 0)$, $(u_1^*, 0, \frac{-u_1^* b_h}{\tilde{b}_h}, \frac{-u_1^* (\tilde{b}_h - b_h)}{\tilde{b}_h}, u_5^*, 0)$, $(u_1^*, 0, 0, -u_1^*, u_5^*, 0)$, $(0, 0, 0, 0, u_5^*, u_6^*)$, and $(u_1^*, 0, \frac{-u_1^* b_h}{\tilde{b}_h}, \frac{-u_1^* (\tilde{b}_h - b_h) + K\tilde{b}_h}{\tilde{b}_h}, 0, 0)$.

From Lemma 5.3.2, the solution of the system is positively invariant; thus, we disregard the solutions $(u_1^*, 0, u_3^*, -u_1^* - u_3^*, u_5^*, 0)$, $(u_1^*, 0, \frac{-u_1^* b_h}{\tilde{b}_h}, \frac{-u_1^* (\tilde{b}_h - b_h)}{\tilde{b}_h}, u_5^*, 0)$, $(u_1^*, 0, 0, -u_1^*, u_5^*, 0)$, $(u_1^*, 0, \frac{-u_1^* b_h}{\tilde{b}_h}, \frac{-u_1^* (\tilde{b}_h - b_h) + K\tilde{b}_h}{\tilde{b}_h}, 0, 0)$ and consider only $(0, 0, 0, 0, u_5^*, u_6^*)$ and $(u_1^*, 0, u_3^*, K - u_1^* - u_3^*, 0, 0)$. The lemma below shows that they are an equilibrium point of the system (3.7).

Lemma 3.2.4. *The system of equation (3.7) admits the equilibrium $(0, 0, 0, 0, 0, 0)$ and $(u_1^*, 0, u_3^*, K - u_1^* - u_3^*, 0, 0)$.*

Proof. Consider the system of equation above. From equation (3.11), since the parameters are all positive, we can conclude that $u_2 = 0$.

Now, substituting u_2 by 0 and multiplying each equation of the system by $u_1 + u_3 + u_4$, the system of equation (3.8)-(3.13) above would become

$$-ab_h u_6 u_1 + \alpha_h(u_1 + u_3 + u_4)^2 - \frac{\alpha_h(u_1 + u_3 + u_4)^3}{K} = 0 \quad (3.14)$$

$$au_6(b_h u_1 + \tilde{b}_h u_3) = 0 \quad (3.15)$$

$$-a\tilde{b}_h u_3 u_6 = 0 \quad (3.16)$$

$$-(\mu_m u_5 - \alpha_m u_5 - \alpha_m u_6)(u_1 + u_3 + u_4) = 0 \quad (3.17)$$

$$-\mu_m u_6(u_1 + u_3 + u_4) = 0 \quad (3.18)$$

From equation (3.16), we get $u_3 = 0$ or $u_6 = 0$. Thus, we consider the following cases.

- Case 1. If $u_3 \neq 0$ and $u_6 = 0$

Then equation (3.14) would become

$$\alpha_h(u_1 + u_3 + u_4)^2 - \frac{\alpha_h(u_1 + u_3 + u_4)^3}{K} = 0$$

Implying that $u_1 + u_3 + u_4 = K$ or $u_4 = K - u_1 - u_3$. Now from equation (3.17), substituting u_6 by 0 and $u_1 + u_3 + u_4$ by K , we get

$$-(\mu_m u_5 - \alpha_m u_5)K = 0.$$

Concluding that $u_5 = 0$, since $K \neq 0$ and $\mu_m \neq \alpha_m$. Thus, for any nonnegative u_1^*, u_3^* and u_4^* we get an equilibrium point $(u_1^*, 0, u_3^*, K - u_1^* - u_3^*, 0, 0)$.

- Case 2. If $u_3 = 0$ and $u_6 \neq 0$

Then equation (3.15) would become $au_6 b_h u_1 = 0$. Consequently, $u_1 = 0$ since $u_6 \neq 0$. Now, substituting u_1, u_3 by 0 to equation (3.18), we get $-\mu_m u_6 u_4 = 0$. Hence, $u_4 = 0$ since $u_6 \neq 0$. Therefore, for any nonnegative u_5^*, u_6^* , we get an equilibrium point $(0, 0, 0, 0, u_5^*, u_6^*)$. Moreover $M^* = u_5^*, u_6^* = 0$ and $u_5^* = u_6^* = 0$.

- Case 3. If $u_3 = 0$ and $u_6 = 0$

Then equation (3.14) would become

$$\alpha_h (u_1 + u_4)^2 - \frac{\alpha_h (u_1 + u_4)^3}{K} = 0.$$

Simplifying the equation we get $u_1 + u_4 = K$. Thus, substituting this to equation (3.17) and u_6, u_3 by 0, we get $-(\mu_m u_5 - \alpha_m u_5)K = 0$. Since $\mu_m \neq \alpha_m$, $u_5 = 0$. Therefore, for any nonnegative u_1^*, u_3^* and u_4^* we get an equilibrium point $(u_1^*, 0, u_3^*, K - u_1^* - u_3^*, 0, 0)$.

□

Next Generation Matrix and Basic Reproduction Number

In this section, we will show the stability of the equilibrium using the next-generation matrix. Since the infected individuals are in u_2 and u_6 , then we can rewrite the system of the equation (3.7) as

$$\mathcal{F} = \begin{pmatrix} \frac{au_6(b_h u_1 + \tilde{b}_h u_3)}{u_1 + u_2 + u_3 + u_4} \\ \frac{ab_m u_2 u_5}{u_1 + u_2 + u_3 + u_4} \end{pmatrix} \quad \mathcal{V} = \begin{pmatrix} (\gamma_h + \delta_h)u_2 \\ \mu_m u_6 \end{pmatrix}$$

where \mathcal{F} is the rate of appearance of new infections in each compartment, and \mathcal{V} is the rate of other transitions between all compartments.

If F is an entry wise nonnegative matrix and V is a non-singular M -matrix, then we have

$$F = \begin{pmatrix} \frac{\partial \mathcal{F}_1}{\partial u_2} & \frac{\partial \mathcal{F}_1}{\partial u_6} \\ \frac{\partial \mathcal{F}_2}{\partial u_2} & \frac{\partial \mathcal{F}_2}{\partial u_6} \end{pmatrix} \quad \text{and} \quad V = \begin{pmatrix} \frac{\partial \mathcal{V}_1}{\partial u_2} & \frac{\partial \mathcal{V}_1}{\partial u_6} \\ \frac{\partial \mathcal{V}_2}{\partial u_2} & \frac{\partial \mathcal{V}_2}{\partial u_6} \end{pmatrix}$$

Thus,

$$F = \begin{pmatrix} \frac{-au_6(b_h u_1 + \tilde{b}_h u_3)}{(u_1 + u_2 + u_3 + u_4)^2} & \frac{a(b_h u_1 + \tilde{b}_h u_3)}{u_1 + u_2 + u_3 + u_4} \\ \frac{ab_m u_5(u_1 + u_3 + u_4)}{(u_1 + u_2 + u_3 + u_4)^2} & 0 \end{pmatrix}, \quad V = \begin{pmatrix} \gamma_h + \delta_h & 0 \\ 0 & \mu_m \end{pmatrix}$$

and $V^{-1} = \begin{pmatrix} \frac{1}{\gamma_h + \delta_h} & 0 \\ 0 & \frac{1}{\mu_m} \end{pmatrix}$. Therefore,

$$\begin{aligned} FV^{-1} &= \begin{pmatrix} \frac{-au_6(b_h u_1 + \tilde{b}_h u_3)}{(u_1 + u_2 + u_3 + u_4)^2} & \frac{a(b_h u_1 + \tilde{b}_h u_3)}{u_1 + u_2 + u_3 + u_4} \\ \frac{ab_m u_5(u_1 + u_3 + u_4)}{(u_1 + u_2 + u_3 + u_4)^2} & 0 \end{pmatrix} \begin{pmatrix} \frac{1}{\gamma_h + \delta_h} & 0 \\ 0 & \frac{1}{\mu_m} \end{pmatrix} \\ &= \begin{pmatrix} \frac{-au_6(b_h u_1 + \tilde{b}_h u_3)}{(\gamma_h + \delta_h)(u_1 + u_2 + u_3 + u_4)^2} & \frac{a(b_h u_1 + \tilde{b}_h u_3)}{\mu_m(u_1 + u_2 + u_3 + u_4)} \\ \frac{ab_m u_5(u_1 + u_3 + u_4)}{(\gamma_h + \delta_h)(u_1 + u_2 + u_3 + u_4)^2} & 0 \end{pmatrix}. \end{aligned}$$

Since the characteristic polynomial is $\det |FV^{-1} - \lambda I|$, we have

$$\det |FV^{-1} - \lambda I| = \begin{vmatrix} \frac{-au_6(b_h u_1 + \tilde{b}_h u_3)}{(\gamma_h + \delta_h)(u_1 + u_2 + u_3 + u_4)^2} - \lambda & \frac{a(b_h u_1 + \tilde{b}_h u_3)}{\mu_m(u_1 + u_2 + u_3 + u_4)} \\ \frac{ab_m u_5(u_1 + u_3 + u_4)}{(\gamma_h + \delta_h)(u_1 + u_2 + u_3 + u_4)^2} & -\lambda \end{vmatrix}.$$

Solving the determinant of the matrix, we get

$$\begin{aligned} \det |FV^{-1} - \lambda I| &= \left(\frac{-au_6(\tilde{b}_h u_3 + b_h u_1)}{(\gamma_h + \delta_h)(u_4 + u_3 + u_2 + u_1)} - \lambda \right) (-\lambda) \\ &\quad - \frac{a^2 b_m (\tilde{b}_h u_3 + b_h u_1) u_5 (u_4 + u_3 + u_1)}{(\gamma_h + \delta_h) \mu_m (u_4 + u_3 + u_2 + u_1)^3} \\ &= \lambda^2 + \lambda \frac{au_6(\tilde{b}_h u_3 + b_h u_1)}{(\gamma_h + \delta_h)(u_4 + u_3 + u_2 + u_1)} \\ &\quad - \frac{a^2 b_m (\tilde{b}_h u_3 + b_h u_1) u_5 (u_4 + u_3 + u_1)}{(\gamma_h + \delta_h) \mu_m (u_4 + u_3 + u_2 + u_1)^3} \end{aligned}$$

Let $u_H = u_1 + u_2 + u_3 + u_4$. Then solving the equation, we have

$$\begin{aligned} \lambda &= \pm \frac{1}{2} \sqrt{\left(\frac{au_6(\tilde{b}_h u_3 + b_h u_1)}{(\gamma_h + \delta_h)u_H^2} \right)^2 - \frac{4a^2 b_m u_5 (\tilde{b}_h u_3 + b_h u_1) (u_H - u_2)}{\mu_m (\gamma_h + \delta_h) u_H^3} - \frac{au_6(\tilde{b}_h u_3 + b_h u_1)}{2(\gamma_h + \delta_h)u_H^2}} \\ &= \pm \frac{a(\tilde{b}_h u_3 + b_h u_1)}{2(\gamma_h + \delta_h)u_H} \sqrt{\frac{u_6^2 \mu_m (\tilde{b}_h u_3 + b_h u_1) - 4b_m u_5 u_H (\gamma_h + \delta_h) (u_H - u_2)}{\mu_m (\tilde{b}_h u_3 + b_h u_1)}} - \frac{au_6(\tilde{b}_h u_3 + b_h u_1)}{2(\gamma_h + \delta_h)u_H^2}} \end{aligned}$$

Simplifying the equation above would give us the eigenvalue

$$\lambda = \frac{a(\tilde{b}_h u_3 + b_h u_1)}{2(\gamma_h + \delta_h)u_H} \left(\frac{-u_6}{u_H} \pm \sqrt{u_6^2 - \frac{4b_m u_5 u_H (\gamma_h + \delta_h) (u_H - u_2)}{\mu_m (\tilde{b}_h u_3 + b_h u_1)}} \right).$$

Now using this eigenvalue, let us determine the stability of the equilibrium points.

Lemma 3.2.5. *The equilibrium point $(u_1^*, 0, u_3^*, u_4^*, 0, 0)$, where $u_4^* = K - u_1^* - u_3^*$, called the Disease Free Equilibrium, of the system of equation (3.7) is locally asymptotically stable.*

Proof. If $u_1 = u_1^*$, $u_2 = 0$, $u_3 = u_3^*$, $u_4^* = K - u_1^* - u_3^*$, then $u_H = u_1 + u_2 + u_3 + u_4 = K$. Therefore, from the above eigenvalues, we have

$$\lambda = \frac{a(\tilde{b}_h u_3^* + b_h u_1^*)}{2(\gamma_h + \delta_h)K} \left(\frac{-0}{K} \pm \sqrt{(0)^2 - \frac{4b_m(0)K(\gamma_h + \delta_h)(K - 0)}{\mu_m(\tilde{b}_h u_3^* + b_h u_1^*)}} \right).$$

Thus, $\lambda = 0 < 1$. Therefore, the system is locally asymptotically stable at the equilibrium point $DFE = (u_1^*, 0, u_3^*, u_4^*, 0, 0)$. \square

Lemma 3.2.6. *The equilibrium point $(0, 0, 0, 0, u_5^*, u_6^*)$, called the Endemic Equilibrium, of the system of equation (3.7) is unstable.*

Proof. From the above eigenvalues,

$$\rho(FV^{-1}) = \lim_{u_1, u_2, u_3, u_4 \rightarrow 0} \lambda = +\infty > 1.$$

Therefore, the system of equation is unstable at $EE = (0, 0, 0, 0, u_5^*, u_6^*)$. \square

Jacobian Matrix

Let $u'(t) = f(u(t), t)$ where $u = (u_1, u_2, u_3, u_4, u_5, u_6)$. In this section, let us confirm the stability result using the Jacobian matrix defined as

$$J(u_1^*, u_2^*, u_3^*, u_4^*, u_5^*, u_6^*) = \begin{pmatrix} \frac{\partial f_1}{\partial u_1} & \frac{\partial f_1}{\partial u_2} & \frac{\partial f_1}{\partial u_3} & \frac{\partial f_1}{\partial u_4} & \frac{\partial f_1}{\partial u_5} & \frac{\partial f_1}{\partial u_6} \\ \frac{\partial f_2}{\partial u_1} & \frac{\partial f_2}{\partial u_2} & \frac{\partial f_2}{\partial u_3} & \frac{\partial f_2}{\partial u_4} & \frac{\partial f_2}{\partial u_5} & \frac{\partial f_2}{\partial u_6} \\ \frac{\partial f_3}{\partial u_1} & \frac{\partial f_3}{\partial u_2} & \frac{\partial f_3}{\partial u_3} & \frac{\partial f_3}{\partial u_4} & \frac{\partial f_3}{\partial u_5} & \frac{\partial f_3}{\partial u_6} \\ \frac{\partial f_4}{\partial u_1} & \frac{\partial f_4}{\partial u_2} & \frac{\partial f_4}{\partial u_3} & \frac{\partial f_4}{\partial u_4} & \frac{\partial f_4}{\partial u_5} & \frac{\partial f_4}{\partial u_6} \\ \frac{\partial f_5}{\partial u_1} & \frac{\partial f_5}{\partial u_2} & \frac{\partial f_5}{\partial u_3} & \frac{\partial f_5}{\partial u_4} & \frac{\partial f_5}{\partial u_5} & \frac{\partial f_5}{\partial u_6} \\ \frac{\partial f_6}{\partial u_1} & \frac{\partial f_6}{\partial u_2} & \frac{\partial f_6}{\partial u_3} & \frac{\partial f_6}{\partial u_4} & \frac{\partial f_6}{\partial u_5} & \frac{\partial f_6}{\partial u_6} \end{pmatrix}.$$

Computing for the partial derivative $\frac{\partial f_i}{\partial u_i}$, for each i , where $i = 1, 2, \dots, 6$, we have

$$\begin{aligned} \frac{\partial f_1}{\partial u_1} &= \frac{-ab_h u_6 (u_2 + u_3 + u_4)}{(u_1 + u_2 + u_3 + u_4)^2} + \alpha_h - \frac{2\alpha_h (u_1 + u_2 + u_3 + u_4)}{K} \\ \frac{\partial f_1}{\partial u_2} &= \frac{ab_h u_6 u_1}{(u_1 + u_2 + u_3 + u_4)^2} + \alpha_h - \frac{2\alpha_h (u_1 + u_2 + u_3 + u_4)}{K} \\ \frac{\partial f_1}{\partial u_3} &= \frac{ab_h u_6 u_1}{(u_1 + u_2 + u_3 + u_4)^2} + \alpha_h - \frac{2\alpha_h (u_1 + u_2 + u_3 + u_4)}{K} \\ \frac{\partial f_1}{\partial u_4} &= \frac{ab_h u_6 u_1}{(u_1 + u_2 + u_3 + u_4)^2} + \alpha_h - \frac{2\alpha_h (u_1 + u_2 + u_3 + u_4)}{K} \end{aligned}$$

and

$$\begin{aligned}
\frac{\partial f_1}{\partial u_5} &= 0 & \frac{\partial f_1}{\partial u_6} &= \frac{-ab_h u_1}{u_1 + u_2 + u_3 + u_4} \\
\frac{\partial f_2}{\partial u_1} &= \frac{ab_h u_6(u_2 + u_3 + u_4) - \tilde{a}\tilde{b}_h u_6 u_3}{(u_1 + u_2 + u_3 + u_4)^2} & \frac{\partial f_2}{\partial u_2} &= \frac{-ab_h u_6 u_1 - \tilde{a}\tilde{b}_h u_6 u_3}{(u_1 + u_2 + u_3 + u_4)^2} - \gamma_h - \delta_h \\
\frac{\partial f_2}{\partial u_3} &= \frac{\tilde{a}\tilde{b}_h u_6(u_1 + u_2 + u_4) - ab_h u_6 u_1}{(u_1 + u_2 + u_3 + u_4)^2} & \frac{\partial f_2}{\partial u_4} &= \frac{-ab_h u_6 u_1 - \tilde{a}\tilde{b}_h u_6 u_3}{(u_1 + u_2 + u_3 + u_4)^2} \\
\frac{\partial f_2}{\partial u_5} &= 0 & \frac{\partial f_2}{\partial u_6} &= \frac{ab_h u_1 + \tilde{a}\tilde{b}_h u_3}{u_1 + u_2 + u_3 + u_4} \\
\frac{\partial f_3}{\partial u_1} &= \frac{\tilde{a}\tilde{b}_h u_6 u_3}{(u_1 + u_2 + u_3 + u_4)^2} & \frac{\partial f_3}{\partial u_2} &= \gamma_h + \frac{\tilde{a}\tilde{b}_h u_6 u_3}{(u_1 + u_2 + u_3 + u_4)^2} \\
\frac{\partial f_3}{\partial u_3} &= \frac{-\tilde{a}\tilde{b}_h u_6(u_1 + u_2 + u_4)}{(u_1 + u_2 + u_3 + u_4)^2} & \frac{\partial f_3}{\partial u_4} &= \frac{\tilde{a}\tilde{b}_h u_6 u_3}{(u_1 + u_2 + u_3 + u_4)^2} \\
\frac{\partial f_3}{\partial u_5} &= 0 & \frac{\partial f_3}{\partial u_6} &= \frac{-\tilde{a}\tilde{b}_h u_3}{u_1 + u_2 + u_3 + u_4} \\
\frac{\partial f_4}{\partial u_1} &= \frac{\partial f_4}{\partial u_3} = \frac{\partial f_4}{\partial u_4} = \frac{\partial f_4}{\partial u_5} = \frac{\partial f_4}{\partial u_6} = 0 & \frac{\partial f_4}{\partial u_2} &= \delta_h \\
\frac{\partial f_5}{\partial u_1} &= \frac{ab_m u_2 u_5}{(u_1 + u_2 + u_3 + u_4)^2} & \frac{\partial f_5}{\partial u_2} &= \frac{-ab_m u_5(u_1 + u_3 + u_4)}{(u_1 + u_2 + u_3 + u_4)^2} \\
\frac{\partial f_5}{\partial u_3} &= \frac{ab_m u_2 u_5}{(u_1 + u_2 + u_3 + u_4)^2} & \frac{\partial f_5}{\partial u_4} &= \frac{ab_m u_2 u_5}{(u_1 + u_2 + u_3 + u_4)^2} \\
\frac{\partial f_5}{\partial u_5} &= \frac{-ab_m u_2}{u_1 + u_2 + u_3 + u_4} - \mu_m + \alpha_m & \frac{\partial f_5}{\partial u_6} &= \alpha_m \\
\frac{\partial f_6}{\partial u_1} &= \frac{-ab_m u_2 u_5}{(u_1 + u_2 + u_3 + u_4)^2} & \frac{\partial f_6}{\partial u_2} &= \frac{ab_m u_5(u_1 + u_3 + u_4)}{(u_1 + u_2 + u_3 + u_4)^2} \\
\frac{\partial f_6}{\partial u_3} &= \frac{-ab_m u_5 u_2}{(u_1 + u_2 + u_3 + u_4)^2} & \frac{\partial f_6}{\partial u_4} &= \frac{-ab_m u_5 u_2}{(u_1 + u_2 + u_3 + u_4)^2} \\
\frac{\partial f_6}{\partial u_5} &= \frac{ab_m u_2}{u_1 + u_2 + u_3 + u_4} & \frac{\partial f_6}{\partial u_6} &= -\mu_m
\end{aligned}$$

From the Jacobian matrix above, the lemma below verified our result for the stability of the disease-free equilibrium point.

Lemma 3.2.7. *The disease-free equilibrium point $DFE = (u_1^*, 0, u_3^*, u_4^*, 0, 0)$ where $u_4^* = K - u_1^* - u_3^*$ of the system of equation (3.7) is locally asymptotically stable. And the endemic equilibrium $(0, 0, 0, 0, u_5^*, u_6^*)$ is locally asymptotically unstable.*

Proof. Let $DFE = (u_1^*, 0, u_3^*, u_4^*, 0, 0)$ where $u_4^* = K - u_1^* - u_3^*$ be an equilibrium point of the system of equation (3.7). Then, the above Jacobian matrix for DFE can be

deduce to

$$J(DFE) = \begin{pmatrix} -\alpha_h & -\alpha_h & -\alpha_h & -\alpha_h & 0 & \frac{-ab_h u_1^*}{K} \\ 0 & -\gamma_h - \delta_h & 0 & 0 & 0 & \frac{ab_h u_1^* + \tilde{a}b_h u_3^*}{K} \\ 0 & \gamma_h & 0 & 0 & 0 & \frac{-\tilde{a}b_h u_3^*}{K} \\ 0 & \delta_h & 0 & 0 & 0 & 0 \\ 0 & 0 & 0 & 0 & -\mu_m + \alpha_m & \alpha_m \\ 0 & 0 & 0 & 0 & 0 & -\mu_m \end{pmatrix}$$

Let $|J(E_1) - \lambda I_6| = 0$. Then

$$\begin{vmatrix} -\alpha_h - \lambda & -\alpha_h & -\alpha_h & -\alpha_h & 0 & \frac{-ab_h u_1^*}{K} \\ 0 & -\gamma_h - \delta_h - \lambda & 0 & 0 & 0 & \frac{ab_h u_1^* + \tilde{a}b_h u_3^*}{K} \\ 0 & \gamma_h & -\lambda & 0 & 0 & \frac{-\tilde{a}b_h u_3^*}{K} \\ 0 & \delta_h & 0 & -\lambda & 0 & 0 \\ 0 & 0 & 0 & 0 & -\mu_m + \alpha_m - \lambda & \alpha_m \\ 0 & 0 & 0 & 0 & 0 & -\mu_m - \lambda \end{vmatrix} = 0.$$

Solving this determinant give us the characteristic polynomial of the system which is

$$(-\lambda)(-\lambda)(-\lambda - \alpha_h)(-\lambda - \gamma_h - \delta_h)(-\lambda - \mu_m)(-\lambda - (\mu_m - \alpha_m)) = 0.$$

Hence the eigenvalues are,

$$\begin{aligned} \lambda &= 0 \text{ (multiplicity 2)} & \lambda &= -\alpha_h & \lambda &= -(\gamma_h + \delta_h) \\ \lambda &= -\mu_m & \lambda &= -(\mu_m - \alpha_m) \end{aligned}$$

Since $\mu_m - \alpha_m > 0$, all eigenvalues are negatives. Therefore, the equilibrium point, $DFE = (u_1^*, 0, u_3^*, u_4^*, 0, 0)$ is locally asymptotically stable.

Similar computations shows that the endemic equilibrium is locally asymptotically unstable. \square

3.2.3 Phase Portrait Analysis

A phase portrait graph of our dynamical system graphically represents the system behavior. It is a geometric representation of the trajectories of a dynamical system in the phase plane. In this section, we will illustrate some simulations performed using Python.

Symbol	Description	Values
a	number of human beaten per mosquito	1 day^{-1}
b_h	probability of becoming infected	0.75 day^{-1}
\tilde{b}_h	probability of becoming infected again	0.375 day^{-1}
α_h	birth rate of human	0.0045 day^{-1}
γ_h	recovery rate of human from first three infection	$0.328833 \text{ day}^{-1}$
δ_h	recovery rate of human from four serotypes	0.1666 day^{-1}
b_m	probability of becoming infectious	0.375 day^{-1}
μ_m	death rate of mosquito	0.02941 day^{-1}
α_m	growth rate of mosquito	0.025 day^{-1}

TABLE 3.2: Values of the parameter used in the numerical simulation

In this study, a numerical simulations are done using 2000 days. Figure 3.2 shows the behavior of the variables S_h , I_h , \tilde{S}_h , R_h , S_m and I_m versus time using the parameters in Table 3.2 that are taken from Bakach [6]. The variable S_h is the red color, I_h is the green, \tilde{S}_h is the blue, R_h is yellow, S_m is the cyan, and I_m is the magenta.

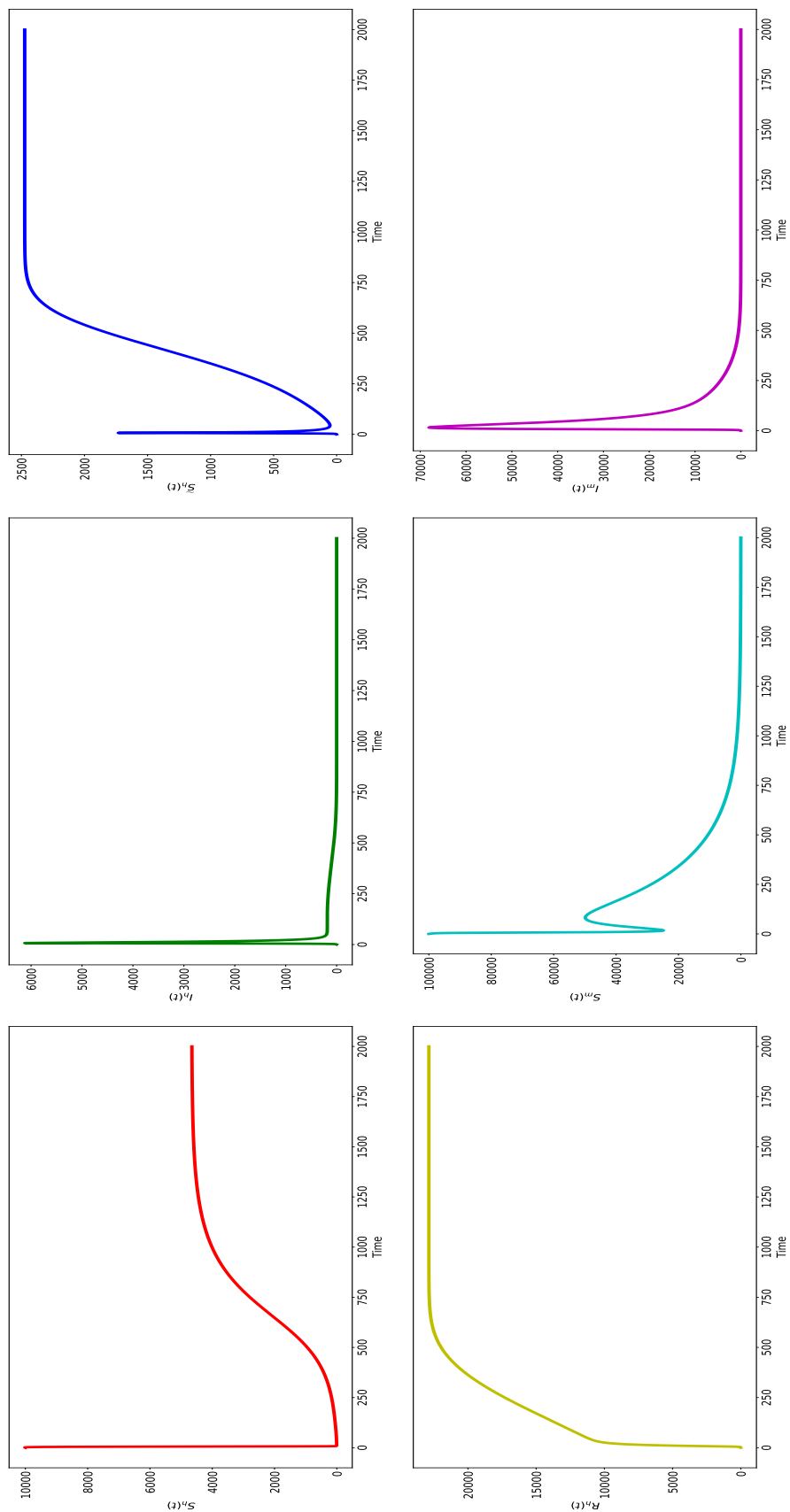


FIGURE 3.2: Behaviour of the solution of each variables in the model with dengvaxia versus time using logarithmic and exponential growth functions for human and mosquito population, respectively.

Initially, the human and mosquito population were healthy, with 10,000 humans and 100,000 mosquitoes populations, respectively, and only ten infected mosquitoes. Since mosquito needs to feed two to three times a day to take a full-blood meal, it takes 11 days for the primary susceptible S_h human population to reach its lowest population at six humans and then exponentially increases to its equilibrium 10,019 population. While it only takes seven days for the infected human I_h population to reach its highest population at 6,084 humans. After such time, a rapid decrease in the population follows. Whereas, for all time t , the recovered human R_h population continuously increases to its maximum population of 22,864 humans.

Note that for a mosquito to be infected by the virus, a mosquito must take its blood meal during viremia, when the infected person has high levels of the dengue virus in the blood. Thus, it takes 16 days for infected mosquito I_m to reach its highest population at 6,8116 mosquitoes before it drops exponentially.

Since humans kill some of these mosquitos and the mosquito's system requires eight to twelve days for the virus to spreads through its body, the population of susceptible mosquito S_m drops for 18 days to its local minimum of 24,814 mosquitos then increases after up to 49,857 mosquitos at 82 days and decreases again afterward.

Moreover, since viremia lasts for 4 to 5 days in primary condition, most people will recover after about a week. It only takes seven days for the secondary susceptible \tilde{S}_h human population to reach its local maximum at 1,730 population, then decreases to 53 population at 44 days and exponentially increases to a maximum of 2,474 population.

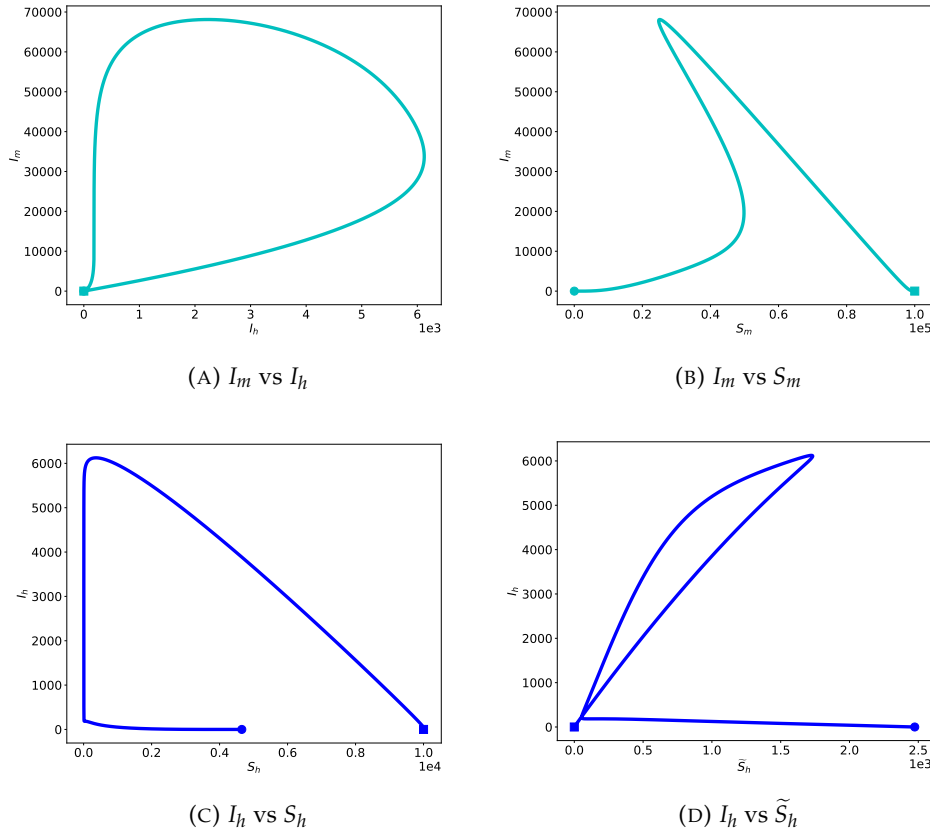


FIGURE 3.3: Phase portrait of the model with dengvaxia showing primary susceptible S_h and secondary susceptible \tilde{S}_h versus infected humans I_h in blue color, and susceptible mosquitoes S_m and infected humans I_h versus infected mosquitoes I_m in cyan color. Square and circle indicates the first and last solution of the variables.

Figure 3.3a shows that in the beginning there are 10 infected mosquito and no infected human. As the infected humans increases, infected mosquitoes also increases. After some time, the two variables become inversely proportional. As infected humans decreases, the infected mosquito continue to increase. Towards the end of time, both variables decreases towards zero.

On the other hand, figure 3.3b shows that at time $t = 0$, there are 100,000 susceptible mosquito and 10 infected mosquitoes. For some time, susceptible mosquitoes decreases while infected mosquitoes increases. When it reaches the maximum of 68117.679 infected mosquitoes, it then decreases while susceptible mosquitoes increases. After some time, both variables decreases towards zero.

For infected humans, figure 3.3c shows that at time $t = 0$, there are no infected humans but have 10,000 primary susceptible humans. For some time, as infected humans increases, primary susceptible humans decreases. Upon reaching 6125.015 infected human populations, both variables decreases. Then primary susceptible humans started to increase but infected humans continue to decrease.

Figure 3.3d shows that at time $t = 0$, there are no infected and secondary susceptible humans. The figure shows that the variables are directly proportional to

each other for an interval of time. For some time, both variables increases up to the maximum of 2474.242 secondary susceptible humans. They then decreases up to 53 secondary susceptible humans. While infected humans continue to decrease, secondary susceptible humans then increases through time.

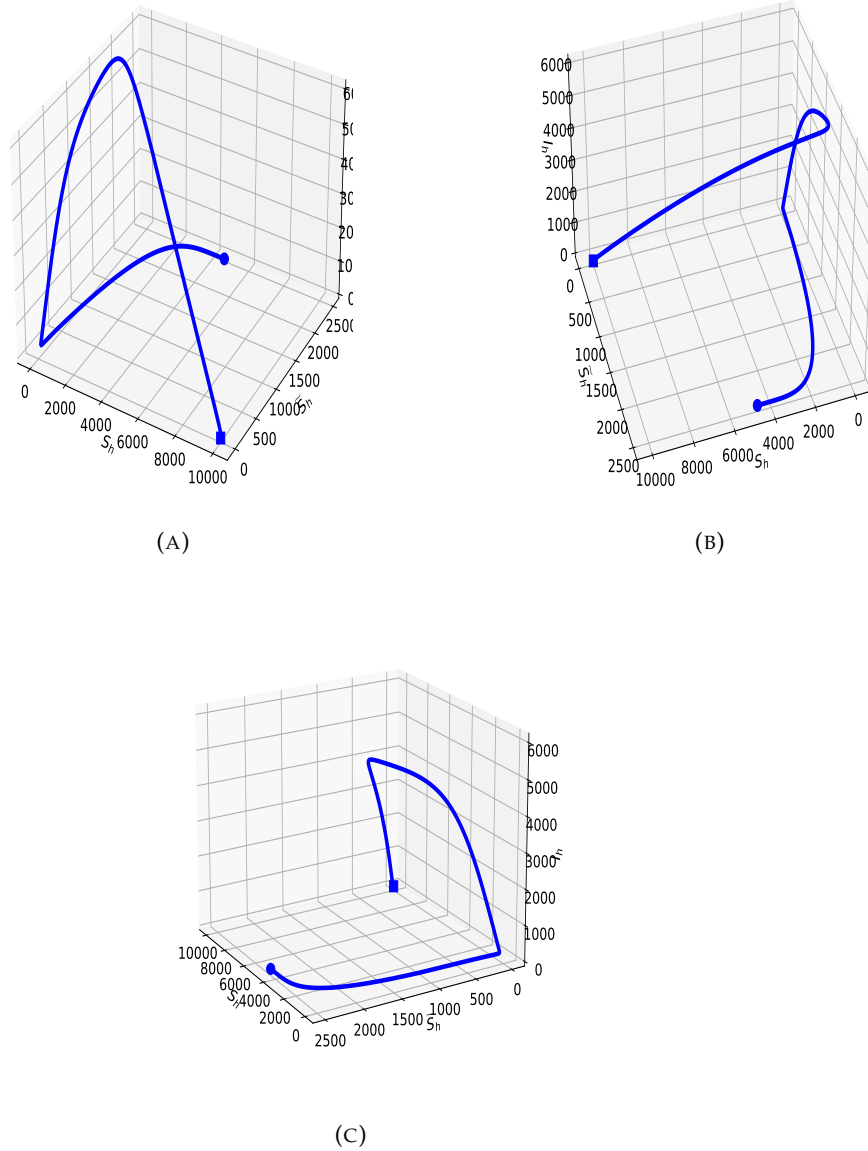


FIGURE 3.4: Three dimensional phase portrait of the primary susceptible human S_h , secondary susceptible \tilde{S}_h , and the infected I_h human population in the model with dengvaxia.

Figure 3.4 graphically shows the system behavior of the primary susceptible human S_h , secondary susceptible \tilde{S}_h , and the infected I_h human population. The solution is positive and bounded, as shown in the previous theorem.

3.3 Comparison against Growth Functions

In this section, we will consider different growth functions for the human population $f(H(t))$ and mosquito population $g(M(t))$ of the system (3.1)-(4.6) of the ordinary differential equation. We consider three growth functions:

- Pop_1 : constant human and mosquitoes population,
- Pop_2 : Gompertz growth function for the human population and an exponential growth function for mosquitoes population,

3.3.1 Constant Human and Mosquito Population

Consider the constant human and mosquito population. For human population, we set $H(t) = H_0$ where H_0 is constant. Then, $H'(t) = f(H(t)) = 0$. Also, for mosquito population we set $M(t) = M_0$ where M_0 is constant. Then $M'(t) = g(M(t)) - \mu_m M(t) = 0$, our model would become

$$\begin{aligned}
 u_1'(t) &= -\frac{ab_h u_6(t) u_1(t)}{H_0} \\
 u_2'(t) &= \frac{au_6(t) (b_h u_1(t) + \tilde{b}_h u_3(t))}{H_0} - \gamma_h u_2(t) - \delta_h u_2(t) \\
 u_3'(t) &= \gamma_h u_2(t) - \frac{\tilde{a} \tilde{b}_h u_3(t) u_6(t)}{H_0} \\
 u_4'(t) &= \delta_h u_2(t) \\
 u_5'(t) &= -\frac{ab_m u_2(t) u_5(t)}{H_0} + \mu_m u_6(t) \\
 u_6'(t) &= \frac{ab_m u_2(t) u_5(t)}{H_0} - \mu_m u_6(t)
 \end{aligned} \tag{3.19}$$

Theorem 3.3.1. Let $(u_1(0), u_2(0), u_3(0), u_4(0), u_5(0), u_6(0))$ be in Ω_{cons} defined by

$$\Omega_{cons} = \{U \in \mathbb{R}_+^6 : u_1 + u_2 + u_3 + u_4 = H_0, u_3 + u_4 = M_0\}.$$

Then, there exists a unique global in time solution $(u_1, u_2, u_3, u_4, u_5, u_6)$ in $\mathcal{C}(\mathbb{R}_+, \Omega_{cons})$.

Proof. The proof follows from the fact that constant population is bounded and well-defined. \square

Equilibrium

If we solve for all possible values of x^* that lie on Ω , we only have $(u_1^*, 0, u_3^*, u_4^*, u_5^*, 0)$. To see this, consider the lemma below.

Lemma 3.3.2. The system of equation (3.19) admits a disease free equilibrium at $E_{cons} = (u_1^*, 0, u_3^*, u_4^*, u_5^*, 0)$.

Proof. Let $u'_1, u'_2, u'_3, u'_4, u'_5, u'_6 = 0$. Since all parameter are positive, then

$$\delta_h u_2 = 0 \implies u_2 = 0$$

Thus, $\frac{ab_m u_2 u_5}{H} - \mu_m u_6 = 0$ becomes

$$\begin{aligned} \frac{ab_m(0)u_5}{H} - \mu_m u_6 &= 0 \\ -\mu_m u_6 &= 0 \end{aligned}$$

Hence, $u_6 = 0$. Since the system of equation contains either u_2 or u_6 or both, which has a zero value, then any nonnegative values of u_1, u_3, u_4, u_5 satisfies the system of equation. Therefore, $(u_1^*, 0, u_3^*, u_4^*, u_5^*, 0)$ is an equilibrium point. \square

Next Generation Matrix and Basic Reproduction Number

Now, let us determine the stability of this equilibrium points by solving for the next generation matrix of the system of equation (3.19). We have

$$\mathcal{F} = \begin{pmatrix} \frac{au_6(b_h u_1 + \tilde{b}_h u_3)}{H_0} \\ \frac{ab_m u_2 u_5}{H_0} \end{pmatrix} \quad \mathcal{V} = \begin{pmatrix} (\gamma_h + \delta_h)u_2 \\ \mu_m u_6 \end{pmatrix}$$

where \mathcal{F} is the rate of appearance of new infections in each compartment and \mathcal{V} is the rate of other transitions between all other compartment. Thus,

$$F = \begin{pmatrix} 0 & \frac{a(b_h u_1 + \tilde{b}_h u_3)}{H_0} \\ \frac{ab_m u_5}{H_0} & 0 \end{pmatrix} \quad \text{and} \quad V = \begin{pmatrix} \gamma_h + \delta_h & 0 \\ 0 & \mu_m \end{pmatrix}.$$

Therefore,

$$\begin{aligned} FV^{-1} &= \begin{pmatrix} 0 & \frac{a(b_h u_1 + \tilde{b}_h u_3)}{H_0} \\ \frac{ab_m u_5}{H_0} & 0 \end{pmatrix} \begin{pmatrix} \frac{1}{\gamma_h + \delta_h} & 0 \\ 0 & \frac{1}{\mu_m} \end{pmatrix} \\ &= \begin{pmatrix} 0 & \frac{a(b_h u_1 + \tilde{b}_h u_3)}{\mu_m H_0} \\ \frac{ab_m u_5}{(\gamma_h + \delta_h) H_0} & 0 \end{pmatrix} \end{aligned}$$

Since the characteristic polynomial is $\det |FV^{-1} - \lambda I|$, we have

$$\begin{aligned} \det |FV^{-1} - \lambda I| &= \begin{vmatrix} -\lambda & \frac{a(b_h u_1 + \tilde{b}_h u_3)}{\mu_m H_0} \\ \frac{ab_m u_5}{(\gamma_h + \delta_h) H_0} & -\lambda \end{vmatrix} \\ &= \lambda^2 - \frac{a^2 b_m u_5 (\tilde{b}_h u_3 + b_h u_1)}{H_0^2 \mu_m (\gamma_h + \delta_h)} \end{aligned}$$

Solving for λ , we get the eigenvalues

$$\lambda = \pm \sqrt{\frac{a^2 b_m u_5 (\tilde{b}_h u_3 + b_h u_1)}{H_0^2 \mu_m (\gamma_h + \delta_h)}} \quad (3.20)$$

Therefore, $\mathcal{R}_0^2 := \frac{a^2 b_m u_5 (\tilde{b}_h u_3 + b_h u_1)}{H_0^2 \mu_m (\gamma_h + \delta_h)}$, and we have the following theorem.

Theorem 3.3.3. *If $\mathcal{R}_0 < 1$, then the disease free equilibrium E_{cons} is asymptotically stable. If $\mathcal{R}_0 > 1$, then the disease free equilibrium E_{cons} is unstable.*

To explain \mathcal{R}_0 biologically, let us consider the following cases.

- Suppose $\mathcal{R}_0 > 1$, that is $\frac{ab_m u_5}{H_0} \left(\frac{a\tilde{b}_h u_3 + ab_h u_1}{H_0} \right) > \mu_m (\gamma_h + \delta_h)$. It means that the severity of the probability of infection to spread on susceptible mosquito $\frac{ab_m u_5}{H_0}$ and susceptible humans $\frac{a\tilde{b}_h u_3 + ab_h u_1}{H_0}$ is greater than the product of mortality rate of mosquito μ_m and the recovery rate of infectious humans $\gamma_h + \delta_h$. In effect, there is a spread of disease in the population, that is, resulting to dengue outbreak. Therefore, if $\mathcal{R}_0 > 1$, then the DFE is unstable.
- Suppose $\mathcal{R}_0 < 1$, that is $\frac{ab_m u_5}{H_0} \left(\frac{a\tilde{b}_h u_3 + ab_h u_1}{H_0} \right) < \mu_m (\gamma_h + \delta_h)$. It means that the severity of the probability of infection to spread on susceptible mosquito $\frac{ab_m u_5}{H_0}$ and susceptible humans $\frac{a\tilde{b}_h u_3 + ab_h u_1}{H_0}$ is lesser than the product of mortality rate of mosquito μ_m and recovery rate of infectious humans $\gamma_h + \delta_h$. Thus, the disease would be lessened, resulting in controlled dengue disease. Therefore, if $\mathcal{R}_0 < 1$, there is an asymptotic stability on the DFE.

Jacobian Matrix

To confirm the theorem above, we compute the Jacobian matrix of the system (3.19). We compute the partial derivatives of f_i with respect to u_i , for $i = 1, 2, \dots, 6$. We

have

$$\begin{array}{lll}
\frac{\partial f_1}{\partial u_1} = \frac{-ab_h u_6}{H_0} & \frac{\partial f_1}{\partial u_2} = \frac{\partial f_1}{\partial u_3} = \frac{\partial f_1}{\partial u_4} = \frac{\partial f_1}{\partial u_5} = 0 & \frac{\partial f_1}{\partial u_6} = \frac{-ab_h u_1}{H_0} \\
\frac{\partial f_2}{\partial u_1} = \frac{ab_h u_6}{H_0} & \frac{\partial f_2}{\partial u_2} = -\gamma_h - \delta_h & \frac{\partial f_2}{\partial u_3} = \frac{\tilde{a}b_h u_6}{H_0} \\
\frac{\partial f_2}{\partial u_4} = \frac{\partial f_2}{\partial u_5} = 0 & \frac{\partial f_2}{\partial u_6} = \frac{ab_h u_1 + \tilde{a}b_h u_3}{H_0} & \frac{\partial f_3}{\partial u_1} = 0 \\
\frac{\partial f_3}{\partial u_2} = \gamma_h & \frac{\partial f_3}{\partial u_3} = \frac{-\tilde{a}b_h u_6}{H_0} & \frac{\partial f_3}{\partial u_4} = \frac{\partial f_3}{\partial u_5} = 0 \\
\frac{\partial f_3}{\partial u_6} = \frac{-\tilde{a}b_h u_3}{H_0} & \frac{\partial f_4}{\partial u_1} = 0 & \frac{\partial f_4}{\partial u_2} = \delta_h \\
\frac{\partial f_4}{\partial u_3} = \frac{\partial f_4}{\partial u_4} = \frac{\partial f_4}{\partial u_5} = \frac{\partial f_4}{\partial u_6} = 0 & \frac{\partial f_5}{\partial u_1} = 0 & \frac{\partial f_5}{\partial u_2} = \frac{-ab_m u_5}{H_0} \\
\frac{\partial f_5}{\partial u_3} = \frac{\partial f_5}{\partial u_4} = 0 & \frac{\partial f_5}{\partial u_5} = \frac{-ab_m u_2}{H_0} & \frac{\partial f_5}{\partial u_6} = \mu_m \\
\frac{\partial f_6}{\partial u_1} = 0 & \frac{\partial f_6}{\partial u_2} = \frac{ab_m u_5}{H_0} & \frac{\partial f_6}{\partial u_3} = 0 \\
\frac{\partial f_6}{\partial u_4} = 0 & \frac{\partial f_6}{\partial u_5} = \frac{ab_m u_2}{H_0} & \frac{\partial f_6}{\partial u_6} = -\mu_m
\end{array}$$

Therefore, we have the following lemma.

Lemma 3.3.4. *The equilibrium point $E_{cons} = (u_1^*, 0, u_3^*, u_4^*, u_5^*, 0)$ is locally asymptotically stable.*

Proof. Let $E_{cons} = (u_1^*, 0, u_3^*, u_4^*, u_5^*, 0)$ be an equilibrium point of the system of equation. Then the above Jacobian matrix for E_{cons} can be deduce to

$$\begin{aligned}
J(E_1) &= \begin{pmatrix} \frac{-ab_h(0)}{H_0} & 0 & 0 & 0 & 0 & \frac{-ab_h u_1^*}{H_0} \\ \frac{ab_h(0)}{H_0} & -\gamma_h - \delta_h & \frac{\tilde{a}b_h(0)}{H_0} & 0 & 0 & \frac{ab_h u_1^* + \tilde{a}b_h u_3^*}{H_0} \\ 0 & \gamma_h & \frac{-\tilde{a}b_h(0)}{H_0} & 0 & 0 & \frac{-\tilde{a}b_h u_3^*}{H_0} \\ 0 & \delta_h & 0 & 0 & 0 & 0 \\ 0 & \frac{-ab_m u_5^*}{H_0} & 0 & 0 & \frac{-ab_m(0)}{H_0} & \mu_m \\ 0 & \frac{ab_m u_5^*}{H_0} & 0 & 0 & \frac{ab_m(0)}{H_0} & -\mu_m \end{pmatrix} \\
&= \begin{pmatrix} 0 & 0 & 0 & 0 & 0 & \frac{-ab_h u_1^*}{H_0} \\ 0 & -\gamma_h - \delta_h & 0 & 0 & 0 & \frac{ab_h u_1^* + \tilde{a}b_h u_3^*}{H_0} \\ 0 & \gamma_h & 0 & 0 & 0 & \frac{-\tilde{a}b_h u_3^*}{H_0} \\ 0 & \delta_h & 0 & 0 & 0 & 0 \\ 0 & \frac{-ab_m u_5^*}{H_0} & 0 & 0 & 0 & \mu_m \\ 0 & \frac{ab_m u_5^*}{H_0} & 0 & 0 & 0 & -\mu_m \end{pmatrix}.
\end{aligned}$$

Let $|J(E_1) - \lambda I_6| = 0$. Then

$$|J(E_1) - \lambda I_6| = \begin{vmatrix} -\lambda & 0 & 0 & 0 & 0 & \frac{-ab_h u_1^*}{H_0} \\ 0 & -\gamma_h - \delta_h - \lambda & 0 & 0 & 0 & \frac{ab_h u_1^* + a\tilde{b}_h u_3^*}{H_0} \\ 0 & \gamma_h & -\lambda & 0 & 0 & \frac{-a\tilde{b}_h u_3^*}{H_0} \\ 0 & \delta_h & 0 & -\lambda & 0 & 0 \\ 0 & \frac{-ab_m u_5^*}{H_0} & 0 & 0 & -\lambda & \mu_m \\ 0 & \frac{ab_m u_5^*}{H_0} & 0 & 0 & 0 & -\mu_m - \lambda \end{vmatrix} = 0.$$

Therefore, solving the equation will determine its characteristic polynomial. We get

$$(-\lambda)^4 \left((-\gamma_h - \delta_h - \lambda)(-\mu_m - \lambda) - \frac{ab_m u_5^* (ab_h u_1^* + a\tilde{b}_h u_3^*)}{H_0^2} \right) = 0$$

Now, let us solve λ for $(-\gamma_h - \delta_h - \lambda)(-\mu_m - \lambda) - \frac{ab_m u_5^* (ab_h u_1^* + a\tilde{b}_h u_3^*)}{H_0^2} = 0$. We have

$$\begin{aligned} & (-\gamma_h - \delta_h - \lambda)(-\mu_m - \lambda) - \frac{ab_m u_5^* (ab_h u_1^* + a\tilde{b}_h u_3^*)}{H_0^2} = 0 \\ & (\gamma_h + \delta_h)\mu_m + (\gamma_h + \delta_h)\lambda + \mu_m\lambda + \lambda^2 - \frac{ab_m u_5^* (ab_h u_1^* + a\tilde{b}_h u_3^*)}{H_0^2} = 0 \\ & \lambda^2 + (\gamma_h + \delta_h + \mu_m)\lambda + (\gamma_h + \delta_h)\mu_m - \frac{ab_m u_5^* (ab_h u_1^* + a\tilde{b}_h u_3^*)}{H_0^2} = 0. \end{aligned}$$

Solving λ by quadratic formula, we have

$$\begin{aligned} \lambda &= \frac{-\gamma_h - \delta_h - \mu_m \pm \sqrt{(\gamma_h + \delta_h + \mu_m)^2 - 4(1) \left((\gamma_h + \delta_h)\mu_m - \frac{ab_m u_5^* (ab_h u_1^* + a\tilde{b}_h u_3^*)}{H_0^2} \right)}}{2} \\ \lambda &= \frac{-\gamma_h - \delta_h - \mu_m}{2} \pm \frac{1}{2} \sqrt{(\gamma_h + \delta_h + \mu_m)^2 - 4(\gamma_h + \delta_h)\mu_m + \frac{4ab_m u_5^* (ab_h u_1^* + a\tilde{b}_h u_3^*)}{H_0^2}} \\ \lambda &= \frac{-\gamma_h - \delta_h - \mu_m}{2} \pm \frac{\sqrt{(\gamma_h + \delta_h - \mu_m)^2 H_0^2 + 4ab_m u_5^* (ab_h u_1^* + a\tilde{b}_h u_3^*)}}{2H_0} \end{aligned}$$

Hence, the eigenvalues are

$$\begin{aligned} \lambda_1 &= 0 \text{ (multiplicity 4)} \\ \lambda_2 &= \frac{-\gamma_h - \delta_h - \mu_m}{2} + \frac{\sqrt{(\gamma_h + \delta_h - \mu_m)^2 H_0^2 + 4ab_m u_5^* (ab_h u_1^* + a\tilde{b}_h u_3^*)}}{2H_0} \\ \lambda_3 &= \frac{-\gamma_h - \delta_h - \mu_m}{2} - \frac{\sqrt{(\gamma_h + \delta_h - \mu_m)^2 H_0^2 + 4ab_m u_5^* (ab_h u_1^* + a\tilde{b}_h u_3^*)}}{2H_0}. \end{aligned}$$

For E_{cons} to be asymptotically stable, the $Re(\lambda_2) < 0$. We have

$$\frac{\sqrt{(\gamma_h + \delta_h - \mu_m)^2 H_0^2 + 4ab_m u_5^* (ab_h u_1^* + a\tilde{b}_h u_3^*)}}{2H_0} < \frac{\gamma_h + \delta_h + \mu_m}{2}.$$

Simplifying the equation would give us

$$\sqrt{(\gamma_h + \delta_h - \mu_m)^2 H_0^2 + 4ab_m u_5^* (ab_h u_1^* + a\tilde{b}_h u_3^*)} < (\gamma_h + \delta_h + \mu_m) H_0.$$

Now taking the square of the inequality, we get

$$(\gamma_h + \delta_h - \mu_m)^2 H_0^2 + 4ab_m u_5^* (ab_h u_1^* + a\tilde{b}_h u_3^*) < (\gamma_h + \delta_h + \mu_m)^2 H_0^2.$$

Combining like terms and then simplifying, we have

$$\begin{aligned} 4ab_m u_5^* (ab_h u_1^* + a\tilde{b}_h u_3^*) &< (\gamma_h + \delta_h + \mu_m)^2 H_0^2 - (\gamma_h + \delta_h - \mu_m)^2 H_0^2 \\ 4ab_m u_5^* (ab_h u_1^* + a\tilde{b}_h u_3^*) &< 4\mu_m(\gamma_h + \delta_h) H_0^2 \\ \frac{a^2 b_m u_5^* (b_h u_1^* + \tilde{b}_h u_3^*)}{\mu_m(\gamma_h + \delta_h) H_0^2} &< 1. \end{aligned}$$

Therefore, we get the same R_0 we obtain from the next generation matrix. That is,

$$\mathcal{R}_0^2 = \frac{a^2 b_m u_5^* (b_h u_1^* + \tilde{b}_h u_3^*)}{\mu_m(\gamma_h + \delta_h) H_0^2} < 1 \text{ is locally asymptotically stable.} \quad \square$$

Numerical Illustrations

To straighten our lemmas above, let us look into the numerical simulation. In this simulation, we let time T be 2000 days with initial condition $(10000, 0, 0, 0, 100000, 10)$. Figure 3.5 shows the behaviour of the variables S_h , I_h , \tilde{S}_h , R_h , S_m and I_m versus time using the parameters in Table 3.2.

Initially, the human S_h and mosquito S_m population are healthy. However, briefly, they decrease exponentially and become infected I_m and I_h . Since humans kill some of these mosquitoes, and once the virus enters the mosquito's system in the blood meal, the virus spreads through the mosquito's body for eight to twelve days, S_h decreases faster than S_m . Hence I_h increases exponentially faster than I_m . Since infected humans I_h suffer for about 3 - 7 days following the infectious mosquito bite, there is an exponential increase of infected humans by then. Nevertheless, it is followed by an overwhelming recovery of the infected that increases the recovered human R_h population and the susceptibility \tilde{S}_h to other DENV strains. For 2000 days, it would only take more or less 40 days for the recovered human population R_h and the population of susceptible humans to other DENV strains \tilde{S}_h to take its equilibrium while the susceptible human S_h population takes its equilibrium at about ten days.

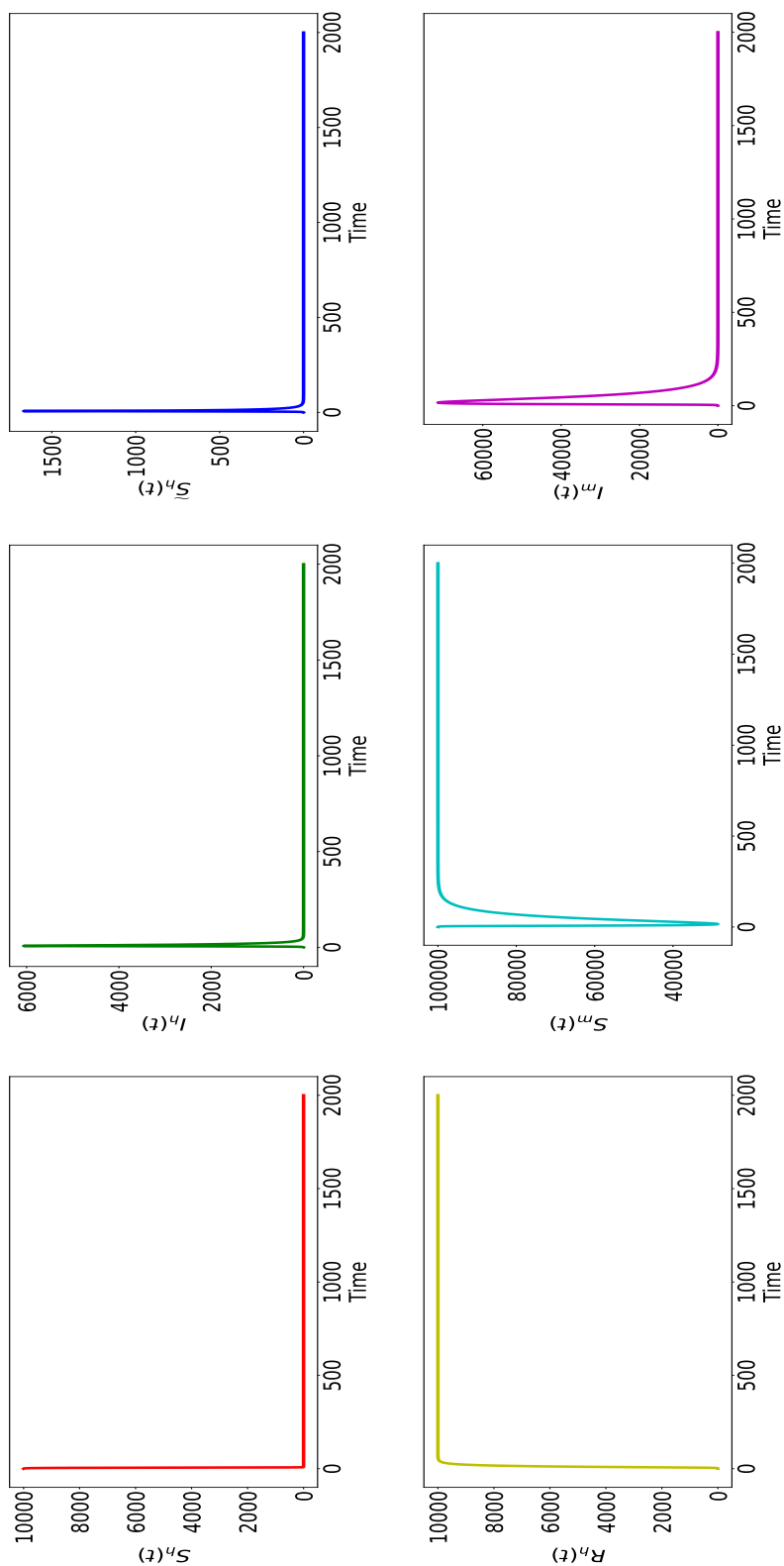


FIGURE 3.5: Behaviour of the solution of each variables in the model 3.19 with dengvaxia versus time using constant growth functions for human and mosquito population. S_h is the red colour figure, I_h is the green, \tilde{S}_h is the blue, R_h is the yellow, S_m is the cyan and I_m is the magenta.

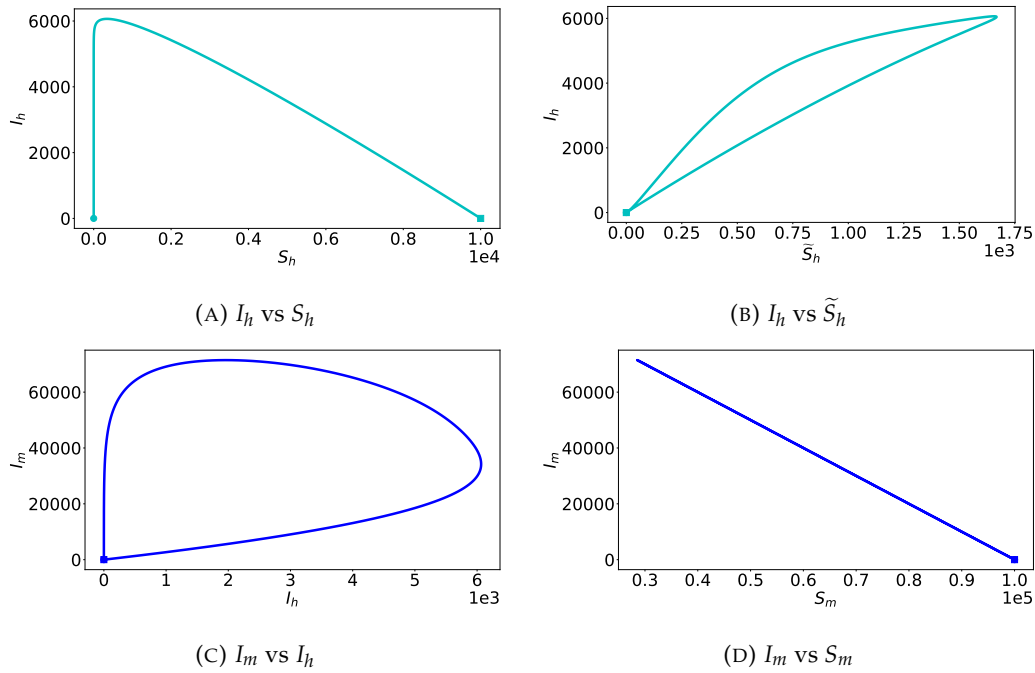


FIGURE 3.6: Phase portrait of the model with dengvaxia using constant growth function showing primary S_h and secondary susceptible \tilde{S}_h versus infected humans I_h in blue color, and susceptible mosquitoes S_m and infected humans I_h versus infected mosquitoes I_m in cyan color. Square and circle indicates the first and last solution of the variables.

For infected humans, figure 3.6a shows that at time $t = 0$, there are no infected humans but have 10,000 primary susceptible humans. For some time, as infected humans increases while primary susceptible humans decreases. Upon reaching 6065.190 infected human populations, both variables decreases thru time.

Figure 3.6b shows that at time $t = 0$, there are no infected and secondary susceptible humans. The figure shows that the variables are directly proportional to each other for all time. For some time, both variables increases up to the maximum of 1668.002 secondary susceptible humans. They then decreases up to the equilibrium.

Figure 3.6c shows that in the beginning there are 10 infected mosquito and no infected human. As the infected humans increases, infected mosquitoes also increases. After some time, the two variables become inversely proportional. As infected humans decreases, the infected mosquito continue to increase. Then both variables decreases towards zero.

On the other hand, figure 3.6d shows that at time $t = 0$, there are 100,000 susceptible mosquito and 10 infected mosquitoes. The figure shows that the two variables are inversely proportional to each other. For some time, susceptible mosquitoes decreases while infected mosquitoes increases. When it reaches the maximum of 71460.393 infected mosquitoes, both variables then decreases towards zero.

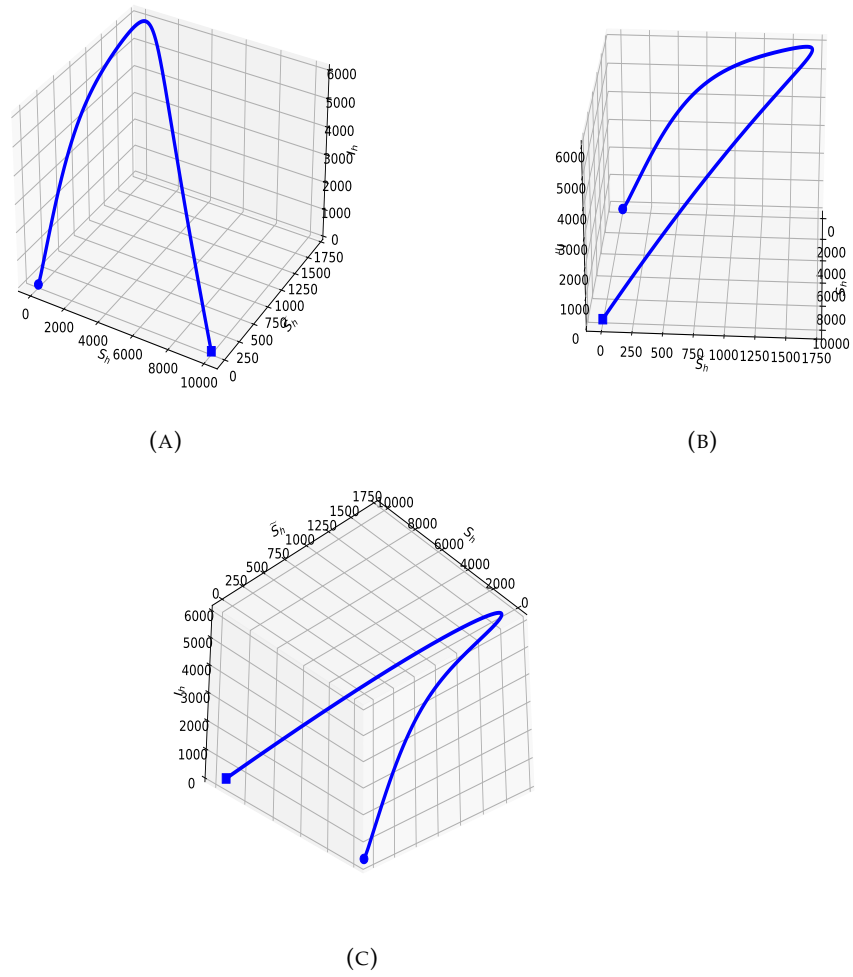


FIGURE 3.7: Phase portrait of the Model

Figure 3.7 graphically shows the system behavior of the primary susceptible human S_h , secondary susceptible \tilde{S}_h , and the infected I_h human population. The solution is indeed positive and bounded, as shown in the previous theorem.

3.3.2 Gompertz Human Population Growth and an Exponential Mosquito Population Growth

Let us consider a human population that agrees with the Gompertz growth equation and a mosquito population that agrees with the exponential growth equation. Then we have $H'(t) = f(H(t)) = r \ln \left(\frac{K}{H(t)} \right) H(t)$ and $M'(t) = (\alpha_m - \mu_m)M(t)$ such that $H(t) = Ke^{\ln \left(\frac{H_0}{K} \right) e^{-rt}}$ and $g(M(t)) = \alpha_m M(t)$. Then our model become

$$\begin{aligned}
 u_1'(t) &= -\frac{ab_h u_6(t) u_1(t)}{Ke^{\ln \left(\frac{H_0}{K} \right) e^{-rt}}} + r \ln \left(\frac{K}{H(t)} \right) H(t) \\
 u_2'(t) &= \frac{au_6(t) (b_h u_1(t) + \tilde{b}_h u_3(t))}{Ke^{\ln \left(\frac{H_0}{K} \right) e^{-rt}}} - \gamma_h u_2(t) - \delta_h u_2(t) \\
 u_3'(t) &= \gamma_h u_2(t) - \frac{a\tilde{b}_h u_3(t) u_6(t)}{Ke^{\ln \left(\frac{H_0}{K} \right) e^{-rt}}} \\
 u_4'(t) &= \delta_h u_2(t) \\
 u_5'(t) &= -\frac{ab_m u_2(t) u_5(t)}{Ke^{\ln \left(\frac{H_0}{K} \right) e^{-rt}}} - \mu_m u_5(t) + \alpha_m u_5(t) + \alpha_m u_6(t) \\
 u_6'(t) &= \frac{ab_m u_2(t) u_5(t)}{Ke^{\ln \left(\frac{H_0}{K} \right) e^{-rt}}} - \mu_m u_6(t)
 \end{aligned} \tag{3.21}$$

Assume that $\alpha_m \leq \mu_m$. We have the following theorems.

Well-posedness and Positivity of the Solution

Theorem 3.3.5. *Let Ω_{Gomp} be the region defined by*

$$\Omega_{Gomp} = \left\{ (u_1, u_2, u_3, u_4, u_5, u_6) \in \mathbb{R}_+^6; 0 \leq u_1 + u_2 + u_3 + u_4 \leq H_0, \right. \\
 \left. 0 \leq u_5 + u_6 \leq M_0 \right\} \tag{3.22}$$

such that $(u_1(0), u_2(0), u_3(0), u_4(0), u_5(0), u_6(0)) \in \Omega$. Then there exists a unique global in time solution $(u_1, u_2, u_3, u_4, u_5, u_6)$ in $\mathcal{C}(\mathbb{R}_+, \mathbb{R}_+^6)$.

Proof. Consider the initial value problem

$$U'(t) = F(t, U(t)) \quad \text{where} \quad U(0) = U_0.$$

Then,

$$\begin{aligned}
f'_1(0, u_2, u_3, u_4, u_5, u_6) &= r \ln \left(\frac{K}{u_2 + u_3 + u_4} \right) (u_2 + u_3 + u_4), \forall u_2, \dots, u_6 \in \Omega \\
f'_2(u_1, 0, u_3, u_4, u_5, u_6) &= \frac{au_6 (b_h u_1 + \tilde{b}_h u_3)}{K e^{\ln \left(\frac{H_0}{K} \right) e^{-rt}}} \geq 0, \forall u_1, u_3, \dots, u_6 \in \Omega \\
f'_3(u_1, u_2, 0, u_4, u_5, u_6) &= \gamma_h u_2, \forall u_1, u_2, u_4, \dots, u_6 \in \Omega \\
f'_4(u_1, u_2, u_3, 0, u_5, u_6) &= \delta_h u_2, \forall u_1, u_2, u_3, u_5, u_6 \in \Omega \\
f'_5(u_1, u_2, u_3, u_4, 0, u_6) &= \alpha_m u_6, \forall u_1, \dots, u_4, u_6 \in \Omega \\
f'_6(u_1, u_2, u_3, u_4, u_5, 0) &= \frac{ab_m u_2 u_5}{K e^{\ln \left(\frac{H_0}{K} \right) e^{-rt}}}, \forall u_1, \dots, u_5 \in \Omega.
\end{aligned}$$

On one hand, note that $H' = r \ln \left(\frac{K}{H} \right) H$ where $H = K e^{\ln \left(\frac{H_0}{K} \right) e^{-rt}}$. Since $e^{-rt} \leq 1$, $\ln \left(\frac{H_0}{K} \right) e^{-rt} \leq \ln \left(\frac{H_0}{K} \right)$. Thus,

$$H \leq K e^{\ln \left(\frac{H_0}{K} \right)} \leq K \frac{H_0}{K} \leq H_0.$$

While $M' = (\alpha_m - \mu_m)M$, then $M = M_0 e^{(\alpha_m - \mu_m)t}$. Since $\alpha_m \leq \mu_m$, we have

$$M(t) = e^{(\alpha_m - \mu_m)t} M_0 \leq M_0.$$

Thus F satisfies the local Lipschitz condition. Therefore, by Cauchy-Lipschitz Theorem, there exist $T > 0$ and a unique solution to equation (3.21) in $\mathcal{C}(\mathbb{R}_+, \mathbb{R}_+^6)$. \square

Equilibrium

Now, solving for all possible values of x^* that lie on Ω_{Comp} we get $(u_1^*, 0, u_3^*, u_4^*, 0, 0)$. To see this, consider the lemma below.

Lemma 3.3.6. *The system of equation (3.21) admits an equilibrium at $E_{Comp} = (u_1^*, 0, u_3^*, u_4^*, 0, 0)$.*

Proof. Let $u'_1, u'_2, u'_3, u'_4, u'_5, u'_6 = 0$. Since all parameter are positive, then

$$\delta_h u_2 = 0 \quad \implies \quad u_2 = 0$$

Thus, $\frac{ab_m u_2 u_5}{K e^{\ln \left(\frac{H_0}{K} \right) e^{-rt}}} - \mu_m u_6 = 0$ becomes

$$\begin{aligned}
\frac{ab_m(0)u_5}{K e^{\ln \left(\frac{H_0}{K} \right) e^{-rt}}} - \mu_m u_6 &= 0 \\
-\mu_m u_6 &= 0.
\end{aligned}$$

Hence, $u_6 = 0$. Now for $-\frac{ab_mu_2u_5}{Ke^{\ln\left(\frac{H_0}{K}\right)e^{-rt}}} - \mu_mu_5 + \alpha_mu_5 + \alpha_mu_6 = 0$, since $u_2 = 0$ and $u_6 = 0$, we have

$$-\frac{ab_m(0)u_5}{Ke^{\ln\left(\frac{H_0}{K}\right)e^{-rt}}} - \mu_mu_5 + \alpha_mu_5 + \alpha_m(0) = 0$$

$$u_5(\alpha_m - \mu_m) = 0.$$

Therefore, $u_5 = 0$, since $\alpha_m - \mu_m < 0$. Since the system of equation contains either u_2, u_5 or u_6 or both, which has a zero value, then any nonnegative values of u_1, u_3, u_4 satisfies the system of equation. Therefore, $E_{Gomp} = (u_1^*, 0, u_3^*, u_4^*, 0, 0)$ is an equilibrium point. \square

Next Generation Matrix and Basic Reproduction Number

Now if we show that the equilibrium point $E_{Gomp} = (u_1^*, 0, u_3^*, u_4^*, 0, 0)$ is asymptotically stable using the eigenvalues from the next generation matrix, then we get the same result as equation (3.20). Then solving for the next generation matrix we get the eigenvalues

$$\lambda = \pm \sqrt{\frac{a^2b_mu_5 \left(\tilde{b}_hu_3 + b_hu_1 \right)}{K^2\mu_m(\gamma_h + \delta_h)}}. \quad (3.23)$$

Jacobian Matrix

Now, let us show that E_{Gomp} is asymptotically stable using the eigenvalue from the Jacobian matrix. Now if we compute the Jacobian Matrix of the system in order to confirm our lambda, then only the $\frac{\partial f_5}{\partial u_i}, i = 1, 2, \dots, 6$, would change. We can get

$$\begin{array}{lll} \frac{\partial f_5}{\partial u_1} = 0 & \frac{\partial f_5}{\partial u_2} = \frac{-ab_mu_5}{K} & \frac{\partial f_5}{\partial u_3} = 0 \\ \frac{\partial f_5}{\partial u_4} = 0 & \frac{\partial f_5}{\partial u_5} = \frac{-ab_mu_2}{K} - \mu_m + \alpha_m & \frac{\partial f_5}{\partial u_6} = \mu_m + \alpha_m \end{array}$$

Therefore, we have the Jacobian matrix

$$J = \begin{pmatrix} \frac{-ab_hu_6}{K} & 0 & 0 & 0 & 0 & \frac{-ab_hu_1}{K} \\ \frac{ab_hu_6}{K} & -\gamma_h - \delta_h & \frac{a\tilde{b}_hu_6}{K} & 0 & 0 & \frac{ab_hu_1 + a\tilde{b}_hu_3}{K} \\ 0 & \gamma_h & \frac{-a\tilde{b}_hu_6}{K} & 0 & 0 & \frac{-a\tilde{b}_hu_3}{K} \\ 0 & \delta_h & 0 & 0 & 0 & 0 \\ 0 & \frac{-ab_mu_5}{K} & 0 & 0 & \frac{-ab_mu_2}{K} - \mu_m + \alpha_m & \mu_m + \alpha_m \\ 0 & \frac{ab_mu_5}{K} & 0 & 0 & \frac{ab_mu_2}{K} & -\mu_m \end{pmatrix}$$

Thus, we have the following theorem.

Lemma 3.3.7. *The equilibrium point $E_{Gomp} = (u_1^*, 0, u_3^*, u_4^*, 0, 0)$ is locally asymptotically stable.*

Proof. Let $E_{Gomp} = (u_1^*, 0, u_3^*, u_4^*, 0, 0)$ be an equilibrium point of the system of equation. Then the above Jacobian matrix can be deduce to

$$J(E_{Gomp}) = \begin{pmatrix} 0 & 0 & 0 & 0 & 0 & \frac{-ab_h u_1^*}{K} \\ 0 & -\gamma_h - \delta_h & 0 & 0 & 0 & \frac{ab_h u_1^* + a\tilde{b}_{hh} u_3^*}{K} \\ 0 & \gamma_h & 0 & 0 & 0 & \frac{-ab_{hh} u_3^*}{K} \\ 0 & \delta_h & 0 & 0 & 0 & 0 \\ 0 & 0 & 0 & 0 & -\mu_m + \alpha_m & \mu_m + \alpha_m \\ 0 & 0 & 0 & 0 & 0 & -\mu_m \end{pmatrix}$$

Therefore, determining its characteristic polynomial, we have

$$|J(E_{Gomp}) - \lambda I_6| = \begin{vmatrix} -\lambda & 0 & 0 & 0 & 0 & \frac{-ab_h u_1^*}{K} \\ 0 & -\gamma_h - \delta_h - \lambda & 0 & 0 & 0 & \frac{ab_h u_1^* + a\tilde{b}_{hh} u_3^*}{K} \\ 0 & \gamma_h & -\lambda & 0 & 0 & \frac{-ab_{hh} u_3^*}{K} \\ 0 & \delta_h & 0 & -\lambda & 0 & 0 \\ 0 & 0 & 0 & 0 & \alpha_m - \lambda & \mu_m + \alpha_m \\ 0 & 0 & 0 & 0 & 0 & -\mu_m - \lambda \end{vmatrix} = 0$$

implying further that

$$-\lambda^3(-\lambda - \gamma_h - \delta_h)(-\lambda - \mu_m)(-\lambda - \mu_m + \alpha_m) = 0.$$

Hence, we get

$$\begin{aligned} \lambda_1 &= 0 \text{ multiplicity } 3 & \lambda_2 &= -\mu_m \\ \lambda_3 &= -\gamma_h - \delta_h & \lambda_4 &= \alpha_m - \mu_m. \end{aligned}$$

Since $\alpha_m - \mu_m < 0$, all the eigenvalues are negative. Therefore, the system of equation is locally asymptotically stable at the equilibrium point $(u_1^*, 0, u_3^*, u_4^*, 0, 0)$. \square

Numerical Illustrations

In this section, we presented the numerical illustration using the Gompertz growth function for human population and exponential growth function for mosquito population. We let the final time T be 2000 days with initial condition $(10000, 0, 0, 0, 100000, 10)$. Using the same parameter value as Table 3.2, $r = 0.00446$, $\mu_h = 0.0000391$ and $K = 100,000,000$, a phase portrait graph of system (3.21) was simulated using the Python program.

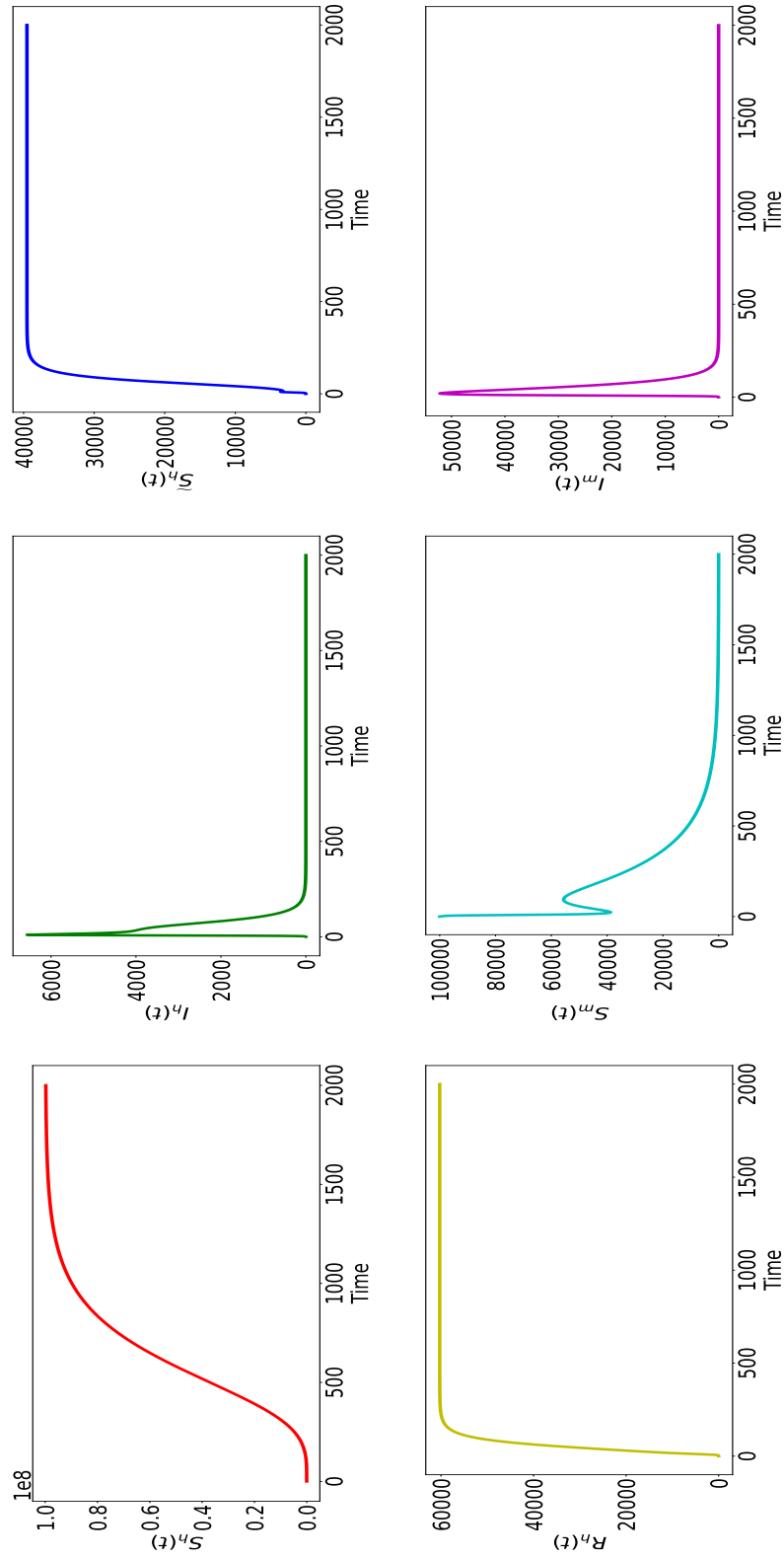


FIGURE 3.8: Behaviour of the solution of each variables in the model 3.19 with dengvaxia versus time using Compertz growth functions for human population and exponential growth function for mosquito population. S_h is the red colour figure, I_h is the green, \tilde{S}_h is the blue, R_h is the yellow, S_m is the cyan and I_m is the magenta.

Figure 3.8 clearly shows a gompertzian growth in the primary susceptible humans. It has the slowest growth at the beginning and towards the end of the time period. It has an early, almost exponential growth rate followed by slower growth rate which reaches a plateau towards the end. On the other hand, secondary susceptible humans follows an increasing linear growth rate for a short time period until it reaches its equilibrium. Moreover, infected humans increases exponentially for 10 days towards its maximum population of 6566.323. It then gradually decreases towards its equilibrium. Whereas recovered humans increases exponentially for 200 days then slowly continuing increasing towards the equilibrium.

For the mosquito population, susceptible humans decreases exponentially for 23 days until it reaches 38733 population, Then it gradually increases up to 55600 population on the 95th day and then decreases towards its equilibrium. Whereas, infected mosquito exponentially increases for 20 days with maximum population of 2199.482 and then exponentially decreases towards its equilibrium.

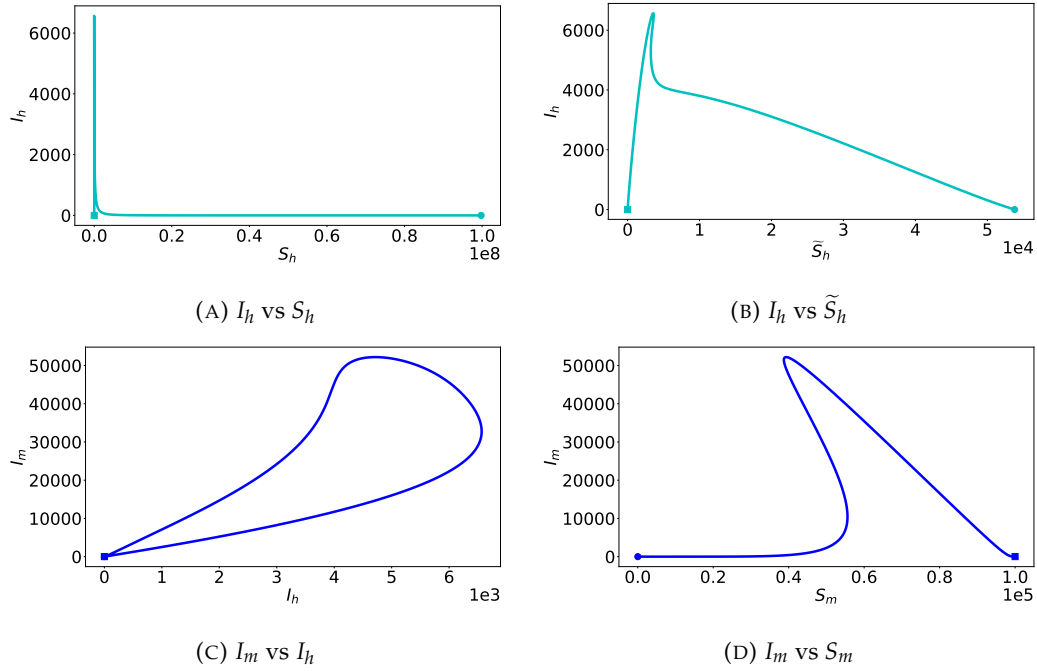


FIGURE 3.9: Phase portrait of the model with dengvaxia using constant growth function showing primary S_h and secondary susceptible \tilde{S}_h versus infected humans I_h in blue color, and susceptible mosquitoes S_m and infected humans I_h versus infected mosquitoes I_m in cyan color. Square and circle indicates the first and last solution of the variables.

For infected humans, figure 3.9a shows that at time $t = 0$, there are no infected humans but have 10,000 primary susceptible humans. For a very short period of time, infected humans increases rapidly while primary susceptible humans increases slowly. Upon reaching the maximum of 6566.323 infected human, infected humans decreases quickly while primary susceptible humans continuous to increase

slowly. Upon reaching the equilibrium of infected humans, primary susceptible humans continues to increase following gompertzian curve.

Figure 3.9b shows that at time $t = 0$, there are no infected and secondary susceptible humans. The figure shows that the variables are directly proportional to each other for all time. For some time, both variables increases up to the maximum of 53787.330 secondary susceptible humans. They then decreases for a short time interval and then increases up to the equilibrium.

Figure 3.9c shows that in the beginning there are 10 infected mosquito and no infected human. As the infected humans increases, infected mosquitoes also increases. After some time, the two variables become inversely proportional. As infected humans decreases, the infected mosquito continue to increase. Then both variables decreases towards zero.

On the other hand, figure 3.9d shows that at time $t = 0$, there are 100,000 susceptible mosquito and 10 infected mosquitoes. The figure shows that the two variables are inversely proportional to each other. For some time, susceptible mosquitoes decreases while infected mosquitoes increases. When it reaches the maximum of 52199.482 infected mosquitoes, infected mosquitoes then decreases while susceptible mosquito increase for a short time period. After then both variables decreases towards zero.

3.4 Choice of Control Strategies

Preventing or reducing dengue virus transmission depends entirely on controlling the mosquito vectors or vaccination. This section applied three control strategies to reduce dengue transmission: vaccination, vector control and the combination of vaccination and vector control.

3.4.1 Vaccination

Dengue fever is the most rapidly spreading mosquito-borne viral disease found in tropical and sub-tropical climates worldwide. It is caused by the single positive-stranded RNA virus of the family *Flaviviridae* that is transmitted to humans through a diurnal mosquito. [56] So far, there is no specific treatment for dengue fever. According to the theory of facilitating antibodies, vaccine research is made more difficult by the need for a vaccine immunizing sustainability and simultaneously against the four serotypes of the virus [50]. Half a dozen vaccine candidates are under study. The most competitive candidate was *Dengvaxia*, by Sanofi Pasteur. Dengvaxia (CYD-TDV) was licensed in December 2015 and has now been approved by regulatory authorities in 20 countries.

CYD-TDV vaccine is for the prevention of dengue disease caused by dengue virus serotypes 1, 2, 3, and 4. It should be administered three doses six months apart of 0.5 mL subcutaneous (SC) administration for individuals aged 9 - 16 years old with laboratory-confirmed previous dengue infection and living in endemic areas.

To account for the vaccine in the model, let us consider the following mathematical model in two different populations.

Constant Human and Mosquito Population of Dengvaxia Model

Let us consider the constant human and mosquito population, that is, $f(H(t)) = 0$ and $g(M(t)) = \mu_m M(t)$. Then our model becomes

$$\begin{aligned}
 u'_1(t) &= -\frac{ab_h u_6(t) u_1(t)}{H_0} - v_1 u_1(t) \\
 u'_2(t) &= \frac{a u_6(t) (b_h u_1(t) + \tilde{b}_h u_3(t))}{H_0} - \gamma_h u_2(t) - \delta_h u_2(t) \\
 u'_3(t) &= \gamma_h u_2(t) - \frac{a \tilde{b}_h u_3(t) u_6(t)}{H_0} - v_3 u_3(t) \\
 u'_4(t) &= \delta_h u_2(t) \\
 u'_5(t) &= -\frac{ab_m u_2(t) u_5(t)}{H_0} + \mu_m u_6(t) \\
 u'_6(t) &= \frac{ab_m u_2(t) u_5(t)}{H_0} - \mu_m u_6(t).
 \end{aligned} \tag{3.24}$$

Where $v_1u_1(t)$ is the vaccination given to the primary susceptible human population, and $v_3u_3(t)$ is the vaccination given to the secondary susceptible human. The total immunity is given by $T'_h(t) = v_1u_1(t) + v_3u_3(t)$.

Note that there exists a unique global in time solution $(u_1, u_2, u_3, u_4, u_5, u_6)$ in $\mathcal{C}(\Omega_{Cons}, \mathbb{R}_+)^6$.

Lemma 3.4.1. *The system of equation (3.24) admits an equilibrium at $E_{VacCons,1} = (0, 0, 0, u_4^*, u_5^*, 0)$.*

Proof. Let $u'_1, u'_2, u'_3, u'_4, u'_5, u'_6 = 0$. Since all parameter are positive, then

$$\delta_h u_2 = 0 \quad \implies \quad u_2 = 0$$

Thus, $\frac{ab_m u_2 u_5}{H} - \mu_m u_6 = 0$ becomes

$$\begin{aligned} \frac{ab_m(0)u_5}{H} - \mu_m u_6 &= 0 \\ -\mu_m u_6 &= 0 \end{aligned}$$

Hence, $u_6 = 0$. Therefore, substituting $u_6 = 0$ and $u_2 = 0$ to both $u'_1 = 0$ and $u'_3 = 0$, we have

$$\begin{aligned} -\frac{ab_h u_6 u_1}{H_0} - v_1 u_1 &= 0 & \gamma_h u_2 - \frac{\tilde{a}b_h u_3 u_6}{H_0} - v_3 u_3 &= 0 \\ -\frac{ab_h(0)u_1}{H_0} - v_1 u_1 &= 0 & \gamma_h(0) - \frac{\tilde{a}b_h u_3(0)}{H_0} - v_3 u_3 &= 0 \\ -v_1 u_1 &= 0 & -v_3 u_3 &= 0 \end{aligned}$$

Since $v_1, v_3 > 0$, $u_1 = 0$ and $u_3 = 0$. Consequently, since system (3.24) contains either u_1, u_2, u_3 or u_6 or both, which has a zero value, then any nonnegative values of u_4^*, u_5^* satisfies the system of equation. Therefore, $E_{VacCons,1} = (0, 0, 0, u_4^*, u_5^*, 0)$ is an equilibrium point. \square

Now, in solving for the next generation matrix, there is no changes in F and V in Section 6.1. Therefore, the eigenvalues of system (3.24) are

$$\lambda = \pm \sqrt{\frac{a^2 b_m u_5 (\tilde{b}_h u_3 + b_h u_1)}{H_0^2 \mu_m (\gamma_h + \delta_h)}}$$

Therefore, we have the following theorem.

Lemma 3.4.2. *The equilibrium point $E_{VacCons,1} = (0, 0, 0, u_4^*, u_5^*, 0)$ of the system of equation (3.24) is locally asymptotically stable.*

Proof. From the above eigenvalues,

$$\rho(FV^{-1}) = \pm \sqrt{\frac{a^2 b_m u_5^* (\tilde{b}_h(0) + b_h(0))}{H_0^2 \mu_m (\gamma_h + \delta_h)}} = 0 < 1.$$

Therefore, the system of equation is locally asymptotically stable at $E_{VacCons,1}$. \square

3.4.2 Vector Control

Vector control is a method to limit or eradicate the vectors which transmit disease pathogens. The most frequent type of vector control uses a variety of strategies such as habitat and environmental control, reducing vector contact, chemical control, and biological control.

Let us consider the following model in two different populations to include vectorial control.

Vector Control with Constant Human and Mosquito Population

Let us consider the constant human and mosquito population where $f(H(t)) = 0$ and $g(M(t)) = \mu_m M(t)$. Then our model would become

$$\begin{aligned}
 u_1'(t) &= -\frac{ab_h u_6(t) u_1(t)}{H_0} \\
 u_2'(t) &= \frac{au_6(t) (b_h u_1(t) + \tilde{b}_h u_3(t))}{H_0} - \gamma_h u_2(t) - \delta_h u_2(t) \\
 u_3'(t) &= \gamma_h u_2(t) - \frac{a\tilde{b}_h u_3(t) u_6(t)}{H_0} \\
 u_4'(t) &= \delta_h u_2(t) \\
 u_5'(t) &= -\frac{ab_m u_2(t) u_5(t)}{H_0} + \mu_m u_6(t) - v_5 u_5(t) \\
 u_6'(t) &= \frac{ab_m u_2(t) u_5(t)}{H_0} - \mu_m u_6(t) - v_6 u_6(t)
 \end{aligned} \tag{3.25}$$

Where $v_5 u_5(t)$ and $v_6 u_6(t)$ are the introduction of vectorial control to the environment resulting to the removal of susceptible and infectious mosquito. The total controlled mosquito control is given by $T'_M(t) = v_5 u_5(t) + v_6 u_6(t)$.

Again there exists a unique global in time solution $(u_1, u_2, u_3, u_4, u_5, u_6)$ in $\mathcal{C}(\Omega_{Cons}, \mathbb{R}_+)^6$.

Lemma 3.4.3. *The system of equation (3.25) admits an equilibrium at $E_{VecCons,1} = (u_1^*, 0, u_3^*, u_4^*, 0, 0)$.*

Proof. Let $u_1', u_2', u_3', u_4', u_5', u_6' = 0$. Since all parameter are positive, then

$$\delta_h u_2 = 0 \implies u_2 = 0$$

Thus, $\frac{ab_m u_2 u_5}{H_0} - \mu_m u_6 - v_6 u_6 = 0$ becomes

$$-\mu_m u_6 - v_6 u_6 = 0$$

$$(-\mu_m - v_6) u_6 = 0$$

Since $-\mu_m - v_6 \neq 0$, $u_6 = 0$. Therefore, substituting $u_6 = 0$ and $u_2 = 0$ to both $u'_5 = 0$, we have

$$\begin{aligned} -\frac{ab_mu_2u_5}{H_0} + \mu_mu_6 - v_5u_5 &= 0 \\ -\frac{ab_m(0)u_5}{H_0} + \mu_m(0) - v_5u_5 &= 0 \\ -v_5u_5 &= 0 \end{aligned}$$

Since $v_5 > 0$, $u_5 = 0$. Consequently, since the system (3.25) contains either u_2 , u_5 or u_6 or both, which has a zero value, then any nonnegative values of u_1^*, u_3^*, u_4^* satisfies the system of equation. Therefore, $E_{VecCons,1} = (u_1^*, 0, u_3^*, u_4^*, 0, 0)$ is an equilibrium point. \square

Since the infected individuals are in u_2 and u_6 , then the next generation matrix is

$$\mathcal{F} = \begin{pmatrix} \frac{au_6(b_hu_1 + \tilde{b}_hu_3)}{H_0} \\ \frac{ab_mu_2u_5}{H_0} \end{pmatrix} \quad \mathcal{V} = \begin{pmatrix} (\gamma_h + \delta_h)u_2 \\ (\mu_m + v_6)u_6 \end{pmatrix}$$

where \mathcal{F} as the appearance of new infections in each compartment and \mathcal{V} as the transitions between all other compartments. Thus,

$$F = \begin{pmatrix} \frac{\partial \mathcal{F}_1}{\partial u_2} & \frac{\partial \mathcal{F}_1}{\partial u_6} \\ \frac{\partial \mathcal{F}_2}{\partial u_2} & \frac{\partial \mathcal{F}_2}{\partial u_6} \end{pmatrix} \quad \text{and} \quad V = \begin{pmatrix} \frac{\partial \mathcal{V}_1}{\partial u_2} & \frac{\partial \mathcal{V}_1}{\partial u_6} \\ \frac{\partial \mathcal{V}_2}{\partial u_2} & \frac{\partial \mathcal{V}_2}{\partial u_6} \end{pmatrix}$$

we have

$$F = \begin{pmatrix} 0 & \frac{a(b_hu_1 + \tilde{b}_hu_3)}{H_0} \\ \frac{ab_mu_5}{H_0} & 0 \end{pmatrix}$$

$$\text{and} \quad V = \begin{pmatrix} \gamma_h + \delta_h & 0 \\ 0 & \mu_m + v_6 \end{pmatrix} \quad \text{where} \quad V^{-1} = \begin{pmatrix} \frac{1}{\gamma_h + \delta_h} & 0 \\ 0 & \frac{1}{\mu_m + v_6} \end{pmatrix}.$$

Consequently,

$$\begin{aligned} FV^{-1} &= \begin{pmatrix} 0 & \frac{a(b_hu_1 + \tilde{b}_hu_3)}{H_0} \\ \frac{ab_mu_5}{H_0} & 0 \end{pmatrix} \begin{pmatrix} \frac{1}{\gamma_h + \delta_h} & 0 \\ 0 & \frac{1}{\mu_m + v_6} \end{pmatrix} \\ &= \begin{pmatrix} 0 & \frac{a(b_hu_1 + \tilde{b}_hu_3)}{H_0(\mu_m + v_6)} \\ \frac{ab_mu_5}{H_0(\gamma_h + \delta_h)} & 0 \end{pmatrix} \end{aligned}$$

Since the characteristic polynomial is $\det |FV^{-1} - \lambda I|$, we have

$$\begin{aligned} \det |FV^{-1} - \lambda I| &= \begin{vmatrix} -\lambda & \frac{a(b_h u_1 + \tilde{b}_h u_3)}{H_0(\mu_m + v_6)} \\ \frac{ab_m u_5}{H_0(\gamma_h + \delta_h)} & -\lambda \end{vmatrix} \\ &= \lambda^2 - \frac{a^2 b_m u_5 (b_h u_1 + \tilde{b}_h u_3)}{H_0^2(\gamma_h + \delta_h)(\mu_m + v_6)} \end{aligned}$$

Therefore, the eigenvalues of system (3.25) are

$$\lambda = \pm \sqrt{\frac{a^2 b_m u_5 (\tilde{b}_h u_3 + b_h u_1)}{H_0^2(\mu_m + v_6)(\gamma_h + \delta_h)}} \quad (3.26)$$

and we have the following theorem.

Lemma 3.4.4. *The equilibrium point $E_{VecCons,1} = (u_1^*, 0, u_3^*, u_4^*, 0, 0)$ of the system of equation (3.25) is locally asymptotically stable.*

Proof. From the above eigenvalues,

$$\rho(FV^{-1}) = \pm \sqrt{\frac{a^2 b_m(0) (\tilde{b}_h u_3^* + b_h u_1^*)}{H_0^2(\mu_m + v_6)(\gamma_h + \delta_h)}} = 0 < 1.$$

Therefore, the system of equation (3.25) is locally asymptotically stable at $E_{VecCons,1}$. \square

Theorem 3.4.5. *The equilibrium point $E_{VecCons,1} = (u_1^*, 0, u_3^*, u_4^*, 0, 0)$ of the system of equation (3.25) is globally asymptotically stable.*

3.4.3 Combination of Vaccination and Vector Control

Let us combine the dengue vaccination and the vectorial control in our model using two growth function.

Constant Human and Mosquito Population with Vaccination and Vector Control

Consider a constant growth for human and mosquito population. We have $f(H(t)) = 0$ and $g(M(t)) = \mu_m M(t)$. Then our model becomes

$$\begin{aligned}
u_1'(t) &= -\frac{ab_h u_6(t) u_1(t)}{H_0} - v_1 u_1(t) \\
u_2'(t) &= \frac{au_6(t) (b_h u_1(t) + \tilde{b}_h u_3(t))}{H_0} - \gamma_h u_2(t) - \delta_h u_2(t) \\
u_3'(t) &= \gamma_h u_2(t) - \frac{a\tilde{b}_h u_3(t) u_6(t)}{H_0} - v_3 u_3(t) \\
u_4'(t) &= \delta_h u_2(t) \\
u_5'(t) &= -\frac{ab_m u_2(t) u_5(t)}{H_0} + \mu_m u_6(t) - v_5 u_5(t) \\
u_6'(t) &= \frac{ab_m u_2(t) u_5(t)}{H_0} - \mu_m u_6(t) - v_6 u_6(t)
\end{aligned} \tag{3.27}$$

where total human immunity is given by $T_H'(t) = v_1 u_1(t) + v_3 u_3(t)$ and total vectorial control is given by $T_M'(t) = v_5 u_5(t) + v_6 u_6(t)$.

There exists a unique global in time solution $(u_1, u_2, u_3, u_4, u_5, u_6)$ in $\mathcal{C}(\Omega_{Cons}, \mathbb{R}_+)^6$.

Lemma 3.4.6. *The system of equation (3.27) admits an equilibrium at $E_{CombCons,1} = (0, 0, 0, u_4^*, 0, 0)$.*

Proof. Let $u_1', u_2', u_3', u_4', u_5', u_6' = 0$. Since all parameter are positive, then

$$\delta_h u_2 = 0 \implies u_2 = 0.$$

Thus, $\frac{ab_m u_2 u_5}{H} - \mu_m u_6 - v_6 u_6 = 0$ becomes

$$\begin{aligned}
\frac{ab_m(0)u_5}{H} - \mu_m u_6 - v_6 u_6 &= 0 \\
(-\mu_m - v_6)u_6 &= 0
\end{aligned}$$

Hence, $u_6 = 0$. Therefore, substituting $u_6 = 0$ to both $u_1' = 0$ and $u_3' = 0$, we have

$$\begin{aligned}
-\frac{ab_h u_6 u_1}{H_0} - v_1 u_1 &= 0 & \gamma_h u_2 - \frac{a\tilde{b}_h u_3 u_6}{H_0} - v_3 u_3 &= 0 \\
-\frac{ab_h(0)u_1}{H_0} - v_1 u_1 &= 0 & \gamma_h(0) - \frac{a\tilde{b}_h u_3(0)}{H_0} - v_3 u_3 &= 0 \\
-v_1 u_1 &= 0 & -v_3 u_3 &= 0
\end{aligned}$$

Since $v_1, v_3 > 0$, $u_1 = 0$ and $u_3 = 0$. Now, substituting $u_6 = 0$ to $-\frac{ab_m u_2 u_5}{H_0} + \mu_m u_6 - v_5 u_5 = 0$, we get

$$\begin{aligned}
-\frac{ab_m(0)u_5}{H_0} + \mu_m(0) - v_5 u_5 &= 0 \\
-v_5 u_5 &= 0 \\
u_5 &= 0
\end{aligned}$$

Consequently, since the system (3.27) contains either u_1, u_2, u_3, u_5 or u_6 or both, which has a zero value, then any nonnegative values of u_4^* satisfies the system of equation. Therefore, $E_{CombCons,1} = (0, 0, 0, u_4^*, 0, 0)$ is an equilibrium point. \square

Now, in solving for the next generation matrix, there is no changes in F and V as in Section 3.3.1. Therefore, the eigenvalues of system are the same as equation (3.26) which are

$$\lambda = \pm \sqrt{\frac{a^2 b_m u_5 (\tilde{b}_h u_3 + b_h u_1)}{H_0^2 (\mu_m + v_6) (\gamma_h + \delta_h)}}.$$

Therefore, we have the following theorem.

Lemma 3.4.7. *The equilibrium point $E_{CombCons,1} = (0, 0, 0, u_4^*, 0, 0)$ of the system of equation (3.27) is locally asymptotically stable.*

Proof. Since $u_1^*, u_3^*, u_5^* = 0$, the above eigenvalues would become

$$\lambda = \pm \sqrt{\frac{a^2 b_m (0) (\tilde{b}_h (0) + b_h (0))}{H_0^2 (\mu_m + v_6) (\gamma_h + \delta_h)}} = 0 < 1.$$

Therefore, the system of equation is locally asymptotically stable at $E_{CombCons,1}$. \square

3.4.4 Summary of the Effective Reproduction Number of Different Control Strategies

Instead of \mathcal{R}_0 , it is more interesting to consider the effective reproduction number R_{eff} . We have

$$\begin{aligned} R_{eff} &= \pm \sqrt{\frac{a^2 b_m u_5 (b_h u_1 + \tilde{b}_h u_3)}{\mu_m H_0^2 (\gamma_h + \delta_h)}} \text{ without control} \\ R_{eff} &= \pm \sqrt{\frac{a^2 b_m u_5 (\tilde{b}_h u_3 + b_h u_1)}{H_0^2 \mu_m (\gamma_h + \delta_h)}} \text{ for vaccination only} \\ R_{eff} &= \pm \sqrt{\frac{a^2 b_m u_5 (\tilde{b}_h u_3 + b_h u_1)}{H_0^2 (\mu_m + v_5) (\gamma_h + \delta_h)}} \text{ for vector control only} \\ R_{eff} &= \pm \sqrt{\frac{a^2 b_m u_5 (\tilde{b}_h u_3 + b_h u_1)}{H_0^2 (\mu_m + v_5) (\gamma_h + \delta_h)}} \text{ for both vaccination and vector control.} \end{aligned}$$

3.5 Optimal Control strategy

In the next section, we determine the optimal control in minimizing infected humans by applying vaccination and vectorial control. Using the constant growth function for human and mosquito population, a numerical simulation is presented using vaccination only and vector control only. For the combination of vaccination and vector control, we use the entomological growth function for mosquito population.

3.5.1 Minimizing Infected Humans by Optimal Vaccination

Let us consider the constant growth population in model for the human population $H'(t) = f(H(t)) = 0$ and a general mosquito growth population $M'(t) = \mu_m M(t) + g(M(t))$. We will now write a control problem that aim to minimize the number of infected human by optimal vaccination. We attribute two control inputs, w_1 and w_3 for the human population. Here, the action of $w_1(t)$ is the percentage of primary susceptible and $w_3(t)$ is the percentage of secondary susceptible individual being vaccinated per unit of time. Furthermore, we assume that both control inputs are measurable functions that takes its values in a positively bounded set $W = [0, w_H]^2$. Thus we consider the objective function

$$\mathcal{J}(w_1, w_3) = \int_0^T \left(u_2(t) + \frac{1}{2} A_1 w_1^2(t) + \frac{1}{2} A_3 w_3^2(t) \right) dt$$

subject to

$$\begin{aligned} u_1'(t) &= -\frac{ab_h u_6(t) u_1(t)}{H_0} - w_1(t) u_1(t) \\ u_2'(t) &= \frac{au_6(t) (b_h u_1(t) + \tilde{b}_h u_3(t))}{H_0} - \gamma_h u_2(t) - \delta_h u_2(t) \\ u_3'(t) &= \gamma_h u_2(t) - \frac{\tilde{a} \tilde{b}_h u_3(t) u_6(t)}{H_0} - w_3(t) u_3(t) \\ u_4'(t) &= \delta_h u_2(t) \\ u_5'(t) &= -\frac{ab_m u_2(t) u_5(t)}{H_0} - \mu_m u_5(t) + g(M(t)) \\ u_6'(t) &= \frac{ab_m u_2(t) u_5(t)}{H_0} - \mu_m u_6(t) \end{aligned} \tag{3.28}$$

for $t \in [0, T]$, with $0 \leq w_1, w_3 \leq w_H$. The variables A_j are the positive weights associated with the control variables w_1 and w_3 , respectively. They corresponds to the effort of vaccinating the primary susceptible human u_1 and the secondary susceptible human u_3 compartment.

Lemma 3.5.1. *There exists an optimal control $w^* = (w_1^*(t), w_3^*(t))$ such that*

$$\mathcal{J}(w_1^*, w_3^*) = \min_{w \in W} \mathcal{J}(w_1, w_3)$$

under the constraint $(u_1, u_2, u_3, u_4, u_5, u_6)$ is a solution to the ordinary differential equation (3.28).

Proof. Let $(w_1^n, w_3^n)_{n \in \mathbb{N}}$ a minimizing sequence of controls in $W = [0, w_H]^2$, i.e.

$$\lim_{n \rightarrow \infty} J(w_1^n, w_3^n) = \inf_{w \in W} J(w_1, w_3).$$

This sequence is bounded by w_H , and using sequential Banach–Alaoglu theorem to extract a subsequence weak* convergent to (w_1^*, w_3^*) in $L^\infty([0, T]; W)$. For $n \in \mathbb{N}$, we denote $(u_1^n, u_2^n, \dots, u_6^n)$ the solution corresponding to the control (w_1^n, w_3^n) . Similarly to Lemma 3.2.2, one can prove that $(u_1^n, u_2^n, \dots, u_6^n)$ is nonnegative and uniformly bounded. Then, $((u_1^n)', (u_2^n)', \dots, (u_6^n)')$ is also bounded, or in other words $(u_1^n, u_2^n, \dots, u_6^n)$ is in $W^{1,\infty}([0, T])$. Thus, from Arzelà–Ascoli theorem, we can extract a subsequence of $((u_1^n, u_2^n, \dots, u_6^n))_n$ that strongly converges to $(u_1^*, u_2^*, \dots, u_6^*)$ in $\mathcal{C}^0([0, T])$. Rewriting (3.28) in integral form, we get

$$\begin{aligned} & \int_0^T (u_1^n(t) - u_0^n) \varphi_1(t) dt - \int_0^T (u_1(t) - u_0) \varphi_1(t) dt \\ &= - \int_0^T \frac{ab_h}{H_0} (u_6^n(s) u_1^n(s) - u_6(s) u_1(s)) + (w_1^n(s) u_1^n(s) - w_1(s) u_1(s)) dt \end{aligned}$$

or again

$$\begin{aligned} & \int_0^T (u_1^n(t) - u_1) dt - \int_0^T (u_0^n - u_0) dt \\ &= - \int_0^T \frac{ab_h}{H_0} ((u_1^n(t) - u_1(t)) u_6^n(t) + (u_6^n(t) - u_6(t)) u_1(t)) \\ & \quad + (w_1^n(t) - w_1(t)) u_1^n(t) + (u_1^n(t) - u_1(t)) w_1(t) dt \end{aligned}$$

that converges to 0 as $n \rightarrow +\infty$. Deal similarly for the remaining equations, the limit $(u_1^*, u_2^*, \dots, u_6^*)$ is then the solution of the system for the limit control (w_1^*, w_3^*) .

Finally,

$$\begin{aligned} \liminf_{n \rightarrow \infty} J(w_1^n, w_3^n) &= \liminf_{n \rightarrow \infty} \left(\int_0^T \left(u_2^n(t) + \frac{1}{2} A_1(w_1^n)^2(t) + \frac{1}{2} A_3(w_3^n)^2(t) \right) dt \right) \\ &\geq \int_0^T \left(u_2^*(t) + \frac{1}{2} A_1(w_1^*)^2(t) + \frac{1}{2} A_3(w_3^*)^2(t) \right) dt \\ &= \mathcal{J}(w_1^*, w_3^*) \end{aligned}$$

by lower semi-continuity of \mathcal{J} . □

Pontryagin's maximum principle is used to find the best possible control for taking a dynamical system from one state to another. It states that it is necessary for any optimal control along with the optimal state trajectory to solve the so-called Hamiltonian system [42] plus the maximum condition of the Hamiltonian. These necessary conditions become sufficient under certain convexity conditions on the objective and

constraint functions. Now let us apply the Pontryagin's Maximum Principle in our system. We state the lemma below.

Lemma 3.5.2. *There exists the adjoint variables $\lambda_i, i = 1, 2, \dots, 6$ of the system (3.28) that satisfy the following backward in time system of ordinary differential equation.*

$$\begin{aligned}
-\frac{d\lambda_1}{dt} &= \lambda_1 \left(\frac{-ab_h u_6}{H_0} - w_1 \right) + \lambda_2 \frac{ab_h u_6}{H_0} \\
-\frac{d\lambda_2}{dt} &= 1 + \lambda_2 (-\gamma_h - \delta_h) + \lambda_3 \gamma_h + \lambda_4 \delta_h - \lambda_5 \frac{ab_m u_5}{H_0} + \lambda_6 \frac{ab_m u_5}{H_0} \\
-\frac{d\lambda_3}{dt} &= \lambda_2 \frac{\tilde{a}b_h u_6}{H_0} + \lambda_3 \left(\frac{-\tilde{a}b_h u_6}{H_0} - w_3 \right) \\
-\frac{d\lambda_4}{dt} &= 0 \\
-\frac{d\lambda_5}{dt} &= \lambda_5 \left(-\frac{ab_m u_2}{H_0} - \mu_m + \frac{\partial g}{\partial u_5} \right) + \lambda_6 \frac{ab_m u_2}{H_0} \\
-\frac{d\lambda_6}{dt} &= -\lambda_1 \frac{ab_h u_1}{H_0} + \lambda_2 \frac{ab_h u_1 + \tilde{a}b_h u_3}{H_0} - \lambda_3 \frac{\tilde{a}b_h u_3}{H_0} + \lambda_5 \frac{\partial g}{\partial u_6} - \lambda_6 \mu_m
\end{aligned} \tag{3.29}$$

with the transversality condition $\lambda(T) = 0$.

Proof. Using the Hamiltonian for system (3.28), we have

$$\begin{aligned}
\mathcal{H} &= \mathcal{L}(w_1, w_3) + \lambda_1(t)u'_1(t) + \lambda_2(t)u'_2(t) \\
&\quad + \lambda_3(t)u'_3(t) + \lambda_4(t)u'_4(t) + \lambda_5(t)u'_5(t) + \lambda_6(t)u'_6(t) \\
&= u_2 + \frac{1}{2}A_1 w_1^2 + \frac{1}{2}A_3 w_3^2 + \lambda_1 \left(-\frac{ab_h u_6 u_1}{H_0} - w_1 u_1 \right) \\
&\quad + \lambda_2 \left(\frac{au_6 (b_h u_1 + \tilde{b}_h u_3)}{H_0} - \gamma_h u_2 - \delta_h u_2 \right) \\
&\quad + \lambda_3 \left(\gamma_h u_2 - \frac{\tilde{a}b_h u_3 u_6}{H_0} - w_3 u_3 \right) + \lambda_4 (\delta_h u_2) \\
&\quad + \lambda_5 \left(-\frac{ab_m u_2 u_5}{H_0} - \mu_m u_5 + g(u_5, u_6) \right) + \lambda_6 \left(\frac{ab_m u_2 u_5}{H_0} - \mu_m u_6 \right)
\end{aligned} \tag{3.30}$$

Therefore, finding the partial derivatives of \mathcal{H} with respect to u_i 's, $i = 1, 2, \dots, 6$, we have

$$\begin{aligned}\frac{\partial \mathcal{H}}{\partial u_1} &= \lambda_1 \left(\frac{-ab_h u_6}{H_0} - w_1 \right) + \lambda_2 \frac{ab_h u_6}{H_0} \\ \frac{\partial \mathcal{H}}{\partial u_2} &= 1 + \lambda_2 (-\gamma_h - \delta_h) + \lambda_3 \gamma_h + \lambda_4 \delta_h - \lambda_5 \frac{ab_m u_5}{H_0} + \lambda_6 \frac{ab_m u_5}{H_0} \\ \frac{\partial \mathcal{H}}{\partial u_3} &= \lambda_2 \frac{\tilde{a}b_h u_6}{H_0} + \lambda_3 \left(\frac{-\tilde{a}b_h u_6}{H_0} - w_3 \right) \\ \frac{\partial \mathcal{H}}{\partial u_4} &= 0 \\ \frac{\partial \mathcal{H}}{\partial u_5} &= \lambda_5 \left(-\frac{ab_m u_2}{H_0} - \mu_m + \frac{\partial g}{\partial u_5} \right) + \lambda_6 \frac{ab_m u_2}{H_0} \\ \frac{\partial \mathcal{H}}{\partial u_6} &= -\lambda_1 \frac{ab_h u_1}{H_0} + \lambda_2 \frac{ab_h u_1 + \tilde{a}b_h u_3}{H_0} - \lambda_3 \frac{\tilde{a}b_h u_3}{H_0} + \lambda_5 \frac{\partial g}{\partial u_6} - \lambda_6 \mu_m.\end{aligned}$$

Then the adjoint system is defined by $\frac{d\lambda_1}{dt} = -\frac{\partial \mathcal{H}}{\partial u_1}, \frac{d\lambda_2}{dt} = -\frac{\partial \mathcal{H}}{\partial u_2}, \frac{d\lambda_3}{dt} = -\frac{\partial \mathcal{H}}{\partial u_3}, \frac{d\lambda_4}{dt} = -\frac{\partial \mathcal{H}}{\partial u_4}, \frac{d\lambda_5}{dt} = -\frac{\partial \mathcal{H}}{\partial u_5}$ and $\frac{d\lambda_6}{dt} = -\frac{\partial \mathcal{H}}{\partial u_6}$. We have the following

$$\begin{aligned}\frac{d\lambda_1}{dt} &= \lambda_1 \left(\frac{ab_h u_6}{H_0} + w_1 \right) - \lambda_2 \frac{ab_h u_6}{H_0} \\ \frac{d\lambda_2}{dt} &= -1 + \lambda_2 (\gamma_h + \delta_h) - \lambda_3 \gamma_h - \lambda_4 \delta_h + \lambda_5 \frac{ab_m u_5}{H_0} - \lambda_6 \frac{ab_m u_5}{H_0} \\ \frac{d\lambda_3}{dt} &= -\lambda_2 \frac{\tilde{a}b_h u_6}{H_0} + \lambda_3 \left(\frac{\tilde{a}b_h u_6}{H_0} + w_3 \right) \\ \frac{d\lambda_4}{dt} &= 0 \\ \frac{d\lambda_5}{dt} &= \lambda_5 \left(\frac{ab_m u_2}{H_0} + \mu_m - \frac{\partial g}{\partial u_5} \right) - \lambda_6 \frac{ab_m u_2}{H_0} \\ \frac{d\lambda_6}{dt} &= \lambda_1 \frac{ab_h u_1}{H_0} - \lambda_2 \frac{ab_h u_1 + \tilde{a}b_h u_3}{H_0} + \lambda_3 \frac{\tilde{a}b_h u_3}{H_0} - \lambda_5 \frac{\partial g}{\partial u_6} + \lambda_6 \mu_m.\end{aligned}$$

□

Theorem 3.5.3. *The optimal control variables, for $j = 1, 3$, are given by*

$$w_j^* = \max \left(0, \min \left(\frac{\lambda_j u_j}{A_j}, w_H \right) \right).$$

Proof. By the Pontryagin maximum principle, the optimal control w^* minimizes the Hamiltonian given by (3.30). We have

$$\frac{\partial H}{\partial w_j} = 0, \quad \text{for all } j = 1, 3 \quad \text{at } w_j = w_j^*.$$

Thus, we get

$$\frac{\partial H}{\partial w_1} = A_1 w_1 - \lambda_1 u_1, \quad \frac{\partial H}{\partial w_3} = A_3 w_3 - \lambda_3 u_3.$$

Implying further that

$$w_1^* = \frac{\lambda_1 u_1}{A_1} \quad w_3^* = \frac{\lambda_3 u_3}{A_3}.$$

Therefore, the optimal control derived from the stationary condition $\frac{d\lambda_i}{dt}$ is given by

$$w_1^* = \begin{cases} 0 & \text{if } \frac{\lambda_1 u_1}{A_1} \leq 0 \\ \frac{\lambda_1 u_1}{A_1} & \text{if } \frac{\lambda_1 u_1}{A_1} < w_H \\ w_H & \text{if } \frac{\lambda_1 u_1}{A_1} \geq w_H \end{cases} \quad w_3^* = \begin{cases} 0 & \text{if } \frac{\lambda_3 u_3}{A_3} \leq 0 \\ \frac{\lambda_3 u_3}{A_3} & \text{if } \frac{\lambda_3 u_3}{A_3} < w_H \\ w_H & \text{if } \frac{\lambda_3 u_3}{A_3} \geq w_H \end{cases}$$

□

Numerical Simulation of Optimal Vaccination using Constant Mosquito Population

This section gives the numerical analyses of the vaccination method through dengue in minimizing the infected human population in the dengue outbreak. We consider a constant growth population for the mosquito population and fixed time T to 100 days or two and a half months, which is around the average infection season duration. The parameters value used are the same as in Table 3.2 and the values of control weights set initially at $A_1 = 0.1$ and $A_3 = 1$. Note that the effort in operating vaccination control w_3 is set higher than the effort in operating vaccination control w_1 , since primary susceptible humans are readily available in the population compared to the secondary susceptible individual, vaccinating them would render effortless.

The optimality system is numerically solved using the following gradient algorithm written in Python.

Algorithm:

Initially we set $u_0 = [1.e4, 0., 0., 0., 1.e5, 1e3]$ with $H_0 = u_0[0] + u_0[1] + u_0[2] + u_0[3]$ and $M_0 = u_0[4] + u_0[5]$. We choose a random positive value for w_1 and w_3 between $]0, 1[$ with $W = (w_1, w_3)$.

While $|H(w_j, u_i, \lambda_i)| > \epsilon$.

1. Solve the direct objective problem for t from 0 to T

$$\begin{aligned} u_1'(t) &= -\frac{ab_h u_6(t) u_1(t)}{H_0} - w_1(t) u_1(t) \\ u_2'(t) &= \frac{au_6(t) (b_h u_1(t) + \tilde{b}_h u_3(t))}{H_0} - \gamma_h u_2(t) - \delta_h u_2(t) \\ u_3'(t) &= \gamma_h u_2(t) - \frac{a\tilde{b}_h u_3(t) u_6(t)}{H_0} - w_3(t) u_3(t) \\ u_4'(t) &= \delta_h u_2(t) \\ u_5'(t) &= -\frac{ab_m u_2(t) u_5(t)}{H_0} + \mu_m u_6(t) \\ u_6'(t) &= \frac{ab_m u_2(t) u_5(t)}{H_0} - \mu_m u_6(t) \end{aligned}$$

2. Solve the adjoint system for t from T to 0

$$\begin{aligned} -\frac{d\lambda_1}{dt} &= \frac{ab_h u_6}{H_0} (-\lambda_1 + \lambda_2) - \lambda_1 w_1 \\ -\frac{d\lambda_2}{dt} &= 1 - \gamma_h (\lambda_2 - \lambda_3) - \delta_h (\lambda_2 - \lambda_4) - \frac{ab_m u_5}{H_0} (\lambda_5 - \lambda_6) \\ -\frac{d\lambda_3}{dt} &= \frac{a\tilde{b}_h u_6}{H_0} (\lambda_2 - \lambda_3) - \lambda_3 w_3 \\ -\frac{d\lambda_4}{dt} &= 0 \\ -\frac{d\lambda_5}{dt} &= \frac{ab_m u_2}{H_0} (-\lambda_5 + \lambda_6) \\ -\frac{d\lambda_6}{dt} &= -\frac{ab_h u_1}{H_0} (\lambda_1 - \lambda_2) + \frac{a\tilde{b}_h u_3}{H_0} (\lambda_2 - \lambda_3) + \mu_m (\lambda_5 - \lambda_6) \end{aligned}$$

3. Using the value of u_i 's in step 1 and λ_i 's in step 2, we solve the $W_{new} = (w_1, w_3)$ such that, for $j = 1, 3$

$$w_j^* = \begin{cases} 0 & \text{if } \frac{\lambda_j u_j}{A_j} \leq 0 \\ \frac{\lambda_j u_j}{A_j} & \text{if } \frac{\lambda_j u_j}{A_j} < w_H \\ w_H & \text{if } \frac{\lambda_j u_j}{A_j} \geq w_H \end{cases}$$

4. Compute $H(w_j, u_i, \lambda_i)$.

A finite difference scheme is used to numerically solve direct and the adjoint system of ordinary differential equations. More precisely, an explicit correction Adams-Bashford and implicit correction Adams-Moulton of order 2 is written in python.

Setting $w_H = 1$ with error $Err = 1$ and tolerance $tol = 0.01$. Note that in the human compartment, the total immunity to dengue by means of implementing the Dengvaxia vaccine is denoted by T_h which is given by $T_h(t) = w_1(t)u_1(t) + w_3(t)u_3(t)$. Using the algorithm above, get the following figure.

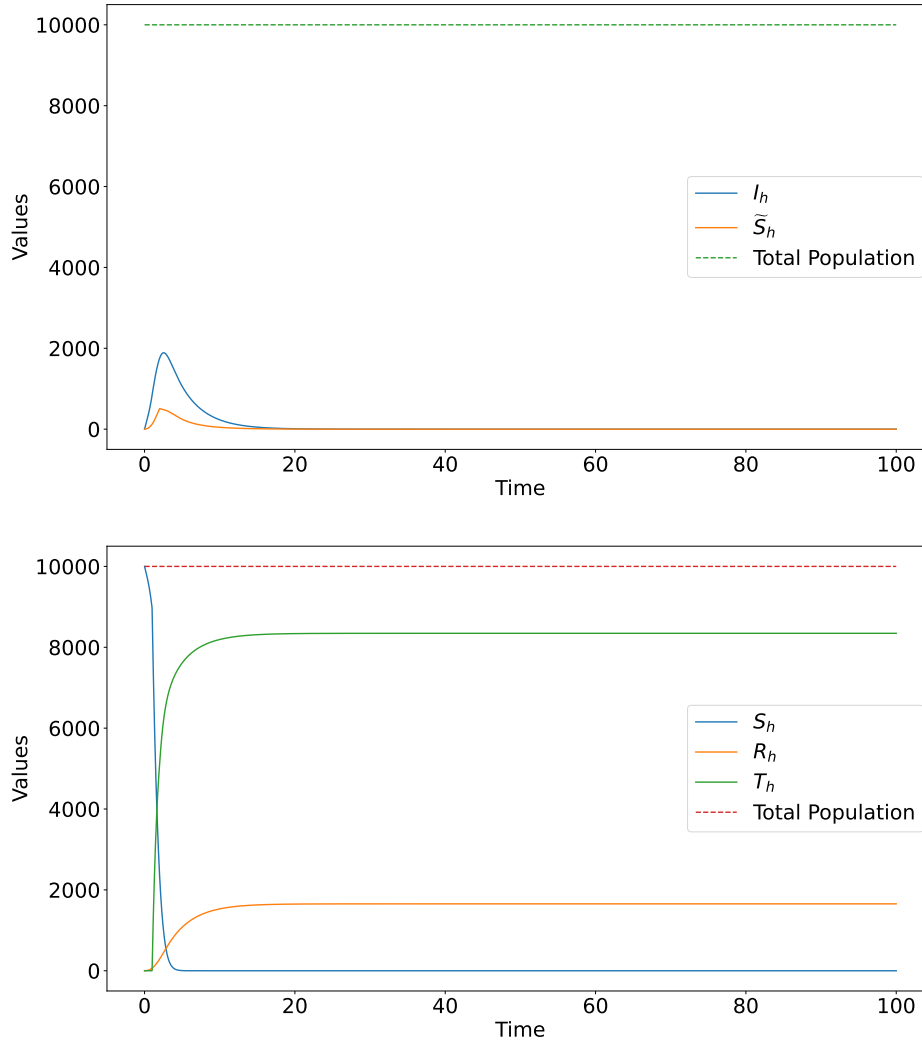


FIGURE 3.10: Behaviour of the solution of infected and secondary susceptible humans (top) and primary susceptible, recovered and totally immune humans (bottom) in optimal vaccination using constant growth function for human and mosquito population.

Figure 3.10 shows that for 100 days, it would only take two days for the infected human u_2 population to reach its highest point at 510 population while it takes around two and a half days for the secondary susceptible u_3 human population to reach its highest point at 1889 individual and then decrease there population going there equilibrium at day 80 and 73, respectively. While both recovered human u_3 and immune human T_h converge at the equilibrium on day 40 at 1654 and

8345 population, respectively. The figure also shows that vaccinating the susceptible human population at day one decreases exponentially to its equilibrium point.

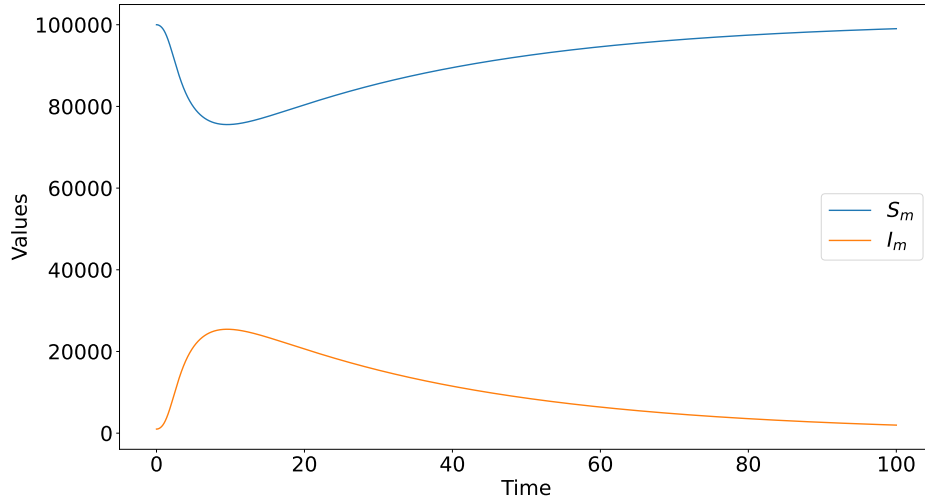


FIGURE 3.11: Behaviour of the solution of susceptible and infected mosquito in optimal vaccination using constant growth function for human and mosquito population.

Figure 3.11 shows that at nine and a half days, susceptible mosquito reaches its lowest point at 75557 population and the highest point of infected mosquito at 25442 population. The figure clearly shows that susceptible mosquito u_5 and infected mosquito u_6 behave opposite. It is because we consider a constant mosquito population.

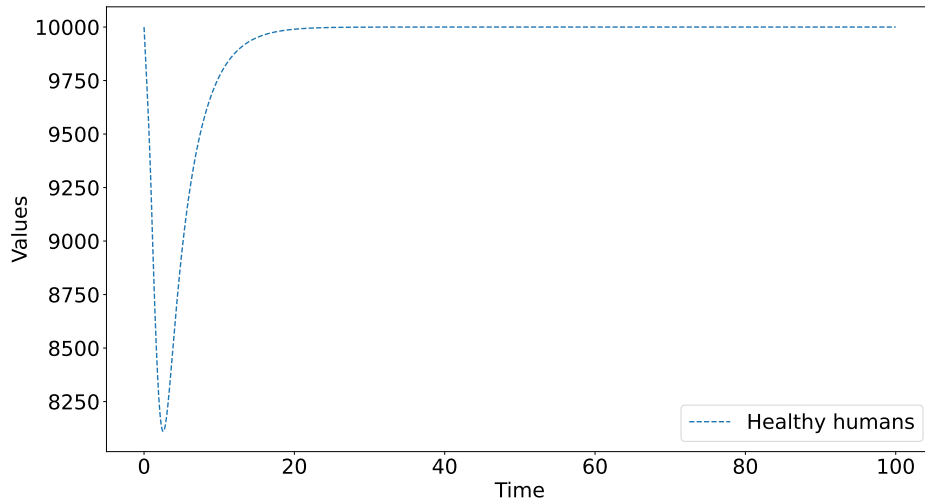


FIGURE 3.12: Behaviour of the solution of healthy humans in optimal vaccination using constant growth function for human and mosquito population.

Healthy human population comprises the combination of primary susceptible human u_1 , secondary susceptible human u_3 , recovered human u_4 and the immune

human T_h . Figure 3.12 shows that for two and a half days, a healthy human population exponentially decreases to its lowest point at 8110 population then increases exponentially to its equilibrium at day 83.

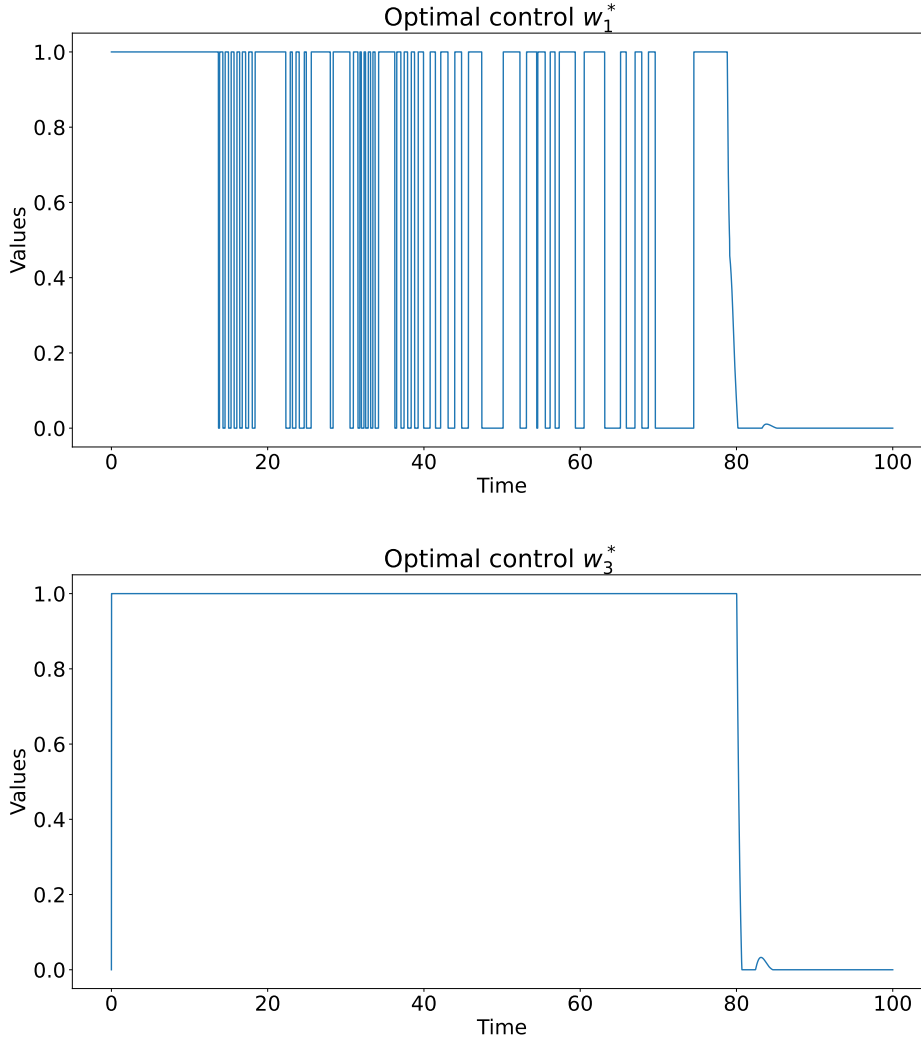


FIGURE 3.13: Behaviour of the solution of optimal control in primary susceptible (top) and secondary susceptible (bottom) humans in optimal vaccination using constant growth function for human and mosquito population.

Figure 3.13 shows that in order to achieve optimal control in minimizing the infected human, we need to constantly vaccine 100% the secondary susceptible u_3 human for 80 days. Then we can stop for two days and resume the vaccination on 82 and a half days with only 3% of the secondary susceptible human. We can only stop the vaccination of secondary susceptible humans on day 85. While for primary susceptible u_1 humans, we can have many breaks between the 80 days. Break starts on day 14, but this is only a short break. Three long breaks are noticeable, on days 47-50, 63-65, and days 69-74.

3.5.2 Minimizing Infected Humans by Optimal Vector Control

In this section we consider minimizing infected humans by applying vector control through pesticide administration. Let us consider the constant growth population model for the human $H'(t) = f(H(t)) = 0$ and a general mosquito growth population $M'(t) = \mu_m M(t) + g(M(t))$. We will now write a control problem that aim to minimize the number of infected human. We attribute a control inputs w_m for the mosquito population. Here, the action of $w_m(t)$ is the percentage of administration of insecticide to the environment per unit of time resulting to the removal of susceptible and infectious mosquito in the system. Furthermore, we assume that the control input is measurable functions that take its values in a positively bounded set $W = [0, w_M]$. Thus we consider the objective function

$$\mathcal{J}(w_m) = \int_0^T \left(u_2(t) + \frac{1}{2} A_m w_m^2(t) \right) dt$$

subject to

$$\begin{aligned} u_1'(t) &= -\frac{ab_h u_6(t) u_1(t)}{H_0} \\ u_2'(t) &= \frac{au_6(t) (b_h u_1(t) + \tilde{b}_h u_3(t))}{H_0} - \gamma_h u_2(t) - \delta_h u_2(t) \\ u_3'(t) &= \gamma_h u_2(t) - \frac{a\tilde{b}_h u_3(t) u_6(t)}{H_0} \\ u_4'(t) &= \delta_h u_2(t) \\ u_5'(t) &= -\frac{ab_m u_2(t) u_5(t)}{H_0} + g(M(t)) - (\mu_m + w_m(t)) u_5(t) \\ u_6'(t) &= \frac{ab_m u_2(t) u_5(t)}{H_0} - \mu_m u_6(t) - w_m(t) u_6(t) \end{aligned} \tag{3.31}$$

for $t \in [0, T]$, with $0 \leq w_m \leq w_M$. The variables A_m are the positive weights associated with the control variables.

Lemma 3.5.4. *There exists an optimal control w_m^* such that*

$$\mathcal{J}(w_m^*) = \min_{w_m \in W} \mathcal{J}(w_m)$$

under the constraint $(u_1, u_2, u_3, u_4, u_5, u_6)$ is a solution to the system (3.31).

Now let us apply the Pontryagin's Maximum Principle in our system. We state the lemma below.

Lemma 3.5.5. *There exists the adjoint variables $\lambda_i, i = 1, 2, \dots, 6$ of the system (3.31) that satisfy the following backward in time system of ordinary differential equation.*

$$\begin{aligned}
-\frac{d\lambda_1}{dt} &= -\lambda_1 \frac{ab_h u_6}{H_0} + \lambda_2 \frac{ab_h u_6}{H_0} \\
-\frac{d\lambda_2}{dt} &= 1 + \lambda_2 (-\gamma_h - \delta_h) + \lambda_3 \gamma_h + \lambda_4 \delta_h - \lambda_5 \frac{ab_m u_5}{H_0} + \lambda_6 \frac{ab_m u_5}{H_0} \\
-\frac{d\lambda_3}{dt} &= \lambda_2 \frac{a\tilde{b}_h u_6}{H_0} - \lambda_3 \frac{a\tilde{b}_h u_6}{H_0} \\
-\frac{d\lambda_4}{dt} &= 0 \\
-\frac{d\lambda_5}{dt} &= \lambda_5 \left(\frac{-ab_m u_2}{H_0} + \frac{\partial g}{\partial u_5} \right) - \lambda_5 (\mu_m + w_m) + \lambda_6 \frac{ab_m u_2}{H_0} \\
-\frac{d\lambda_6}{dt} &= -\lambda_1 \frac{ab_h u_1}{H_0} + \lambda_2 \frac{ab_h u_1 + a\tilde{b}_h u_3}{H_0} - \lambda_3 \frac{a\tilde{b}_h u_3}{H_0} + \lambda_5 \frac{\partial g}{\partial u_6} - \lambda_6 (\mu_m + w_m)
\end{aligned}$$

with the transversality condition $\lambda(T) = 0$.

Proof. Using the Hamiltonian for equation (3.31), we have

$$\begin{aligned}
\mathcal{H} &= \mathcal{L}(w_m) + \lambda_1(t)u'_1(t) + \lambda_2(t)u'_2(t) \\
&\quad + \lambda_3(t)u'_3(t) + \lambda_4(t)u'_4(t) + \lambda_5(t)u'_5(t) + \lambda_6(t)u'_6(t) \\
&= u_2 + \frac{1}{2}A_m w_m^2 + \lambda_1 \left(-\frac{ab_h u_6 u_1}{H_0} \right) + \lambda_3 \left(\gamma_h u_2 - \frac{a\tilde{b}_h u_3 u_6}{H_0} \right) \\
&\quad + \lambda_2 \left(\frac{au_6 (b_h u_1 + \tilde{b}_h u_3)}{H_0} - \gamma_h u_2 - \delta_h u_2 \right) + \lambda_4 (\delta_h u_2) \\
&\quad + \lambda_5 \left(-\frac{ab_m u_2 u_5}{H_0} + g(M) - (\mu_m + w_m)u_5 \right) \\
&\quad + \lambda_6 \left(\frac{ab_m u_2 u_5}{H_0} - \mu_m u_6 - w_m u_6 \right)
\end{aligned} \tag{3.32}$$

Therefore, finding the partial derivatives of \mathcal{H} with respect to u_i 's, $i = 1, 2, \dots, 6$, we have

$$\begin{aligned}
\frac{\partial \mathcal{H}}{\partial u_1} &= -\lambda_1 \frac{ab_h u_6}{H_0} + \lambda_2 \frac{ab_h u_6}{H_0} \\
\frac{\partial \mathcal{H}}{\partial u_2} &= 1 + \lambda_2 (-\gamma_h - \delta_h) + \lambda_3 \gamma_h + \lambda_4 \delta_h - \lambda_5 \frac{ab_m u_5}{H_0} + \lambda_6 \frac{ab_m u_5}{H_0} \\
\frac{\partial \mathcal{H}}{\partial u_3} &= \lambda_2 \frac{a\tilde{b}_h u_6}{H_0} - \lambda_3 \frac{a\tilde{b}_h u_6}{H_0} \\
\frac{\partial \mathcal{H}}{\partial u_4} &= 0 \\
\frac{\partial \mathcal{H}}{\partial u_5} &= \lambda_5 \left(\frac{-ab_m u_2}{H_0} + \frac{\partial g}{\partial u_5} \right) - \lambda_5 (\mu_m + w_m) + \lambda_6 \frac{ab_m u_2}{H_0} \\
\frac{\partial \mathcal{H}}{\partial u_6} &= -\lambda_1 \frac{ab_h u_1}{H_0} + \lambda_2 \frac{ab_h u_1 + a\tilde{b}_h u_3}{H_0} - \lambda_3 \frac{a\tilde{b}_h u_3}{H_0} + \lambda_5 \frac{\partial g}{\partial u_6} - \lambda_6 (\mu_m + w_m)
\end{aligned}$$

Then the adjoint system is defined by $\frac{d\lambda_i}{dt} = -\frac{\partial \mathcal{H}}{\partial u_i}$ for $i = 1, 2, \dots, 6$. We have the following

$$\begin{aligned}\frac{d\lambda_1}{dt} &= \lambda_1 \frac{ab_h u_6}{H_0} - \lambda_2 \frac{ab_h u_6}{H_0} \\ \frac{d\lambda_2}{dt} &= -1 + \lambda_2 (\gamma_h + \delta_h) - \lambda_3 \gamma_h - \lambda_4 \delta_h + \lambda_5 \frac{ab_m u_5}{H_0} - \lambda_6 \frac{ab_m u_5}{H_0} \\ \frac{d\lambda_3}{dt} &= -\lambda_2 \frac{\tilde{a}b_h u_6}{H_0} + \lambda_3 \frac{\tilde{a}b_h u_6}{H_0} \\ \frac{d\lambda_4}{dt} &= 0 \\ \frac{d\lambda_5}{dt} &= \lambda_5 \left(\frac{ab_m u_2}{H_0} - \frac{\partial g}{\partial u_5} \right) + \lambda_5 (\mu_m + w_m) - \lambda_6 \frac{ab_m u_2}{H_0} \\ \frac{d\lambda_6}{dt} &= \lambda_1 \frac{ab_h u_1}{H_0} - \lambda_2 \frac{ab_h u_1 + \tilde{a}b_h u_3}{H_0} + \lambda_3 \frac{\tilde{a}b_h u_3}{H_0} - \lambda_5 \frac{\partial g}{\partial u_6} + \lambda_6 (\mu_m + w_m)\end{aligned}$$

□

Theorem 3.5.6. *The optimal control variables, for $j = 5, 6$, are given by*

$$w_m^*(t) = \max \left(0, \min \left(\frac{\lambda_5 u_5 + \lambda_6 u_6}{A_m}, w_M \right) \right).$$

Proof. By the Pontryagin maximum principle, the optimal control w_m^* should be the one that minimizes, at each instant t , the Hamiltonian given by (3.32). Therefore, we get

$$\frac{\partial H}{\partial w_m} = A_m w_m - \lambda_5 u_5 - \lambda_6 u_6.$$

In effect, we get

$$w_m^* = \frac{\lambda_5 u_5 + \lambda_6 u_6}{A_m}$$

Therefore, the optimal control derived from the stationary condition $\frac{d\lambda_i}{dt}$ is given by

$$w_m^* = \begin{cases} 0 & \text{if } \frac{\lambda_5 u_5 + \lambda_6 u_6}{A_m} \leq 0 \\ \frac{\lambda_5 u_5 + \lambda_6 u_6}{A_m} & \text{if } \frac{\lambda_5 u_5 + \lambda_6 u_6}{A_m} < w_M \\ w_M & \text{if } \frac{\lambda_5 u_5 + \lambda_6 u_6}{A_m} \geq w_M \end{cases}$$

□

Numerical Simulation of Optimal Vector using Constant Mosquito Population

This section gives the numerical analyses of the vector control method through pesticide administration in minimizing the infected human population in the dengue outbreak. We consider a constant growth population for the mosquito population and fixed time T to 100 days or two and a half months, which is around the average infection season duration. The parameters value used are the same as in Table 3.2

and the values of control weights set initially at $A_m = 1$. The optimality system is numerically solved using the same gradient algorithm as in Section 3.5.1.

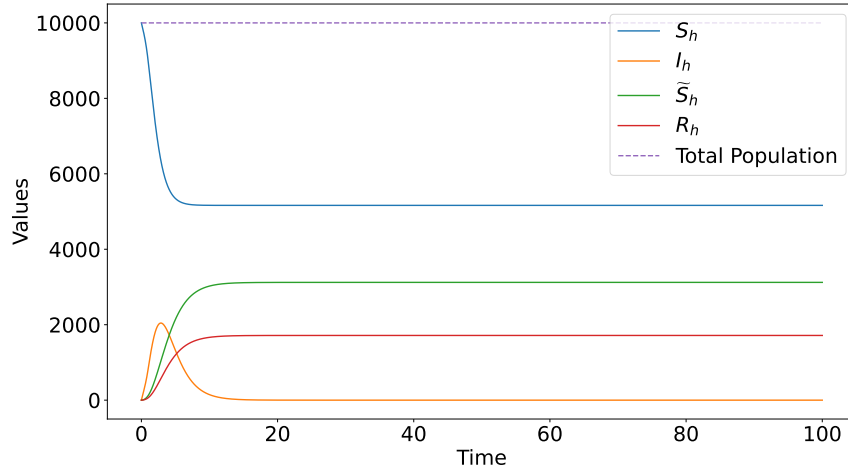


FIGURE 3.14: Behaviour of the solution of the variables in the human compartments in optimal vector control using constant growth function for human and mosquito population.

Figure 3.14 shows that for 100 days, it would take at most three days for the infected human population to reach its maximum at 2044 population. It then decreases exponentially towards its equilibrium. On the other hand, secondary susceptible humans increases exponentially for approximately 20 days towards its equilibrium with 3121 maximum population.

Furthermore, primary susceptible humans decreases while recovered humans increases over time with minimum population of 3121 and maximum population of 1715 individuals, respectively.

Figure 3.15 shows that vector control is an effective method in minimizing the mosquito population. For ten days, susceptible mosquito decreases until it reaches almost zero population. While infected mosquito increases only for at most two days with 2688 maximum population.

Totally controlled mosquitoes means those mosquitoes who have been eliminated in the process of applying insecticide. The figure shows that the totally controlled mosquito increases exponentially and reaches its equilibrium for a short time only. This strengthens further the conclusion that vector control is an effective method in minimizing the mosquito population.

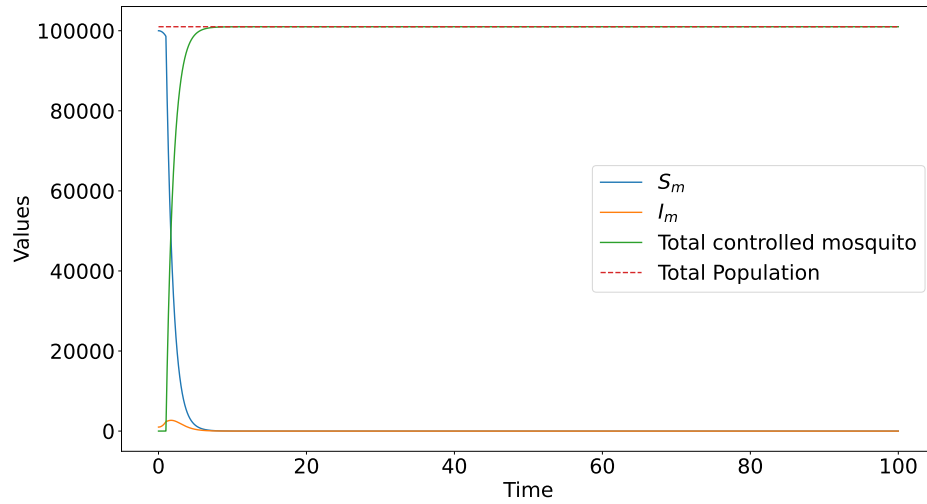


FIGURE 3.15: Behaviour of the solution of susceptible, infected and total controlled mosquito in optimal vector control using constant growth function for human and mosquito population.

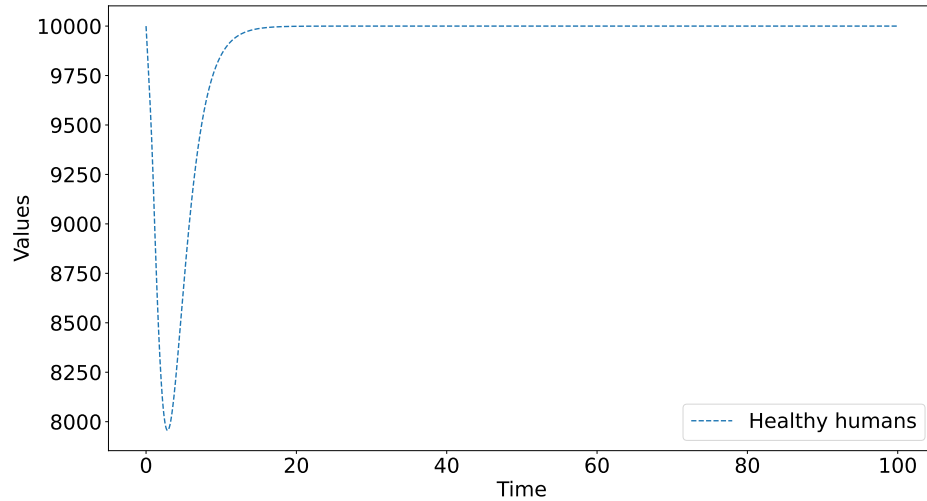


FIGURE 3.16: Behaviour of the solution of healthy humans in optimal vector control using constant growth function for human and mosquito population.

Healthy human population comprises the combination of primary susceptible human u_1 , secondary susceptible human u_3 , recovered human u_4 and the immune human T_h . Figure 3.16 shows that for at most three days, a healthy human population exponentially decreases to its lowest point at 7955 population then increases exponentially to its equilibrium at day 22. The figure shows that vector control is more effective in maintaining a healthy human population. With the difference of only 155 population, vector control has less minimum population than vaccination but vector control reaches the equilibrium faster than vaccination.

Figure 3.17 shows that in order to achieve optimal control in minimizing the infected human, we need to constantly apply insecticide for 34.5 days. After then

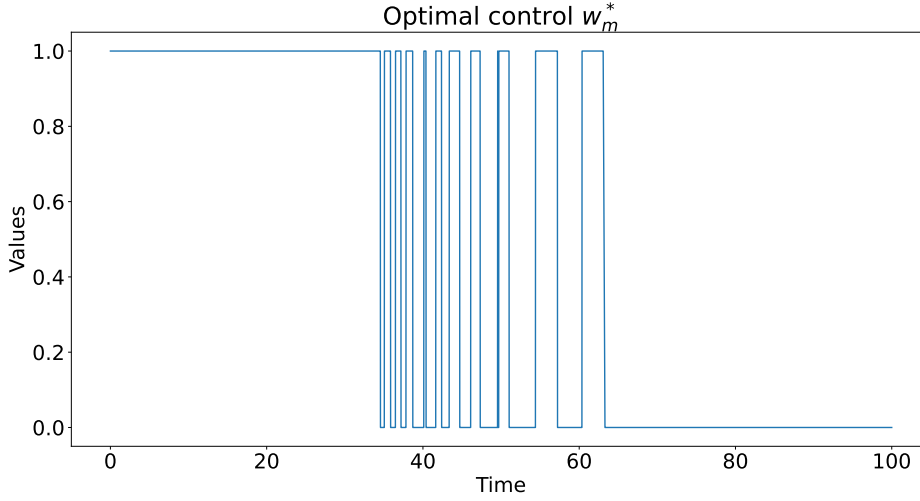


FIGURE 3.17: Behaviour of the solution of optimal control of mosquitoes in optimal vector control using constant growth function for human and mosquito population.

there is a bang-bang control. The figure shows that we can stop the application of insecticide on the 63rd day.

3.5.3 Minimizing Infected Humans by both Optimal Vaccination and Vector Control

In this section, we combine the vaccination and vector control as a strategy in minimizing infected humans. We write a control problem that aim to minimize the number of infected human population. We attribute three control inputs, w_1 and w_3 for the human population and w_m for the mosquito population. Here, the action of $w_1(t)$ is the percentage of primary susceptible and $w_3(t)$ is the percentage of secondary susceptible individual being vaccinated per unit of time implying the removal of infected human individuals from the system. While the action of $w_m(t)$ is the percentage of administration of insecticide to the environment per unit of time resulting to the removal of susceptible and infected mosquito in the system. Furthermore, we assume that all control inputs are measurable functions that takes its values in a positively bounded set $W = [0, w_H, w_M]$. Thus we consider the objective function

$$\mathcal{J}(w_1, w_3, w_m) = \int_0^T \left(u_2(t) + \frac{1}{2} A_1 w_1^2(t) + \frac{1}{2} A_3 w_3^2(t) + \frac{1}{2} A_m w_m^2(t) \right) dt$$

subject to

$$\begin{aligned}
u_1'(t) &= -\frac{ab_h u_6(t) u_1(t)}{H_0} - w_1(t) u_1(t) \\
u_2'(t) &= \frac{au_6(t) (b_h u_1(t) + \tilde{b}_h u_3(t))}{H_0} - \gamma_h u_2(t) - \delta_h u_2(t) \\
u_3'(t) &= \gamma_h u_2(t) - \frac{\tilde{a} \tilde{b}_h u_3(t) u_6(t)}{H_0} - w_3(t) u_3(t) \\
u_4'(t) &= \delta_h u_2(t) \\
u_5'(t) &= -\frac{ab_m u_2(t) u_5(t)}{H_0} + g(M(t)) - (\mu_m + w_m(t)) u_5(t) \\
u_6'(t) &= \frac{ab_m u_2(t) u_5(t)}{H_0} - \mu_m u_6(t) - w_m(t) u_6(t)
\end{aligned} \tag{3.33}$$

for $t \in [0, T]$, with $0 \leq w_1, w_3 \leq w_H$, $0 \leq w_m \leq w_M$. The variables A_j are the positive weights associated with the control variables w_j , $j = 1, 3, m$, respectively,

Lemma 3.5.7. *There exists an optimal control $w^* = (w_1^*(t), w_3^*(t), w_m^*(t))$ such that*

$$\mathcal{J}(w_1^*, w_3^*, w_m^*) = \min_{w \in W} \mathcal{J}(w_1, w_3, w_m)$$

under the constraint $(u_1, u_2, u_3, u_4, u_5, u_6)$ is a solution to the system (4.13).

Now let us apply Pontryagin's Maximum Principle in our system. We state the lemma below.

Lemma 3.5.8. *There exist the adjoint variables $\lambda_i, i = 1, 2, \dots, 6$ of the system (4.13) that satisfy the following backward in time system of ordinary differential equations:*

$$\begin{aligned}
-\frac{d\lambda_1}{dt} &= \lambda_1 \left(\frac{-ab_h u_6}{H_0} - w_1 \right) + \lambda_2 \frac{ab_h u_6}{H_0} \\
-\frac{d\lambda_2}{dt} &= 1 + \lambda_2 (-\gamma_h - \delta_h) + \lambda_3 \gamma_h + \lambda_4 \delta_h - \lambda_5 \frac{ab_m u_5}{H_0} + \lambda_6 \frac{ab_m u_5}{H_0} \\
-\frac{d\lambda_3}{dt} &= \lambda_2 \frac{\tilde{a} \tilde{b}_h u_6}{H_0} + \lambda_3 \left(\frac{-\tilde{a} \tilde{b}_h u_6}{H_0} - w_3 \right) \\
-\frac{d\lambda_4}{dt} &= 0 \\
-\frac{d\lambda_5}{dt} &= \lambda_5 \left(\frac{-ab_m u_2}{H_0} + \frac{\partial g}{\partial u_5} \right) - \lambda_5 (\mu_m + w_m) + \lambda_6 \frac{ab_m u_2}{H_0} \\
-\frac{d\lambda_6}{dt} &= -\lambda_1 \frac{ab_h u_1}{H_0} + \lambda_2 \frac{ab_h u_1 + \tilde{a} \tilde{b}_h u_3}{H_0} - \lambda_3 \frac{\tilde{a} \tilde{b}_h u_3}{H_0} + \lambda_5 \frac{\partial g}{\partial u_6} - \lambda_6 (\mu_m + w_m)
\end{aligned}$$

with the transversality condition $\lambda(T) = 0$.

Proof. Using the Hamiltonian for (4.13), we have

$$\begin{aligned}
\mathcal{H} &= \mathcal{L}(w_1, w_3, w_m) + \lambda_1(t)u'_1(t) + \lambda_2(t)u'_2(t) \\
&\quad + \lambda_3(t)u'_3(t) + \lambda_4(t)u'_4(t) + \lambda_5(t)u'_5(t) + \lambda_6(t)u'_6(t) \\
&= \frac{1}{2} (u_2^2 + A_1 w_1^2 + A_3 w_3^2 + A_m w_m^2) \\
&\quad + \lambda_1 \left(-\frac{ab_h u_6 u_1}{H_0} - w_1 u_1 \right) + \lambda_3 \left(\gamma_h u_2 - \frac{\tilde{a} \tilde{b}_h u_3 u_6}{H_0} - w_3 u_3 \right) \\
&\quad + \lambda_2 \left(\frac{a u_6 (b_h u_1 + \tilde{b}_h u_3)}{H_0} - \gamma_h u_2 - \delta_h u_2 \right) + \lambda_4 (\delta_h u_2) \\
&\quad + \lambda_5 \left(-\frac{ab_m u_2 u_5}{H_0} + g(M) - \mu_m u_5 - w_m u_5 \right) \\
&\quad + \lambda_6 \left(\frac{ab_m u_2 u_5}{H_0} - \mu_m u_6 - w_m u_6 \right). \tag{3.34}
\end{aligned}$$

Therefore, finding the partial derivatives of \mathcal{H} with respect to u_i 's, $i = 1, 2, \dots, 6$, we have

$$\begin{aligned}
\frac{\partial \mathcal{H}}{\partial u_1} &= \lambda_1 \left(-\frac{ab_h u_6}{H_0} - w_1 \right) + \lambda_2 \frac{ab_h u_6}{H_0} \\
\frac{\partial \mathcal{H}}{\partial u_2} &= 1 + \lambda_2 (-\gamma_h - \delta_h) + \lambda_3 \gamma_h + \lambda_4 \delta_h - \lambda_5 \frac{ab_m u_5}{H_0} + \lambda_6 \frac{ab_m u_5}{H_0} \\
\frac{\partial \mathcal{H}}{\partial u_3} &= \lambda_2 \frac{\tilde{a} \tilde{b}_h u_6}{H_0} + \lambda_3 \left(-\frac{\tilde{a} \tilde{b}_h u_6}{H_0} - w_3 \right) \\
\frac{\partial \mathcal{H}}{\partial u_4} &= 0 \\
\frac{\partial \mathcal{H}}{\partial u_5} &= \lambda_5 \left(-\frac{ab_m u_2}{H_0} + \frac{\partial g}{\partial u_5} \right) - \lambda_5 (\mu_m + w_m) + \lambda_6 \frac{ab_m u_2}{H_0} \\
\frac{\partial \mathcal{H}}{\partial u_6} &= -\lambda_1 \frac{ab_h u_1}{H_0} + \lambda_2 \frac{ab_h u_1 + \tilde{a} \tilde{b}_h u_3}{H_0} - \lambda_3 \frac{\tilde{a} \tilde{b}_h u_3}{H_0} + \lambda_5 \frac{\partial g}{\partial u_6} - \lambda_6 (\mu_m + w_m).
\end{aligned}$$

Then the adjoint system is defined by $\frac{d\lambda_i}{dt} = -\frac{\partial \mathcal{H}}{\partial u_i}$ for $i = 1, 2, \dots, 6$. □

Theorem 3.5.9. *The optimal control variables are given by*

$$\begin{aligned}
w_1^*(t) &= \max \left(0, \min \left(\frac{\lambda_1 u_1}{A_1}, w_H \right) \right) \\
w_3^*(t) &= \max \left(0, \min \left(\frac{\lambda_3 u_3}{A_3}, w_H \right) \right) \\
w_m^*(t) &= \max \left(0, \min \left(\frac{\lambda_5 u_5 + \lambda_6 u_6}{A_m}, w_M \right) \right)
\end{aligned}$$

Proof. By the Pontryagin maximum principle, the optimal control w^* minimizes, at each instant t , the Hamiltonian given by (4.14). We have

$$\frac{\partial \mathcal{H}}{\partial w_j} = 0, \quad \text{for all } j = 1, 3, m \quad \text{at } w_j = w_j^*.$$

Therefore, we get

$$\begin{aligned} \frac{\partial \mathcal{H}}{\partial w_1} &= A_1 w_1 - \lambda_1 u_1, \\ \frac{\partial \mathcal{H}}{\partial w_3} &= A_3 w_3 - \lambda_3 u_3, \\ \frac{\partial \mathcal{H}}{\partial w_m} &= A_m w_m - \lambda_5 u_5 - \lambda_6 u_6, \end{aligned}$$

and

$$w_1 = \frac{\lambda_1 u_1}{A_1}, \quad w_3 = \frac{\lambda_3 u_3}{A_3}, \quad w_m = \frac{\lambda_5 u_5 + \lambda_6 u_6}{A_m}.$$

□

3.5.4 Numerical Simulation of the Optimal Control Problem

In this section, we presented numerical simulations showing the difference in minimizing the infected human during the dengue outbreak between the three methods: vaccination, vector control, and the combination of the vaccination and vector control. The optimal control are (w_1^*, w_3^*) , (w_5^*, w_6^*) and $(w_1^*, w_3^*, w_5^*, w_6^*)$, respectively.

We consider a constant growth function for human population $f(H(t)) = 0$ and an entomological growth function for the mosquito population $g(M(t)) = \alpha_m M e^{-\beta_m M}$. The parameters value used presented in Table 3.2 which is taken from Bakach et al. [6] and the author estimates some from Indonesia, with the similar environmental condition as the Philippines. Notice that we set $\alpha_m < \mu_m$, by Theorem 4.2.1 the global stability corresponds to E_1 . In this situation, E_2 is biologically thus we do not take it into consideration.

The control weights A_1 and A_3 are the efforts in vaccinating the human population while A_m is the effort to eliminate the mosquito population by means of administering insecticides. Since primary susceptible humans are readily available in the population compared to the secondary susceptible humans, the efforts used in vaccinating them would be less than the effort exerted in vaccinating the secondary susceptible. Thus, A_3 is set higher than A_1 . While insecticide administration in susceptible mosquitoes and infected mosquitoes uses the same effort and achieves a similar result. Hence, we initially set the control weights as $A_1 = 0.1$, $A_3 = 1$ and $A_m = 1$. Note that the values of A_1, A_3, A_m do not change the convergence of optimal control.

The optimality system is numerically solved using the same gradient algorithm describe in Section 3.5.1. In here, we set $u_0 = [1.e4, 0., 0., 0., 1.e5, 1.e3]$ with $H_0 = u_0[0] + u_0[1] + u_0[2] + u_0[3]$ and $M_0 = u_0[4] + u_0[5]$. We choose a random

positive value for w_1 , w_3 and w_m between $]0, 1[$ with $W = (w_1, w_3, w_m)$ such that $|\mathcal{H}(w_j, u_i, \lambda_i)| > \epsilon$. Note that the initial choice of w does not affect the convergence of the solution.

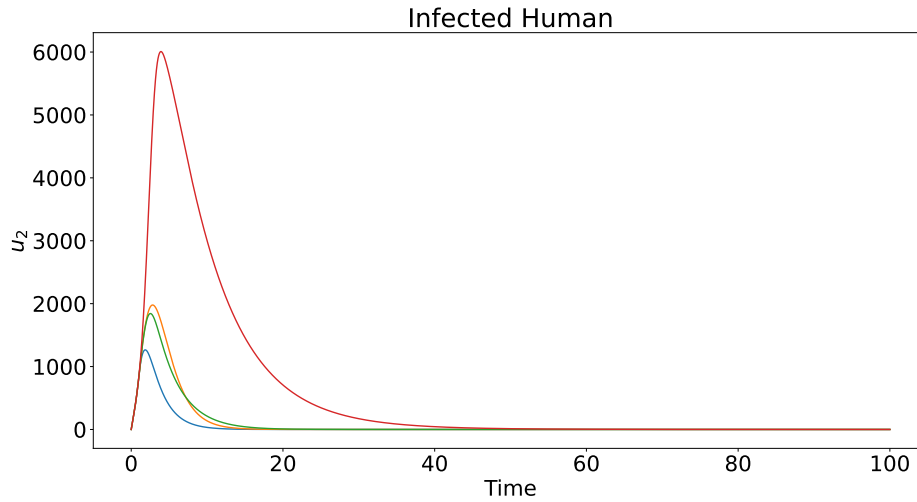


FIGURE 3.18: Response comparison of the infected human compartment in the 4 control strategies: vaccination only (green), vector control only (orange), vaccination and vector control (blue), and without control (red).

Figure 3.18 shows in minimizing the infected human that the combination of Dengvaxia and vector control is the most effective method. It would only take 30 days to reach equilibrium, resulting in the total elimination of infected humans with a maximum of 12.55% (1,255) infected humans over time. Nevertheless, vector control stands out if we compare only the vaccination and vector control method. It would only take 34 days with a maximum population of 19.68% (1,968) infected humans for vector control to eliminate infected humans. In comparison, vaccination takes 45 days, with 18.42% (1,842) infected humans. Without control, infected humans would slowly decrease after reaching 60.07% (6,007) but would never annihilate. Vaccinating secondary humans would only take 48 days to reach equilibrium with a maximum of 54.94% (5,494) infected humans over time.

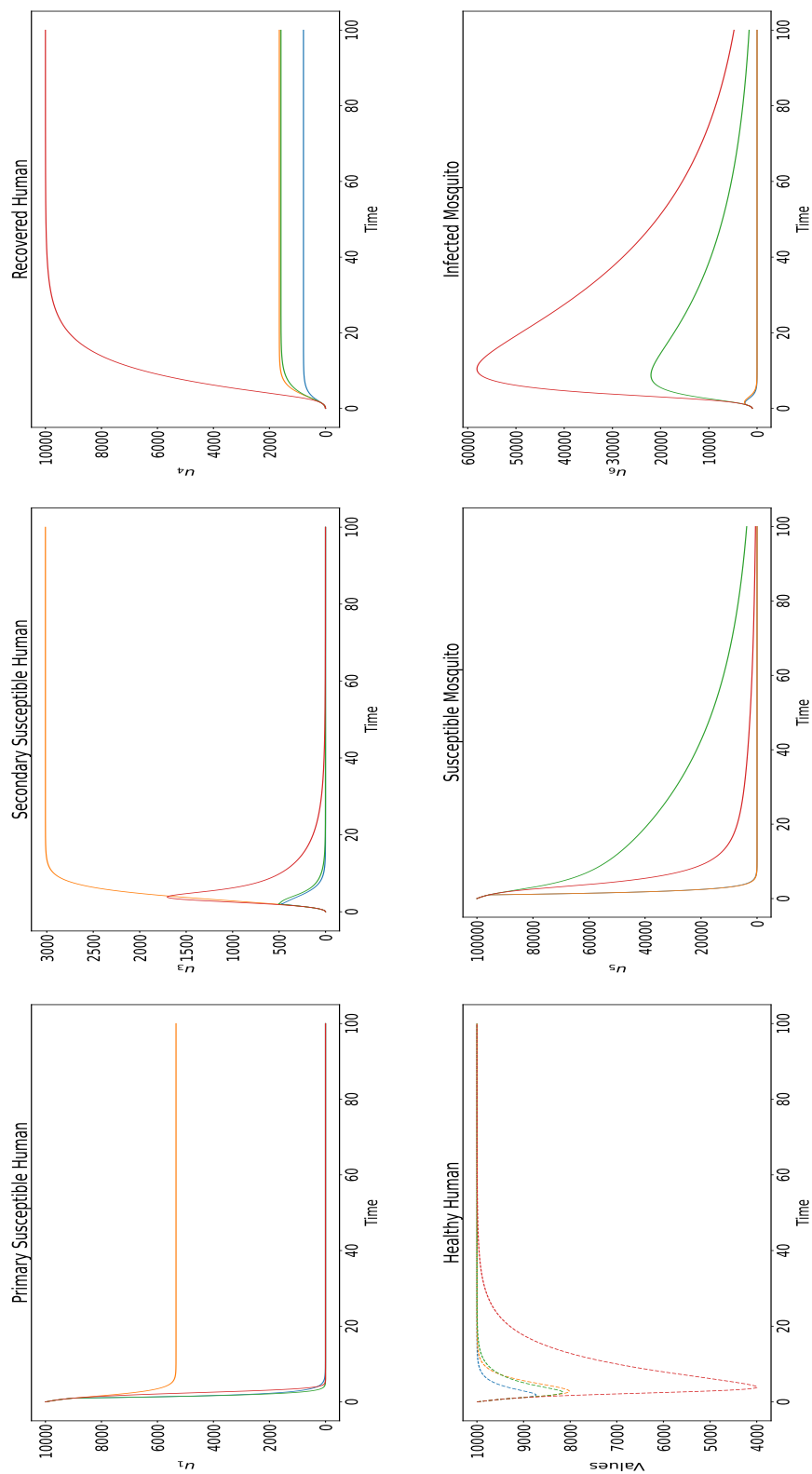


FIGURE 3.19: Response comparison of each variables in the model with 4 control strategies: vaccination (green), vector control (orange), the combination of vaccination and vector control (blue), and without control (red).

Figure 3.19 shows no significant difference between the three methods concerning the primary and secondary susceptibles to reach its equilibrium point. It takes seven and a half days for vaccination and 14 days to combine vaccination and vector control to reach zero primary susceptible individuals. Moreover, it takes 42 days for vaccination and 30 days for the combination to reach zero secondary susceptible individuals. For vector control, it takes 20 days to reach an equilibrium of 53.36% (5336) primary susceptible humans and 34 days to reach 30.15% (3015) secondary susceptible humans.

Note that in the human compartment, the total immunity to dengue by means of implementing the Dengvaxia vaccine is denoted by T_h which is given by $T_h(t) = w_1(t)u_1(t) + w_3(t)u_3(t)$. Thus, a healthy human combines immune human T_h , primary susceptible u_1 , secondary susceptible u_3 , and the recovered u_4 humans. The figure shows that the combination of vaccination and vector control is the best method in maximizing the healthy human population. It only takes 26 days to combine vaccination and vector control methods to reach the equilibrium of healthy humans. Its minimum population is 8.73% (8,734) on day 1.8.

In contrast, there is no significant difference in the vector and vaccination method alone in the healthy human population. The vector method takes 29 days to reach its equilibrium with 8.02% (8,021) minimum population on 2.8 days. The vaccination required 39 days to reach an equilibrium with 8.16% (8,157) minimum population on 2.5 days. Without any control strategies applied to the healthy human population, it requires a much higher time to reach its equilibrium with 4% (4,000) minimum population.

For the recovered human compartment, the figure shows that the human population would eventually recover through time without control strategies applied to the variables. It supports that dengue infection lasts only three to seven days following the infectious mosquito bite, and a spontaneous, full health recovery follows. However, comparing the three control methods, the combination of vaccination and vector control methods stands out. It only requires 26 days to reach its equilibrium at 0.79% (787) recovered human population. At the same time, there is no significant difference between vaccination alone and vector control alone. Both require 32 days to reach its equilibrium at 1.59% (1,590) and 1.65% (1,646) recovered human, respectively.

Now, minimizing the susceptible mosquito population, no control applied to the variables is better than vaccination. It decreases faster with 0.56% (556) minimum susceptible mosquito population while vaccination decreases slower with 3.69% (3,692) minimum population at the end of time. Nevertheless, the vector control method and the combination of vaccination and vector control are the better methods for controlling the mosquito population. They annihilate the susceptible mosquito population.

Minimizing the infected mosquito, either vector control alone or combining vaccination and vector control is the best method. There is no significant difference between the two. They both require minimum time for the infected mosquito to reach zero population and with only 2.6% (2596) and 2.52% (2521) maximum population for the vector control only and the combination, respectively. However, vaccination is better compared to the one without control. The infected mosquito has a 58.09% (58,092) maximum population without applying a control strategy, while the vaccination has a 22% (22,006) maximum population.

Now, let us show the controlled variable's behavior by comparing the vaccination, vector control only, and the combination of vaccination and vector control.

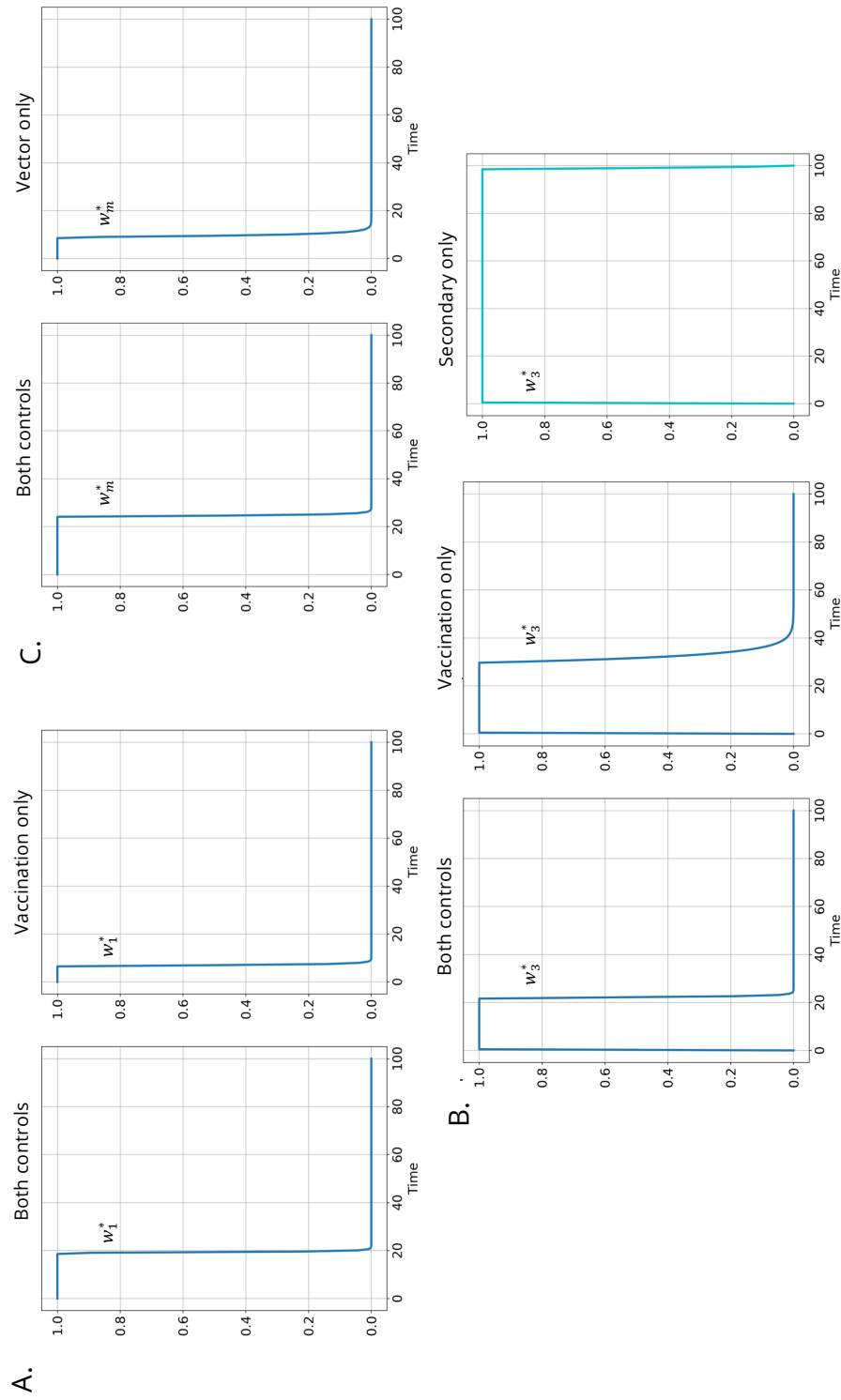


FIGURE 3.20: Optimal control of the (A) primary susceptible and (B) secondary susceptible human compartment using vaccination only versus the combination of both control strategies. Optimal control of (C) mosquitoes compartment using vector control only versus the combination of both control strategies. Cyan curve represents optimal control of vaccination of secondary humans only

Figure 3.20 shows that concerning vaccination only, vaccinating the primary susceptible human population requires a shorter time compared to the secondary susceptible human. It takes ten days and 40 days to vaccinate primary and secondary susceptible human populations, respectively. Nevertheless, applying both control strategies takes only approximately 20-22 days. While minimizing the mosquito population, the vector control method is better than combining the two strategies. It takes approximately 15-18 days to administer insecticide to the mosquito population while applying both control strategies takes 22-24 days.

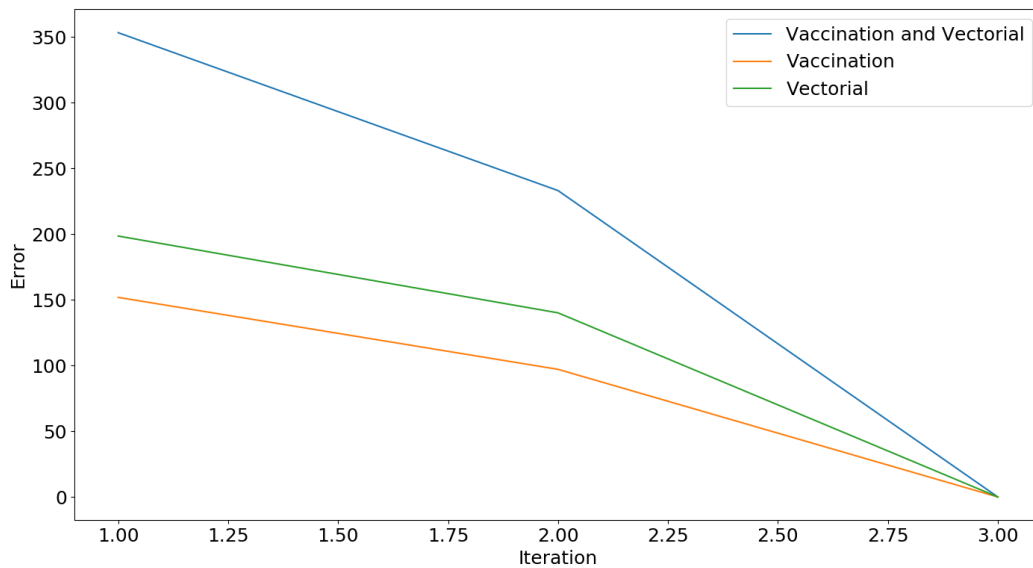


FIGURE 3.21: Convergence of the Error in each control strategies

Figure 3.21 shows the convergence of the error to zero. In general, the gradient method converges rapidly. Here only 3 steps are necessary.

Chapter 4

A Dengue-Dengvaxia Model: Comparison Between Vaccination and Vector Control

This chapter focuses on a dengue-dengvaxia models with entomological growth of mosquitoes. The results in this chapter were published in the article *Optimal Control of a Dengue-Dengvaxia Model: Comparison Between Vaccination and Vector Control*, *Comput. Math. Biophys.* 2021; 9:198–213.

4.1 Description of the Model with Vaccination

Based on the Ross-type model, we assumed that dengue viruses are virulent with no other microorganism attacking the human body.

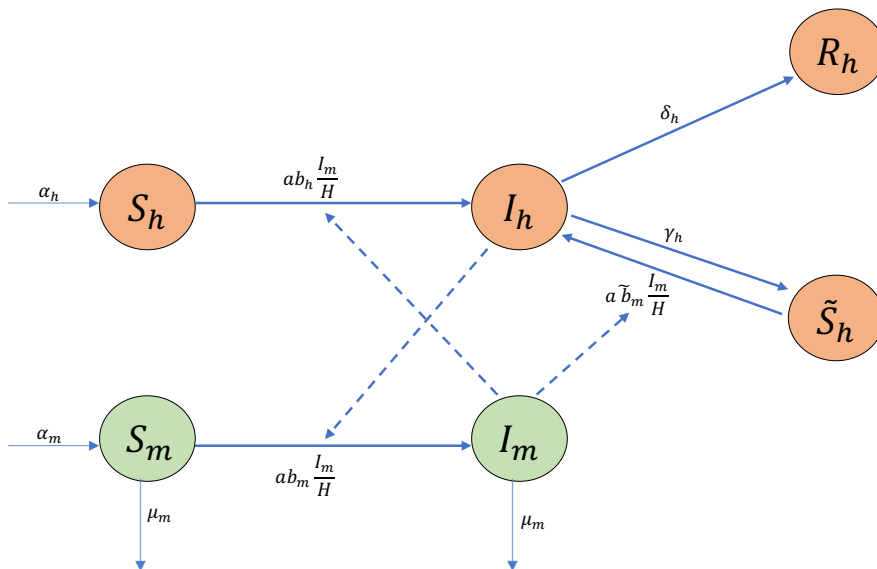


FIGURE 4.1: Compartmental representation of the model with vaccination considering individuals who have previous dengue infections.

Let H be the human population subdivided into primary susceptible S_h , secondary susceptible \tilde{S}_h , infected I_h and removed R_h . Primary susceptible humans are individuals who have not yet been infected by dengue, while secondary susceptible humans are individuals who previously had dengue infection.

Let M be the population of female mosquitoes split into two groups of susceptible S_m and infectious I_m mosquitoes. Figure 4.1 describes the flow of dengue disease. In this chapter, we introduce a mathematical model of dengue that considers the vaccine that should be given to people who are already infected by one type of virus.

Since humans have a meager mortality rate compared to mosquitoes, we neglect the natural death of humans but still consider their growth. The following system of ordinary equations governed the dynamics of humans.

$$S'_h(t) = -\frac{ab_h I_m(t)}{H(t)} S_h(t) + f(H(t)) \quad (4.1)$$

$$I'_h(t) = \frac{a I_m(t)}{H(t)} (b_h S_h(t) + \tilde{b}_h \tilde{S}_h(t)) - \gamma_h I_h(t) - \delta_h I_h(t) \quad (4.2)$$

$$\tilde{S}'_h(t) = \gamma_h I_h(t) - \frac{a \tilde{b}_h I_m(t)}{H(t)} \tilde{S}_h(t) \quad (4.3)$$

$$R'_h(t) = \delta_h I_h(t). \quad (4.4)$$

While the dynamics of mosquitoes are as follows

$$S'_m(t) = -\frac{ab_m I_h(t)}{H(t)} S_m(t) - \mu_m S_m(t) + g(M(t)) \quad (4.5)$$

$$I'_m(t) = \frac{ab_m I_h(t)}{H(t)} S_m(t) - \mu_m I_m(t). \quad (4.6)$$

Note that the total human population is given by $H = S_h + I_h + \tilde{S}_h + R_h$ and the total mosquito population is given by $M = S_m + I_m$. The function $f(H(t))$ is the change in the total human population, while $g(M(t))$ is the change in the total mosquito population. In this study, we will consider different growth model for human and mosquito population. Since human have a meager mortality rate compared to mosquitoes, we neglect the natural death of the humans.

4.2 Study of the Model with Entomological Growth

Let us consider an entomological growth population model for the mosquito population and a constant human population. We have $H'(t) = f(H(t)) = 0$ and $g(M(t)) = \alpha_m M e^{-\beta_m M}$, as in Bilman et al. [9], where β_m is the characteristic of

the competition effect per individual. Then our model would become

$$\begin{aligned}
u_1'(t) &= -\frac{ab_h u_6(t)u_1(t)}{H_0} \\
u_2'(t) &= \frac{au_6(t) \left(b_h u_1(t) + \tilde{b}_h u_3(t) \right)}{H_0} - \gamma_h u_2(t) - \delta_h u_2(t) \\
u_3'(t) &= \gamma_h u_2(t) - \frac{a\tilde{b}_h u_3(t)u_6(t)}{H_0} \\
u_4'(t) &= \delta_h u_2(t) \\
u_5'(t) &= -\frac{ab_m u_2(t)u_5(t)}{H_0} - \mu_m u_5(t) + \alpha_m M e^{-\beta_m M} \\
u_6'(t) &= \frac{ab_m u_2(t)u_5(t)}{H_0} - \mu_m u_6(t)
\end{aligned} \tag{4.7}$$

Now, let us prove that our new model is bounded and well-defined.

Well-posedness and Positivity of the Solution

Theorem 4.2.1. *The domain Ω defined by*

$$\Omega_{Ento} = \left\{ U \in \mathbb{R}_+^6 : 0 \leq u_1 + u_2 + u_3 + u_4 = H_0, 0 \leq u_5 + u_6 \leq \max \left(\frac{\alpha_m}{\beta_m \mu_m}, M_0 \right) \right\}$$

is positively invariant. In particular, for an initial datum $U(0)$ in Ω_{Ento} , there exists a unique global in time solution U in $\mathcal{C}(\mathbb{R}_+, \Omega_{Ento})$.

Proof. Consider the initial value problem

$$U'(t) = F(t, U(t)) \quad \text{where} \quad U(0) = U_0.$$

The right-hand-side F satisfies the local Lipschitz condition. Therefore, the Cauchy-Lipschitz theorem ensure the local well-posedness. Then,

$$\begin{aligned}
f_1(0, u_2, u_3, u_4, u_5, u_6) &= 0, \forall u_2, \dots, u_6 \in \Omega_{Ento} \\
f_2(u_1, 0, u_3, u_4, u_5, u_6) &= \frac{au_6 \left(b_h u_1 + \tilde{b}_h u_3 \right)}{H} \geq 0, \forall u_1, u_3, \dots, u_6 \in \Omega_{Ento} \\
f_3(u_1, u_2, 0, u_4, u_5, u_6) &= \gamma_h u_2, \forall u_1, u_2, u_4, \dots, u_6 \in \Omega_{Ento} \\
f_4(u_1, u_2, u_3, 0, u_5, u_6) &= \delta_h u_2, \forall u_1, u_2, u_3, u_5, u_6 \in \Omega_{Ento} \\
f_5(u_1, u_2, u_3, u_4, 0, u_6) &= \alpha_m u_6 e^{-\beta_m u_6}, \forall u_1, \dots, u_4, u_6 \in \Omega_{Ento} \\
f_6(u_1, u_2, u_3, u_4, u_5, 0) &= \frac{ab_m u_2 u_5}{H}, \forall u_1, \dots, u_5 \in \Omega_{Ento}
\end{aligned}$$

We write

$$\begin{aligned}\alpha_m M e^{-\beta_m M} &= \frac{\alpha_m M}{e^{\beta_m M}} = \frac{\alpha_m M}{\sum_{n \geq 0} \frac{(\beta_m M)^n}{n!}} \\ &= \frac{\alpha_m M}{1 + \beta_m M + \frac{\beta_m^2 M^2}{2} + \frac{\beta_m^3 M^3}{6} + \dots} \\ &\leq \frac{\alpha_m}{\beta_m}\end{aligned}$$

Then $M'(t) \leq \frac{\alpha_m}{\beta_m} - \mu_m M(t)$ and by Gronwall's lemma

$$M(t) \leq e^{-\mu_m t} \left(M_0 - \frac{\alpha_m}{\beta_m \mu_m} \right) + \frac{\alpha_m}{\beta_m \mu_m} \leq \max \left(\frac{\alpha_m}{\beta_m \mu_m}, M_0 \right)$$

□

Equilibrium

Now, solving for all possible values of x^* that lie on Ω_{Ento} we get $E_{Ento,1} = (u_1^*, 0, u_3^*, u_4^*, 0, 0)$ and $E_{Ento,2} = (u_1^*, 0, u_3^*, u_4^*, \frac{1}{\beta_m} \ln \left(\frac{\alpha_m}{\mu_m} \right), 0)$. We state the following lemma.

Lemma 4.2.2. *The system of equation (4.7) admits an equilibria at $E_{Ento,1} = (u_1^*, 0, u_3^*, u_4^*, 0, 0)$ and $E_{Ento,2} = (u_1^*, 0, u_3^*, u_4^*, \frac{1}{\beta_m} \ln \left(\frac{\alpha_m}{\mu_m} \right), 0)$.*

Proof. Let $u'_1, u'_2, u'_3, u'_4, u'_5, u'_6 = 0$. Since all parameter are positive, then

$$\delta_h u_2 = 0 \quad \implies \quad u_2 = 0.$$

Now for $\frac{ab_m u_2 u_5}{H_0} - \mu_m u_6$, since $u_2 = 0$, we have

$$\begin{aligned}\frac{ab_m(0)u_5}{H_0} - \mu_m u_6 &= 0 \\ -\mu_m u_6 &= 0.\end{aligned}$$

Therefore, $u_6 = 0$. Thus, for $-\frac{ab_m u_2 u_5}{H_0} - \mu_m u_5 + \alpha_m(u_5 + u_6)e^{-\beta_m(u_5 + u_6)} = 0$ becomes

$$\begin{aligned}-\frac{ab_m(0)}{H_0} - \mu_m u_5 + \alpha_m(u_5 + (0))e^{-\beta_m(u_5 + (0))} &= 0 \\ -\mu_m u_5 + \alpha_m u_5 e^{-\beta_m u_5} &= 0 \\ u_5(-\mu_m + \alpha_m e^{-\beta_m u_5}) &= 0\end{aligned}$$

Hence, $u_5 = 0$ or $-\mu_m + \alpha_m e^{-\beta_m u_5} = 0$. If $-\mu_m + \alpha_m e^{-\beta_m u_5} = 0$, then $e^{-\beta_m u_5} = \frac{\mu_m}{\alpha_m}$.

Thus, $u_5 = \frac{1}{\beta_m} \ln \left(\frac{\alpha_m}{\mu_m} \right)$. Since the system of equation contains either u_2 or u_6 or both, which has a zero value, then any nonnegative values of u_1, u_3, u_4 satisfies the system of equation. Therefore, $E_{Ento,1} = (u_1^*, 0, u_3^*, u_4^*, 0, 0)$ and

$E_{Ento,2} = (u_1^*, 0, u_3^*, u_4^*, \frac{1}{\beta_m} \ln \left(\frac{\alpha_m}{\mu_m} \right), 0)$ are an equilibrium point of the system (4.7).

□

Next Generation Matrix and Basic Generation Matrix

Since the infected individuals are in u_2 and u_6 , then we can rewrite the system of the equations as

$$\mathcal{F} = \begin{pmatrix} \frac{au_6(b_h u_1 + \tilde{b}_h u_3)}{H_0} \\ \frac{ab_m u_2 u_5}{H_0} \end{pmatrix} \quad \mathcal{V} = \begin{pmatrix} (\gamma_h + \delta_h)u_2 \\ \mu_m u_6 \end{pmatrix}$$

where \mathcal{F} is the rate of appearance of new infections in each compartment and \mathcal{V} is the rate of other transitions between all compartments. Thus,

$$F = \begin{pmatrix} 0 & \frac{a(b_h u_1 + \tilde{b}_h u_3)}{H_0} \\ \frac{ab_m u_5}{H_0} & 0 \end{pmatrix}, V = \begin{pmatrix} \gamma_h + \delta_h & 0 \\ 0 & \mu_m \end{pmatrix}$$

and $V^{-1} = \begin{pmatrix} \frac{1}{\gamma_h + \delta_h} & 0 \\ 0 & \frac{1}{\mu_m} \end{pmatrix}$. Therefore, the next generation matrix is

$$FV^{-1} = \begin{pmatrix} 0 & \frac{a(b_h u_1 + \tilde{b}_h u_3)}{\mu_m H_0} \\ \frac{ab_m u_5}{(\gamma_h + \delta_h)H_0} & 0 \end{pmatrix}.$$

It follows that by [67] the basic reproduction number, denoted by $\rho(FV^{-1})$, where ρ is the spectral radius, is given by

$$\rho(FV^{-1}) = \sqrt{\frac{a^2 b_m u_5 (b_h u_1 + \tilde{b}_h u_3)}{\mu_m H_0^2 (\gamma_h + \delta_h)}}. \quad (4.8)$$

Now using this eigenvalue, we determine the local stability of the equilibrium points $E_{Ento,1}$ and $E_{Ento,2}$.

Proposition 4.2.3.

1. The disease free equilibrium $E_{Ento,1} = (u_1^*, 0, u_3^*, u_4^*, 0, 0) = (S_h^*, 0, \tilde{S}_h^*, R_h^*, 0, 0)$ is locally asymptotically stable.
2. If $\alpha_m > \mu_m$ and $\mathcal{R}_0 < 1$ where $\mathcal{R}_0 = \sqrt{\frac{a^2 b_m \ln\left(\frac{\alpha_m}{\mu_m}\right) (b_h S_h^* + \tilde{b}_h \tilde{S}_h^*)}{H_0^2 \mu_m \beta_m (\gamma_h + \delta_h)}}$, then the disease free equilibrium point $E_{Ento,2} = (u_1^*, 0, u_3^*, u_4^*, \frac{1}{\beta_m} \ln\left(\frac{\alpha_m}{\mu_m}\right), 0) = (S_h^*, 0, \tilde{S}_h^*, R_h^*, \frac{1}{\beta_m} \ln\left(\frac{\alpha_m}{\mu_m}\right), 0)$ is locally asymptotically stable.

Proof. 1. From the above eigenvalues,

$$\rho(FV^{-1}) = \sqrt{\frac{a^2 b_m(0) (\tilde{b}_h u_3^* + b_h u_1^*)}{H_0^2 \mu_m (\gamma_h + \delta_h)}} = 0$$

Therefore, the system of equation is local asymptotically stable at $E_{Ento,1}$.

2. Similarly,

$$\mathcal{R}_0 = \sqrt{\frac{a^2 b_m u_5^* (b_h u_1^* + \tilde{b}_h u_3^*)}{\mu_m H_0^2 (\gamma_h + \delta_h)}} = \sqrt{\frac{a^2 b_m \ln\left(\frac{\alpha_m}{\mu_m}\right) (\tilde{b}_h u_3^* + b_h u_1^*)}{\mu_m H_0^2 \beta_m (\gamma_h + \delta_h)}}.$$

Therefore, if $\alpha_m > \mu_m$ and $\mathcal{R}_0 < 1$, the system of equation is local asymptotically stable at $E_{Ento,2}$. □

The basic reproduction number \mathcal{R}_0 has a biological meaning when $\alpha_m > \mu_m$. It means that the average number of new infected humans is proportional to the proportion $\frac{u_5^*}{H_0}$ of susceptible mosquitoes among the human population. The terms $\frac{u_1^*}{H_0}$, and $\frac{u_3^*}{H_0}$ proportion of primary and secondary susceptible humans respectively. The terms $\frac{ab_h}{\mu_m(\gamma_h + \delta_h)}$, and $\frac{a\tilde{b}_h}{\mu_m(\gamma_h + \delta_h)}$ represent the transmission rate due by biting during the infection period $1/(\gamma_h + \delta_h)$ and mosquitoes life expectancy $1/\mu_m$.

Jacobian Matrix

To confirm the stability, we compute the Jacobian Matrix of the system in order to confirm our lambda, then only the $\frac{\partial f_5}{\partial u_i}$, $i = 1, 2, \dots, 6$, would change. We can get

$$\begin{aligned} \frac{\partial f_5}{\partial u_1} &= 0 & \frac{\partial f_5}{\partial u_2} &= \frac{-ab_m u_5}{H_0} \\ \frac{\partial f_5}{\partial u_3} &= 0 & \frac{\partial f_5}{\partial u_4} &= 0 \\ \frac{\partial f_5}{\partial u_5} &= \frac{-ab_m u_2}{H_0} - \mu_m + \alpha_m e^{-\beta_m M} (1 - \beta_m M) & \frac{\partial f_5}{\partial u_6} &= \alpha_m e^{-\beta_m M} (1 - \beta_m M) \end{aligned}$$

Therefore, we get the Jacobian Matrix

$$J = \begin{pmatrix} \frac{-ab_h u_6}{H_0} & 0 & 0 & 0 & 0 & \frac{-ab_h u_1}{H_0} \\ \frac{ab_h u_6}{H_0} & -\gamma_h - \delta_h & \frac{a\tilde{b}_h u_6}{H_0} & 0 & 0 & \frac{ab_h u_1 + a\tilde{b}_h u_3}{H_0} \\ 0 & \gamma_h & \frac{-ab_h u_6}{H_0} & 0 & 0 & \frac{-ab_h u_3}{H_0} \\ 0 & \delta_h & 0 & 0 & 0 & 0 \\ 0 & \frac{-ab_m u_5}{H_0} & 0 & 0 & \frac{-ab_m u_2}{H_0} - \mu_m + \alpha_m e^{-\beta_m M} (1 - \beta_m M) & \alpha_m e^{-\beta_m M} (1 - \beta_m M) \\ 0 & \frac{ab_m u_5}{H_0} & 0 & 0 & \frac{ab_m u_2}{H_0} & -\mu_m \end{pmatrix}$$

Thus, we have the following theorem.

Lemma 4.2.4. *The disease-free equilibrium point $E_{Ento,1} = (u_1^*, 0, u_3^*, u_4^*, 0, 0)$ is locally asymptotically stable.*

Proof. Let $E_{Ento,1} = (u_1^*, 0, u_3^*, u_4^*, 0, 0)$ be an equilibrium point of the system of equation (4.7). Then the above Jacobian matrix for $E_{Ento,1}$ can be deduce to

$$J(E_{Ento,1}) = \begin{pmatrix} 0 & 0 & 0 & 0 & 0 & \frac{-ab_h u_1^*}{H_0} \\ 0 & -\gamma_h - \delta_h & 0 & 0 & 0 & \frac{ab_h u_1^* + a\tilde{b}_h u_3^*}{H_0} \\ 0 & \gamma_h & 0 & 0 & 0 & \frac{-ab_h u_3^*}{H_0} \\ 0 & \delta_h & 0 & 0 & 0 & 0 \\ 0 & 0 & 0 & 0 & -\mu_m + \alpha_m & \alpha_m \\ 0 & 0 & 0 & 0 & 0 & -\mu_m \end{pmatrix}.$$

Let $|J(E_{Ento,1}) - \lambda I_6| = 0$. Then

$$|J(E_{Ento,1}) - \lambda I_6| = \begin{vmatrix} -\lambda & 0 & 0 & 0 & 0 & \frac{-ab_h u_1^*}{H_0} \\ 0 & -\gamma_h - \delta_h - \lambda & 0 & 0 & 0 & \frac{ab_h u_1^* + a\tilde{b}_h u_3^*}{H_0} \\ 0 & \gamma_h & -\lambda & 0 & 0 & \frac{-ab_h u_3^*}{H_0} \\ 0 & \delta_h & 0 & -\lambda & 0 & 0 \\ 0 & 0 & 0 & 0 & -\mu_m + \alpha_m - \lambda & \alpha_m \\ 0 & 0 & 0 & 0 & 0 & -\mu_m - \lambda \end{vmatrix}.$$

Therefore, solving the determinant above would determine its characteristic polynomial. We have

$$-\lambda^3(-\lambda - \gamma_h - \delta_h)(-\lambda - \mu_m)(-\lambda - \mu_m + \alpha_m) = 0.$$

Hence, we get

$$\lambda_1 = 0 \text{ multiplicity } 3$$

$$\lambda_2 = -\gamma_h - \delta_h$$

$$\lambda_3 = -\mu_m$$

$$\lambda_4 = -\mu_m + \alpha_m.$$

Since $\alpha_m - \mu_m \leq 0$, all the eigenvalues are negative, implying further that the system of equation is locally asymptotically stable at the $E_{Ento,1}$. \square

Lemma 4.2.5. *The endemic equilibrium point $(u_1^*, 0, u_3^*, u_4^*, \frac{1}{\beta_m} \ln \left(\frac{\alpha_m}{\mu_m} \right), 0)$ is locally asymptotically stable if $\alpha_m > \mu_m$ and $\mathcal{R}_0 < 1$.*

Proof. Let $E_{Ento,2} = (u_1^*, 0, u_3^*, u_4^*, \frac{1}{\beta_m} \ln(\frac{\alpha_m}{\mu_m}), 0)$ be an equilibrium point of the system of equation (??). Then the above Jacobian matrix for $E_{Ento,2}$ can be deduce to

$$J(E_{Ento,2}) = \begin{pmatrix} 0 & 0 & 0 & 0 & 0 & \frac{-ab_h u_1^*}{H_0} \\ 0 & -\gamma_h - \delta_h & 0 & 0 & 0 & \frac{ab_h u_1^* + a\tilde{b}_h u_3^*}{H_0} \\ 0 & \gamma_h & 0 & 0 & 0 & \frac{-ab_h u_3^*}{H_0} \\ 0 & \delta_h & 0 & 0 & 0 & 0 \\ 0 & \frac{-ab_m \ln(\frac{\alpha_m}{\mu_m})}{H_0 \beta_m} & 0 & 0 & -\mu_m \ln(\frac{\alpha_m}{\mu_m}) & \mu_m (1 - \ln(\frac{\alpha_m}{\mu_m})) \\ 0 & \frac{ab_m \ln(\frac{\alpha_m}{\mu_m})}{H_0 \beta_m} & 0 & 0 & 0 & -\mu_m \end{pmatrix}.$$

Let $|J(E_{Ento,2}) - \lambda I_6| = 0$. Then

$$\begin{vmatrix} -\lambda & 0 & 0 & 0 & 0 & \frac{-ab_h u_1^*}{H_0} \\ 0 & -\gamma_h - \delta_h - \lambda & 0 & 0 & 0 & \frac{ab_h u_1^* + a\tilde{b}_h u_3^*}{H_0} \\ 0 & \gamma_h & -\lambda & 0 & 0 & \frac{-ab_h u_3^*}{H_0} \\ 0 & \delta_h & 0 & -\lambda & 0 & 0 \\ 0 & \frac{-ab_m \ln(\frac{\alpha_m}{\mu_m})}{H_0 \beta_m} & 0 & 0 & \mu_m \ln(\frac{\mu_m}{\alpha_m}) - \lambda & \mu_m (1 - \ln(\frac{\alpha_m}{\mu_m})) \\ 0 & \frac{ab_m \ln(\frac{\alpha_m}{\mu_m})}{H_0 \beta_m} & 0 & 0 & 0 & -\mu_m - \lambda \end{vmatrix} = 0.$$

Therefore, solving the determinant above would determine its characteristic polynomial. We have

$$(-\lambda)^3 \left(-\mu_m \ln\left(\frac{\alpha_m}{\mu_m}\right) - \lambda \right) \begin{vmatrix} -\gamma_h - \delta_h - \lambda & \frac{ab_h u_1^* + a\tilde{b}_h u_3^*}{H_0} \\ \frac{ab_m \ln(\frac{\alpha_m}{\mu_m})}{H_0 \beta_m} & -\mu_m - \lambda \end{vmatrix} = 0.$$

Solving the determinant of the remaining 2x2 matrix, we get

$$(-\gamma_h - \delta_h - \lambda)(-\mu_m - \lambda) - \frac{ab_m \ln(\frac{\alpha_m}{\mu_m})}{H_0 \beta_m} \cdot \frac{ab_h u_1^* + a\tilde{b}_h u_3^*}{H_0} = 0.$$

Expanding the equation above give us the quadratic equation

$$\lambda^2 + \lambda(\gamma_h + \delta_h + \mu_m) + \left(\mu_m(\gamma_h + \delta_h) - \frac{ab_m \ln(\frac{\alpha_m}{\mu_m}) (ab_h u_1^* + a\tilde{b}_h u_3^*)}{H_0^2 \beta_m} \right) = 0$$

Using quadratic formula to solve λ , we get

$$\lambda = -\frac{\gamma_h + \delta_h + \mu_m}{2} \pm \sqrt{\frac{(\gamma_h + \delta_h + \mu_m)^2 - 4 \left(\mu_m(\gamma_h + \delta_h) - \frac{ab_m \ln(\frac{\alpha_m}{\mu_m}) (ab_h u_1^* + a\tilde{b}_h u_3^*)}{H_0^2 \beta_m} \right)}{2}}$$

Since $\ln\left(\frac{\alpha_m}{\mu_m}\right) \frac{ab_m}{H_0} \left(\frac{a\tilde{b}_h u_3 + ab_h u_1}{H_0}\right) < \mu_m \beta_m (\gamma_h + \delta_h)$, we have

$$\lambda < -\frac{\gamma_h + \delta_h + \mu_m}{2} \pm \frac{\sqrt{(\gamma_h + \delta_h + \mu_m)^2 - 4\left(\mu_m(\gamma_h + \delta_h) - \frac{1}{\beta_m} \cdot \mu_m \beta_m (\gamma_h + \delta_h)\right)}}{2}$$

Simplifying this we get

$$\lambda < -\frac{\gamma_h + \delta_h + \mu_m}{2} \pm \frac{\sqrt{(\gamma_h + \delta_h + \mu_m)^2 - 4(\mu_m(\gamma_h + \delta_h) - \mu_m(\gamma_h + \delta_h))}}{2}$$

That is,

$$\lambda < -\frac{\gamma_h + \delta_h + \mu_m}{2} \pm \frac{\gamma_h + \delta_h + \mu_m}{2}$$

Therefore,

$$\begin{aligned} \lambda &< -\frac{\gamma_h + \delta_h + \mu_m}{2} + \frac{\gamma_h + \delta_h + \mu_m}{2} & \lambda &< -\frac{\gamma_h + \delta_h + \mu_m}{2} - \frac{\gamma_h + \delta_h + \mu_m}{2} \\ \lambda &= 0 & \lambda &< -(\gamma_h + \delta_h + \mu_m) \end{aligned}$$

Thus, the eigenvalues of system are

$$\lambda = 0 \quad (\text{multiplicity } 4)$$

$$\lambda = -\mu_m \ln\left(\frac{\alpha_m}{\mu_m}\right)$$

$$\lambda < -(\gamma_h + \delta_h + \mu_m)$$

which are negative if $\alpha_m > \mu_m$ and $\mathcal{R}_0 > 1$. Therefore, the system of equation is locally asymptotically stable at the equilibrium point $E_{Ento,2}$. \square

Theorem 4.2.6.

1. If $\alpha_m < \mu_m$, then $E_{Ento,1}$ is globally asymptotically stable.
2. If $\alpha_m > \mu_m$ and $\mathcal{R}_0 > 1$, then $E_{Ento,2}$ is globally asymptotically stable.

Proof. From the fourth equation of system (4.7), we can deduce that u_4 is increasing. Since u_4 is bounded by H_0 , u_4 has a limit u_4^* as $t \rightarrow +\infty$. Thus, integrating the equation gives

$$u_4(t) - u_4(0) = \delta_h \int_0^t u_2(s) ds.$$

Thus

$$u_4^* - u_4(0) = \delta_h \int_0^\infty u_2(s) ds$$

which is finite. Implying further that $u_2(s) \rightarrow 0$ as $s \rightarrow +\infty$.

Now, adding the fifth and six equation of system (4.7) gives us

$$u'_5 + u'_6 = M' = g(M) = \alpha_m M e^{-\beta_m M} - \mu_m M.$$

As in Theorem 3.2.3, if $\alpha_m < \mu_m$, then $M(t) \rightarrow 0$ as $t \rightarrow +\infty$. Thus, by positivity of the solution u_5 and u_6 goes to 0 as $t \rightarrow +\infty$.

From $u_1' = -\frac{ab_h u_6 u_1}{H_0} \leq 0$, the function u_1 is a decreasing non-negative function bounded by H_0 . Thus, as $t \rightarrow +\infty$, $u_1 \rightarrow u_1^*$.

The solution of the third equation $u_3' + \frac{ab_h u_6 u_3}{H_0} = \gamma_h u_2$, can be written as

$$u_3(t) = E(t)u_3(0) + \int_0^t E(t-s)\gamma_h u_2(s)ds$$

with $E(t) = e^{-\frac{ab_h}{H_0} \int_0^t u_6(s)ds}$. Since, for all $t \geq 0$, $0 \leq u_2(t), u_3(t) \leq H_0, 0 \leq u_6(t) \leq M_0$, then $u_2 \rightarrow 0, u_3 \rightarrow u_3^*$ when $t \rightarrow +\infty$.

When $\alpha_m \geq \mu_m$, let us denote $M^* = \frac{1}{\beta_m} \ln \left(\frac{\alpha_m}{\mu_m} \right)$. Since $M'(t) = (\alpha_m e^{-\beta M} - \mu_m)M$, if $M(t) < M^*$, then M is increasing and bounded by above, while if $M(t) > M^*$, then M is decreasing and bounded by below. In particular, $M(t)$ has a limit when $t \rightarrow +\infty$. Using now the local asymptotic stability with $\mathcal{R}_0 < 1$, this limit is equal to M^* . \square

Numerical Illustrations

In this section, we presented the numerical illustration using the constant human population and entomological growth function for mosquito population. We let the final time T be 2000 days with initial condition $(10000, 0, 0, 0, 100000, 10)$. Using the same parameter value as Table 3.2 and $\beta_m = 0.375$, a phase portrait graph of system (4.7) was simulated using the Python program.

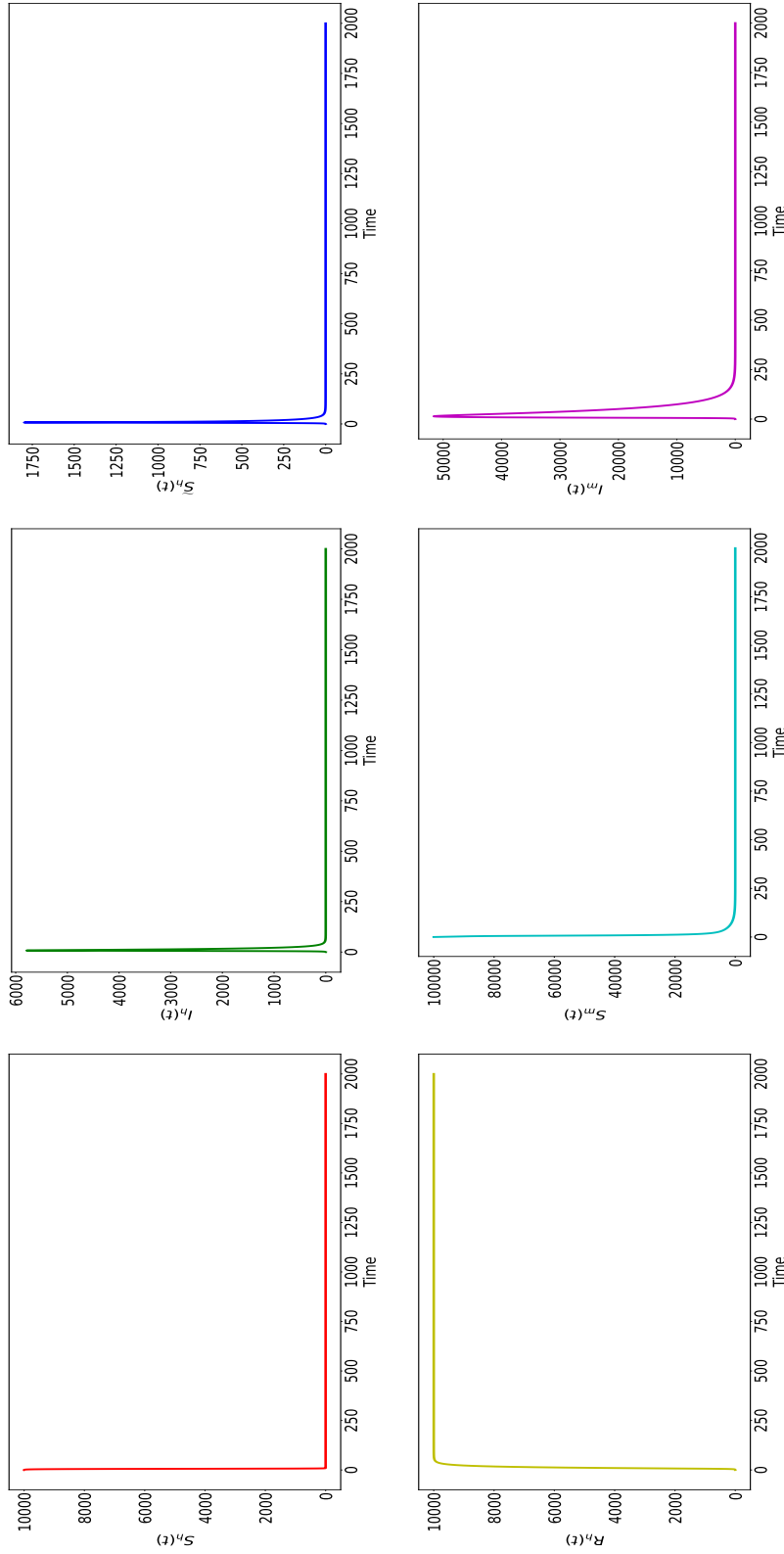


FIGURE 4.2: Behaviour of the solution of each variables in the model ?? with dengvaxia versus time using constant growth functions for human population and entomological growth function for mosquito population. S_h is the red colour figure, I_h is the green, \tilde{S}_h is the blue, R_h is the yellow, S_m is the cyan and I_m is the magenta.

Figure 4.2 shows that for 9 days susceptible humans decreases exponentially towards its equilibrium. On the other hand, infected and secondary susceptible humans increases exponentially. Upon reaching the maximum of 5790.384 infected and 1798.828 secondary susceptible humans, they then decrease towards their equilibrium on the 60th day. As a consequence, recovered humans exponentially increase for 60 days towards its equilibrium.

For the mosquito population, susceptible humans decreases rapidly for 120 days then follows by a smooth decrease towards its equilibrium. Whereas, infected mosquito exponentially increase for 14 days with maximum population of 51603.490 and then exponentially decreases towards its equilibrium.

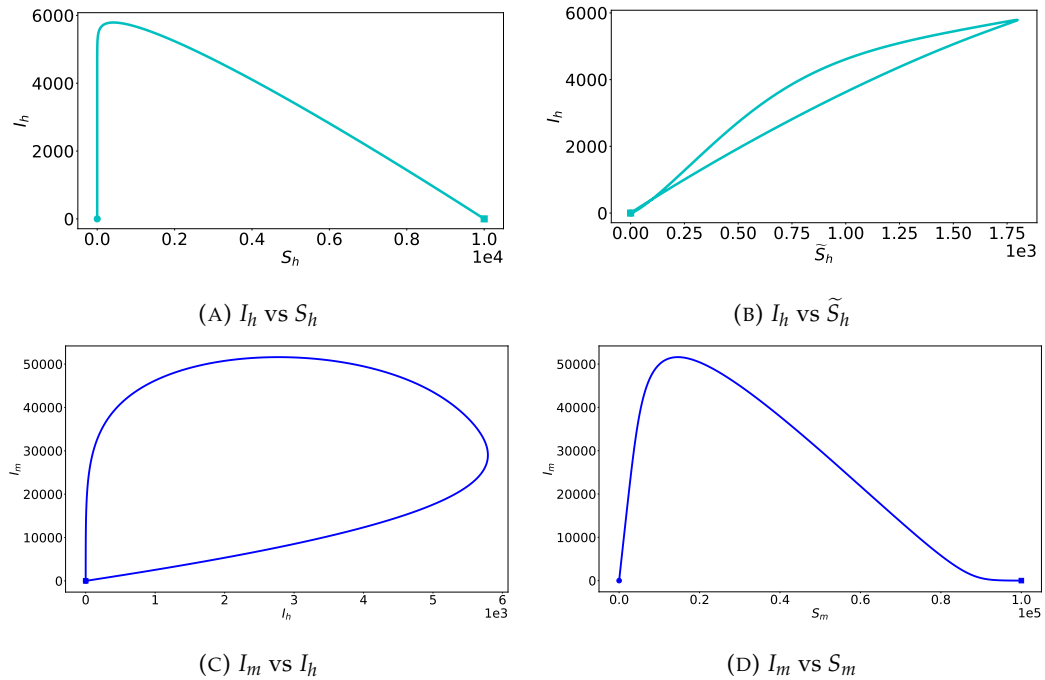


FIGURE 4.3: Phase portrait of the model with dengvaxia using constant growth function showing primary S_h and secondary susceptible \tilde{S}_h versus infected humans I_h in blue color, and susceptible mosquitoes S_m and infected humans I_h versus infected mosquitoes I_m in cyan color. Square and circle indicates the first and last solution of the variables.

For infected humans, figure 4.3a shows that at time $t = 0$, there are no infected humans but have 10,000 primary susceptible humans. For a period of time, infected humans increases while primary susceptible humans decreases. Upon reaching the maximum of 5790.384 infected human, it then decreases while primary susceptible humans continues to decrease.

Figure 4.3b shows that infected and secondary susceptible humans are directly proportional to each other for all time. For some time, both variables increase up to the maximum of 1798.828 secondary susceptible humans. Then they decrease towards the total elimination.

Figure 4.3c shows that in the beginning there are 10 infected mosquito and no infected human. As the infected humans increases, infected mosquitoes also increases. After some time, the two variables become inversely proportional. As infected humans decreases, the infected mosquito continue to increase. Then both variables decreases towards zero.

On the other hand, figure 4.3d shows that at time $t = 0$, there are 100,000 susceptible mosquito and 10 infected mosquitoes. The figure shows that the two variables are inversely proportional to each other. For some time, susceptible mosquitoes decreases while infected mosquitoes increases slowly. Then an exponentially increase of infected mosquito follows. When it reaches the maximum of 51603.490 infected mosquitoes, it then decreases while susceptible mosquito continues to decrease towards zero.

4.3 Choice of Control Strategies

Preventing or reducing dengue virus transmission depends entirely on controlling the mosquito vectors or vaccination. This section applied three control strategies to reduce dengue transmission: vaccination, vector control and the combination of vaccination and vector control. We applied this control strategies to model (4.7).

4.3.1 Vaccination

Dengue fever is the most rapidly spreading mosquito-borne viral disease found in tropical and sub-tropical climates worldwide. It is caused by the single positive-stranded RNA virus of the family *Flaviviridae* that is transmitted to humans through a diurnal mosquito. [56] So far, there is no specific treatment for dengue fever. According to the theory of facilitating antibodies, vaccine research is made more difficult by the need for a vaccine immunizing sustainability and simultaneously against the four serotypes of the virus [50]. Half a dozen vaccine candidates are under study. The most competitive candidate was *Dengvaxia*, by Sanofi Pasteur. Dengvaxia (CYD-TDV) was licensed in December 2015 and has now been approved by regulatory authorities in 20 countries.

CYD-TDV vaccine is for the prevention of dengue disease caused by dengue virus serotypes 1, 2, 3, and 4. It should be administered three doses six months apart of 0.5 mL subcutaneous (SC) administration for individuals aged 9 - 16 years old with laboratory-confirmed previous dengue infection and living in endemic areas.

To account for the vaccine in the model, let us consider the following mathematical model in two different populations.

Let us consider an entomological growth for the mosquito population and constant human population. We have $f(H(t)) = 0$ and $g(M(t)) = \alpha_m M e^{-\beta_m M}$. Then our model becomes

$$\begin{aligned}
u_1'(t) &= -\frac{ab_h u_6(t) u_1(t)}{H_0} - v_1 u_1(t) \\
u_2'(t) &= \frac{au_6(t) (b_h u_1(t) + \tilde{b}_h u_3(t))}{H_0} - \gamma_h u_2(t) - \delta_h u_2(t) \\
u_3'(t) &= \gamma_h u_2(t) - \frac{a\tilde{b}_h u_3(t) u_6(t)}{H_0} - v_3 u_3(t) \\
u_4'(t) &= \delta_h u_2(t) \\
u_5'(t) &= -\frac{ab_m u_2(t) u_5(t)}{H_0} - \mu_m u_5(t) + \alpha_m M e^{-\beta_m M} \\
u_6'(t) &= \frac{ab_m u_2(t) u_5(t)}{H_0} - \mu_m u_6(t)
\end{aligned} \tag{4.9}$$

Where $v_1 u_1(t)$ is the vaccination given to the primary susceptible human population, and $v_3 u_3(t)$ is the vaccination given to the secondary susceptible human. The total immunity is given by $T'(t) = v_1 u_1(t) + v_3 u_3(t)$.

Note that there exists a unique global in time solution $(u_1, u_2, u_3, u_4, u_5, u_6)$ in $\mathcal{C}(\Omega_{Ento}, \mathbb{R}_+)^6$.

Lemma 4.3.1. *The system of equation (4.9) admits two equilibria $E_{VacEnto,1} = (0, 0, 0, u_4^*, 0, 0)$ and $E_{VacEnto,2} = (0, 0, 0, u_4^*, \frac{1}{\beta_m} \ln\left(\frac{\alpha_m}{\mu_m}\right), 0)$.*

Proof. Let $u_1', u_2', u_3', u_4', u_5', u_6' = 0$. Since all parameter are positive, then

$$\delta_h u_2 = 0 \implies u_2 = 0$$

Now for $\frac{ab_m u_2 u_5}{H_0} - \mu_m u_6 = 0$, since $u_2 = 0$, we have

$$\begin{aligned}
\frac{ab_m(0)u_5}{H_0} - \mu_m u_6 &= 0 \\
-\mu_m u_6 &= 0
\end{aligned}$$

Therefore, $u_6 = 0$. Consequently, substituting $u_6 = 0$ and $u_2 = 0$ to both $u_1' = 0$ and $u_3' = 0$, we have

$$\begin{aligned}
-\frac{ab_h u_6 u_1}{H_0} - v_1 u_1 &= 0 & \gamma_h u_2 - \frac{a\tilde{b}_h u_3 u_6}{H_0} - v_3 u_3 &= 0 \\
-\frac{ab_h(0)u_1}{H_0} - v_1 u_1 &= 0 & \gamma_h(0) - \frac{a\tilde{b}_h u_3(0)}{H_0} - v_3 u_3 &= 0 \\
-v_1 u_1 &= 0 & -v_3 u_3 &= 0
\end{aligned}$$

Since $v_1, v_3 > 0$, $u_1 = 0$ and $u_3 = 0$. For $-\frac{ab_mu_2u_5}{H_0} - \mu_mu_5 + \alpha_m(u_5 + u_6)e^{-\beta_m(u_5+u_6)} = 0$ becomes

$$\begin{aligned} -\frac{ab_m(0)}{H_0} - \mu_mu_5 + \alpha_m(u_5 + (0))e^{-\beta_m(u_5+(0))} &= 0 \\ -\mu_mu_5 + \alpha_mu_5e^{-\beta_mu_5} &= 0 \\ u_5(-\mu_m + \alpha_me^{-\beta_mu_5}) &= 0 \end{aligned}$$

Hence, $u_5 = 0$ or $-\mu_m + \alpha_me^{-\beta_mu_5} = 0$. If $-\mu_m + \alpha_me^{-\beta_mu_5} = 0$, then $e^{-\beta_mu_5} = \frac{\mu_m}{\alpha_m}$. Thus, $u_5 = \frac{1}{\beta_m} \ln\left(\frac{\alpha_m}{\mu_m}\right)$. Consequently, since the system (4.9) contains either u_1, u_2, u_3 or u_6 or both, which has a zero value, then any nonnegative values of u_4^* satisfies the system of equation. Therefore, $E_{VacEnto,1} = (0, 0, 0, u_4^*, 0, 0)$ and $E_{VacEnto,2} = (0, 0, 0, u_4^*, \frac{1}{\beta_m} \ln\left(\frac{\alpha_m}{\mu_m}\right), 0)$ is an equilibrium point of system (4.9). \square

As in Section 6.1, one gets

$$\lambda = \pm \sqrt{\frac{a^2b_mu_5(\tilde{b}_hu_3 + b_hu_1)}{H_0^2\mu_m(\gamma_h + \delta_h)}},$$

and, we have the following lemma.

Lemma 4.3.2. *The equilibrium points $E_{VacEnto,1} = (0, 0, 0, u_4^*, 0, 0)$ and $E_{VacEnto,2} = (0, 0, 0, u_4^*, \frac{1}{\beta_m} \ln\left(\frac{\alpha_m}{\mu_m}\right), 0)$ of the system of equation (4.9) are locally asymptotically stable.*

4.3.2 Vector Control

Vector control is a method to limit or eradicate the vectors which transmit disease pathogens. The most frequent type of vector control uses a variety of strategies such as habitat and environmental control, reducing vector contact, chemical control, and biological control.

Let us consider the following model in two different populations to include vectorial control.

Our model would become

$$\begin{aligned} u_1'(t) &= -\frac{ab_hu_6(t)u_1(t)}{H_0} \\ u_2'(t) &= \frac{au_6(t)(b_hu_1(t) + \tilde{b}_hu_3(t))}{H_0} - \gamma_hu_2(t) - \delta_hu_2(t) \\ u_3'(t) &= \gamma_hu_2(t) - \frac{a\tilde{b}_hu_3(t)u_6(t)}{H_0} \\ u_4'(t) &= \delta_hu_2(t) \\ u_5'(t) &= -\frac{ab_mu_2(t)u_5(t)}{H_0} - \mu_mu_5(t) + \alpha_mMe^{-\beta_mM} - v_5u_5(t) \\ u_6'(t) &= \frac{ab_mu_2(t)u_5(t)}{H_0} - \mu_mu_6(t) - v_5u_6(t) \end{aligned} \tag{4.10}$$

Where $v_5 u_5(t)$ is the vectorial control given to the susceptible mosquito population, and $v_5 u_6(t)$ is the vectorial control to infectious mosquito. The total mosquito control is given by $T'_M(t) = v_5 u_5(t) + v_6 u_6(t)$.

Again there exists a unique global in time solution $(u_1, u_2, u_3, u_4, u_5, u_6)$ in $\mathcal{C}(\Omega_{Ento}, \mathbb{R}_+)^6$.

Lemma 4.3.3. *The system of equation (4.10) admits two equilibria $E_{VecEnto,1} = (u_1^*, 0, u_3^*, u_4^*, 0, 0)$ and $E_{VecEnto,2} = (u_1^*, 0, u_3^*, u_4^*, \frac{1}{\beta_m} \ln \left(\frac{\alpha_m}{v_5 + \mu_m} \right), 0)$.*

Proof. Let $u'_1, u'_2, u'_3, u'_4, u'_5, u'_6 = 0$. Since all parameter are positive, then

$$\delta_h u_2 = 0 \quad \implies \quad u_2 = 0$$

Now for $\frac{ab_m u_2 u_5}{H_0} - \mu_m u_6 - v_5 u_6 = 0$, since $u_2 = 0$, we have

$$\begin{aligned} \frac{ab_m(0)u_5}{H_0} - \mu_m u_6 - v_5 u_6 &= 0 \\ (-\mu_m - v_5)u_6 &= 0 \end{aligned}$$

Since $-\mu_m - v_5 \neq 0$, $u_6 = 0$. Consequently, substituting $u_6 = 0$ and $u_2 = 0$ to $u'_5 = 0$, we have

$$\begin{aligned} -\frac{ab_m u_2 u_5}{H_0} - \mu_m u_5 + \alpha_m (u_5 + u_6) e^{-\beta_m (u_5 + u_6)} - v_5 u_5 &= 0 \\ -\frac{ab_m(0)u_5}{H_0} - \mu_m u_5 + \alpha_m (u_5 + (0)) e^{-\beta_m (u_5 + (0))} - v_5 u_5 &= 0 \\ -\mu_m u_5 + \alpha_m u_5 e^{-\beta_m u_5} - v_5 u_5 &= 0 \\ \left(-\mu_m + \alpha_m e^{-\beta_m u_5} - v_5 \right) u_5 &= 0 \end{aligned}$$

Implying that

$$\begin{aligned} -\mu_m + \alpha_m e^{-\beta_m u_5} - v_5 &= 0 & \text{or} & & u_5 &= 0 \\ \alpha_m e^{-\beta_m u_5} &= v_5 + \mu_m \\ -\beta_m u_5 &= \ln \left(\frac{v_5 + \mu_m}{\alpha_m} \right) \\ u_5 &= \frac{1}{\beta_m} \ln \left(\frac{\alpha_m}{v_5 + \mu_m} \right) \end{aligned}$$

Consequently, since system (4.10) contains either u_2 , or u_6 or both, which has a zero value, then any nonnegative values of u_1^* , u_3^* and u_4^* satisfies the system of equation. Therefore, $E_{VecEnto,1} = (u_1^*, 0, u_3^*, u_4^*, 0, 0)$ and $E_{VecEnto,2} = (u_1^*, 0, u_3^*, u_4^*, \frac{1}{\beta_m} \ln \left(\frac{\alpha_m}{v_5 + \mu_m} \right), 0)$ is an equilibrium point of system (4.10). \square

Now, in solving for the next generation matrix, since equation (3.25) and (4.10) have the same u'_2 and u'_6 , then they have the same next generation matrix where the

eigenvalues are

$$\lambda = \pm \sqrt{\frac{a^2 b_m u_5 (\tilde{b}_h u_3 + b_h u_1)}{H_0^2 (\mu_m + v_5) (\gamma_h + \delta_h)}} \quad (4.11)$$

Therefore, we have the following theorem.

Lemma 4.3.4. *The diseases free equilibrium point $E_{VecEnto,1} = (u_1^*, 0, u_3^*, u_4^*, 0, 0)$ of the system of equation (4.10) is locally asymptotically stable. While the endemic equilibrium point $E_{VecEnto,2} = \left(u_1^*, 0, u_3^*, u_4^*, \frac{1}{\beta_m} \ln \left(\frac{\alpha_m}{v_5 + \mu_m} \right), 0\right)$ is locally asymptotically stable if $\mathcal{R}_0 < 1$.*

Proof. For $E_{VecEnto,1}$, since $u_5^* = 0$, $\mathcal{R}_0 = 0 < 1$. Thus, $E_{VecEnto,1}$ is locally asymptotically stable.

For $E_{VecEnto,2}$ since $u_5^* = \frac{1}{\beta_m} \ln \left(\frac{\alpha_m}{v_5 + \mu_m} \right)$, the above eigenvalues will become

$$\mathcal{R}_0 = \sqrt{\frac{a^2 b_m \left(\frac{1}{\beta_m} \ln \left(\frac{\alpha_m}{v_5 + \mu_m} \right) \right) (\tilde{b}_h u_3^* + b_h u_1^*)}{H_0^2 (\mu_m + v_5) (\gamma_h + \delta_h)}}$$

Consequently,

$$\begin{aligned} \mathcal{R}_0^2 &= \frac{a^2 b_m \ln \left(\frac{\alpha_m}{v_5 + \mu_m} \right) (\tilde{b}_h u_3^* + b_h u_1^*)}{H_0^2 \beta_m (\mu_m + v_5) (\gamma_h + \delta_h)} \\ &= \frac{\ln \left(\frac{\alpha_m}{v_5 + \mu_m} \right) \frac{a b_m}{H_0} \left(\frac{\tilde{a} b_h u_3^* + a b_h u_1^*}{H_0} \right)}{\beta_m (\mu_m + v_5) (\gamma_h + \delta_h)}, \end{aligned}$$

if $\mathcal{R}_0 < 1$, the system is locally asymptotically stable at $E_{VecEnto,2}$. □

Following Theorem 4.2.6, we can also prove the theorem below.

Theorem 4.3.5. 1. *If $\alpha_m < \mu_m + v_5$, then $E_{VecEnto,1}$ is globally asymptotically stable.*

2. *If $\alpha_m > \mu_m + v_5$ and $\mathcal{R}_0 < 1$, then $E_{VecEnto,2}$ is globally asymptotically stable.*

4.3.3 Combination of Vaccination and Vector Control

Let us combine the dengue vaccination and the vectorial control in our model using two growth function.

Then our model becomes

$$\begin{aligned}
u_1'(t) &= -\frac{ab_h u_6(t) u_1(t)}{H_0} - v_1 u_1(t) \\
u_2'(t) &= \frac{au_6(t) (b_h u_1(t) + \tilde{b}_h u_3(t))}{H_0} - \gamma_h u_2(t) - \delta_h u_2(t) \\
u_3'(t) &= \gamma_h u_2(t) - \frac{a\tilde{b}_h u_3(t) u_6(t)}{H_0} - v_3 u_3(t) \\
u_4'(t) &= \delta_h u_2(t) \\
u_5'(t) &= -\frac{ab_m u_2(t) u_5(t)}{H_0} - \mu_m u_5(t) + \alpha_m M e^{-\beta_m M} - v_5 u_5(t) \\
u_6'(t) &= \frac{ab_m u_2(t) u_5(t)}{H_0} - \mu_m u_6(t) - v_5 u_6(t)
\end{aligned} \tag{4.12}$$

where the total human immunity is given by $T_H'(t) = v_1 u_1(t) + v_3 u_3(t)$ and total vectorial control is given by $T_M'(t) = v_5 u_5(t) + v_5 u_6(t)$.

There exists a unique global in time solution $(u_1, u_2, u_3, u_4, u_5, u_6)$ in $\mathcal{C}(\Omega_{Ento}, \mathbb{R}_+)^6$.

Lemma 4.3.6. *The system of equation (4.12) admits two equilibria $E_{CombEnto,1} = (0, 0, 0, u_4^*, 0, 0)$ and $E_{CombEnto,2} = (0, 0, 0, u_4^*, \frac{1}{\beta_m} \ln\left(\frac{\alpha_m}{\mu_m + v_5}\right), 0)$.*

Proof. Let $u_1', u_2', u_3', u_4', u_5', u_6' = 0$. Since all parameter are positive, then

$$\delta_h u_2 = 0 \quad \implies \quad u_2 = 0.$$

Thus, $\frac{ab_m u_2 u_5}{H} - \mu_m u_6 - v_5 u_6 = 0$ becomes

$$\begin{aligned}
\frac{ab_m(0)u_5}{H} - \mu_m u_6 - v_5 u_6 &= 0 \\
(-\mu_m - v_5)u_6 &= 0.
\end{aligned}$$

Hence, $u_6 = 0$. Therefore, substituting $u_6 = 0$ to both $u_1' = 0$ and $u_3' = 0$, we have

$$\begin{aligned}
-\frac{ab_h u_6 u_1}{H_0} - v_1 u_1 &= 0 & \gamma_h u_2 - \frac{a\tilde{b}_h u_3 u_6}{H_0} - v_3 u_3 &= 0 \\
-\frac{ab_h(0)u_1}{H_0} - v_1 u_1 &= 0 & \gamma_h(0) - \frac{a\tilde{b}_h u_3(0)}{H_0} - v_3 u_3 &= 0 \\
-v_1 u_1 &= 0 & -v_3 u_3 &= 0
\end{aligned}$$

Since $v_1, v_3 > 0$, $u_1 = 0$ and $u_3 = 0$. Now, substituting $u_6 = 0$ to $-\frac{ab_m u_2 u_5}{H_0} - \mu_m u_5 + \alpha_m(u_5 + u_6)e^{-\beta_m(u_5 + u_6)} - v_5 u_5 = 0$, we get

$$\begin{aligned}
-\frac{ab_m(0)u_5}{H_0} - \mu_m u_5 + \alpha_m(u_5 + 0)e^{-\beta_m(u_5 + 0)} - v_5 u_5 &= 0 \\
-\mu_m u_5 + \alpha_m u_5 e^{-\beta_m u_5} - v_5 u_5 &= 0 \\
u_5(-\mu_m + \alpha_m e^{-\beta_m u_5} - v_5) &= 0
\end{aligned}$$

implying further that

$$\begin{aligned}
 u_5 = 0 \quad \text{or} \quad & -\mu_m + \alpha_m e^{-\beta_m u_5} - v_5 = 0 \\
 & e^{-\beta_m u_5} = \frac{\mu_m + v_5}{\alpha_m} \\
 & u_5 = \frac{1}{\beta_m} \ln \left(\frac{\alpha_m}{\mu_m + v_5} \right)
 \end{aligned}$$

Consequently, since the system (4.12) contains either u_1, u_2, u_3 or u_6 or both, which has a zero value, then any nonnegative values of u_4^* satisfies the system of equation. Therefore, the equilibrium point of the system of equation (4.12) are $E_{CombEnto,1} = (0, 0, 0, u_4^*, 0, 0)$ and $E_{CombEnto,2} = \left(0, 0, 0, u_4^*, \frac{1}{\beta_m} \ln \left(\frac{\alpha_m}{\mu_m + v_5} \right), 0\right)$. \square

The next generation matrix remains the same as in Section 4.2. Thus the eigenvalues of system are

$$\lambda = \pm \sqrt{\frac{a^2 b_m u_5 (\tilde{b}_h u_3 + b_h u_1)}{H_0^2 (\mu_m + v_5) (\gamma_h + \delta_h)}}.$$

Therefore, we have the following theorem.

Lemma 4.3.7. *The disease free equilibrium point $E_{CombEnto,1} = (0, 0, 0, u_4^*, 0, 0)$ and the endemic equilibrium point $E_{CombEnto,2} = \left(0, 0, 0, u_4^*, \frac{1}{\beta_m} \ln \left(\frac{\alpha_m}{\mu_m + v_5} \right), 0\right)$ of the system of equation (4.12) are locally asymptotically stable.*

Proof. Since $u_1^*, u_3^* = 0$ in either $E_{CombEnto,1}$ and $E_{CombEnto,2}$,

$$\tilde{b}_h u_3 + b_h u_1 = \tilde{b}_h(0) + b_h(0) = 0.$$

Thus the above eigenvalues will banished. Consequently, the system of equation is locally asymptotically stable at $E_{CombEnto,1}$ and $E_{CombEnto,2}$. \square

Following Theorem 4.2.6, we can also prove the theorem below.

Theorem 4.3.8. 1. *If $\alpha_m < \mu_m + v_5$, then $E_{CombEnto,1}$ is globally asymptotically stable.*

2. *If $\alpha_m > \mu_m + v_5$ and $\mathcal{R}_0 < 1$, then $E_{CombEnto,2}$ is globally asymptotically stable.*

4.4 Optimal Control strategy

Assume that both control inputs are piecewise continuous functions that take its values in a positively bounded set $W = [0, w_H]^2 \times [0, w_M]^2$. Thus we consider the objective function

$$\mathcal{J}(w_1, w_3, w_m) = \int_0^T u_2(t) + \frac{1}{2} (A_1 w_1^2(t) + A_3 w_3^2(t) + A_m w_m^2(t)) dt$$

subject to

$$\begin{aligned}
u_1'(t) &= -\frac{ab_h u_6(t) u_1(t)}{H_0} - w_1(t) u_1(t) \\
u_2'(t) &= \frac{au_6(t) (b_h u_1(t) + \tilde{b}_h u_3(t))}{H_0} - \gamma_h u_2(t) - \delta_h u_2(t) \\
u_3'(t) &= \gamma_h u_2(t) - \frac{a\tilde{b}_h u_3(t) u_6(t)}{H_0} - w_3(t) u_3(t) \\
u_4'(t) &= \delta_h u_2(t) \\
u_5'(t) &= -\frac{ab_m u_2(t) u_5(t)}{H_0} + g(M(t)) - \mu_m u_5(t) - w_m(t) u_5(t) \\
u_6'(t) &= \frac{ab_m u_2(t) u_5(t)}{H_0} - \mu_m u_6(t) - w_m(t) u_6(t)
\end{aligned} \tag{4.13}$$

for $t \in [0, T]$, with $0 \leq w_1, w_3 \leq w_H$, $0 \leq w_m \leq w_M$ and $w = (w_1, w_3, w_m)$. The variables A_j are the positive weights associated with the control variables w_j , $j = 1, 3, m$, respectively.

Lemma 4.4.1. *There exists an optimal control $w^* = (w_1^*(t), w_3^*(t), w_m^*(t))$ such that*

$$\mathcal{J}(w_1^*, w_3^*, w_m^*) = \min_{w \in W} \mathcal{J}(w_1, w_3, w_m)$$

under the constraint $(u_1, u_2, u_3, u_4, u_5, u_6)$ is a solution of (4.13).

Pontryagin's maximum principle is used to find the best possible control for taking a dynamical system from one state to another. It states that it is necessary for any optimal control along with the optimal state trajectory to solve the so-called Hamiltonian system [42]. We state the lemma below.

Lemma 4.4.2. *There exist the adjoint variables $\lambda_i, i = 1, 2, \dots, 6$ of the system (4.13) that satisfy the following backward in time system of ordinary differential equations:*

$$\begin{aligned}
-\frac{d\lambda_1}{dt} &= \lambda_1 \left(\frac{-ab_h u_6}{H_0} - w_1 \right) + \lambda_2 \frac{ab_h u_6}{H_0} \\
-\frac{d\lambda_2}{dt} &= 1 + \lambda_2 (-\gamma_h - \delta_h) + \lambda_3 \gamma_h + \lambda_4 \delta_h - \lambda_5 \frac{ab_m u_5}{H_0} + \lambda_6 \frac{ab_m u_5}{H_0} \\
-\frac{d\lambda_3}{dt} &= \lambda_2 \frac{a\tilde{b}_h u_6}{H_0} + \lambda_3 \left(\frac{-a\tilde{b}_h u_6}{H_0} - w_3 \right) \\
-\frac{d\lambda_4}{dt} &= 0 \\
-\frac{d\lambda_5}{dt} &= \lambda_5 \left(\frac{-ab_m u_2}{H_0} + \frac{\partial g}{\partial u_5} \right) - \lambda_5 (\mu_m + w_m) + \lambda_6 \frac{ab_m u_2}{H_0} \\
-\frac{d\lambda_6}{dt} &= -\lambda_1 \frac{ab_h u_1}{H_0} + \lambda_2 \frac{ab_h u_1 + a\tilde{b}_h u_3}{H_0} - \lambda_3 \frac{a\tilde{b}_h u_3}{H_0} + \lambda_5 \frac{\partial g}{\partial u_6} - \lambda_6 (\mu_m + w_m)
\end{aligned}$$

with the transversality condition $\lambda(T) = 0$.

Proof. Using the Hamiltonian for (4.13), we have

$$\begin{aligned}
\mathcal{H} &= \mathcal{L}(w_1, w_3, w_m) + \lambda_1(t)u'_1(t) + \lambda_2(t)u'_2(t) + \lambda_3(t)u'_3(t) \\
&\quad + \lambda_4(t)u'_4(t) + \lambda_5(t)u'_5(t) + \lambda_6(t)u'_6(t) \\
&= \frac{1}{2} (u_2^2 + A_1 w_1^2 + A_3 w_3^2 + A_m w_m^2) \\
&\quad + \lambda_1 \left(-\frac{ab_h u_6 u_1}{H_0} - w_1 u_1 \right) + \lambda_3 \left(\gamma_h u_2 - \frac{\tilde{a} \tilde{b}_h u_3 u_6}{H_0} - w_3 u_3 \right) \\
&\quad + \lambda_2 \left(\frac{a u_6 (b_h u_1 + \tilde{b}_h u_3)}{H_0} - \gamma_h u_2 - \delta_h u_2 \right) + \lambda_4 (\delta_h u_2) \\
&\quad + \lambda_5 \left(-\frac{ab_m u_2 u_5}{H_0} + g(M) - \mu_m u_5 - w_m u_5 \right) \\
&\quad + \lambda_6 \left(\frac{ab_m u_2 u_5}{H_0} - \mu_m u_6 - w_m u_6 \right). \tag{4.14}
\end{aligned}$$

Therefore, finding the partial derivatives of \mathcal{H} with respect to u_i 's, $i = 1, 2, \dots, 6$, we have

$$\begin{aligned}
\frac{\partial \mathcal{H}}{\partial u_1} &= \lambda_1 \left(-\frac{ab_h u_6}{H_0} - w_1 \right) + \lambda_2 \frac{ab_h u_6}{H_0} \\
\frac{\partial \mathcal{H}}{\partial u_2} &= 1 + \lambda_2 (-\gamma_h - \delta_h) + \lambda_3 \gamma_h + \lambda_4 \delta_h - \lambda_5 \frac{ab_m u_5}{H_0} + \lambda_6 \frac{ab_m u_5}{H_0} \\
\frac{\partial \mathcal{H}}{\partial u_3} &= \lambda_2 \frac{\tilde{a} \tilde{b}_h u_6}{H_0} + \lambda_3 \left(\frac{-\tilde{a} \tilde{b}_h u_6}{H_0} - w_3 \right) \\
\frac{\partial \mathcal{H}}{\partial u_4} &= 0 \\
\frac{\partial \mathcal{H}}{\partial u_5} &= \lambda_5 \left(-\frac{ab_m u_2}{H_0} + \frac{\partial g}{\partial u_5} \right) - \lambda_5 (\mu_m + w_m) + \lambda_6 \frac{ab_m u_2}{H_0} \\
\frac{\partial \mathcal{H}}{\partial u_6} &= -\lambda_1 \frac{ab_h u_1}{H_0} + \lambda_2 \frac{ab_h u_1 + \tilde{a} \tilde{b}_h u_3}{H_0} - \lambda_3 \frac{\tilde{a} \tilde{b}_h u_3}{H_0} + \lambda_5 \frac{\partial g}{\partial u_6} - \lambda_6 (\mu_m + w_m).
\end{aligned}$$

Then the adjoint system is defined by $\frac{d\lambda_i}{dt} = -\frac{\partial \mathcal{H}}{\partial u_i}$ for $i = 1, 2, \dots, 6$. \square

Theorem 4.4.3. *The optimal control variables are given by*

$$\begin{aligned}
w_1^*(t) &= \max \left(0, \min \left(\frac{\lambda_1 u_1}{A_1}, w_H \right) \right) \\
w_3^*(t) &= \max \left(0, \min \left(\frac{\lambda_3 u_3}{A_3}, w_H \right) \right) \\
w_m^*(t) &= \max \left(0, \min \left(\frac{\lambda_5 u_5 + \lambda_6 u_6}{A_m}, w_M \right) \right)
\end{aligned}$$

Proof. By the Pontryagin maximum principle, the optimal control w^* minimizes, at each instant t , the Hamiltonian given by (4.14). We have

$$\frac{\partial H}{\partial w_j} = 0, \quad \text{for all } j = 1, 3, m \quad \text{at } w_j = w_j^*.$$

Therefore, we get

$$\frac{\partial \mathcal{H}}{\partial w_1} = A_1 w_1 - \lambda_1 u_1, \quad \frac{\partial \mathcal{H}}{\partial w_3} = A_3 w_3 - \lambda_3 u_3, \quad \frac{\partial \mathcal{H}}{\partial w_m} = A_m w_m - \lambda_5 u_5 - \lambda_6 u_6,$$

and

$$w_1 = \frac{\lambda_1 u_1}{A_1}, \quad w_3 = \frac{\lambda_3 u_3}{A_3}, \quad w_m = \frac{\lambda_5 u_5 + \lambda_6 u_6}{A_m}.$$

□

4.4.1 Numerical Simulation of Optimal Control

Numerical simulations show the difference in minimizing the infected human during the dengue outbreak between the three methods: vaccination, vector control, and the combination of the vaccination and vector control.

Symbol	Description	Values
a	number of human beaten per mosquito	1 day^{-1}
b_h	probability of becoming infected	0.75 day^{-1}
\tilde{b}_h	probability of becoming infected again	0.375 day^{-1}
α_h	growth rate of human	0.0045 day^{-1}
γ_h	recovery rate of human from first infection	$0.328833 \text{ day}^{-1}$
δ_h	recovery rate of human from the second infection	0.1666 day^{-1}
b_m	probability of becoming infectious	0.375 day^{-1}
μ_m	death rate of mosquito	0.02941 day^{-1}
α_m	growth rate of mosquito	0.025 day^{-1}

TABLE 4.1: Parameter values used in the numerical simulations.

The parameters are presented in Table 4.1, which is taken from [6]. Notice that $\alpha_m < \mu_m$, by Theorem 4.3.8 the global stability corresponds to $E_{CombEnto,1}$. Here $E_{CombEnto,2}$ is biologically not meaningful in this situation. The author estimated some from Indonesia, where environmental conditions are similar to the Philippines. The control weights A_1 and A_3 are the efforts in vaccinating the human population. In contrast, the control weights A_m is the effort to eliminate the mosquito population by means of administering insecticides. Since primary susceptible humans are readily available in the population compared to the secondary susceptible humans, the efforts used in vaccinating them would be less than the effort exerted in vaccinating the secondary susceptible. Thus, A_3 is set higher than A_1 . While insecticide administration in susceptible mosquitoes and infected mosquitoes uses the same effort and achieves a similar result. Hence, we initially set the control weights as

$A_1 = 0.1$, $A_3 = 1$ and $A_m = 1$. Note that the values of A_1, A_3, A_m do not change the convergence of optimal control

A finite difference scheme is used to numerically solve direct and the adjoint system of ordinary differential equations. More precisely, an explicit correction Adams-Bashford and implicit correction Adams-Moulton of order 2 is written in python. The optimality of the system is numerically solved using Algorithm 1 with $\epsilon = 0.01$.

Algorithm 1 Computation of optimal control of dengue-dengvaxia

Given $U^0 = (10^4, 0, 0, 0, 10^5, 10^3)$ as initial datum, a final time $T > 0$ and a tolerance $\epsilon > 0$.

Let w_1^0, w_2^0, w_m^0 randomly chosen following $\mathcal{N}(0, 1)$.

while $\|\nabla \mathcal{H}(w^n, U^n, \lambda^n)\| > \epsilon$ **do**,
 solve the forward system u^n ,
 solve the backward system λ^n ,
 update w^n
 solve the gradient $\nabla \mathcal{H}(w^n, U^n, \lambda^n)$

$w^* = w^n$.

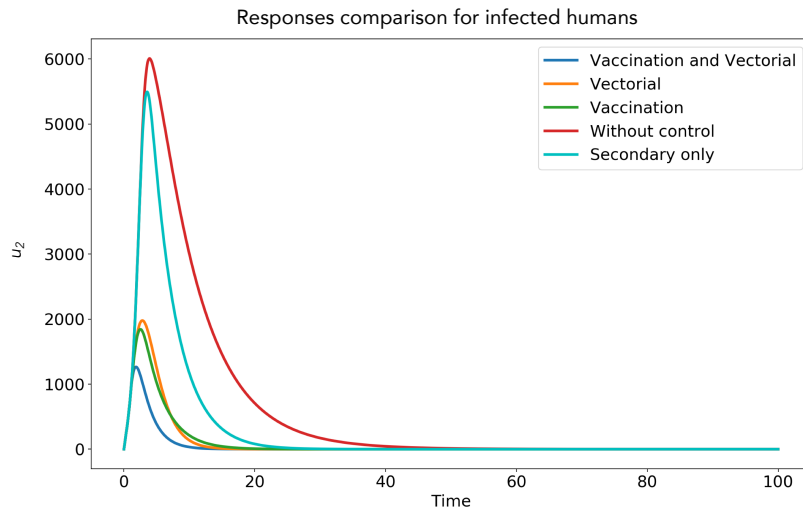


FIGURE 4.4: Behaviour of infected humans I_h with respect to time without control (red), for the optimal control related to the vaccination only (green), related to the vector only (orange), and with both control (blue). Cyan curve corresponds to optimal control of vaccination of secondary humans only.

Figure 4.4 shows in minimizing the infected human that the combination of Dengvaxia and vector control is the most effective method. It would only take 30 days to reach equilibrium, resulting in the total elimination of infected humans with a maximum of 12.55% (1,255) infected humans over time. Nevertheless, vector control stands out if we compare only the vaccination and vector control method. It would only take 34 days with a maximum population of 19.68% (1,968) infected humans for vector control to eliminate infected humans. In comparison, vaccination takes 45 days, with 18.42% (1,842) infected humans. Without control, infected

humans would slowly decrease after reaching 60.07% (6,007) but would never annihilate. Vaccinating secondary humans would only take 48 days to reach equilibrium with a maximum of 54.94% (5,494) infected humans over time.

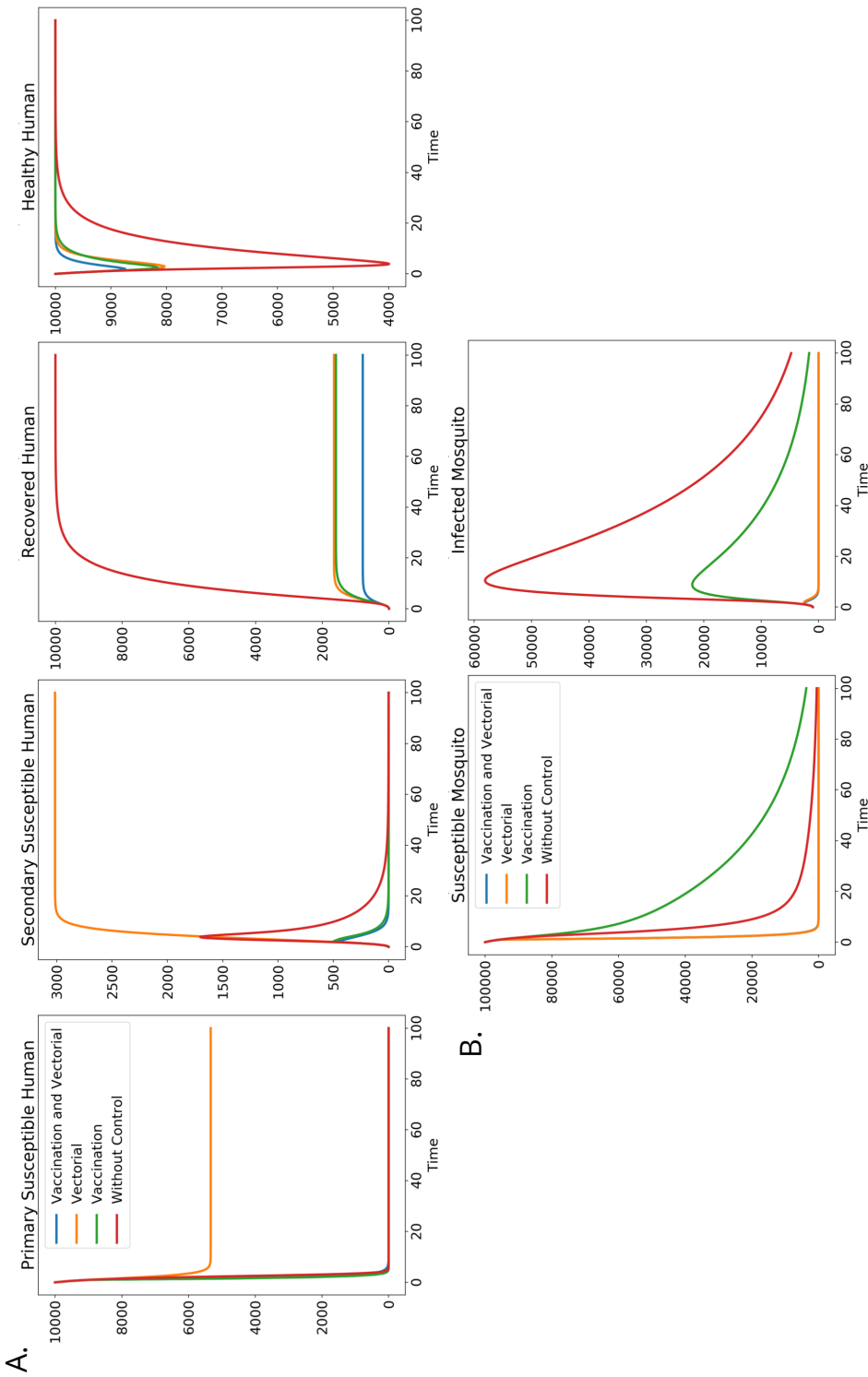


FIGURE 4.5: Behaviour of (A) human compartment and (B) mosquito compartment with respect to time without control (red), for the optimal control related to the vaccination only (green), and with both control (blue).

Figure 4.5 shows no significant difference between the three methods concerning the primary and secondary susceptibles to reach its equilibrium point. It takes seven and a half days for vaccination and 14 days to combine vaccination and vector control to reach zero primary susceptible individuals. Moreover, it takes 42 days for vaccination and 30 days for the combination to reach zero secondary susceptible individuals. For vector control, it takes 20 days to reach an equilibrium of 53.36% (5336) primary susceptible humans and 34 days to reach 30.15% (3015) secondary susceptible humans.

Note that in the human compartment, the total immunity to dengue by means of implementing the Dengvaxia vaccine is denoted by T_h which is given by $T_h(t) = w_1(t)u_1(t) + w_3(t)u_3(t)$. Thus, a healthy human combines immune human T_h , primary susceptible u_1 , secondary susceptible u_3 , and the recovered u_4 humans. The figure shows that the combination of vaccination and vector control is the best method in maximizing the healthy human population. It only takes 26 days to combine vaccination and vector control methods to reach the equilibrium of healthy humans. Its minimum population is 8.73% (8,734) on day 1.8.

In contrast, there is no significant difference in the vector and vaccination method alone in the healthy human population. The vector method takes 29 days to reach its equilibrium with 8.02% (8,021) minimum population on 2.8 days. The vaccination required 39 days to reach an equilibrium with 8.16% (8,157) minimum population on 2.5 days. Without any control strategies applied to the healthy human population, it requires a much higher time to reach its equilibrium with 4% (4,000) minimum population.

For the recovered human compartment, the figure shows that the human population would eventually recover through time without control strategies applied to the variables. It supports that dengue infection lasts only three to seven days following the infectious mosquito bite, and a spontaneous, full health recovery follows. However, comparing the three control methods, the combination of vaccination and vector control methods stands out. It only requires 26 days to reach its equilibrium at 0.79% (787) recovered human population. At the same time, there is no significant difference between vaccination alone and vector control alone. Both require 32 days to reach its equilibrium at 1.59% (1,590) and 1.65% (1,646) recovered human, respectively.

Now, minimizing the susceptible mosquito population, no control applied to the variables is better than vaccination. It decreases faster with 0.56% (556) minimum susceptible mosquito population while vaccination decreases slower with 3.69% (3,692) minimum population at the end of time. Nevertheless, the vector control method and the combination of vaccination and vector control are the better methods for controlling the mosquito population. They annihilate the susceptible mosquito population.

Minimizing the infected mosquito, either vector control alone or combining vaccination and vector control is the best method. There is no significant difference between the two. They both require minimum time for the infected mosquito to reach zero population and with only 2.6% (2596) and 2.52% (2521) maximum population for the vector control only and the combination, respectively. However, vaccination is better compared to the one without control. The infected mosquito has a 58.09% (58,092) maximum population without applying a control strategy, while the vaccination has a 22% (22,006) maximum population.

Now, let us show the controlled variable's behavior by comparing the vaccination, vector control only, and the combination of vaccination and vector control.

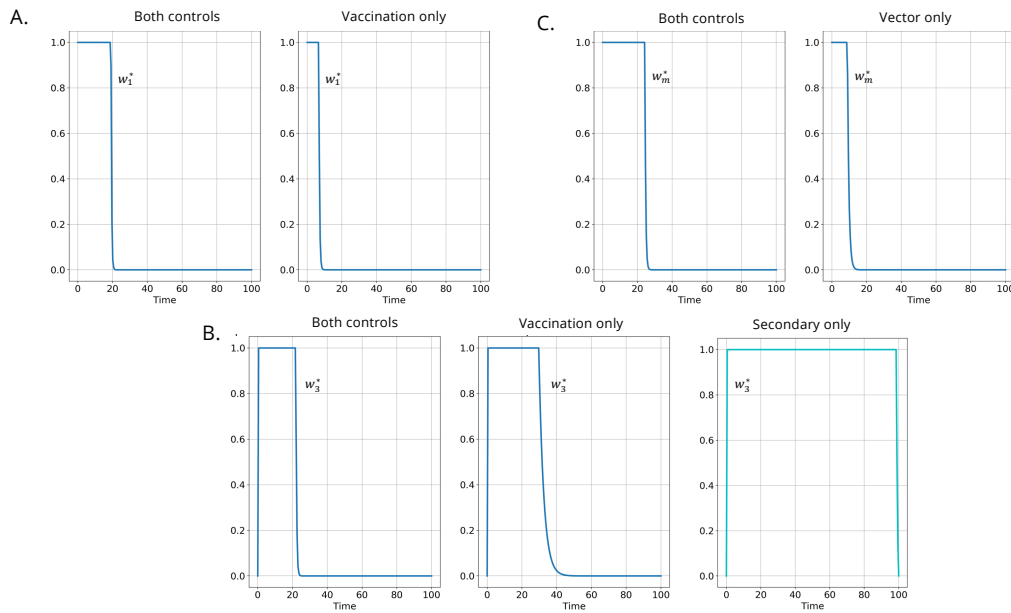


FIGURE 4.6: Optimal control of the (A) primary susceptible and (B) secondary susceptible human compartment using vaccination only versus the combination of both control strategies. Optimal control of (C) mosquitoes compartment using vector control only versus the combination of both control strategies. Cyan curve represents optimal control of vaccination of secondary humans only

Figure 4.6 shows that concerning vaccination only, vaccinating the primary susceptible human population requires a shorter time compared to the secondary susceptible human. It takes ten days and 40 days to vaccinate primary and secondary susceptible human populations, respectively. Nevertheless, applying both control strategies takes only approximately 20-22 days. While minimizing the mosquito population, the vector control method is better than combining the two strategies. It takes approximately 15-18 days to administer insecticide to the mosquito population while applying both control strategies takes 22-24 days.

Chapter 5

A Model of Dengue accounting for the Life Cycle

In this chapter, we introduced a ROSS-type model of dengue accounting for mosquitoes' life cycle. The qualitative study of this model was also discussed, as the identifiability of the parameters involved. An optimal control strategy using copepods and pesticides was added to the model. The numerical simulations of the optimal control use the effectivity of *Mesocyclops aspericornis*, a Philippines specie of copepod, to eliminate larvae and thermal fogging to eliminate adult mosquitoes.

5.1 Life Cycle of Mosquitoes

Mosquitoes have a complex life cycle. They change their shape and habitat as they develop.

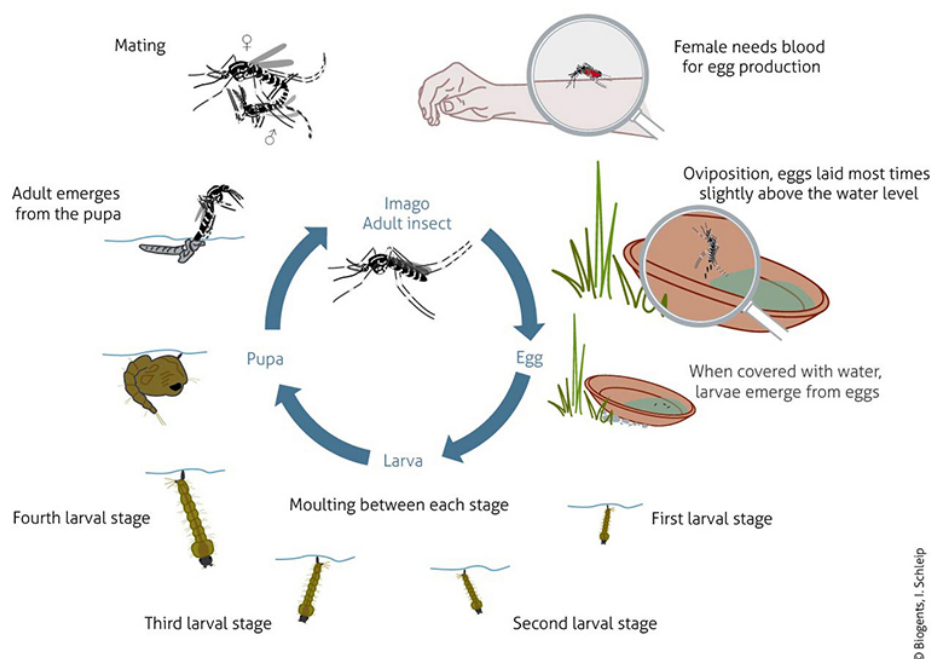


FIGURE 5.1: Life cycle of *Aedes* mosquitoes.

Only female adult mosquitoes lay eggs. They lay their eggs which stick like glue, above the water line on the inner walls of containers that are or will be filled with water. This oviposition site includes the wall of a cavity, such as a hollow stump, or a container, such as a bucket or a discarded vehicle tire. Only a tiny amount of water is needed to lay eggs. The egg hatch into larvae when water inundates the eggs by any means, such as rain or filling water by people. But mosquito eggs can survive drying out for up to 8 months or even in winter in the southern United States [20]. When that happens, they have to withstand considerable desiccation before that hatch [59]. Once they achieve a suitable desiccation level, they can enter diapause for several months. *Aedes* eggs in diapause tend to hatch irregularly over an extended period of time.

Larvae live in water, and they feed on microorganisms and particulate organic matter. They develop through four stages, or instars. In the first to fourth instar, the larvae molt, shedding their skins to allow for further growth. On the fourth instar, when the larva is fully grown, they metamorphose into a new form called pupae. Pupa still lives in water but they do not feed. After two days, they fully developed into adult mosquito forms and breaks through the skin of the pupa. Adult mosquito is no longer aquatic, it has a terrestrial habitat and is able to fly. This entire life cycle of mosquito last for eight to ten days at room temperature, depending on the level of feeding.

Dengue viruses are spread to people through the bites of infected *Aedes* species mosquitoes (*Ae. aegypti* or *Ae. albopictus*). These are the same types of mosquitoes that spread Zika and chikungunya viruses [18].

Dengue can also spread from mother to child. A pregnant woman already infected with dengue can pass the virus to her fetus during pregnancy or around the time of birth.

Rarely, dengue can also be transmitted through infected blood, laboratory, or healthcare setting exposures, i.e., through blood transfusion, organ transplant, or through a needle stick injury.

5.2 Description of the model

In this section, we presented a new model that involves the mosquitoes aquatic stage. Based on the Ross-type model, we assumed that dengue viruses are virulent and no other microorganism attacking the body and it is not transmitted from mother to child.

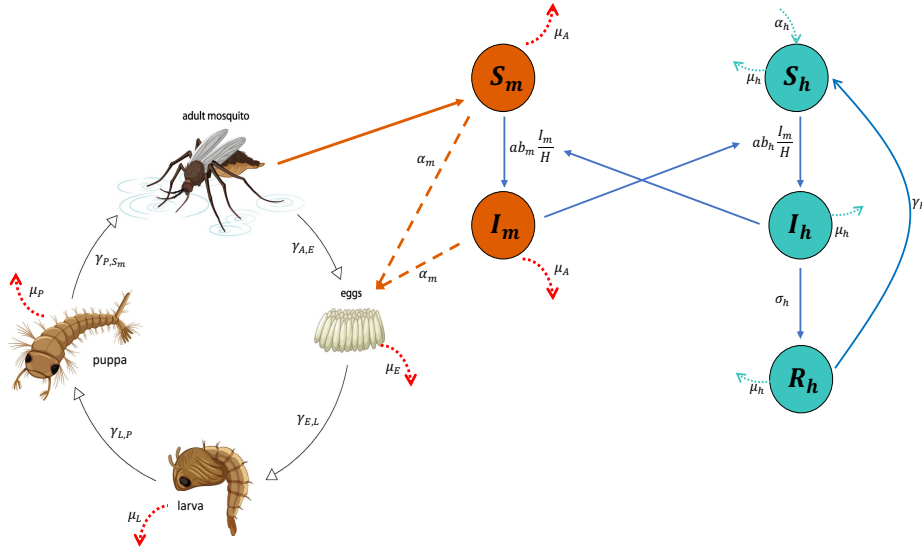


FIGURE 5.2: Compartmental representation

Let M_Y and M_A represents the young and adult mosquito population, respectively. Thus M_Y is subdivided into the three aquatic stage, i.e., eggs E , larvae L , and pupae P , and M_A is subdivided into susceptible S_m and infected I_m mosquitoes. In this study, we assumed that adult mosquito cannot pass the virus to its eggs. That is, we assume that eggs reproduce by either susceptible or infected mosquito is not a genetic carrier of dengue virus. α_m represents mosquitoes birth rate through egg production. Thus, $\alpha_m S_m$ and $\alpha_m I_m$ represents the rate of egg laying of susceptible mosquitoes and infected mosquitoes, respectively. As mosquito evolved from one life stage to another, we use the parameter $\gamma_{i,j}$ as the conversation between state variables. μ_i represents the death rate in each state variables. With total population of $M_Y = E + L + P$, the dynamics of the metamorphosis of young mosquito is govern by the equation below.

$$E'(t) = \alpha_m(S_m(t) + I_m(t)) - \gamma_{E,L}E(t) - \mu_E E(t) \quad (5.1)$$

$$L'(t) = \gamma_{E,L}E(t) - \gamma_{L,P}L(t) - \mu_L L(t) \quad (5.2)$$

$$P'(t) = \gamma_{L,P}L(t) - \gamma_{P,S_m}P(t) - \mu_P P(t). \quad (5.3)$$

When pupa fully developed it breaks through its skin and become an adult mosquito. Adult mosquito is longer aquatic and is able to fly. We denote $\gamma_{P,S_m} P e^{-\beta_m P}$ as the transition rate of pupae to adult mosquito. The pupal competition is translated by $e^{-\beta_m P}$ meaning that the death rate increases with the pupae density P [11]. In this study, we assume that all emerging adults are susceptible. $ab_m I_h$ represents the probability of susceptible mosquito to be infectious once it bites an infected humans. The parameter a represents the average mosquito bites and b_m is the transmission probability from infected humans to susceptible mosquito. With total population of $M_A = S_m + I_m$, the dynamics of the interaction of adult mosquito is govern by the equation below.

$$S'_m(t) = \gamma_{P,S_m} P(t) e^{-\beta_m P(t)} - \mu_A S_m(t) - ab_m I_h(t) S_m(t) \quad (5.4)$$

$$I'_m(t) = ab_m I_h(t) S_m(t) - \mu_A I_m(t) \quad (5.5)$$

Since humans have a meager mortality rate compared to mosquitoes, we neglect the human death rate. Let H be the human population subdivided into susceptible S_h , infected I_h and recovered R_h humans. The dynamics of human population is given by

$$S'_h(t) = \gamma_h R_h(t) - ab_h I_m(t) S_h(t) \quad (5.6)$$

$$I'_h(t) = ab_h I_m(t) S_h(t) - \sigma_h I_h(t) \quad (5.7)$$

$$R'_h(t) = \sigma_h I_h(t) - \gamma_h R_h(t) \quad (5.8)$$

In this chapter, susceptible humans represents both primary and secondary susceptible. Thus as humans recovered ($\gamma_h R_h$ is the recovery rate of humans from dengue infection) from one, two or three types of dengue virus, it goes back to being susceptible to the other type of the virus. Since an individual being infected by all types of dengue virus is a rare case, we neglect the total immunity. The probability of susceptible humans to be infected with dengue is given by $ab_h I_m$, where b_h represents the probability of transmission of virus from infected mosquito to susceptible humans.

5.3 Qualitative Study of the Model

Let $U(t) = (E(t), L(t), P(t), S_m(t), I_m(t), S_h(t), I_h(t), R_h(t))^T$. Then the system above can be rewritten in compact form as

$$U'(t) = f(t, U(t)), \quad (5.9)$$

where

$$f(t, U) = \begin{pmatrix} \alpha_m(S_m + I_m) - \gamma_{E,L}E - \mu_E E \\ \gamma_{E,L}E - \gamma_{L,P}L - \mu_L L \\ \gamma_{L,P}L - \gamma_{P,S_m}P - \mu_P P \\ \gamma_{P,S_m}Pe^{-\beta_m P} - \mu_A S_m - ab_m I_h S_m \\ ab_m I_h S_m - \mu_A I_m \\ \gamma_h R_h - ab_h I_m S_h \\ ab_h I_m S_h - \sigma_h I_h \\ \sigma_h I_h - \gamma_h R_h \end{pmatrix} \quad (5.10)$$

5.3.1 Well-posedness and Positivity of the Solution

Lemma 5.3.1. *Let $(E(0), L(0), P(0), S_m(0), I_m(0), S_h(0), I_h(0), R_h(0))$ be a nonnegative initial datum with $H(0) = S_h(0) + I_h(0) + R_h(0) > 0$, $M_A = S_m(0) + I_m(0) > 0$ and $M_Y(0) = E(0) + L(0) + P(0) > 0$. Then there exist a time $T > 0$ and a unique solution $(E, L, P, S_m, I_m, S_h, I_h, R_h)$ in $\mathcal{C}([0, T], \mathbb{R})^8$.*

Proof. Consider the initial value problem $U'(t) = f(t, U(t))$ where $U(0) = U_0$. The function $f(t, U(t))$ is \mathcal{C}^1 on $[0, T]$ and thus, U satisfies the local Lipschitz condition. Therefore, by Cauchy-Lipschitz Theorem, there exist $T > 0$ and a unique solution to equation (5.10) in $\mathcal{C}([0, T], \mathbb{R})^8$. \square

Now we will show that if the solution exists then it is positive and bounded.

Lemma 5.3.2. *The solution is nonnegative and bounded for all time.*

Proof. Let $U = (E, L, P, S_m, I_m, S_h, I_h, R_h) \in \mathbb{R}_+^8$ be the solution of the system of equation (5.10). In proving for positivity, we assume that the parameters are positive for

all time $t > 0$. We have

$$\begin{aligned}
f_1(E = 0, L, P, S_m, I_m, S_h, I_h, R_h) &= \alpha_m(S_m + I_m) - \gamma_{E,L}E - \mu_E E \\
&= \alpha_m(S_m + I_m) \leq 0 \quad \forall L, P, S_m, I_m, S_h, I_h, R_h \geq 0 \\
f_2(E, L = 0, P, S_m, I_m, S_h, I_h, R_h) &= \gamma_{E,L}E - \gamma_{L,P}L - \mu_L L \\
&= \gamma_{E,L}E > 0 \quad \forall E, P, S_m, I_m, S_h, I_h, R_h \geq 0 \\
f_3(E, L, P = 0, S_m, I_m, S_h, I_h, R_h) &= \gamma_{L,P}L - \gamma_{P,S_m}P - \mu_P P \\
&= \gamma_{L,P}L > 0 \quad \forall E, L, S_m, I_m, S_h, I_h, R_h \geq 0 \\
f_4(E, L, P, S_m = 0, I_m, S_h, I_h, R_h) &= \gamma_{P,S_m}P e^{-\beta_m P} - \mu_A S_m - ab_m I_h S_m \\
&= \gamma_{P,S_m}P e^{-\beta_m P} > 0 \quad \forall E, L, P, I_m, S_h, I_h, R_h \geq 0 \\
f_5(E, L, P, S_m, I_m = 0, S_h, I_h, R_h) &= ab_m I_h S_m - \mu_A I_m \\
&= ab_m I_h S_m > 0 \quad \forall E, L, P, S_m, S_h, I_h, R_h \geq 0 \\
f_6(E, L, P, S_m, I_m, S_h = 0, I_h, R_h) &= \gamma_h R_h - ab_h I_m S_h \\
&= \gamma_h R_h > 0 \quad \forall E, L, P, S_m, I_m, I_h, R_h \geq 0 \\
f_7(E, L, P, S_m, I_m, S_h, I_h = 0, R_h) &= ab_h I_m S_h - \sigma_h I_h \\
&= ab_h I_m S_h > 0 \quad \forall E, L, P, S_m, I_m, S_h, R_h \geq 0 \\
f_8(E, L, P, S_m, I_m, S_h, I_h, R_h = 0) &= \sigma_h I_h - \gamma_h R_h \\
&= \sigma_h I_h > 0 \quad \forall E, L, P, S_m, I_m, S_h, I_h \geq 0
\end{aligned}$$

Hence, we have shown that for all time $t > 0$, the solution $E, L, P, S_m, I_m, S_h, I_h$ and R_h remains nonnegative.

Since we consider a constant human population $H'(t) = 0$, then

$$H(t) = H_0 = \text{constant}$$

and the human components, being nonnegative, are bounded by H_0 .

Now, note that mosquito population is the combination of young and adult mosquito. Let $\mu_m = \min(\mu_E, \mu_L, \mu_P, \mu_A)$, then

$$\begin{aligned}
M' &= (E + L + P + S_m + I_m)' \\
&= \alpha_m(S_m + I_m) - \mu_E E - \mu_L L - \mu_P P - \mu_A(S_m + I_m) - \gamma_{P,S_m}P(1 - e^{-\beta_m P}) \\
&\leq (\alpha_m - \mu_m)M
\end{aligned}$$

Therefore, from Grönwall's Lemma,

$$M(t) \leq e^{(\alpha_m - \mu_m)t} M_0.$$

If $\alpha_m \leq \mu_m$, then $\alpha_m - \mu_m \leq 0$ and $M(t) = e^{(\alpha_m - \mu_m)t} M_0 \leq M_0$. On the other hand, if $\alpha_m - \mu_m > 0$ and $M(t) \leq e^{(\alpha_m - \mu_m)t} M_0$, which is finite for all finite time t and infinite only when $t = +\infty$.

□

From lemma 5.3.1 and lemma 5.3.2, we can deduce the global well-posedness theorem below.

Theorem 5.3.3. *Let $(E(0), L(0), P(0), S_m(0), I_m(0), S_h(0), I_h(0), R_h(0))$ be in Ω . Then there exists a unique global in time solution $(E, L, P, S_m, I_m, S_h, I_h, R_h)$ in $\mathcal{C}(\mathbb{R}_+, \Omega)$ ⁸.*

5.3.2 Equilibrium of the Model

Let $(E^*, L^*, P^*, S_m^*, I_m^*, S_h^*, I_h^*, R_h^*)$ be an equilibrium point of the system of equation (5.10). Then solving the system of equation below

$$\alpha_m(S_m + I_m) - \gamma_{E,L}E - \mu_E E = 0 \quad (5.11)$$

$$\gamma_{E,L}E - \gamma_{L,P}L - \mu_L L = 0 \quad (5.12)$$

$$\gamma_{L,P}L - \gamma_{P,S_m}P - \mu_P P = 0 \quad (5.13)$$

$$\gamma_{P,S_m}P e^{-\beta_m P} - \mu_A S_m - ab_m I_h S_m = 0 \quad (5.14)$$

$$ab_m I_h S_m - \mu_A I_m = 0 \quad (5.15)$$

$$\gamma_h R_h - ab_h I_m S_h = 0 \quad (5.16)$$

$$ab_h I_m S_h - \sigma_h I_h = 0 \quad (5.17)$$

$$\sigma_h I_h - \gamma_h R_h = 0 \quad (5.18)$$

would give us the equilibrium points $\mathcal{E}_{DFE} = (E^*, L^*, P^*, S_m^*, 0, S_h^*, 0, 0)$ and $\mathcal{E}_{EE} = (E^*, L^*, P^*, S_m^*, I_m^*, S_h^*, I_h^*, R_h^*)$. To show this, consider the lemma below.

Lemma 5.3.4. *The system of equation (5.10) admits a positive disease free equilibrium $\mathcal{E}_{DFE} = (E^*, L^*, P^*, S_m^*, 0, S_h^*, 0, 0)$ and an endemic equilibrium $\mathcal{E}_{EE} = (E^*, L^*, P^*, S_m^*, I_m^*, S_h^*, I_h^*, R_h^*)$.*

Proof. Suppose $I_h \neq 0$. Expressing each equation in the system in terms of P, I_m and I_h we can have from equation (5.13),

$$L = \frac{\gamma_{P,S_m} + \mu_P}{\gamma_{L,P}} P. \quad (5.19)$$

From equation (5.12), solving for E we get

$$\begin{aligned} \gamma_{E,L}E &= (\gamma_{L,P} + \mu_L)L \\ E &= \frac{\gamma_{L,P} + \mu_L}{\gamma_{E,L}} L \end{aligned}$$

Substituting equation (5.19) to the equation above would give us

$$E = \frac{(\gamma_{L,P} + \mu_L)(\gamma_{P,S_m} + \mu_P)}{\gamma_{E,L}\gamma_{L,P}} P \quad (5.20)$$

Now, adding equation (5.14) and (5.15) we get

$$\begin{aligned}\gamma_{P,S_m} P e^{-\beta_m P} - \mu_A S_m - \mu_A I_m &= 0 \\ \mu_A (S_m + I_m) &= \gamma_{P,S_m} P e^{-\beta_m P} \\ S_m + I_m &= \frac{\gamma_{P,S_m} P e^{-\beta_m P}}{\mu_A}\end{aligned}$$

From equation (5.11), solving for $S_m + I_m$ we have

$$\begin{aligned}\alpha_m (S_m + I_m) &= (\gamma_{E,L} + \mu_E) E \\ S_m + I_m &= \frac{(\gamma_{E,L} + \mu_E) E}{\alpha_m}\end{aligned}$$

Now, equating the two equations above and substituting equation (5.20) to E , we have

$$\begin{aligned}\frac{\gamma_{P,S_m} P e^{-\beta_m P}}{\mu_A} &= \frac{(\gamma_{E,L} + \mu_E) \cdot \frac{(\gamma_{L,P} + \mu_L)(\gamma_{P,S_m} + \mu_P) P}{\gamma_{E,L} \gamma_{L,P}}}{\alpha_m} \\ \frac{\gamma_{P,S_m} P e^{-\beta_m P}}{\mu_A} &= \frac{(\gamma_{E,L} + \mu_E)(\gamma_{L,P} + \mu_L)(\gamma_{P,S_m} + \mu_P) P}{\alpha_m \gamma_{E,L} \gamma_{L,P}} \\ e^{-\beta_m P} &= \frac{\mu_A (\gamma_{E,L} + \mu_E)(\gamma_{L,P} + \mu_L)(\gamma_{P,S_m} + \mu_P)}{\alpha_m \gamma_{E,L} \gamma_{L,P} \gamma_{P,S_m}} \\ e^{\beta_m P} &= \frac{\alpha_m \gamma_{E,L} \gamma_{L,P} \gamma_{P,S_m}}{\mu_A (\gamma_{E,L} + \mu_E)(\gamma_{L,P} + \mu_L)(\gamma_{P,S_m} + \mu_P)}\end{aligned}$$

Applying \ln to both sides of the equation would give us

$$\beta_m P = \ln \frac{\alpha_m \gamma_{E,L} \gamma_{L,P} \gamma_{P,S_m}}{\mu_A (\gamma_{E,L} + \mu_E)(\gamma_{L,P} + \mu_L)(\gamma_{P,S_m} + \mu_P)}$$

Therefore,

$$P = \frac{1}{\beta_m} \ln \left(\frac{\alpha_m \gamma_{E,L} \gamma_{L,P} \gamma_{P,S_m}}{\mu_A (\gamma_{E,L} + \mu_E)(\gamma_{L,P} + \mu_L)(\gamma_{P,S_m} + \mu_P)} \right) \quad (5.21)$$

Solving S_m from equation (5.14), we get

$$S_m = \frac{\gamma_{P,S_m} P e^{-\beta_m P}}{\mu_A + ab_m I_h}.$$

From equation (5.15), solving for I_m , we have

$$\begin{aligned}I_m &= \frac{ab_m I_h S_m}{\mu_A} \\ &= \frac{ab_m I_h \cdot \frac{\gamma_{P,S_m} P e^{-\beta_m P}}{\mu_A + ab_m I_h}}{\mu_A}\end{aligned}$$

Thus,

$$I_m = \frac{ab_m I_h \gamma_{P,S_m} P e^{-\beta_m P}}{\mu_A (\mu_A + ab_m I_h)} \quad (5.22)$$

Solving R_h from equation (5.18), we can get

$$R_h = \frac{\sigma_h I_h}{\gamma_h}. \quad (5.23)$$

From equation (5.17), solving for S_h we have

$$S_h = \frac{\sigma_h I_h}{ab_h I_m} \quad (5.24)$$

Therefore the endemic equilibrium of the system of equation (5.10) is $\mathcal{E}_{EE} = (E^*, L^*, P^*, S_m^*, I_m^*, S_h^*, I_h^*, R_h^*)$ where

$$\begin{aligned} E^* &= \frac{(\gamma_{L,P} + \mu_L)(\gamma_{P,S_m} + \mu_P)}{\gamma_{E,L}\gamma_{L,P}} P^* \\ L^* &= \frac{\gamma_{P,S_m} + \mu_P}{\gamma_{L,P}} P^* \\ P^* &= \frac{1}{\beta_m} \ln \left(\frac{\alpha_m \gamma_{E,L} \gamma_{L,P} \gamma_{P,S_m}}{\mu_A (\gamma_{E,L} + \mu_E) (\gamma_{L,P} + \mu_L) (\gamma_{P,S_m} + \mu_P)} \right) \\ S_m^* &= \frac{\gamma_{P,S_m} P^* e^{-\beta_m P^*}}{\mu_A + ab_m I_h^*} \\ I_m^* &= \frac{ab_m I_h^* \gamma_{P,S_m} P^* e^{-\beta_m P^*}}{\mu_A (\mu_A + ab_m I_h^*)} \\ S_h^* &= \frac{\sigma_h I_h^*}{ab_h I_m^*} \\ I_h^* &= I_h^* \\ R_h^* &= \frac{\sigma_h I_h^*}{\gamma_h}. \end{aligned}$$

Now if $I_h^* = 0$ then $I_m^* = R_h^* = 0$ and $S_h^* = H$. Hence the disease free equilibrium is $\mathcal{E}_{DFE} = (E^*, L^*, P^*, S_m^*, 0, H, 0, 0)$, where

$$\begin{aligned} E^* &= \frac{(\gamma_{L,P} + \mu_L)(\gamma_{P,S_m} + \mu_P)}{\gamma_{E,L}\gamma_{L,P}} P^* \\ L^* &= \frac{\gamma_{P,S_m} + \mu_P}{\gamma_{L,P}} P^* \\ P^* &= \frac{1}{\beta_m} \ln \left(\frac{\alpha_m \gamma_{E,L} \gamma_{L,P} \gamma_{P,S_m}}{\mu_A (\gamma_{E,L} + \mu_E) (\gamma_{L,P} + \mu_L) (\gamma_{P,S_m} + \mu_P)} \right) \\ S_m^* &= \frac{\gamma_{P,S_m} P^* e^{-\beta_m P^*}}{\mu_A} \end{aligned}$$

□

5.3.3 Next Generation Matrix and Basic Reproduction Number

In this section, will obtain the basic reproduction number using the next generation matrix.

Since the infected individuals are in I_h and I_m , if \mathcal{F} is the rate of appearance of new infections in each compartment and \mathcal{V} is the rate of other transitions between all compartments, then we can have

$$\mathcal{F} = \begin{pmatrix} ab_m I_h S_m \\ ab_h I_m S_h \end{pmatrix} \quad \text{and} \quad \mathcal{V} = \begin{pmatrix} \mu_A I_m \\ \sigma_h I_h \end{pmatrix}$$

where

$$F = \begin{pmatrix} 0 & ab_m S_m \\ ab_h S_h & 0 \end{pmatrix} \quad \text{and} \quad V = \begin{pmatrix} \mu_A & 0 \\ 0 & \sigma_h \end{pmatrix}.$$

Thus, solving for FV^{-1} , we have

$$\begin{aligned} FV^{-1} &= \begin{pmatrix} 0 & ab_m S_m \\ ab_h S_h & 0 \end{pmatrix} \begin{pmatrix} \frac{1}{\mu_A} & 0 \\ 0 & \frac{1}{\sigma_h} \end{pmatrix} \\ &= \begin{pmatrix} 0 & \frac{ab_m S_m}{\sigma_h} \\ \frac{ab_h S_h}{\mu_A} & 0 \end{pmatrix}. \end{aligned}$$

Hence, solving the determinant of the characteristic polynomial $\det |FV^{-1} - \lambda I|$, we have

$$\begin{aligned} \det |FV^{-1} - \lambda I| &= \begin{vmatrix} -\lambda & \frac{ab_m S_m}{\sigma_h} \\ \frac{ab_h S_h}{\mu_A} & -\lambda \end{vmatrix} \\ &= \lambda^2 - \frac{a^2 b_h b_m S_m S_h}{\mu_A \sigma_h} \\ \lambda &= \pm \sqrt{\frac{a^2 b_h b_m S_m S_h}{\mu_A \sigma_h}}. \end{aligned}$$

Therefore, the basic reproduction is

$$\begin{aligned} \mathcal{R}_0 &:= \sqrt{\frac{a^2 b_h b_m S_m^* S_h^*}{\mu_A \sigma_h}} \\ &= \sqrt{\frac{a^2 b_h b_m H(\gamma_{E,L} + \mu_E)(\gamma_{L,P} + \mu_L)(\gamma_{P,S_m} + \mu_P) \ln \left(\frac{\alpha_m \gamma_{E,L} \gamma_{L,P} \gamma_{P,S_m}}{\mu_A (\gamma_{E,L} + \mu_E)(\gamma_{L,P} + \mu_L)(\gamma_{P,S_m} + \mu_P)} \right)}{\mu_A \sigma_h \alpha_m \beta_m \gamma_{E,L} \gamma_{L,P}}}. \end{aligned} \quad (5.25)$$

We will use now Jacobian matrix to get more details about the stability.

5.3.4 Jacobian Matrix

Computing for the partial derivative $\frac{\partial f_i}{\partial U}$, for each $U = E, L, P, S_m, I_m, S_h, I_h, R_h$, and $i = 1, 2, \dots, 8$, we have $J(U)$ equal to

$$\begin{pmatrix} -\gamma_{E,L} - \mu_E & 0 & 0 & \alpha_m & \alpha_m & 0 & 0 & 0 \\ \gamma_{E,L} & -\gamma_{L,P} - \mu_L & 0 & 0 & 0 & 0 & 0 & 0 \\ 0 & \gamma_{L,P} & -\gamma_{P,S_m} - \mu_P & 0 & 0 & 0 & 0 & 0 \\ 0 & 0 & \gamma_{P,S_m} e^{-\beta_m P} (1 - \beta_m P) & -\mu_A - ab_m I_h & 0 & 0 & -ab_m S_m & 0 \\ 0 & 0 & 0 & ab_m I_h & -\mu_A & 0 & ab_m S_m & 0 \\ 0 & 0 & 0 & 0 & -ab_h S_h & -ab_h I_m & 0 & \gamma_h \\ 0 & 0 & 0 & 0 & ab_h S_h & ab_h I_m & -\sigma_h & 0 \\ 0 & 0 & 0 & 0 & 0 & 0 & \sigma_h & -\gamma_h \end{pmatrix}$$

Now let us verify the stability of the equilibrium point using Jacobian matrix.

Note that

$$\mathcal{N}_Y := \frac{\alpha_m \gamma_{E,L} \gamma_{L,P} \gamma_{P,S_m}}{\mu_A (\gamma_{E,L} + \mu_E) (\gamma_{L,P} + \mu_L) (\gamma_{P,S_m} + \mu_P)}$$

$$\mathcal{R}_0 := \sqrt{\frac{a^2 b_h b_m H (\gamma_{E,L} + \mu_E) (\gamma_{L,P} + \mu_L) (\gamma_{P,S_m} + \mu_P) \ln(\mathcal{N}_Y)}{\mu_A \sigma_h \alpha_m \beta_m \gamma_{E,L} \gamma_{L,P}}}.$$

Lemma 5.3.5. Assume $\mathcal{N}_Y > 1$ and $\mathcal{R}_0 < 1$. Then the disease free equilibrium $\mathcal{E}_{DFE} = (E^*, L^*, P^*, S_m^*, 0, H, 0, 0)$ of the system of equation (5.10) is locally asymptotically stable.

Proof. To simplify the writing, we denote $R_Y = \left(1 + \frac{\mu_E}{\gamma_{E,L}}\right) \left(1 + \frac{\mu_L}{\gamma_{L,P}}\right) \left(1 + \frac{\mu_P}{\gamma_{P,S_m}}\right)$. The Jacobian matrix above for \mathcal{E}_{DFE} can be deduce to

$$J(\mathcal{E}_{DFE}) = \begin{pmatrix} -\gamma_{E,L} - \mu_E & 0 & 0 & \alpha_m & \alpha_m & 0 & 0 & 0 \\ \gamma_{E,L} & -\gamma_{L,P} - \mu_L & 0 & 0 & 0 & 0 & 0 & 0 \\ 0 & \gamma_{L,P} & -\gamma_{P,S_m} - \mu_P & 0 & 0 & 0 & 0 & 0 \\ 0 & 0 & \frac{\mu_A \gamma_{P,S_m} R_Y}{\alpha_m} \left(1 - \ln \frac{\alpha_m}{\mu_A R_Y}\right) & -\mu_A & 0 & 0 & \frac{-ab_m \gamma_{P,S_m} R_Y}{\alpha_m \beta_m} \ln \left(\frac{\alpha_m}{\mu_A R_Y}\right) & 0 \\ 0 & 0 & 0 & 0 & -\mu_A & 0 & \frac{-ab_m \gamma_{P,S_m} R_Y}{\alpha_m \beta_m} \ln \left(\frac{\alpha_m}{\mu_A R_Y}\right) & 0 \\ 0 & 0 & 0 & 0 & -ab_h H & 0 & 0 & \gamma_h \\ 0 & 0 & 0 & 0 & ab_h H & 0 & -\sigma_h & 0 \\ 0 & 0 & 0 & 0 & 0 & 0 & \sigma_h & -\gamma_h \end{pmatrix}$$

Let $|J(\mathcal{E}_{DFE}) - \lambda I_8| = 0$. Then we can have

$$\begin{vmatrix} -\gamma_{E,L} - \mu_E - \lambda & 0 & 0 & \alpha_m & \alpha_m & 0 & 0 & 0 \\ \gamma_{E,L} & -\gamma_{L,P} - \mu_L - \lambda & 0 & 0 & 0 & 0 & 0 & 0 \\ 0 & \gamma_{L,P} & -\gamma_{P,S_m} - \mu_P - \lambda & 0 & 0 & 0 & 0 & 0 \\ 0 & 0 & \frac{\mu_A \gamma_{P,S_m} R_Y}{\alpha_m} \left(1 - \ln \frac{\alpha_m}{\mu_A R_Y}\right) & -\mu_A - \lambda & 0 & 0 & \frac{-ab_m \gamma_{P,S_m} R_Y}{\alpha_m \beta_m} \ln \left(\frac{\alpha_m}{\mu_A R_Y}\right) & 0 \\ 0 & 0 & 0 & 0 & -\mu_A - \lambda & 0 & \frac{-ab_m \gamma_{P,S_m} R_Y}{\alpha_m \beta_m} \ln \left(\frac{\alpha_m}{\mu_A R_Y}\right) & 0 \\ 0 & 0 & 0 & 0 & -ab_h H & -\lambda & 0 & \gamma_h \\ 0 & 0 & 0 & 0 & ab_h H & 0 & -\sigma_h - \lambda & 0 \\ 0 & 0 & 0 & 0 & 0 & 0 & \sigma_h & -\gamma_h - \lambda \end{vmatrix} = 0$$

Solving the determinant of this matrix give us

$$\begin{aligned}
0 = & (-\lambda)(-\gamma_h - \lambda)(-\gamma_{E,L} - \mu_E - \lambda)(-\mu_A - \lambda)(-\gamma_{P,S_m} - \mu_P - \lambda)(-\gamma_{L,P} - \mu_L - \lambda) \\
& \left[(-\mu_A - \lambda)(-\sigma_h - \lambda) - (ab_h H) \left(\frac{ab_m \gamma_{P,S_m} R_Y}{\alpha_m \beta_m} \ln \left(\frac{\alpha_m}{\mu_A R_Y} \right) \right) \right] \\
& + (-\lambda)(-\gamma_h - \lambda)(-\gamma_{E,L})(-\gamma_{L,P}) \left(\frac{\mu_A \gamma_{P,S_m} R_Y}{\alpha_m} \left(1 - \ln \frac{\alpha_m}{\mu_A R_Y} \right) \right) (\alpha_m) \\
& \left[(-\mu_A - \lambda)(-\sigma_h - \lambda) - (ab_h H) \left(\frac{ab_m \gamma_{P,S_m} R_Y}{\alpha_m \beta_m} \ln \left(\frac{\alpha_m}{\mu_A R_Y} \right) \right) \right]
\end{aligned}$$

Simplifying the equation above gives us

$$\begin{aligned}
0 = & (-\lambda)(-\gamma_h - \lambda)(-\gamma_{E,L} - \mu_E - \lambda)(-\mu_A - \lambda)(-\gamma_{P,S_m} - \mu_P - \lambda)(-\gamma_{L,P} - \mu_L - \lambda) \\
& [(-\mu_A - \lambda)(-\sigma_h - \lambda) - \sigma_h \mu_A \mathcal{R}_0^2] \\
& + (-\lambda)(-\gamma_h - \lambda) \left(\mu_A \gamma_{E,L} \gamma_{L,P} \gamma_{P,S_m} R_Y \left(1 - \ln \frac{\alpha_m}{\mu_A R_Y} \right) \right) \\
& [(-\mu_A - \lambda)(-\sigma_h - \lambda) - \sigma_h \mu_A \mathcal{R}_0^2]
\end{aligned}$$

Factoring out the common term, we have

$$\begin{aligned}
0 = & (-\lambda)(-\gamma_h - \lambda) [(-\mu_A - \lambda)(-\sigma_h - \lambda) - \sigma_h \mu_A \mathcal{R}_0^2] \\
& \left[(-\gamma_{E,L} - \mu_E - \lambda)(-\mu_A - \lambda)(-\gamma_{P,S_m} - \mu_P - \lambda)(-\gamma_{L,P} - \mu_L - \lambda) \right. \\
& \left. + \mu_A \gamma_{E,L} \gamma_{L,P} \gamma_{P,S_m} R_Y \left(1 - \ln \frac{\alpha_m}{\mu_A R_Y} \right) \right]
\end{aligned}$$

Let S and T be equal to $(-\mu_A - \lambda)(-\sigma_h - \lambda) - \sigma_h \mu_A \mathcal{R}_0^2$ and $(-\gamma_{E,L} - \mu_E - \lambda)(-\mu_A - \lambda)(-\gamma_{P,S_m} - \mu_P - \lambda)(-\gamma_{L,P} - \mu_L - \lambda) + \mu_A \gamma_{E,L} \gamma_{L,P} \gamma_{P,S_m} R_Y \left(1 - \ln \frac{\alpha_m}{\mu_A R_Y} \right)$, respectively. Then we have

$$0 = (-\lambda) \cdot (-\gamma_h - \lambda) \cdot S \cdot T$$

Now, note that expanding S would give us

$$\begin{aligned}
S &= \lambda^2 + (\sigma_h + \mu_A)\lambda + (\sigma_h \mu_A - \sigma_h \mu_A \mathcal{R}_0^2) \\
&= \lambda^2 + (\sigma_h + \mu_A)\lambda + \sigma_h \mu_A (1 - \mathcal{R}_0^2)
\end{aligned}$$

and expanding T gives us

$$\begin{aligned}
T &= \lambda^4 + \left[(\gamma_{P,S_m} + \mu_P) + (\gamma_{L,P} + \mu_L) + \mu_A \right] \lambda^3 \\
&+ \left[(\gamma_{E,L} + \mu_E)(\gamma_{P,S_m} + \mu_P) + (\gamma_{E,L} + \mu_E)(\gamma_{L,P} + \mu_L) + (\gamma_{P,S_m} + \mu_P)(\gamma_{L,P} + \mu_L) + \mu_A(\gamma_{P,S_m} + \mu_P) + \mu_A(\gamma_{L,P} + \mu_L) \right] \lambda^2 \\
&+ \mu_A \left[(\gamma_{E,L} + \mu_E)(\gamma_{P,S_m} + \mu_P) + (\gamma_{E,L} + \mu_E)(\gamma_{L,P} + \mu_L) + (\gamma_{P,S_m} + \mu_P)(\gamma_{L,P} + \mu_L) + \frac{\gamma_{E,L} \gamma_{L,P} \gamma_{P,S_m} R_Y}{\mu_A} \right] \lambda \\
&+ \mu_A \gamma_{E,L} \gamma_{L,P} \gamma_{P,S_m} R_Y \left(2 - \ln \frac{\alpha_m}{\mu_A R_Y} \right)
\end{aligned}$$

Observe that there is no sign change in $S(\lambda)$ and $T(\lambda)$ if $\mathcal{R}_0 < 1$. By Descartes' rule of sign [5], the polynomials S and T has 0 positive roots.

For $S(-\lambda)$ we have

$$\begin{aligned} S(-\lambda) &= (-\lambda)^2 + (\sigma_h + \mu_A)(-\lambda) + \sigma_h \mu_A (1 - \mathcal{R}_0^2) \\ &= \lambda^2 - (\sigma_h + \mu_A)\lambda + \sigma_h \mu_A (1 - \mathcal{R}_0^2) \end{aligned}$$

Thus, there are 2 sign change in $S(-\lambda)$. Implying further that the polynomial S has 2 negative roots. Whence by Descartes rule of sign, the possible combination of roots are

No. of Positive Roots	No. of Negative Roots	No. of Non-real Roots	Total No. of Solutions
0	2	0	2
0	0	2	2

Doing the same process for T , we can conclude that all eigenvalues of the characteristics polynomial

$$0 = -\lambda \cdot (-\lambda - \gamma_h) \cdot S \cdot T$$

are negative. Consequently, the disease free equilibrium \mathcal{E}_{DFE} is locally asymptotically stable. \square

5.3.5 Parameter Identifiability

The dynamic system given by equation (5.9) is **identifiable** if θ can be uniquely determined from the measurable system output $Y(t)$; otherwise, it is said to be **unidentifiable**.

Definition 5.3.6. [45] A system structure is said to be **globally identifiable** if for any two parameter vectors θ_1 and θ_2 in the parameter space Θ , $Y(U, \theta_1) = Y(U, \theta_2)$ holds if and only if $\theta_1 = \theta_2$.

Now let us determine the global identifiability of the parameters using the study proposed by Denis-Vidal and Joly-Blanchard [26]. We choose $Y = (E, L, P, S_m, I_m, S_h, I_h)$. From $f(U, \theta_1) = f(U, \theta_2)$, we have

$$\alpha_{m,1}(S_m + I_m) - (\gamma_{\{E,L\},1} + \mu_{E,1})E = \alpha_{m,2}(S_m + I_m) - (\gamma_{\{E,L\},2} + \mu_{E,2})E \quad (5.26)$$

$$\gamma_{\{E,L\},1}E - \gamma_{\{L,P\},1}L - \mu_{L,1}L = \gamma_{\{E,L\},2}E - \gamma_{\{L,P\},2}L - \mu_{L,2}L \quad (5.27)$$

$$\gamma_{\{L,P\},1}L - \gamma_{\{P,S_m\},1}P - \mu_{P,1}P = \gamma_{\{L,P\},2}L - \gamma_{\{P,S_m\},2}P - \mu_{P,2}P \quad (5.28)$$

$$\gamma_{\{P,S_m\},1}Pe^{-\beta_{m,1}P} - \mu_{A,1}S_m - a_1b_{m,1}I_hS_m = \gamma_{\{P,S_m\},2}Pe^{-\beta_{m,2}P} - \mu_{A,2}S_m - a_2b_{m,2}I_hS_m \quad (5.29)$$

$$a_1b_{m,1}I_hS_m - \mu_{A,1}I_m = a_2b_{m,2}I_hS_m - \mu_{A,2}I_m \quad (5.30)$$

$$\gamma_{h,1}R_h - a_1b_{h,1}I_mS_h = \gamma_{h,2}R_h - a_2b_{h,2}I_mS_h \quad (5.31)$$

$$a_1b_{h,1}I_mS_h - \sigma_{h,1}I_h = a_2b_{h,2}I_mS_h - \sigma_{h,2}I_h \quad (5.32)$$

$$\sigma_{h,1}I_h - \gamma_{h,1}R_h = \sigma_{h,2}I_h - \gamma_{h,2}R_h \quad (5.33)$$

Now solving each equation above, we can solve the identifiability of each parameters.

- For α_m : Using equation (5.26), we can imply that $\alpha_{m,1}(S_m + I_m) = \alpha_{m,2}(S_m + I_m)$. Thus $\alpha_{m,1} = \alpha_{m,2}$, so the parameters α_m and β_m are identifiable.
- For $\gamma_{E,L}$: Using equation (5.27), we can imply that $\gamma_{\{E,L\},1}E = \gamma_{\{E,L\},2}E$, implying further that the parameter $\gamma_{E,L}$ is identifiable.
- For $\gamma_{L,P}$: Using equation (5.28), we can imply that $\gamma_{\{L,P\},1}L = \gamma_{\{L,P\},2}L$, implying further that the parameter $\gamma_{L,P}$ is identifiable.
- For γ_{P,S_m} and β_m : Using equation (5.29), we can imply that $\gamma_{\{P,S_m\},1}Pe^{-\beta_{m,1}P} = \gamma_{\{P,S_m\},2}Pe^{-\beta_{m,2}P}$, implying further that the parameter γ_{P,S_m} is identifiable.
- For μ_E : Using equation (5.26), we have $\frac{\gamma_{\{E,L\},1}}{\gamma_{\{E,L\},2}} = \frac{\mu_{E,1}}{\mu_{E,2}}$. Thus, μ_E is unidentifiable but the sum $(\gamma_{E,L} + \mu_E)$ is identifiable.
- For μ_L : Using equation (5.27), we have $\frac{\gamma_{\{L,P\},1}}{\gamma_{\{L,P\},2}} = \frac{\mu_{L,1}}{\mu_{L,2}}$. Thus, μ_L is unidentifiable. However, since $\gamma_{L,P}$ is identifiable, the sum $(\gamma_{L,P} + \mu_L)$ is identifiable.
- For μ_P : Using equation (5.28), we have $\frac{\gamma_{\{P,S_m\},1}}{\gamma_{\{P,S_m\},2}} = \frac{\mu_{P,1}}{\mu_{P,2}}$. Thus, μ_P is unidentifiable. However, since γ_{P,S_m} is identifiable, the sum $(\gamma_{P,S_m} + \mu_P)$ is identifiable.
- For μ_A : Using equation (5.30), we can imply that $\mu_{A,1}I_m = \mu_{A,2}I_m$. Thus the parameter μ_A is identifiable.
- For γ_h : Using equation (5.31), we can imply that $\gamma_{h,1}R_h = \gamma_{h,2}R_h$. Thus the parameter γ_h is identifiable.
- For σ_h : Using equation (5.32), we can imply that $\sigma_{h,1}I_h = \sigma_{h,2}I_h$. Thus the parameter σ_h is identifiable.
- For ab_m : Using again equation (5.30), we can imply that $a_1b_{m,1}I_hS_m = a_2b_{m,2}I_hS_m$. Thus we can imply further that $\frac{a_1}{a_2} = \frac{b_{m,1}}{b_{m,2}}$. Thus the parameters a and b_m are unidentifiable. However, the product ab_m is identifiable.
- For ab_h : Using again equation (5.32), we can imply that $a_1b_{h,1}I_mS_h = a_2b_{h,2}I_mS_h$. Thus we can imply further that $\frac{a_1}{a_2} = \frac{b_{h,1}}{b_{h,2}}$. Thus the parameters a and b_h are unidentifiable. However, the product ab_m is identifiable.

From this result we have the following theorem.

Theorem 5.3.7. *The parameters $(\alpha_m, \gamma_{E,L}, \gamma_{L,P}, \gamma_{P,S_m}, \beta_m, \mu_E, \mu_L, \mu_P, \mu_A, \gamma_h, \sigma_h, ab_m, ab_h)$ are globally identifiable but the rest is not.*

5.4 Optimal Control strategies : Copepods and Pesticides

Our aim in this section to minimize the number of infected humans by controlling the vector population. We attribute two control inputs, w_Y for the percentage of young mosquitoes exposed to copepods and w_A for the percentage of adult

mosquitoes exposed to pesticides. According to mosquitoesreviews.com, Copepods are natural enemies of the first and second instar (the smallest sizes) of mosquito larvae. Also according to [25], large sized cyclopoid copepods (having body size greater than 1.0 mm) act as predators of mosquito larvae which strongly influence the mosquito larval population. Furthermore, we assume that both control inputs are mesurable continuous functions that takes its values in a positively bounded set $W = [0, w_{Y,max}] \times [0, w_{A,max}]$. Thus we consider the objective function

$$\mathcal{J}(w_Y, w_A) = \int_0^T \left(I_h(t) + \frac{1}{2} A_Y w_Y^2(t) + \frac{1}{2} A_A w_A^2(t) \right) dt$$

subject to

$$\begin{aligned} E'(t) &= \alpha_m(S_m(t) + I_m(t)) - \gamma_{E,L}E(t) - \mu_E E(t) \\ L'(t) &= \gamma_{E,L}E(t) - \gamma_{L,P}L(t) - \mu_L L(t) - w_Y L(t) \\ P'(t) &= \gamma_{L,P}L(t) - \gamma_{P,S_m}P(t) - \mu_P P(t) \\ S'_m(t) &= \gamma_{P,S_m}P(t)e^{-\beta_m P(t)} - \mu_A S_m(t) - ab_m I_h(t)S_m(t) - w_A S_m(t) \\ I'_m(t) &= ab_m I_h(t)S_m(t) - \mu_A I_m(t) - w_A I_m(t) \\ S'_h(t) &= \gamma_h R_h(t) - ab_h I_m(t)S_h(t) \\ I'_h(t) &= ab_h I_m(t)S_h(t) - \sigma_h I_h(t) \\ R'_h(t) &= \sigma_h I_h(t) - \gamma_h R_h(t) \end{aligned} \tag{5.34}$$

for $t \in [0, T]$, with $0 \leq w_Y, w_A \leq w_M$. The variables A_Y, A_A are the positive weights associated with the control variables w_Y and w_A , respectively. They corresponds to the efforts rendered in exposing the larvae L and the adult mosquitoes S_m, I_m compartments.

Lemma 5.4.1. *There exists an optimal control $w^* = (w_Y^*(t), w_A^*(t))$ such that*

$$\mathcal{J}(w_Y^*, w_A^*) = \min_{w \in W} \mathcal{J}(w_Y, w_A)$$

under the constraint $(E, L, P, S_m, I_m, S_h, I_h, R_h)$ is a solution to the ordinary differential equation (5.34).

Proof. This lemma can be proven using the similar arguments as Lemma 3.5.1. \square

Lemma 5.4.2. *There exists the adjoint variables $\lambda_i, i = 1, 2, \dots, 6$ of the system (5.34) that satisfy the following backward in time system of ordinary differential equation.*

$$\begin{aligned}
-\frac{d\lambda_1}{dt} &= -(\lambda_1 - \lambda_2)\gamma_{E,L} - \lambda_1\mu_E \\
-\frac{d\lambda_2}{dt} &= -(\lambda_2 - \lambda_3)\gamma_{L,P} - \lambda_2(\mu_L + w_Y) \\
-\frac{d\lambda_3}{dt} &= -(\lambda_3 - \lambda_4(1 - \beta_m P)e^{-\beta_m P})\gamma_{P,S_m} - \lambda_3\mu_P \\
-\frac{d\lambda_4}{dt} &= \lambda_1\alpha_m - \lambda_4(\mu_A + w_A) - (\lambda_4 - \lambda_5)ab_m I_h \\
-\frac{d\lambda_5}{dt} &= \lambda_1\alpha_m - \lambda_5(\mu_A + w_A) - (\lambda_6 - \lambda_7)ab_m S_h \\
-\frac{d\lambda_6}{dt} &= -(\lambda_6 - \lambda_7)ab_h I_m \\
-\frac{d\lambda_7}{dt} &= 1 - (\lambda_4 - \lambda_5)ab_m S_m - (\lambda_7 - \lambda_8)\sigma_h \\
-\frac{d\lambda_8}{dt} &= -(\lambda_8 - \lambda_6)\gamma_h
\end{aligned} \tag{5.35}$$

with the transversality condition $\lambda(T) = 0$.

Proof. Using the Hamiltonian for system (5.34), we have

$$\begin{aligned}
\mathcal{H} &= \mathcal{L}(w_Y, w_A) + \lambda_1(t)E'(t) + \lambda_2(t)L'(t) + \lambda_3(t)P'(t) \\
&\quad + \lambda_4(t)S'_m(t) + \lambda_5(t)I'_m(t) + \lambda_6(t)S'_h(t) + \lambda_7(t)I'_h(t) + \lambda_8(t)R'_h(t) \\
&= I_h + \frac{1}{2}A_Y w_Y^2 + \frac{1}{2}A_A w_A^2 + \lambda_1(\alpha_m(S_m + I_m) - \gamma_{E,L}E - \mu_E E) \\
&\quad + \lambda_2(\gamma_{E,L}E - \gamma_{L,P}L - \mu_L L - w_Y L) + \lambda_3(\gamma_{L,P}L - \gamma_{P,S_m}P - \mu_P P) \\
&\quad + \lambda_4(\gamma_{P,S_m}P e^{-\beta_m P} - \mu_A S_m - ab_m I_h S_m - w_A S_m) + \lambda_5(ab_m I_h S_m - \mu_A I_m - w_A I_m) \\
&\quad + \lambda_6(\gamma_h R_h - ab_h I_m S_h) + \lambda_7(ab_h I_m S_h - \sigma_h I_h) + \lambda_8(\sigma_h I_h - \gamma_h R_h)
\end{aligned} \tag{5.36}$$

To prove this, we determine the partial derivatives of \mathcal{H} with respect to each variables then set the adjoint system as $\frac{d\lambda_1}{dt} = -\frac{\partial \mathcal{H}}{\partial E}, \frac{d\lambda_2}{dt} = -\frac{\partial \mathcal{H}}{\partial L}, \frac{d\lambda_3}{dt} = -\frac{\partial \mathcal{H}}{\partial P}, \frac{d\lambda_4}{dt} = -\frac{\partial \mathcal{H}}{\partial S_m},$

$\frac{d\lambda_5}{dt} = -\frac{\partial \mathcal{H}}{\partial I_m}$, $\frac{d\lambda_6}{dt} = -\frac{\partial \mathcal{H}}{\partial S_h}$, $\frac{d\lambda_7}{dt} = -\frac{\partial \mathcal{H}}{\partial I_h}$ and $\frac{d\lambda_8}{dt} = -\frac{\partial \mathcal{H}}{\partial R_h}$. We have the following

$$\begin{aligned}\frac{d\lambda_1}{dt} &= (\lambda_1 - \lambda_2)\gamma_{E,L} + \lambda_1\mu_E \\ \frac{d\lambda_2}{dt} &= (\lambda_2 - \lambda_3)\gamma_{L,P} + \lambda_2(\mu_L + w_Y) \\ \frac{d\lambda_3}{dt} &= (\lambda_3 - \lambda_4(1 - \beta_m P)e^{-\beta_m P})\gamma_{P,S_m} + \lambda_3\mu_P \\ \frac{d\lambda_4}{dt} &= -\lambda_1\alpha_m + \lambda_4(\mu_A + w_A) + (\lambda_4 - \lambda_5)ab_m I_h \\ \frac{d\lambda_5}{dt} &= -\lambda_1\alpha_m + \lambda_5(\mu_A + w_A) + (\lambda_6 - \lambda_7)ab_m S_h \\ \frac{d\lambda_6}{dt} &= (\lambda_6 - \lambda_7)ab_h I_m \\ \frac{d\lambda_7}{dt} &= -1 + (\lambda_4 - \lambda_5)ab_m S_m + (\lambda_7 - \lambda_8)\sigma_h \\ \frac{d\lambda_8}{dt} &= (\lambda_8 - \lambda_6)\gamma_h.\end{aligned}$$

□

Theorem 5.4.3. *The optimal control variables are given by*

$$\begin{aligned}w_Y^* &= \max \left(0, \min \left(\frac{\lambda_2 L}{A_Y}, w_{Y,max} \right) \right) \\ w_A^* &= \max \left(0, \min \left(\frac{\lambda_4 S_m + \lambda_5 I_m}{A_A}, w_{A,max} \right) \right).\end{aligned}$$

Proof. By the Pontryagin maximum principle, the optimal control w^* minimizes the Hamiltonian given by equation (5.36). Now, setting the partial derivative of H with respect to the control variables to zero, then solving w_Y and w_A , we get

$$w_Y^* = \frac{\lambda_2 L}{A_Y} \qquad w_A^* = \frac{\lambda_4 S_m + \lambda_5 I_m}{A_A}.$$

Therefore, the optimal control derived from the stationary condition $\frac{d\lambda_i}{dt}$ is given by

$$w_Y^* = \begin{cases} 0 & \text{if } \frac{\lambda_2 L}{A_Y} \leq 0 \\ \frac{\lambda_2 L}{A_Y} & \text{if } \frac{\lambda_2 L}{A_Y} < w_M \\ w_M & \text{if } \frac{\lambda_2 L}{A_Y} \geq w_M \end{cases} \qquad w_A^* = \begin{cases} 0 & \text{if } \frac{\lambda_4 S_m + \lambda_5 I_m}{A_A} \leq 0 \\ \frac{\lambda_4 S_m + \lambda_5 I_m}{A_A} & \text{if } \frac{\lambda_4 S_m + \lambda_5 I_m}{A_A} < w_M \\ w_M & \text{if } \frac{\lambda_4 S_m + \lambda_5 I_m}{A_A} \geq w_M \end{cases}.$$

□

5.4.1 Numerical Simulation of Optimal Control Strategies: Copepodes vs Pesticides

In this section, we will show a numerical simulations of the optimal control strategy in minimizing infected humans. The optimal control is (w_Y^*, w_A^*) where w_Y is the percentage of young mosquitoes exposed to copepodes and w_A is the percentage of adult mosquitoes exposed to pesticides.

The control weights A_Y is the efforts rendered in exposing young mosquito population to copepodes while the control weights A_A is the effort in eliminating adult mosquito population by means of administering insecticides. Since adults mosquitoes is more visible compare to the young mosquitoes, eliminating them would render an effortless job. Thus, A_Y is set smaller than A_A . Hence, we initially set the control weights as $A_A = 10$ and $A_Y = 1$. Note that the values of A_Y and A_A does not change the convergence of optimal control.

Parameters	Description	Value	Source
α_m	Oviposition	1 day^{-1}	[13]
$\gamma_{E,L}$	Transformation from egg to larva	$0.330000 \text{ day}^{-1}$	[13]
$\gamma_{L,P}$	Transformation from larvae to pupa	$0.140000 \text{ day}^{-1}$	[13]
γ_{P,S_m}	Transformation from pupa to adult mosquito	$0.346000 \text{ day}^{-1}$	[13]
μ_E	Mortality rates of egg	$0.050000 \text{ day}^{-1}$	[13]
μ_L	Mortality rates of larva	$0.050000 \text{ day}^{-1}$	[13]
μ_P	Mortality rates of pupa	$0.016700 \text{ day}^{-1}$	[13]
μ_A	Mortality rates of mosquito	$0.042000 \text{ day}^{-1}$	[13]
γ_h	Rate of decline in human immunity to disease	$0.575000 \text{ day}^{-1}$	[43]
σ_h	Rate of cure for disease	$0.328833 \text{ day}^{-1}$	[43]
ab_m	Probability of susceptible mosquitoes to be infectious	$0.375000 \text{ day}^{-1}$	[43]
ab_h	Probability of susceptible humans to be infected	$0.750000 \text{ day}^{-1}$	[43]
$\frac{1}{\beta_m}$	carrying capacity of pupae (ha^{-1})	$250000 \text{ hectare}^{-1}$	[30]

TABLE 5.1: Value of the Parameters used for the simulations.

Considering a constant growth function for human and mosquito population, the optimality of the system is numerically solved using a gradient method programmed in Python. The algorithm are describe below and the parameters value used are presented in Table 6.2. The optimality of the system is numerically solved using Algorithm 2 with $\epsilon = 0.01$.

Algorithm 2 Computation of optimal control of the model (5.34)

Given $U^0 = (9.4e7, 5.e4, 1.e4, 94.4e4, 5.6e4, 8768197, 1895, 1878)$ as initial datum , a final time $T > 0$ and a tolerance $\varepsilon > 0$.
 Let w_Y^0, w_A^0 randomly chosen following $\mathcal{N}(0, 1)$.
while $\|\nabla \mathcal{H}(w^n, U^n, \lambda^n)\| > \varepsilon$ **do**,
 solve the forward system u^n ,
 solve the backward system λ^n ,
 update w^n
 solve the gradient $\nabla \mathcal{H}(w^n, U^n, \lambda^n)$
 $w^* = w^n$.

Using the algorithm above with a tolerance of 10^{-2} , we get the following results.

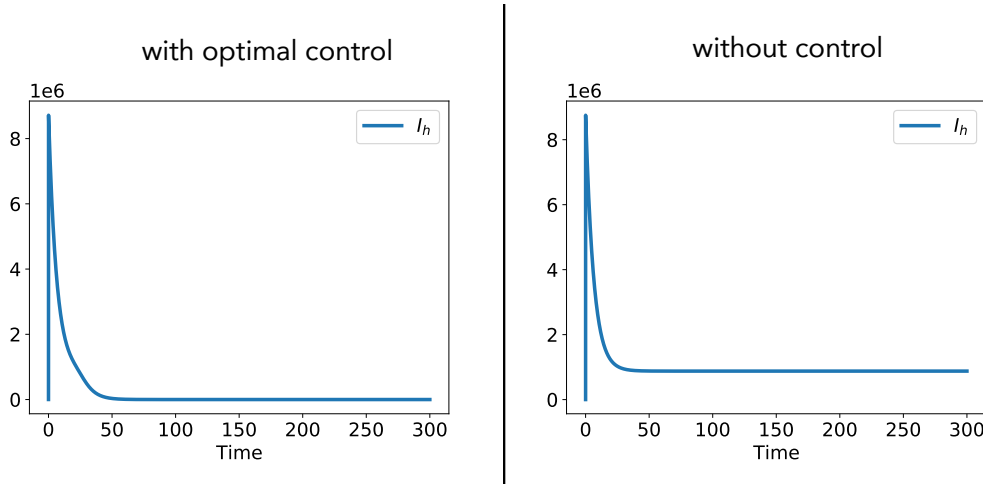


FIGURE 5.3: Optimal solutions of the infected human compartment in the model (5.34) with $w_{Y,max} = 23.96, w_{A,max} = 1$.

Figure 5.3 shows the behavior of infected humans if we apply with and without control strategies. It shows that using control strategies would eliminate infected humans over time, with an 8,715,766.164 maximum population. Having no control strategy increases this at 8,752,880.738 infected humans and an equilibrium of 877,196 infected humans over time.

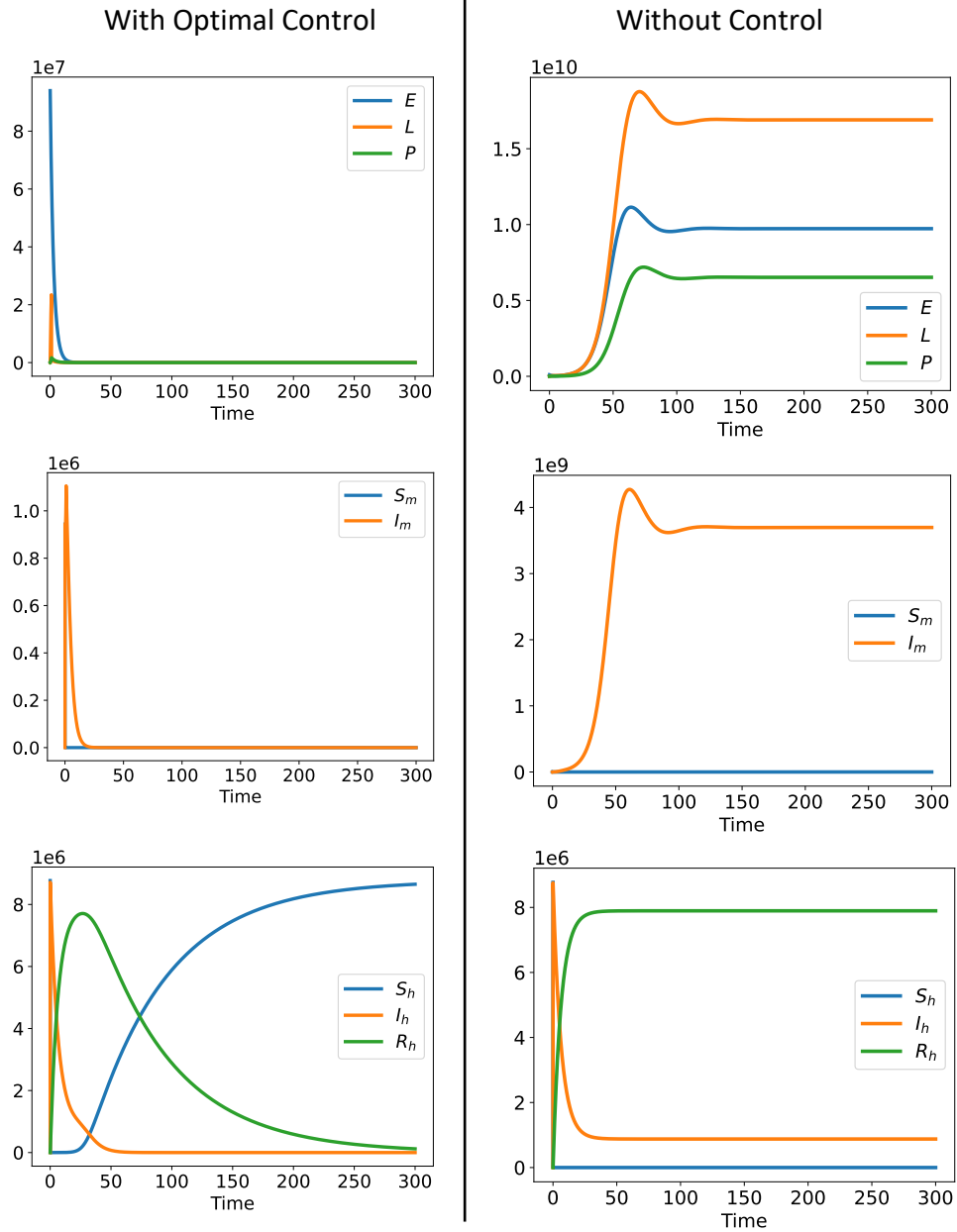


FIGURE 5.4: Optimal solutions of each compartments in model (5.34) with $w_{Y,max} = 23.96, w_{A,max} = 1$.

Figure 5.4 shows the behavior of each variable in the compartment. The figure shows that applying copepods and pesticides eliminates the mosquito population. With the control strategy, young and infected adult mosquito populations are eliminated quickly. It only has 1,105,864.772 and 23,443,653.571 maximum infected mosquito and larvae populations. This population increases to 8,752,880.738 and 18,763,929,783.442 infected mosquito and larvae populations without control strategies. The figure clearly shows that controlling the mosquito population is an

effective method of managing the human population.

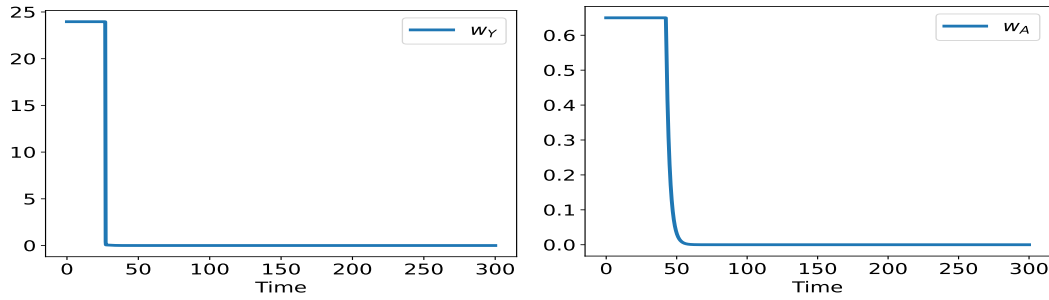


FIGURE 5.5: Optimal solutions of control variables in model (5.34) with $w_{Y,max} = 23.96, w_{A,max} = 1$.

The simulation was done assuming that the *Aedes Aegypti* does not become resistant to the insecticide and that it is financially possible to apply insecticide at all times. Figure 5.5 shows that setting $w_{Y,max} = 23.96, w_{A,max} = 1$ takes 26 days and 42 days of continuous application of copepod and pesticide, respectively. It then slowly minimizes the application toward its equilibrium.

Influence of the copepods number

One *Mesocyclops aspericornis*, a Philippine species of copepod, is capable of eating an average of 23.96 among 50 *Aedes aegypti* larvae [53]. In this section, we compare the optimal control by varying the maximum number of copepod N exposed to larvae as $w_{Y,max} = (23.96/50)N = 0.4792N$. From the figure above, we consider increasing the effort by setting N equal to 20 and 200. With this, we get the figure below.

The simulation was done assuming *Mesocyclops aspericornis* have no predators in the laying sites. Figure 5.6 shows the influence of increasing the number of copepods N exposed to larvae on the control variables. It shows that the application of the control strategies, both w_Y^* and w_A^* , decreases as N increases. The figures show that in $N = 2$, you need to increase the effort at day one by a hundred percent and then continuously apply copepod and pesticide for 43 days and 52 days, respectively. While with 20 *Mesocyclops aspericornis*, it decreases to 27 days and 43 days of continuous application of copepod and pesticide, respectively. Since we assume there is no copepod predator in the laying site, applying 200 copepods in the laying site requires only 26 and 41 days of copepod and pesticide to eliminate the mosquito population.

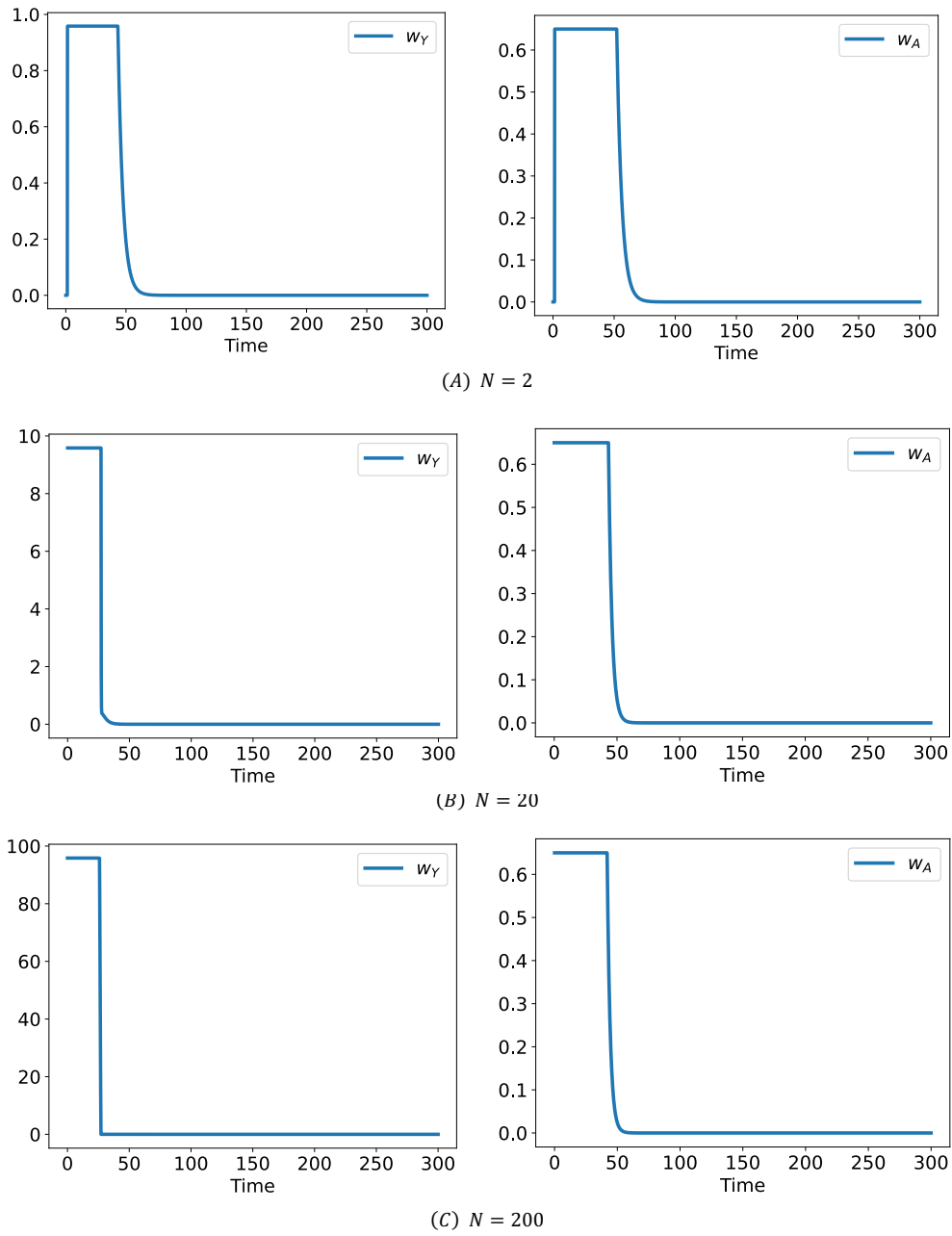


FIGURE 5.6: Optimal solutions of the control variables for different maximum number of copepod.

Considering all Control Strategies: Copepods, Pesticides and Vaccination

Now, let us include vaccination in our control strategy. We attribute three control inputs, w_Y for the percentage of young mosquitoes exposed to copepods, w_A for the percentage of adult mosquitoes exposed to pesticides and w_H for the efforts in vaccinating susceptible humans. Furthermore, we assume that both control inputs are measurable continuous functions that takes its values in a positively bounded set

$W = [0, w_{Y,max}] \times [0, w_{A,max}] \times [0, w_{H,max}]$. Thus we consider the objective function

$$\mathcal{J}(w_Y, w_A, w_H) = \int_0^T \left(I_h(t) + \frac{1}{2} A_Y w_Y^2(t) + \frac{1}{2} A_A w_A^2(t) + \frac{1}{2} A_H w_H^2(t) \right) dt$$

subject to

$$\begin{aligned} E'(t) &= \alpha_m(S_m(t) + I_m(t)) - \gamma_{E,L}E(t) - \mu_E E(t) \\ L'(t) &= \gamma_{E,L}E(t) - \gamma_{L,P}L(t) - \mu_L L(t) - w_Y L(t) \\ P'(t) &= \gamma_{L,P}L(t) - \gamma_{P,S_m}P(t) - \mu_P P(t) \\ S'_m(t) &= \gamma_{P,S_m}P(t)e^{-\beta_m P} - \mu_A S_m(t) - ab_m I_h(t)S_m(t) - w_A S_m(t) \\ I'_m(t) &= ab_m I_h(t)S_m(t) - \mu_A I_m(t) - w_A I_m(t) \\ S'_h(t) &= \gamma_h R_h(t) - ab_h I_m(t)S_h(t) - w_H S_h(t) \\ I'_h(t) &= ab_h I_m(t)S_h(t) - \sigma_h I_h(t) \\ R'_h(t) &= \sigma_h I_h(t) - \gamma_h R_h(t) \end{aligned} \tag{5.37}$$

for $t \in [0, T]$, with $0 \leq w_Y, w_A \leq w_M$ and $0 \leq w_H$. The variables A_Y, A_A, A_H are the positive weights associated with the control variables w_Y, w_A and w_H , respectively. They corresponds to the efforts rendered in exposing the larvae L , the adult mosquitoes S_m, I_m and susceptible humans S_h to the control strategy.

Lemma 5.4.4. *There exists an optimal control $w^* = (w_Y^*(t), w_A^*(t), w_H^*(t))$ such that*

$$\mathcal{J}(w_Y^*, w_A^*, w_H^*) = \min_{w \in W} \mathcal{J}(w_Y, w_A, w_H)$$

under the constraint $(E, L, P, S_m, I_m, S_h, I_h, R_h)$ is a solution to the ordinary differential equation (5.37).

Proof. This lemma can be proven using the similar arguments as Lemma 3.5.1. \square

Lemma 5.4.5. *There exists the adjoint variables $\lambda_i, i = 1, 2, \dots, 6$ of the system (5.37) that satisfy the following backward in time system of ordinary differential equation.*

$$\begin{aligned}
-\frac{\partial \lambda_1(t)}{\partial t} &= -\lambda_1 \mu_E + (\lambda_2 - \lambda_1) \gamma_{E,L} \\
-\frac{\partial \lambda_2(t)}{\partial t} &= -\lambda_2 (\mu_L + w_Y) + (\lambda_3 - \lambda_2) \gamma_{L,P} \\
-\frac{\partial \lambda_3(t)}{\partial t} &= -\lambda_3 \mu_P + (\lambda_4 (1 - \beta_m P) e^{-\beta_m P} - \lambda_3) \gamma_{P,S_m} \\
-\frac{\partial \lambda_4(t)}{\partial t} &= \lambda_1 \alpha_m - \lambda_4 (\mu_A + w_A) + (\lambda_5 - \lambda_4) a b_m I_h(t) \\
-\frac{\partial \lambda_5(t)}{\partial t} &= \lambda_1 \alpha_m - \lambda_5 (\mu_A + w_A) + (\lambda_7 - \lambda_6) a b_h S_h(t) \\
-\frac{\partial \lambda_6(t)}{\partial t} &= -\lambda_6 w_H + (\lambda_7 - \lambda_6) a b_h I_m(t) \\
-\frac{\partial \lambda_7(t)}{\partial t} &= 1 + (\lambda_5 - \lambda_4) a b_m S_m(t) - \lambda_7 \sigma_h \\
-\frac{\partial \lambda_8(t)}{\partial t} &= (\lambda_6 - \lambda_8) \gamma_h.
\end{aligned}$$

with the transversality condition $\lambda(T) = 0$. Moreover, the optimal control variables are given by

$$\begin{aligned}
w_Y^* &= \max \left(0, \min \left(\frac{\lambda_2 L}{A_Y}, w_M \right) \right) \\
w_A^* &= \max \left(0, \min \left(\frac{\lambda_4 S_m + \lambda_5 I_m}{A_A}, w_M \right) \right) \\
w_H^* &= \max \left(0, \min \left(\frac{\lambda_6 S_h}{A_H}, w_H \right) \right).
\end{aligned}$$

Proof. Using the Hamiltonian for the system (5.37), we have

$$\begin{aligned}
\mathcal{H} &= \mathcal{L}(w_Y, w_A, w_H) + \lambda_1(t)E'(t) + \lambda_2(t)L'(t) + \lambda_3(t)P'(t) \\
&\quad + \lambda_4(t)S'_m(t) + \lambda_5(t)I'_m(t) + \lambda_6(t)S'_h(t) + \lambda_7(t)I'_h(t) + \lambda_8(t)R'_h(t) \\
&= I_h(t) + \frac{1}{2}A_Y w_Y^2(t) + \frac{1}{2}A_A w_A^2(t) + \frac{1}{2}A_H w_H^2(t) \\
&\quad + \lambda_1 \left(\alpha_m(S_m(t) + I_m(t)) - \gamma_{E,L}E(t) - \mu_E E(t) \right) \\
&\quad + \lambda_2 \left(\gamma_{E,L}E(t) - \gamma_{L,P}L(t) - \mu_L L(t) - w_Y L(t) \right) \\
&\quad + \lambda_3 \left(\gamma_{L,P}L(t) - \gamma_{P,S_m}P(t) - \mu_P P(t) \right) \\
&\quad + \lambda_4 \left(\gamma_{P,S_m}P(t)e^{-\beta_m P} - \mu_A S_m(t) - ab_m I_h(t)S_m(t) - w_A S_m(t) \right) \\
&\quad + \lambda_5 \left(ab_m I_h(t)S_m(t) - \mu_A I_m(t) - w_A I_m(t) \right) \\
&\quad + \lambda_6 \left(\gamma_h R_h(t) - ab_h I_m(t)S_h(t) - w_H S_h(t) \right) \\
&\quad + \lambda_7 \left(ab_h I_m(t)S_h(t) - \sigma_h I_h(t) \right) + \lambda_8 \left(\sigma_h I_h(t) - \gamma_h R_h(t) \right).
\end{aligned}$$

Now, taking the partial derivative of \mathcal{H} with respect to U , we have

$$\begin{aligned}
\frac{\partial \mathcal{H}}{\partial E} &= \lambda_1(-\gamma_{E,L} - \mu_E) + \lambda_2 \gamma_{E,L} \\
\frac{\partial \mathcal{H}}{\partial L} &= \lambda_2(-\gamma_{L,P} - \mu_L - w_Y) + \lambda_3 \gamma_{L,P} \\
\frac{\partial \mathcal{H}}{\partial P} &= \lambda_3(-\gamma_{P,S_m} - \mu_P) + \lambda_4 \gamma_{P,S_m}(1 - \beta_m P)e^{-\beta_m P} \\
\frac{\partial \mathcal{H}}{\partial S_m} &= \lambda_1 \alpha_m + \lambda_4(-\mu_A - ab_m I_h(t) - w_A) + \lambda_5 ab_m I_h(t) \\
\frac{\partial \mathcal{H}}{\partial I_m} &= \lambda_1 \alpha_m + \lambda_5(-\mu_A - w_A) - \lambda_6 ab_h S_h(t) + \lambda_7 ab_h S_h(t) \\
\frac{\partial \mathcal{H}}{\partial S_h} &= \lambda_6(-ab_h I_m(t) - w_H) + \lambda_7 ab_h I_m(t) \\
\frac{\partial \mathcal{H}}{\partial I_h} &= 1 - \lambda_4 ab_m S_m(t) + \lambda_5 ab_m S_m(t) - \lambda_7 \sigma_h + \lambda_8 \sigma_h \\
\frac{\partial \mathcal{H}}{\partial R_h} &= \lambda_6 \gamma_h - \lambda_8 \gamma_h.
\end{aligned}$$

Therefore, the adjoint system of equation (5.37) is

$$\begin{aligned}
\frac{\partial \lambda_1(t)}{\partial t} &= -\lambda_1 \mu_E + (\lambda_2 - \lambda_1) \gamma_{E,L} \\
\frac{\partial \lambda_2(t)}{\partial t} &= -\lambda_2 (\mu_L + w_Y) + (\lambda_3 - \lambda_2) \gamma_{L,P} \\
\frac{\partial \lambda_3(t)}{\partial t} &= -\lambda_3 \mu_P + (\lambda_4 - \lambda_3 (1 - \beta_m P) e^{-\beta_m P}) \gamma_{P,S_m} \\
\frac{\partial \lambda_4(t)}{\partial t} &= \lambda_1 \alpha_m - \lambda_4 (\mu_A + w_A) + (\lambda_5 - \lambda_4) a b_m I_h(t) \\
\frac{\partial \lambda_5(t)}{\partial t} &= \lambda_1 \alpha_m - \lambda_5 (\mu_A + w_A) + (\lambda_7 - \lambda_6) a b_h S_h(t) \\
\frac{\partial \lambda_6(t)}{\partial t} &= -\lambda_6 w_H + (\lambda_7 - \lambda_6) a b_h I_m(t) \\
\frac{\partial \lambda_7(t)}{\partial t} &= 1 + (\lambda_5 - \lambda_4) a b_m S_m(t) + (\lambda_8 - \lambda_7) \sigma_h \\
\frac{\partial \lambda_8(t)}{\partial t} &= (\lambda_6 - \lambda_8) \gamma_h.
\end{aligned}$$

Now, setting the partial derivative of \mathcal{H} with respect to the control variables to zero, then solving w_Y and w_A , we get

$$w_Y^* = \frac{\lambda_2 L}{A_Y} \quad w_A^* = \frac{\lambda_4 S_m + \lambda_5 I_m}{A_A} \quad w_H^* = \frac{\lambda_6 S_h}{A_H}.$$

Therefore, the optimal control derived from the stationary condition $\frac{d\lambda_i}{dt}$ is given by

$$\begin{aligned}
w_Y^* &= \begin{cases} 0 & \text{if } \frac{\lambda_2 L}{A_Y} \leq 0 \\ \frac{\lambda_2 L}{A_Y} & \text{if } \frac{\lambda_2 L}{A_Y} < w_M \\ w_M & \text{if } \frac{\lambda_2 L}{A_Y} \geq w_M \end{cases} & w_A^* = \begin{cases} 0 & \text{if } \frac{\lambda_4 S_m + \lambda_5 I_m}{A_A} \leq 0 \\ \frac{\lambda_4 S_m + \lambda_5 I_m}{A_A} & \text{if } \frac{\lambda_4 S_m + \lambda_5 I_m}{A_A} < w_M \\ w_H & \text{if } \frac{\lambda_4 S_m + \lambda_5 I_m}{A_A} \geq w_M \end{cases} \\
w_H^* &= \begin{cases} 0 & \text{if } \frac{\lambda_6 S_h}{A_H} \leq 0 \\ \frac{\lambda_6 S_h}{A_H} & \text{if } \frac{\lambda_6 S_h}{A_H} < w_H \\ w_H & \text{if } \frac{\lambda_6 S_h}{A_H} \geq w_H \end{cases}
\end{aligned}$$

□

Now let us incorporate vaccination into our control strategy and compare it with its different combinations. To perform our simulation, we choose the upper bound in our optimal control, reflecting most of the Philippines' conditions. Herein, $w_{Y,max}$ is set to 23.96, corresponding to the average number of larvae eaten by 50 *Mesocyclops aspericornis* copepods [53]. In the Philippines, thermal fogging is the main way to apply pesticides. It is conducted using a PULSFOG™ machine loaded with a pyrethroid insecticide. Using the study by Mistica, M.S et al. [47], wherein they used the water-based pyrethroid called Aqua-Resigen®, we use the efficacy they evaluated as $w_{A,max} = 0.65$. Finally, the dengvaxia efficacy provides $w_{H,max} = 0.8$

[35, 64]. Using Algorithm 2 with $\epsilon = 0.01$, we numerically solved the optimality of the system. In doing so, we get the graph in Figure 5.7 and Figure 5.8.

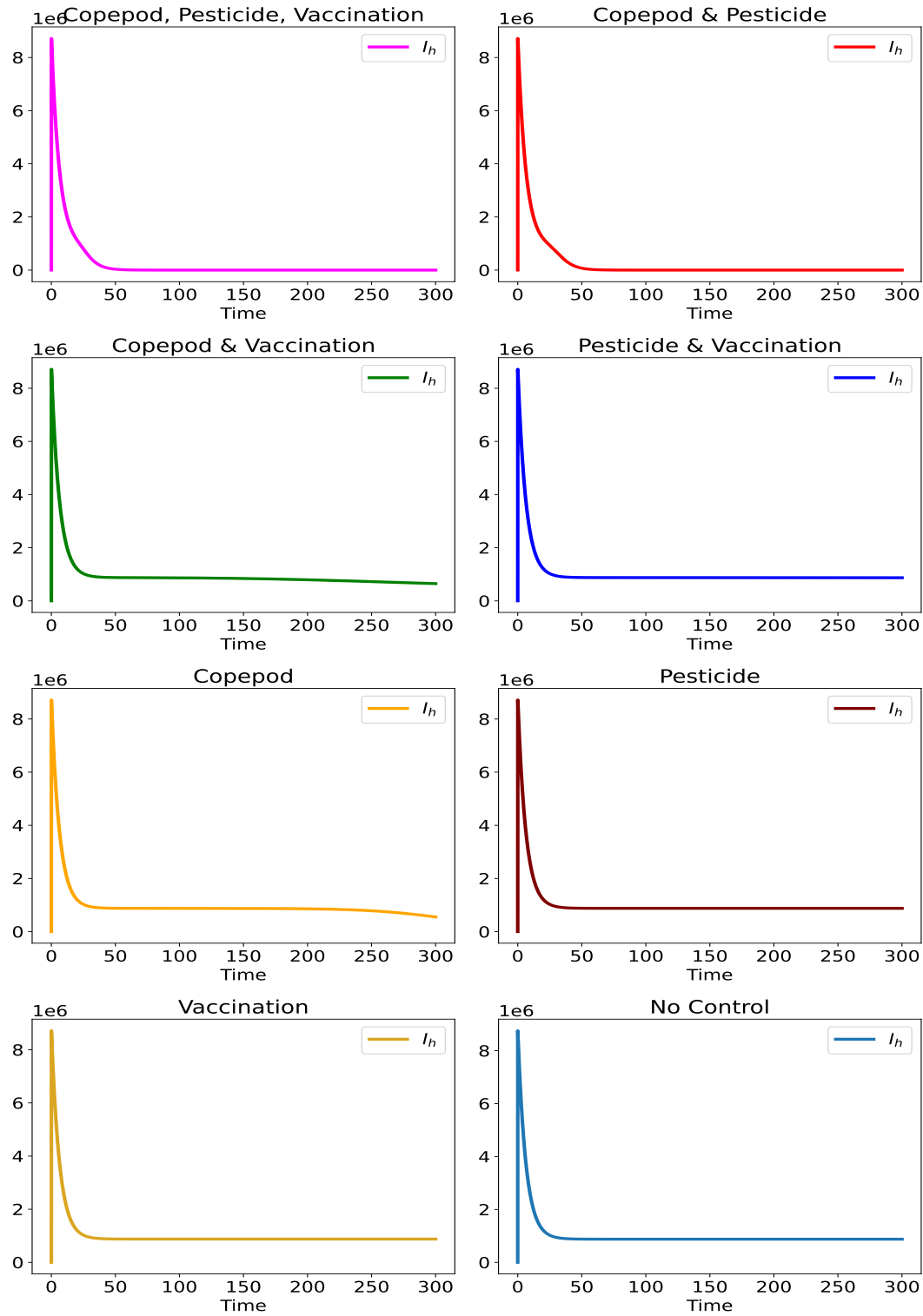


FIGURE 5.7: Optimal solutions of the infected human in the model with different control strategies.

Figure 5.7 shows the behavior of the infected human compartments on the different combinations of control strategies and no control strategy applied. It shows

that the variety of the three techniques (copepod, pesticide, and vaccination) or the combination of the two approaches (copepod and pesticide) is the best strategy for minimizing infected humans. The two methods have no significant difference in the number of maximum infected humans. They both have an 8,715,766.164 maximum infected human population.

Concerning the individual application of the control strategies, applying the copepod is the best strategy for minimizing infected humans. It had a minimum population at the end of the time of 552,606.823 infected humans, whereas pesticide and vaccination had 877,121.808 and 877,190.111 infected humans population at the end of time. On the other hand, not applying a control strategy is not the best choice. It increases the number of infected humans significantly, with an 8,752,880.738 population. However, it does not eliminate the infected humans and has 877,196.995 infected humans at the end of time.

Similarly, for the behavior of infected mosquitoes, figure 5.8 shows that in minimizing the infected mosquito, there is no significant difference in the combination of the three strategies (copepod, pesticide, and vaccination) and the two strategies (the combination of copepod and pesticide). Both methods have a 1,105,864.772 maximum infected mosquito population on day one and equilibrium at 1,105,864.772 infected mosquito population. On the other hand, combining pesticides and vaccination is not a good strategy since it is slow in minimizing the infected mosquito population and has 6,886,581.680 maximum infected mosquitoes.

Meanwhile, for the individual application of the control strategy, copepod alone is the best control in minimizing infected mosquitoes. It prevents the increase of infected mosquitoes with a 2,305,570.072 maximum infected mosquito population, exponentially decreasing over time towards equilibrium. Conversely, vaccination alone is not a good strategy for minimizing the number of infected mosquitoes. It has 4,272,649,867.795 maximum infected mosquito and an equilibrium at 3,697,402,540 infected mosquito.

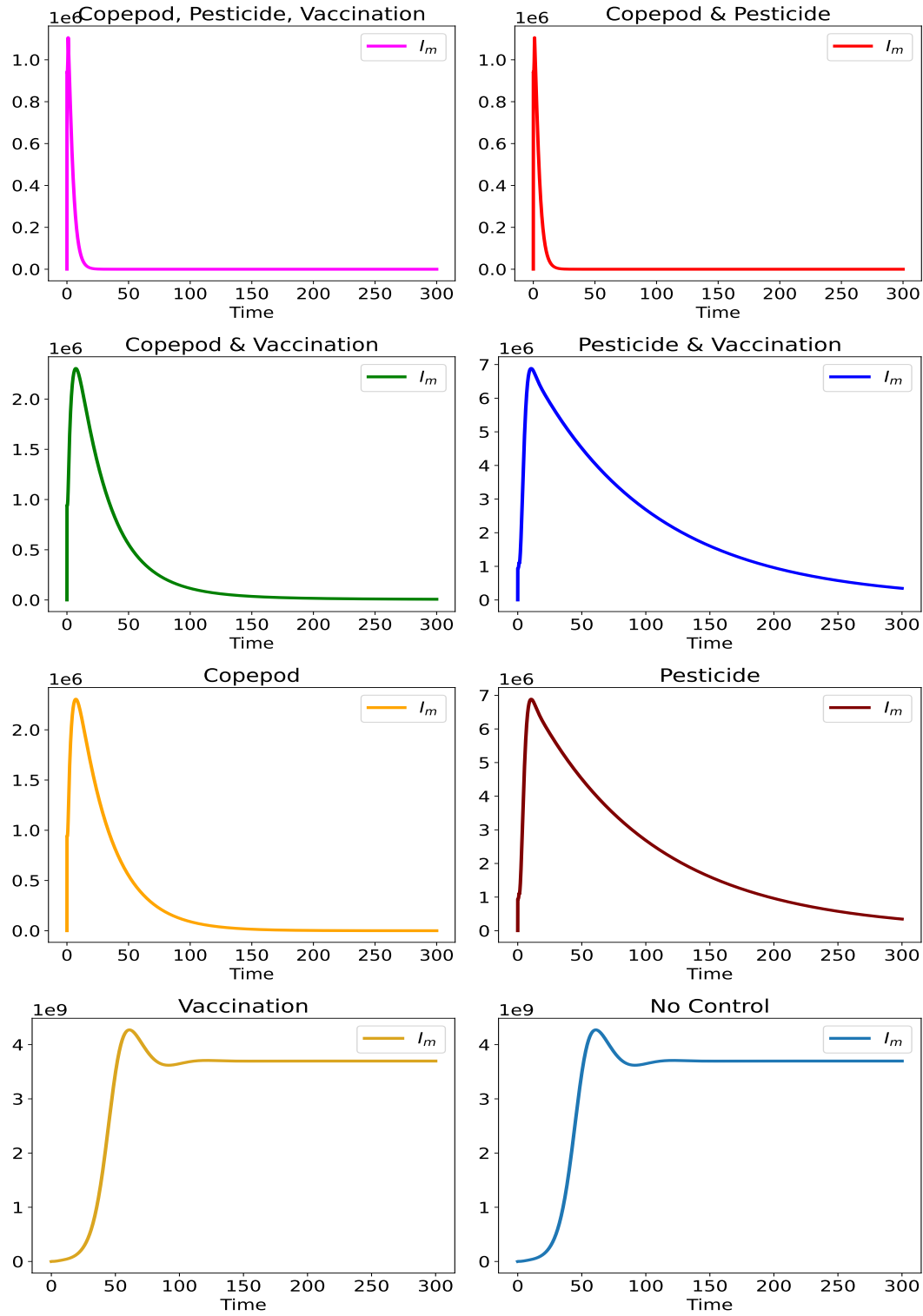


FIGURE 5.8: Optimal solutions of the infected mosquito in the model with different control strategies.

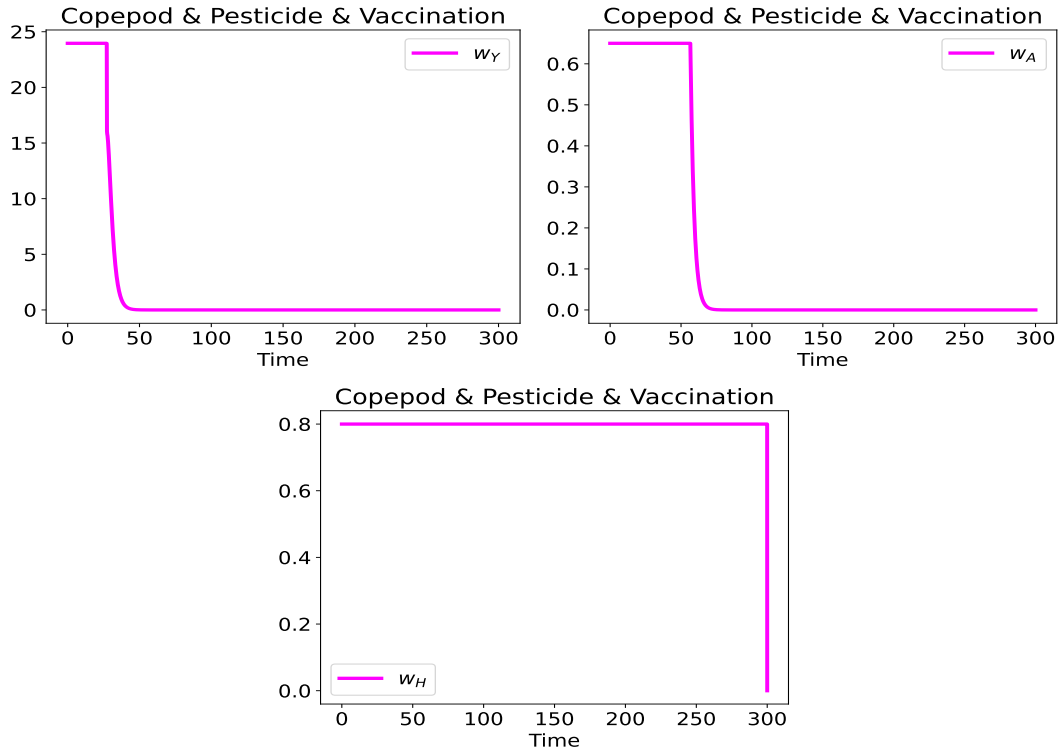


FIGURE 5.9: Optimal solution of the control variables in the model with Copepod, Pesticide and Vaccination control.

Figure 5.9 shows the behavior of the optimal control variables in applying the copepod, pesticide, and vaccination. It shows that the copepod and pesticide should be continuously used for 27 and 56 days, respectively, before a rapid decrease toward equilibrium. However, vaccination should always be done until the end of time.

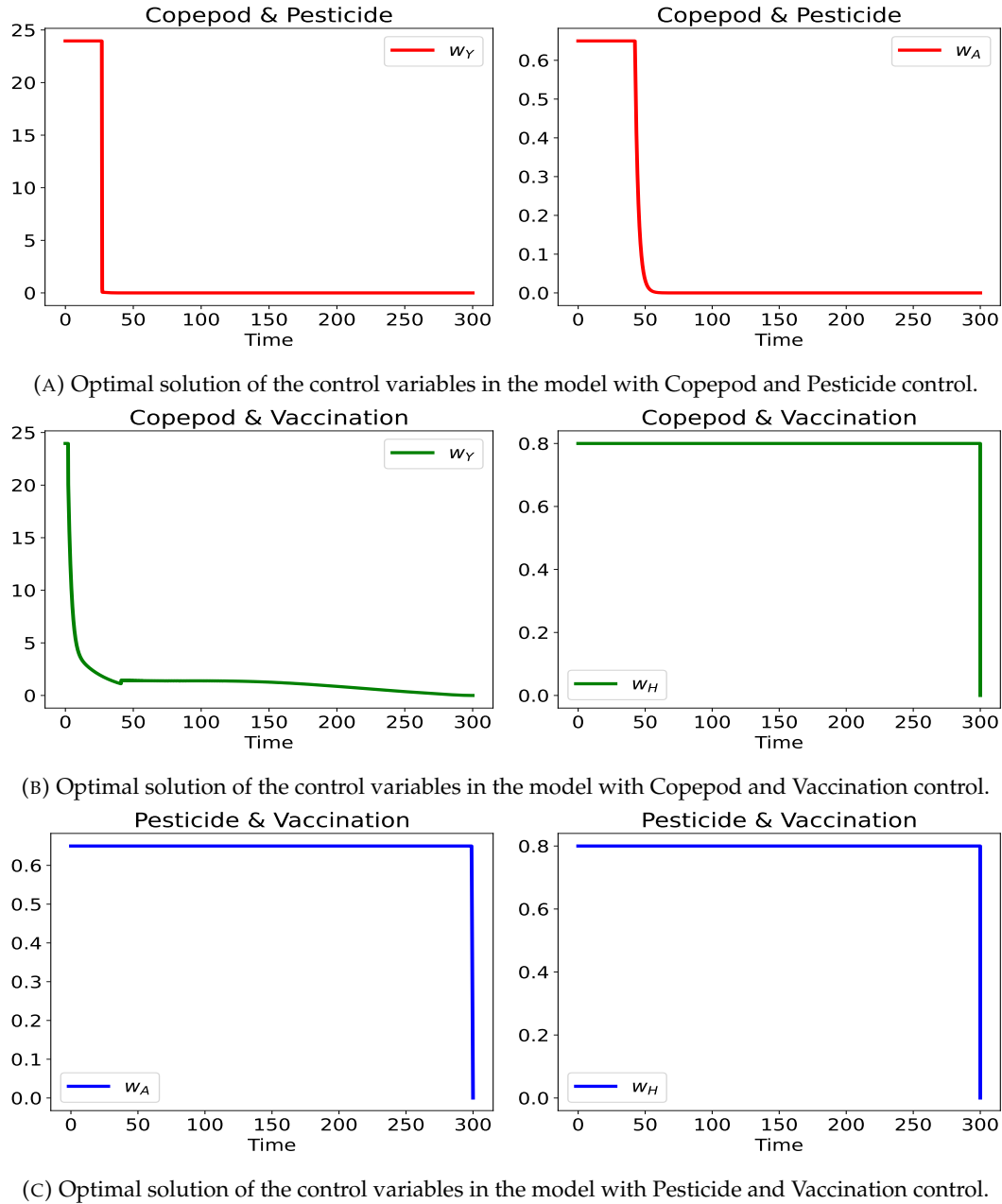


FIGURE 5.10: Optimal solution of the control variables in the model using the different combination of the control strategies.

Figure 5.10 shows the behavior of the control variables by applying a different combination of control strategies. It shows that combining copepod and pesticide is the best control strategy since it requires a shorter time of application. It takes 26 days for copepod application and 42 days for pesticide administration. However, combining copepod and vaccination is better than pesticide and vaccination. Copepod and vaccination methods take only two days for a copepod applicant. In contrast, combining pesticide and vaccination methods is not a good strategy since they must be constantly applied until the end.

5.4.2 Influence of the starting date of control

In this section, we will determine the influence of the optimal control not starting at day zero. We consider three dates, day 40 or the day during the growth; day 64 at the peak; and day 150 at the endemic equilibrium.

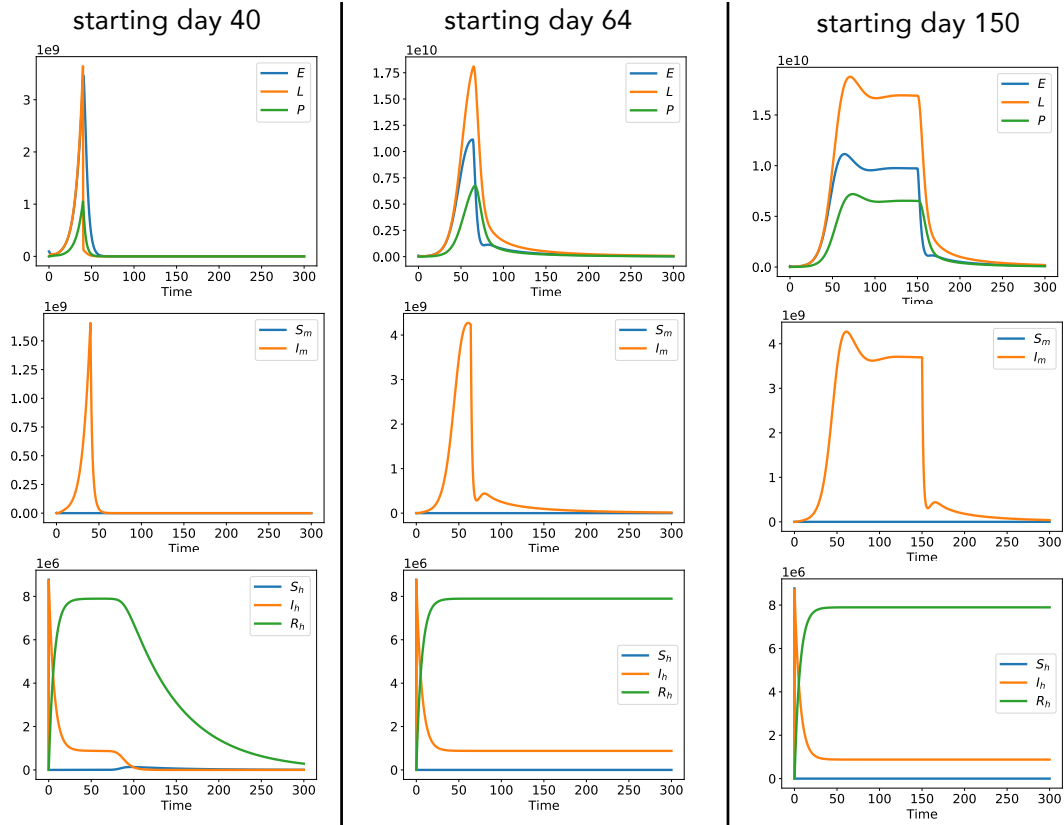


FIGURE 5.11: Optimal solution of the control variables starting control at day 40, 64 and 150.

Figure 5.11 shows the behavior of each variable influenced by the different starting dates of the control inputs. It clearly shows that starting the control inputs earlier in time is the best choice. It prohibits the number of young mosquitoes from increasing and restrains infected mosquitoes from spreading. In effect, the figure shows that starting the control at day 64 and day 150 will not eliminate the infected human compartments.

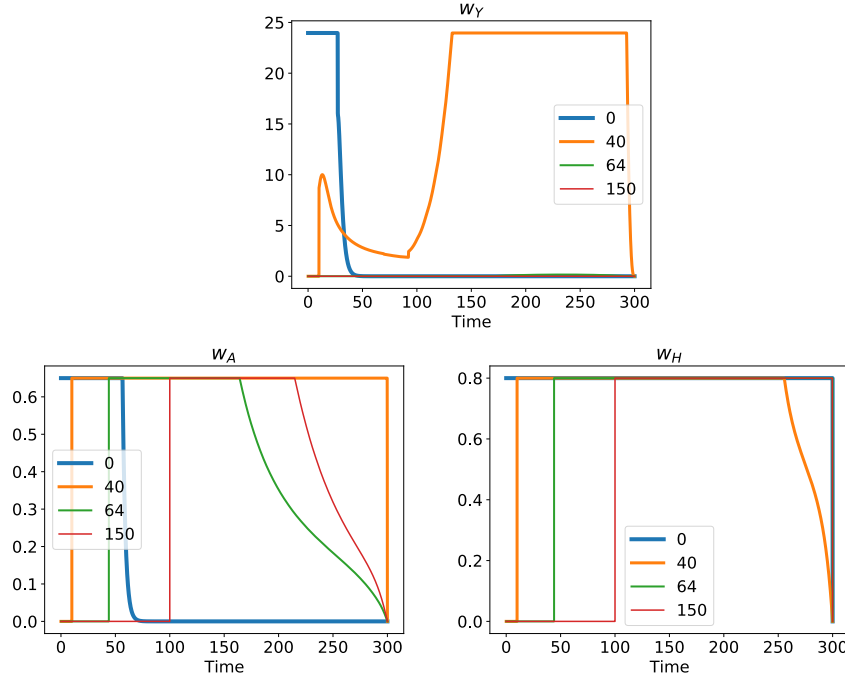


FIGURE 5.12: P control at day 40, 64 and 150.

Figure 5.12 shows the behavior of each optimal control variable influenced by the different starting dates of the control inputs. It shows that the later the starting date of the control inputs the longer the days of application.

5.5 Comparison with larval and pupal competition

In the above section, we considered the pupal competition only. Now the transition rate of pupae to adult mosquito is given by $\gamma_{P,S_m} P e^{-\beta_m(P+L)}$, meaning that the death rate increases with the pupae density P and the larvae density L . Equation (5.4) becomes

$$S'_m(t) = \gamma_{P,S_m} P(t) e^{-\beta_m(P(t)+L(t))} - \mu_A S_m(t) - ab_m I_h(t) S_m(t). \quad (5.38)$$

The system remains globally well-posed and its positive disease free equilibrium $\mathcal{E}_{DFE} = (E^*, L^*, P^*, S_m^*, 0, S_h^*, 0, 0)$ is written as

$$\begin{aligned} E^* &= \frac{(\gamma_{L,P} + \mu_L)(\gamma_{P,S_m} + \mu_P)}{\gamma_{E,L}\gamma_{L,P}} P^* \\ L^* &= \frac{\gamma_{P,S_m} + \mu_P}{\gamma_{L,P}} P^* \\ P^* &= \frac{\gamma_{L,P}}{\beta_m(\gamma_{L,P} + \gamma_{P,S_m} + \mu_P)} \ln \left(\frac{\alpha_m \gamma_{E,L} \gamma_{L,P} \gamma_{P,S_m}}{\mu_A(\gamma_{E,L} + \mu_E)(\gamma_{L,P} + \mu_L)(\gamma_{P,S_m} + \mu_P)} \right) \\ S_m^* &= \frac{\gamma_{P,S_m} P^* e^{-\beta_m P^*}}{\mu_A} \end{aligned}$$

Finally, the second and third equations of the adjoint problem become

$$\begin{aligned} -\frac{d\lambda_2}{dt} &= -(\lambda_2 - \lambda_3)\gamma_{L,P} - \lambda_2(\mu_L + w_Y) + \lambda_4(\beta_m P)e^{-\beta_m(P+L)}\gamma_{P,S_m} \\ -\frac{d\lambda_3}{dt} &= -(\lambda_3 - \lambda_4(1 - \beta_m P)e^{-\beta_m(P+L)})\gamma_{P,S_m} - \lambda_3\mu_P \end{aligned} \quad (5.39)$$

The figures below show the solution with competition induced by larvae and pupae with $\beta_m = 1/(3.59 \times 250000)$, and by pupae only with $\beta_m = 1/(250000)$. Similar results are observed considering pupal competition only and larval competition. Note that, when considering competition induced by pupae only, the number of larvae L is 2.59 times greater than the number of pupae at the equilibrium.

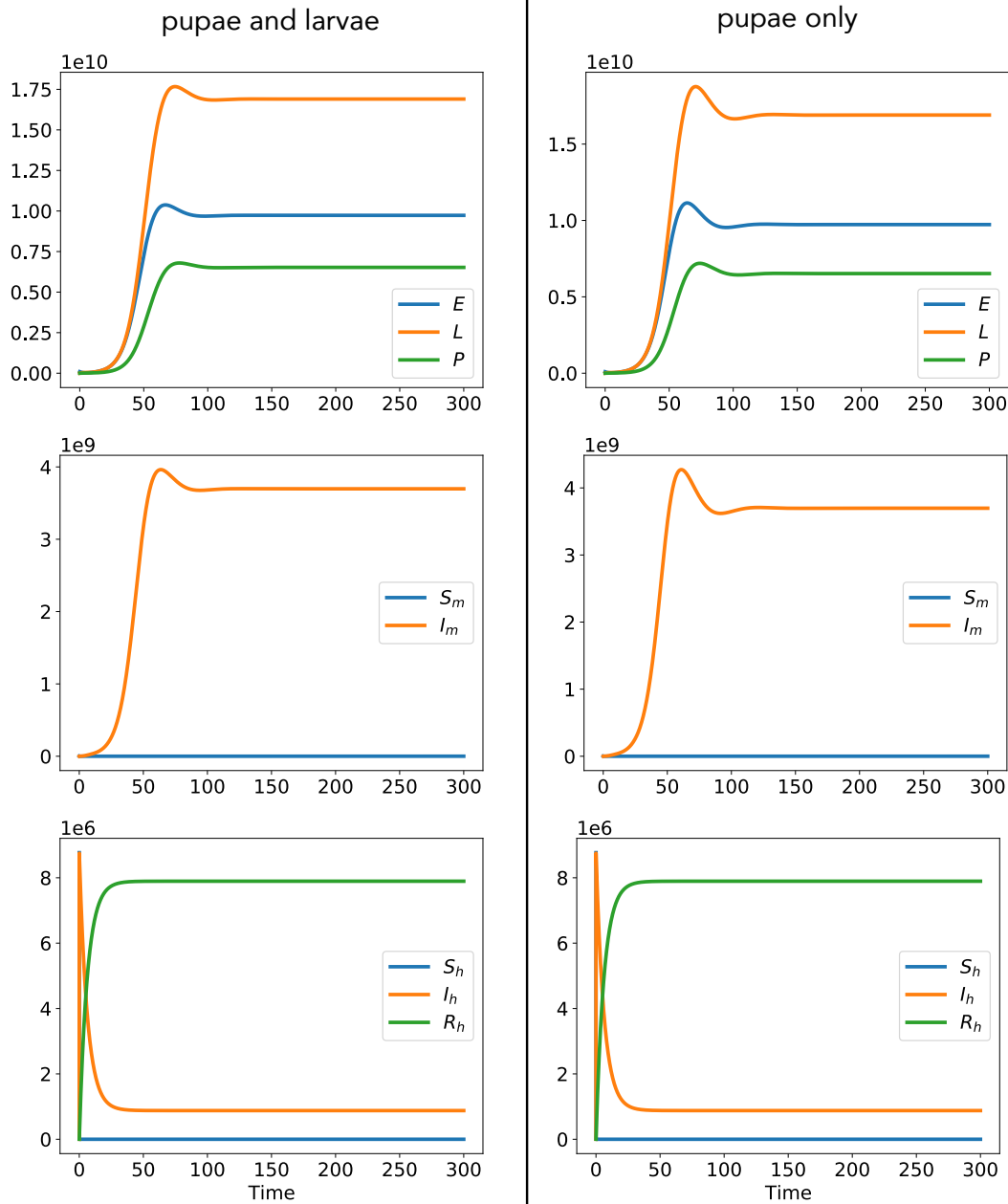


FIGURE 5.13: Comparison of the solution considering competition induced by larvae and pupae (left), and by pupae only (right).

Figure 5.13 shows the behaviour of each variables in the competition induced by larvae and pupae and pupae alone. The figure shows that each variables behaves the same but the mosquito population increases whereas the human population stays the same. For young mosquitoes with competition induced by larvae and pupae, there are 10,375,262,030, 17,669,725,442 and 6,795,266,115 maximum population for eggs, larvae, pupae, respectively. But for competition induced by pupae only, there are only 11,146,838,868, 18,763,929,783 and 7,194,524,993 maximum egg, larvae and pupae population. For adult mosquitoes with competition induced by larvae and pupae, there are 944000 and 3962681700 maximum population for susceptible and infected mosquitoes, respectively. But for competition induced by pupae only,

there are 948030 and 4272650088 maximum population for susceptible and infected mosquitoes, respectively.

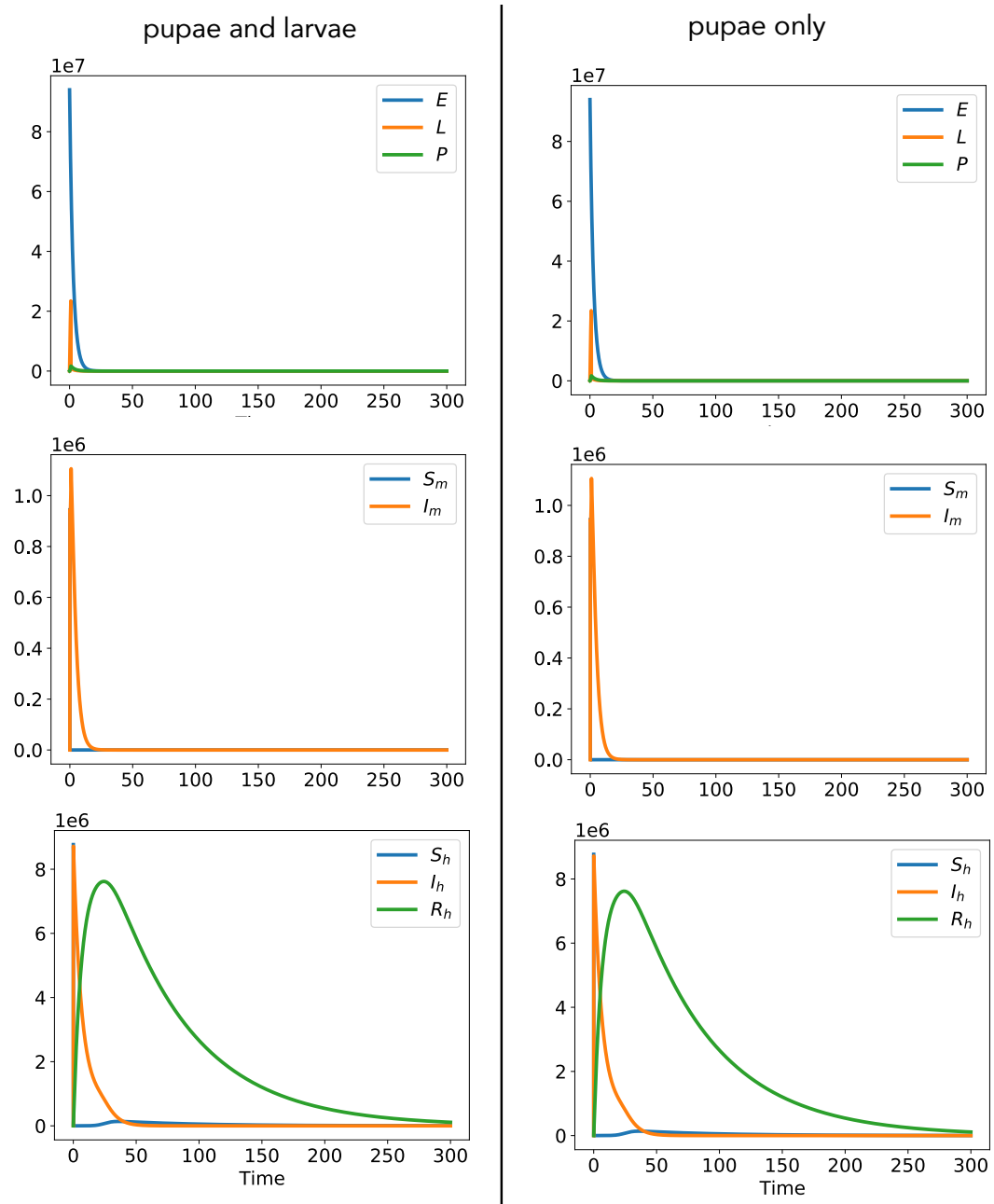


FIGURE 5.14: Comparison of the optimal solution considering competition induced by larvae and pupae (left), and by pupae only (right).

Chapter 6

A Model of Dengue accounting for the Spatial Distribution

There is no gray host for the dengue virus. It is circulating between humans and mosquitoes. Thus, the mosquitoes' spatial distribution highly affects the disease's epidemiology. In this chapter, we introduce a dengue mathematical model that considers adult mosquitoes' spatial distribution.

Spatial analysis is a study that entails using topological, geometric, or geographic properties of a subject. The existence of information regarding the spatial spread of dengue is a crucial ingredient in controlling the spread of the disease. It is important to study because each area has different characteristics, such as land surface elevation, soil type, population density, and many more [57]. A geographic distribution map is handy for empirically studying the relationship between geography and disease and is helpful in the implementation of intervention plans. This chapter assumes that only adult mosquitoes move while humans are immobile. Mosquitoes' movements are governed by their habits. Thus, a summary of the random walk model was included for mosquito feeding and laying habits to understand better how the dynamics are constructed.

6.1 Adult Mosquitoes Habits

6.1.1 Feeding Habits

Like all other animals, mosquitoes need energy and nutrients for survival and reproduction. Plant materials and blood are useful sources of this.

Only female mosquitoes bite. They are attracted by several things like infrared light, light, perspiration, body odor, lactic acid and carbon dioxide. Mouth-part of many female mosquitoes are adapted for piercing the skin of animal hosts and sucking their blood as ectoparasites. During the blood meal, the female mosquitoes lands on the host skin and sticks their proboscis. Their saliva contains anticoagulants proteins that prevents blood clotting. They then sucks the host blood into their abdomen. *A. Aegypti* mosquitoes needs 5 μL per serving [23]. In many female mosquito species, nutrients obtain from blood meal is essential for the production of eggs, whereas in many other species, obtaining nutrients from a blood meal enables

the mosquito to lay more eggs. Among humans, mosquitoes preferred feeding those with type O blood [61], heavy breathers, an abundance of skin bacteria, high body heat, and pregnant women [21]. Individuals' attractiveness to mosquitoes also has a heritable, genetically-controlled component. [29]

Blood-sucking species of mosquitoes are selective feeders that prefer a particular host species. But they relax this selectivity when they experience severe competition and scarcity of food, and/or defensive activity on the part of the hosts. If humans are scarce, mosquitoes resort to feed on monkeys, while others prefer on equines, rodents, birds, bats and pigs, which is where so many of our cross-species disease fears originate from.[41] Some mosquitoes ignores humans altogether and feed exclusively on birds, while most will eat whatever is available. Some of the other most popular dining options for mosquitoes include amphibians, snakes, reptiles, squirrels, rabbits and other small mammals. Mosquitoes also target larger animals, such as horses, cows and primates, as well as kangaroos and wallabies [39]. Even fish may be attacked by some mosquito species if they expose themselves above water level, as mudskippers do [63]. Comparably, mosquitoes may sometimes feed on insects in nature. *A. Aegypti* and *Culex tarsalis* are attracted and feed on insect larvae and they live to produce viable eggs [60]. While *Anopheles Stephensi* is attracted to and can feed successfully on larvae of moth species known as *Manduca sexta* and *Heliothis subflexa* [34].

Plant nectar is a common energy source for diet across mosquito species, particularly male mosquitoes, which are exclusively dependent on plant nectar or alternative sugar sources for survival. The design of efficient sugar-baited traps for mosquitoes would greatly benefit the prevention of vector-borne illness. Plant preference is likely driven by an innate attraction that may be enhanced by experience, as mosquitoes learn to recognize available sugar rewards [70]. It varies among mosquito species, geographical habitats, and seasonal availability. Nectar-seeking involves the integration of at least three sensory systems: olfaction, vision and taste. But altogether mosquitoes can discriminate between rich and poor sugar sources to choose plants that offer higher glycogen, lipid, and protein content [73]. Below are the preferred plant of different mosquito species from Barredo and DeGennaro [7].

6.1.2 Breeding Sites

The dengue vectors, are container breeders; they breed in a wide variety of artificial and natural wet containers/receptacles, preferably with dark coloured surfaces and holding clear (unpolluted) water [46].

Some mosquitoes like living near people, while others prefer forests, marshes, or tall grasses. All mosquitoes like water because mosquito larvae and pupae live in the water with little or no flow [16].

Different types of water attract different types of mosquitoes.

Mosquito Species	Nectar Source
<i>Aedes aegypti</i>	<i>Asclepias syriaca</i> (milkweed) Plant extract <i>Impatiens walleriana</i> Live plants
<i>Anopheles gambiae</i>	<i>Mangifera indica</i> <i>Delonix regia</i> Live plants <i>Parthenium hysterophorus</i> Live plants <i>Acacia macrostachya</i> <i>Acacia albida</i>
<i>Culex pipiens</i>	<i>A. syriaca</i> (milkweed) Live Flower, extract, and synthetic blend <i>I. walleriana</i>
<i>Culex pipiens pallens</i>	<i>Ligustrum quihoui</i> (waxyleaf privet) <i>Broussonetia papyrifera</i> (paper mulberry) <i>L. quihoui</i> <i>Abelia chinensis</i> <i>Nerium indicum</i>

TABLE 6.1: Preferred plants of different mosquito species from Barredo and DeGennaro [7].

- Permanent water mosquitoes: These mosquitoes tend to lay their eggs in permanent-to-semi-permanent bodies of water.
- Floodwater mosquitoes: These mosquitoes lay their eggs in moist soil or in containers above the water line. The eggs dry out, then hatch when rain floods the soil or container.

6.2 Summary of Random Walk Modelling

Mathematicians have long been researching qualitative models that describe the process of dispersal. The common of which are random walk types. The invention of the term 'random walk' was indebted to Karl Pearson, who wrote a letter entitled "The problem of random walk" published in the journal *Nature* on 27 July 1905 [37].

A *random walk* is a random process that describes a walker's path consisting of a sequence of discrete random steps with a fixed length. It is used in an essential model in time series forecasting known as the random walk model. This model assumes that in each period, the variable takes a random step away from its previous value; the steps are independently and identically distributed in size [49]. Meaning that the first difference of the variable is a series to which the mean model should be applied.

Below, we will introduce the fundamental theory and equations of random walks from the paper of Codling et al. [22].

6.2.1 Reaction-Diffusion Equation

Consider a mosquito that moves randomly in one direction with a fixed step δ on time τ . Let $p(m, n)$ be the probability that the mosquito reaches the point $m\delta$ after n time steps.

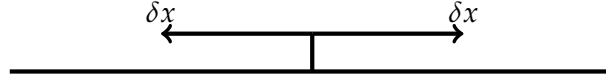


FIGURE 6.1: Mosquito can move left or right.

Suppose that to reach $m\delta$ after $n\tau$, we need a step to the right and b steps to the left. Then

$$m = a - b \quad \text{and} \quad n = a + b.$$

The number of possible path is

$$\frac{n!}{a!b!} = \frac{n!}{a!(n-a)!} = \binom{n}{a},$$

and the total number of path with n steps is 2^n and the probability is

$$p(m, n) = \binom{n}{a} \frac{1}{2^n}.$$

Note that

$$\sum_{m=-n}^n p(m, n) = \sum_{a=0}^n \binom{n}{a} \left(\frac{1}{2}\right)^{n-a} \left(\frac{1}{2}\right)^a = \left(\frac{1}{2} + \frac{1}{2}\right)^n = 1,$$

and $p(m, n)$ follows a binomial law. Thanks to the Stirling formula

$$n! \simeq_{n \rightarrow +\infty} (2\pi n)^{1/2} e^{n \ln n - n},$$

we have

$$\begin{aligned} p(m, n) &\simeq_{n \rightarrow +\infty} \frac{1}{2^n} \frac{(2\pi n)^{1/2}}{(2\pi a)^{1/2} (2\pi(n-a))^{1/2}} e^{(n \ln n - n) - (a \ln a - a) - ((n-a) \ln(n-a) - (n-a))} \\ &\simeq_{n \rightarrow +\infty} \left(\frac{2}{\pi n}\right)^{1/2} e^{-\frac{m^2}{2n}}. \end{aligned}$$

We deduce

$$\frac{p\left(\frac{x}{\delta}, \frac{t}{\tau}\right)}{2\delta} \simeq \left(\frac{\tau}{2\pi t \delta^2}\right)^{1/2} e^{-\frac{x^2}{2t} \frac{\tau}{\delta^2}}.$$

Assume that

$$\lim_{\delta, \tau \rightarrow 0} \frac{\delta^2}{2\tau} = D,$$

where $D > 0$ is the diffusion coefficient, we obtain

$$K(x, t) = \lim_{\delta, \tau \rightarrow 0} \frac{p\left(\frac{x}{\delta}, \frac{t}{\tau}\right)}{2\delta} = \left(\frac{1}{4\pi Dt}\right)^{1/2} e^{-\frac{x^2}{4Dt}}. \quad (6.1)$$

Theorem 6.2.1. *The function $K : (x, t) \in \mathbb{R}^d \times \mathbb{R}_+^* \rightarrow K(t, x)$ is the fundamental solution of the heat equation*

$$\begin{aligned} \frac{\partial K}{\partial t} - D\Delta K &= 0 \\ K(x, 0) &= 0, \end{aligned}$$

with

$$\int_{\mathbb{R}^d} K(x, t) dx = 1.$$

Proof. For equation (6.1) taking it's partial derivative with respect to t and x , respectively would give us

$$\begin{aligned} \frac{\partial K}{\partial t} &= \left(\frac{1}{4\pi Dt}\right)^{\frac{1}{2}} e^{-\frac{x^2}{4Dt}} [x^2(4Dt)^{-2}(4D)] + e^{-\frac{x^2}{4Dt}} \left[\left(-\frac{1}{2}\right) (4\pi Dt)^{-\frac{3}{2}} (4\pi D) \right] \\ &= \left(\frac{1}{4\pi Dt}\right)^{\frac{1}{2}} e^{-\frac{x^2}{4Dt}} [4Dx^2(4Dt)^{-2} - 2\pi D(4\pi Dt)^{-1}] \\ &= \left(\frac{1}{4\pi Dt}\right)^{\frac{1}{2}} e^{-\frac{x^2}{4Dt}} [4\pi^2 x^2 D(4\pi Dt)^{-2} - 2\pi D(4\pi Dt)^{-1}] \\ &= \left(\frac{1}{4\pi Dt}\right)^{\frac{3}{2}} e^{-\frac{x^2}{4Dt}} (2\pi D) \left(\frac{x^2}{2Dt} - 1\right) \end{aligned}$$

and

$$\begin{aligned} \frac{\partial K}{\partial x} &= \left(\frac{1}{4\pi Dt}\right)^{\frac{1}{2}} e^{-\frac{x^2}{4Dt}} [-2x(4Dt)^{-1}] \\ &= \left(\frac{1}{4\pi Dt}\right)^{\frac{1}{2}} e^{-\frac{x^2}{4Dt}} [-2x(4\pi Dt)^{-1}(\pi)] \\ &= -\left(\frac{1}{4\pi Dt}\right)^{\frac{3}{2}} e^{-\frac{x^2}{4Dt}} (2\pi x). \end{aligned}$$

Thus, the Laplacian of K is given by

$$\begin{aligned} \Delta K &= -\left(\frac{1}{4\pi Dt}\right)^{\frac{3}{2}} \left[e^{-\frac{x^2}{4Dt}} (2\pi) + 2\pi x e^{-\frac{x^2}{4Dt}} (-2x)(4Dt)^{-1} \right] \\ &= \left(\frac{1}{4\pi Dt}\right)^{\frac{3}{2}} e^{-\frac{x^2}{4Dt}} (2\pi) (2\pi x^2(4\pi Dt)^{-1} - 1) \\ &= \left(\frac{1}{4\pi Dt}\right)^{\frac{3}{2}} e^{-\frac{x^2}{4Dt}} (2\pi) \left(\frac{x^2}{2Dt} - 1\right). \end{aligned}$$

Therefore,

$$\frac{\partial K}{\partial t} - D\Delta K = 0.$$

Note that as $t \rightarrow 0$, $e^{-\frac{x^2}{4Dt}} = 0$ while $\left(\frac{1}{4\pi Dt}\right)^{1/2}$ approaches infinity. But $e^{-\frac{x^2}{4Dt}}$ approaches 0 faster than the later. Thus,

$$\begin{aligned} K(x, 0) &= \lim_{t \rightarrow 0} \left(\frac{1}{4\pi Dt} \right)^{1/2} e^{-\frac{x^2}{4Dt}} \\ &= \lim_{t \rightarrow 0} \left(\frac{1}{4\pi Dt} \right)^{1/2} \lim_{t \rightarrow 0} e^{-\frac{x^2}{4Dt}} \\ &= 0. \end{aligned}$$

Now, taking the integral of $K(x, t)$ with respect to x , would give us

$$\begin{aligned} \int_{\mathbb{R}^d} K(x, t) dx &= \int_{\mathbb{R}^d} \left(\frac{1}{4\pi Dt} \right)^{1/2} e^{-\frac{x^2}{4Dt}} dx \\ &= \int_{\mathbb{R}^d} \left(\frac{1}{4\pi Dt} \right)^{1/2} e^{-\left(\frac{x}{(4Dt)^{1/2}}\right)^2} dx. \end{aligned}$$

Let $z = \frac{x}{(4Dt)^{1/2}}$. Then $(4Dt)^{1/2} dz = dx$. Thus for each time $t > 0$,

$$\begin{aligned} \int_{\mathbb{R}^d} K(x, t) dx &= \frac{1}{\pi^{1/2}} \int_{\mathbb{R}^d} e^{-z^2} dz \\ &= \frac{1}{\pi^{1/2}} \prod_{i=1}^n \int_{-\infty}^{\infty} e^{-z_i^2} dz_i \\ &= 1. \end{aligned}$$

□

Corollary 6.2.2. Let $u_0 \in L^\infty(\mathbb{R})$.

1. The function

$$u(x, t) = \int_{\mathbb{R}^d} K(x - y, t) u_0(y) dy = K \star u_0(x)$$

is a solution of the initial value problem

$$\begin{aligned} \frac{\partial u}{\partial t} - D\Delta u &= 0 \\ u(x, 0) &= u_0(x) \end{aligned}$$

2. The function

$$u(x, t) = \int_{\mathbb{R}^d} K(x - y, t) u_0(y) dy + \int_0^t \int_{\mathbb{R}^d} K(x - y, t - s) f(y, s) dy ds$$

is a solution of the reaction-diffusion problem

$$\begin{aligned}\frac{\partial u}{\partial t} - D\Delta u &= f \\ u(x, 0) &= u_0(x)\end{aligned}$$

In particular, if $f = f(t, u)$ is Lipschitz with respect to u , there exists a unique local in time strong solution.

Proof. 1. Let $x_0 \in \mathbb{R}^d$, $\epsilon > 0$. Choose $\delta > 0$ such that

$$|u(y) - u(x_0)| < \epsilon \quad \text{if} \quad |y - x_0| < \delta, y \in \mathbb{R}^d \quad (6.2)$$

Thus, $u(x, 0) = u_0(x)$.

Now note that $y - x_0 = y - x + x - x_0$. By triangle property,

$$|y - x_0| \leq |y - x| + |x - x_0|.$$

Since $|y - x_0| < \delta$, $|x - x_0| < \frac{\delta}{2}$. By Theorem 6.2.1,

$$\begin{aligned}|u(x, t) - u(x_0)| &= \left| \int_{\mathbb{R}^d} K(x - y, t) |u(y) - u(x_0)| dy \right| \\ &\leq \int_{B(x_0, \delta)} K(x - y, t) |u(y) - u(x_0)| dy \\ &\quad + \int_{\mathbb{R}^d - B(x_0, \delta)} K(x - y, t) |u(y) - u(x_0)| dy\end{aligned}$$

Let I be the first term and J the second term of the right-hand side of the equation above. Then by equation 6.2 and Theorem 6.2.1,

$$I \leq \epsilon \int_{B(x_0, \delta)} K(x - y, t) dy \leq \epsilon(1) \leq \epsilon.$$

Furthermore,

$$\begin{aligned}|u(y) - u(x_0)| &\leq |u(y)| + |u(x_0)| \\ &\leq \|u_0\| + \|u_0\| \\ &\leq 2\|u_0\|.\end{aligned}$$

Implying further that

$$\begin{aligned}
 J &\leq 2\|u_0\|_{L^\infty} \int_{\mathbb{R}^d - B(x_0, \delta)} K(x-y, t) dy \\
 &\leq 2\|u_0\|_{L^\infty} \int_{\mathbb{R}^d - B(x_0, \delta)} \left(\frac{1}{4\pi Dt} \right)^{1/2} e^{-\frac{(x-y)^2}{4Dt}} dy \\
 &\leq \frac{2\|u_0\|}{(4\pi Dt)^{1/2}} \int_{\mathbb{R}^d - B(x_0, \delta)} e^{-\frac{(x-y)^2}{4Dt}} dy \\
 &\leq \frac{2\|u_0\|}{(4\pi Dt)^{1/2}} \int_{\mathbb{R}^d - B(x_0, \delta)} e^{-\frac{(y-x_0)^2}{4Dt}} dy
 \end{aligned}$$

Let $z = \frac{y-x}{(4Dt)^{1/2}}$. Then $(4Dt)^{1/2}dz = dy$. Thus

$$J \leq \frac{2\|u_0\|}{\pi^{1/2}} \int_{\mathbb{R}^d - B(x_0, \delta/\sqrt{t})} e^{-\frac{z^2}{16}} dz$$

Note that as $t \rightarrow 0^+$, $\int_{\mathbb{R}^d - B(x_0, \delta/\sqrt{t})} e^{-\frac{z^2}{16}} dz \rightarrow 0$. Hence, $J = 0$. Thus if $|x - x_0| \leq \frac{\delta}{2}$ and $t > 0$ is small enough, $|u(x, t) - u(x_0)| < 2\epsilon$.

2. Let $u(x, t) = \int_{\mathbb{R}^d} K(x-y, t)u_0(y)dy + \int_0^t \int_{\mathbb{R}^d} K(x-y, t-s)f(y, s)dyds$. Then

$$\begin{aligned}
 \frac{\partial u}{\partial t} - D\Delta u &= \frac{\partial}{\partial t} \left(\int_{\mathbb{R}^d} K(x-y, t)u_0(y)dy + \int_0^t \int_{\mathbb{R}^d} K(x-y, t-s)f(y, s)dyds \right) \\
 &\quad - D \frac{\partial^2}{\partial x^2} \left(\int_{\mathbb{R}^d} K(x-y, t)u_0(y)dy + \int_0^t \int_{\mathbb{R}^d} K(x-y, t-s)f(y, s)dyds \right) \\
 &= \frac{\partial}{\partial t} \left(\int_{\mathbb{R}^d} K(x-y, t)u_0(y)dy \right) \\
 &\quad + \frac{\partial}{\partial t} \left(\int_0^t \int_{\mathbb{R}^d} K(x-y, t-s)f(y, s)dyds \right) \\
 &\quad - D \frac{\partial^2}{\partial x^2} \left(\int_{\mathbb{R}^d} K(x-y, t)u_0(y)dy \right) \\
 &\quad - D \frac{\partial^2}{\partial x^2} \left(\int_0^t \int_{\mathbb{R}^d} K(x-y, t-s)f(y, s)dyds \right) \\
 &= \left(\frac{\partial}{\partial t} - D \frac{\partial^2}{\partial x^2} \right) \int_{\mathbb{R}^d} K(x-y, t)u_0(y)dy \\
 &\quad + \left(\frac{\partial}{\partial t} - D \frac{\partial^2}{\partial x^2} \right) \int_0^t \int_{\mathbb{R}^d} K(x-y, t-s)f(y, s)dyds
 \end{aligned}$$

By (1), $\left(\frac{\partial}{\partial t} - D \frac{\partial^2}{\partial x^2} \right) \int_{\mathbb{R}^d} K(x-y, t)u_0(y)dy = 0$. Thus, we only have

$$u_t - D\Delta u = \left(\frac{\partial}{\partial t} - D \frac{\partial^2}{\partial x^2} \right) \int_0^t \int_{\mathbb{R}^d} K(x-y, t-s)f(y, s)dyds.$$

Now we change variables, to write

$$u_t - D\Delta u = \left(\frac{\partial}{\partial t} - D \frac{\partial^2}{\partial x^2} \right) \int_0^t \int_{\mathbb{R}^d} K(y, s)f(x-y, t-s)dyds.$$

For $s = t > 0$, we compute that

$$\begin{aligned} \frac{\partial}{\partial t} \left(\int_0^t \int_{\mathbb{R}^d} K(y, s) f(x - y, t - s) dy ds \right) &= \int_0^t \int_{\mathbb{R}^d} K(y, s) f_t(x - y, t - s) dy ds \\ &\quad + \int_{\mathbb{R}^d} K(y, t) f(x - y, 0) dy \end{aligned}$$

and

$$D \frac{\partial^2}{\partial x^2} \left(\int_0^t \int_{\mathbb{R}^d} K(y, s) f(x - y, t - s) dy ds \right) = \int_0^t \int_{\mathbb{R}^d} K(y, s) f_{x_1 x_2}(x - y, t - s) dy ds.$$

Hence, we have

$$\begin{aligned} u_t - D\Delta u &= \int_0^t \int_{\mathbb{R}^d} K(y, s) \left[\left(\frac{\partial}{\partial t} - D \frac{\partial^2}{\partial x^2} \right) f(x - y, t - s) \right] dy ds \\ &\quad + \int_{\mathbb{R}^d} K(y, t) f(x - y, 0) dy \\ &= \int_\epsilon^t \int_{\mathbb{R}^d} K(y, s) \left[\left(-\frac{\partial}{\partial s} - D \frac{\partial^2}{\partial y^2} \right) f(x - y, t - s) \right] dy ds \quad (6.3) \\ &\quad + \int_0^\epsilon \int_{\mathbb{R}^d} K(y, s) \left[\left(-\frac{\partial}{\partial s} - D \frac{\partial^2}{\partial y^2} \right) f(x - y, t - s) \right] dy ds \\ &\quad + \int_{\mathbb{R}^d} K(y, t) f(x - y, 0) dy \end{aligned}$$

Let I be the first term, J be the second term and G be the third term of the right-hand side of the equation above. Then

$$\begin{aligned} |J| &\leq (\|f_t\|_{L^\infty} + D\|H^2 f\|_{L^\infty}) \int_0^\epsilon \int_{\mathbb{R}^d} K(y, s) dy ds \\ &\leq (\|f_t\|_{L^\infty} + D\|H^2 f\|_{L^\infty}) \int_0^\epsilon \int_{\mathbb{R}^d} \left(\frac{1}{4\pi Ds} \right)^{1/2} e^{-\frac{y^2}{4Ds}} dy ds \\ &\leq (\|f_t\|_{L^\infty} + D\|H^2 f\|_{L^\infty}) \int_0^\epsilon \left[\pi^{-1/2} \int_{\mathbb{R}^d} e^{-z^2} dz \right] ds \\ &\leq (\|f_t\|_{L^\infty} + D\|H^2 f\|_{L^\infty}) \int_0^\epsilon \left[\pi^{-1/2} \pi^{1/2} \right] ds \\ &\leq \epsilon C \end{aligned}$$

We also have, by integration by parts

$$\begin{aligned} I &= \int_\epsilon^t \int_{\mathbb{R}^d} \left[\left(-\frac{\partial}{\partial s} - D \frac{\partial^2}{\partial y^2} \right) K(y, s) \right] f(x - y, t - s) dy ds \\ &\quad + \int_{\mathbb{R}^d} K(y, \epsilon) f(x - y, t - \epsilon) dy \\ &\quad - \int_{\mathbb{R}^d} K(y, t) f(x - y, 0) dy \quad (6.4) \\ &= \int_{\mathbb{R}^d} K(y, \epsilon) f(x - y, t - \epsilon) dy - \int_{\mathbb{R}^d} K(y, t) f(x - y, 0) dy \end{aligned}$$

Since K solves the heat equation. Combining equations (6.3, 6.4) and J , we have

$$\begin{aligned} u_t(x, t) - D\Delta(x, t) &= \lim_{\epsilon \rightarrow 0} \int_{\mathbb{R}^d} K(y, \epsilon) f(x - y, t - \epsilon) dy \\ &= f(x, t) \end{aligned}$$

for $x \in \mathbb{R}^d$ and $t > 0$.

□

Remark 6.2.3. *Similar results remains true in a bounded domain Ω .*

6.2.2 Advection-Diffusion Equation

This section will discuss a random walk with a preferred direction or bias and a possible waiting time between movement steps.

Consider that at each time step t , a mosquito moves a distance δ to the left or right with probabilities l and r , respectively, or stays in the exact location, with probability $1 - l - r$. If the mosquito is at location x at the time $t + \tau$, there are three possibilities for its location at time t :

- it was at $x - \delta$ and then moved to the right,
- it was at $x + \delta$ and then moved to the left, and
- it was at x and did not moved at all.

Thus the probability that at time $t + \tau$ the mosquito is at distance x , is given by

$$p(x, t + \tau) = p(x, t)(1 - l - r) + p(x - \delta, t)r + p(x + \delta, t)l. \quad (6.5)$$

Taylor's expansions are written

$$\begin{aligned} p(x + \delta, t) &= p(x, t) + \delta \frac{\partial p}{\partial x} + \frac{\delta^2}{2} \frac{\partial^2 p}{\partial x^2} + O(\delta^3) \\ p(x - \delta, t) &= p(x, t) - \delta \frac{\partial p}{\partial x} + \frac{\delta^2}{2} \frac{\partial^2 p}{\partial x^2} + O(\delta^3). \end{aligned}$$

Then by subtracting, respectively adding these equations, gives us

$$\begin{aligned} \frac{\partial p}{\partial x} &= \frac{p(x + \delta, t) - p(x, t)}{\delta} + O(\delta) = \frac{p(x, t) - p(x - \delta, t)}{\delta} + O(\delta) = \lim_{\delta \rightarrow 0} \frac{p(x, t) - p(x - \delta, t)}{\delta} \\ \frac{\partial^2 p}{\partial x^2} &= \frac{p(x + \delta, t) - 2p(x, t) + p(x - \delta, t)}{\delta^2} + O(\delta^2) \\ \frac{\partial p}{\partial t} &= \frac{p(x, t + \tau) - p(x, t)}{\tau} + O(\tau) \end{aligned}$$

Let τ, δ be small. Then, the partial derivative of (6.5) with respect to time t gives

$$\frac{\partial p}{\partial t} = -\frac{\delta \epsilon}{\tau} \frac{\partial p}{\partial x} + \frac{k \delta^2}{2\tau} \frac{\partial^2 p}{\partial x^2} + O(\tau^2) + O(\delta^3)$$

with $\epsilon = r - l$; $k = l + r$ and where $O(\tau^2)$ and $O(\delta^3)$ represents higher order terms. Note that δ^2/τ is positive and finite as $\delta, \tau \rightarrow 0$ since the difference $\epsilon = r - l$ between the probabilities of moving left and right is proportional to δ , and that $\epsilon \rightarrow 0$ as $\delta, \tau \rightarrow 0$. Thus the probabilities r and l are not fixed, but vary with the spatial and

temporal step sizes such that the limit

$$u = \lim_{\delta, \tau \rightarrow 0} \frac{\delta \epsilon}{\tau}, \quad D = k \lim_{\delta, \tau \rightarrow 0} \frac{\delta^2}{2\tau}$$

exists and are positive and finite. Implying further that the limits of the terms $O(\tau^2)$ and $O(\tau^3)$ tends to zero. Hence we have the advection-diffusion equation

$$\frac{\partial p}{\partial t} = -u \frac{\partial p}{\partial x} + D \frac{\partial^2 p}{\partial x^2} \quad (6.6)$$

where the first term on the right-hand side represents advection due to the bias in the probability of moving in the preferred direction and the second terms represents diffusion.

For an N -dimensional lattice, the standard drift-diffusion equation is given by

$$\frac{\partial p}{\partial t} = -u \cdot \nabla p + D \Delta^2 p$$

where u is the average drift velocity, ∇ is the gradient operator and Δ^2 is the Laplacian. Assuming an initial Dirac delta function distribution $p(x, 0) = \delta_d(x_1), \dots, \delta_d(x_N)$, the equation above has the solution

$$p(x, t) = \frac{1}{(4\pi Dt)^{N/2}} \exp\left(-\frac{|x - ut|^2}{4Dt}\right). \quad (6.7)$$

6.2.3 Fokker-Plank Equation

This section will extend a simple random walk in two or more dimensions to include the probability of spatially dependent movements.

Consider a mosquito that moves in a two-dimensional lattice. Suppose that at each time step τ , the mosquito move a distance δ either upward, downward, to the left or to the right with probabilities dependent on location given by $u(x, y)$, $d(x, y)$, $l(x, y)$ and $r(x, y)$, respectively where $u + d + l + r \leq 1$, or remain at the same location with probability $1 - u(x, y) - l(x, y) - d(x, y) - r(x, y)$. Then the probability that the mosquito is at a distance x at time t is given by

$$\begin{aligned} p((x, y), t) &= p((x, y), t)(1 - u(x, y) - l(x, y) - d(x, y) - r(x, y)) \\ &\quad + p((x - \delta, y), t)l(x, y) + p((x + \delta, y), t)r(x, y) \\ &\quad + p((x, y - \delta), t)d(x, y) + p((x, y + \delta), t)u(x, y) \end{aligned}$$

For $i = 1, 2$, the limit

$$b_i = \lim_{\delta, \tau, \epsilon_i \rightarrow 0} \frac{\epsilon_i \delta}{\tau}, \quad a_{ii} = \lim_{\delta, \tau \rightarrow 0} \frac{k_i \delta^2}{2\tau}$$

tends to constants with $\epsilon_1 = r - l$, $\epsilon_2 = u - d$, $k_1 = r + l$ and $k_2 = u + d$. Thus, we have the Fokker-Planck diffusion equation

$$\frac{\partial p}{\partial t} = -\nabla \cdot (up) + \nabla \cdot (D\nabla p) \quad (6.8)$$

with

$$u(x, y) = \begin{pmatrix} b_1(x, y) \\ b_2(x, y) \end{pmatrix},$$

$$D(x, y) = \begin{pmatrix} a_{11}(x, y) & 0 \\ 0 & a_{22}(x, y) \end{pmatrix}.$$

6.3 Dengue Model with Spatial Distribution

In this section we presented a new model for dengue that involves the spatial spread of adult mosquitoes. We follow the method proposed by Bourhis et al. [10] for the fly spread.

Consider a domain $\Omega \subset \mathbb{R}^2$. The propensity of adult mosquito to leave the determined focal point (x, y) can be defined by the diffusion coefficient

$$D(x, y) = D_{min} + \alpha \mathcal{F}_l(x, y) + \beta \mathcal{F}_f(x, y) \quad (6.9)$$

where D_{min} is the minimal diffusion value in the absence of resources perception, $\mathcal{F}_l(x, y)$ and $\mathcal{F}_f(x, y)$ are the dispersion kernels that covered the entire landscape of the laying and food resources respectively. That is, the mosquitoes moves in random direction D_{min} if they see no resources. But if they see food source, the mosquitoes would prefer to move in that direction $\beta \mathcal{F}_f(x, y)$. The same is true for laying sites $\alpha \mathcal{F}_l(x, y)$. The coefficients α and β is used to weight the differential impact of resources on the diffusion intensity. And the dispersion kernels $\mathcal{F}_l(x, y)$ and $\mathcal{F}_f(x, y)$ is defined as

$$\mathcal{F}_f(x, y) = \frac{\sum_{\Omega} K_f(d) \times \mathbb{1}_f(x, y)}{\sum_{\Omega} K_f(d)}$$

$$\mathcal{F}_l(x, y) = \frac{\sum_{\Omega} K_l(d) \times \mathbb{1}_l(x, y)}{\sum_{\Omega} K_l(d)}$$

with

$$K_f(d) = e^{-c_f d}$$

$$K_l(d) = e^{-c_l d}$$

as the kernels for feeding sites $K_f(d)$ and ovipositing sites $K_l(d)$ where d is the distance to the focal point and c_f and c_l tune the perception ranges of feeding and laying sites, respectively.

Defining the population density of adults mosquito for every $(x, y) \in \Omega$ and we have

$$\begin{aligned} \frac{\partial S_m(t, x, y)}{\partial t} = & \gamma_{P, S_m} P(t, x, y) e^{-\beta_m P(t, x, y)} - \mu_A S_m(t, x, y) \\ & - ab_m I_h(t, x, y) S_m(t, x, y) + \frac{\partial}{\partial x} \left(D(x, y) \frac{\partial S_m}{\partial x} \right) \\ & + \frac{\partial}{\partial y} \left(D(x, y) \frac{\partial S_m}{\partial y} \right) \end{aligned} \quad (6.10)$$

$$\begin{aligned} \frac{\partial I_m(t, x, y)}{\partial t} = & ab_m I_h(t, x, y) S_m(t, x, y) - \mu_A I_m(t, x, y) \\ & + \frac{\partial}{\partial x} \left(D(x, y) \frac{\partial I_m}{\partial x} \right) + \frac{\partial}{\partial y} \left(D(x, y) \frac{\partial I_m}{\partial y} \right) \end{aligned} \quad (6.11)$$

6.4 Well-posedness of the Model

To simplify, we assume in this section that $D(x, y) = D$ constant. For $x \in \Omega, t > 0$, with initial datum $(E(0), L(0), P(0), S_m(0), I_m(0), S_h(0), I_h(0), R_h(0))$ and Neumann boundary condition $\partial E = \partial L = \partial P = \partial S_m = \partial I_m = \partial S_h = \partial I_h = \partial R_h = 0$ on $\partial\Omega$. Consider the system of mixed ODE and PDE below

$$E' = \alpha_m(S_m + I_m) - \gamma_{E, L} E - \mu_E E \quad (6.12)$$

$$L' = \gamma_{E, L} E - \gamma_{L, P} L - \mu_L L \quad (6.13)$$

$$P' = \gamma_{L, P} L - \gamma_{P, S_m} P - \mu_P P \quad (6.14)$$

$$\frac{\partial S_m}{\partial t} - D\Delta S_m = \gamma_{P, S_m} P e^{-\beta_m P} - \mu_A S_m - ab_m I_h S_m \quad (6.15)$$

$$\frac{\partial I_m}{\partial t} - D\Delta I_m = ab_m I_h S_m - \mu_A I_m \quad (6.16)$$

$$S_h' = \gamma_h R_h - ab_h I_m S_h \quad (6.17)$$

$$I_h' = ab_h I_m S_h - \sigma_h I_h \quad (6.18)$$

$$R_h' = \sigma_h I_h - \gamma_h R_h \quad (6.19)$$

Lemma 6.4.1. *If the solution of the system above exists, then it is of the form $(E, L, P, S_m, I_m, S_h, I_h, R_h)$ such that*

$$\begin{aligned}
 E &= e^{-(\gamma_{E,L} + \mu_E)t} E_0 + \alpha_m \int_0^t e^{-(\gamma_{E,L} + \mu_E)(t-s)} (S_m + I_m) ds \\
 L &= e^{-(\gamma_{L,P} + \mu_L)t} L_0 + \gamma_{E,L} \int_0^t e^{-(\gamma_{L,P} + \mu_L)(t-s)} E ds \\
 P &= e^{-(\gamma_{P,S_m} + \mu_P)t} P_0 + \gamma_{L,P} \int_0^t e^{-(\gamma_{P,S_m} + \mu_P)(t-s)} L ds \\
 S_m &= K(., t) S_{m,0} + \int_0^t K(., t - \Delta) (\gamma_{P,S_m} P e^{-\beta_m P} - ab_m I_h S_m) ds \\
 I_m &= K(., t) I_{m,0} + ab_m \int_0^t K(., t - \Delta) I_h S_m ds \\
 S_h &= S_{h,0} + \int_0^t (\gamma_h R_h - ab_h I_m S_h) ds \\
 I_h &= e^{-\sigma_h t} I_{h,0} + ab_h \int_0^t e^{-\sigma_h(t-s)} I_m S_h ds \\
 R_h &= e^{-\gamma_h t} R_{h,0} + \sigma_h \int_0^t e^{-\gamma_h(t-s)} I_h ds
 \end{aligned} \tag{6.20}$$

Proof. Rewriting equation (6.12) would give us

$$E' + (\gamma_{E,L} + \mu_E)E = \alpha_m(S_m + I_m).$$

Multiplying both side of the equation by the integrating factor $e^{\int (\gamma_{E,L} + \mu_E) dt} = e^{(\gamma_{E,L} + \mu_E)t}$ we will have

$$\frac{d}{dt} \left(e^{(\gamma_{E,L} + \mu_E)t} E \right) = e^{(\gamma_{E,L} + \mu_E)t} \alpha_m(S_m + I_m).$$

Hence, integrating both sides of the equation will give us

$$\begin{aligned}
 \int_0^t \frac{d}{ds} \left(e^{(\gamma_{E,L} + \mu_E)s} E \right) ds &= \int_0^t e^{(\gamma_{E,L} + \mu_E)s} \alpha_m(S_m + I_m) ds \\
 e^{(\gamma_{E,L} + \mu_E)t} E &= \alpha_m \int_0^t e^{(\gamma_{E,L} + \mu_E)s} (S_m + I_m) ds + Constant
 \end{aligned}$$

Note that for $t = 0$, we have $E(0) = E_0$. Thus, determining the *Constant* and solving for E , we get

$$E = e^{-(\gamma_{E,L} + \mu_E)t} E_0 + \alpha_m \int_0^t e^{-(\gamma_{E,L} + \mu_E)(t-s)} (S_m + I_m) ds.$$

Applying the same procedure for the ordinary differential equation in (6.13)-(6.19), we get

$$\begin{aligned}
L &= e^{-(\gamma_{L,P} + \mu_L)t} L_0 + \gamma_{E,L} \int_0^t e^{-(\gamma_{L,P} + \mu_L)(t-s)} E ds \\
P &= e^{-(\gamma_{P,S_m} + \mu_P)t} P_0 + \gamma_{L,P} \int_0^t e^{-(\gamma_{P,S_m} + \mu_P)(t-s)} L ds \\
S_h &= S_{h,0} + \int_0^t (\gamma_h R_h - ab_h I_m S_h) ds \\
I_h &= e^{-\sigma_h t} I_{h,0} + ab_h \int_0^t e^{-\sigma_h(t-s)} I_m S_h ds \\
R_h &= e^{-\gamma_h t} R_{h,0} + \sigma_h \int_0^t e^{-\gamma_h(t-s)} I_h ds
\end{aligned}$$

Now, for the partial differential equation (6.15) and (6.16), we have

$$\begin{aligned}
S'_m - D\Delta S_m &= \gamma_{P,S_m} P e^{-\beta_m P} - (\mu_A + ab_m I_h) S_m \\
I'_m - D\Delta I_m &= ab_m I_h S_m - \mu_A I_m
\end{aligned}$$

By Corollary 6.2.2, the solution of the reaction-diffusion problem above is

$$\begin{aligned}
S_m &= K(., t) S_{m,0} + \int_0^t K(., t-s) (\gamma_{P,S_m} P e^{-\beta_m P} - ab_m I_h S_m) ds \\
I_m &= K(., t) I_{m,0} + ab_m \int_0^t K(., t-s) I_h S_m ds
\end{aligned}$$

where K is the kernels defined as the solution of the diffusion equation with boundary conditions

$$\begin{aligned}
\frac{\partial K}{\partial t} - D\Delta K &= f & \text{for } x \in \Omega, t > 0 \\
K(x, 0) &= K_0
\end{aligned}$$

where $\int_{\mathbb{R}^d} K(t, x) dx = 1$. □

We will denote by Φ the right-hand side of equation (6.20), that is,

$$\Phi = (\Phi_E, \Phi_L, \Phi_P, \Phi_{S_m}, \Phi_{I_m}, \Phi_{S_h}, \Phi_{I_h}, \Phi_{R_h}).$$

Lemma 6.4.2. Let $U = (E, L, P, S_m, I_m, S_h, I_h, R_h)$ in B_T the ball defined by

$$B_T := \left\{ U \in L^\infty(\mathbb{R}_+, L^\infty(\Omega))^8 : \sup_{t \in [0, T]} \|U(t, \cdot) - U_0\|_{L^\infty(\Omega)} \leq r \right\}. \quad (6.21)$$

There exists a time $T > 0$ such that $\Phi(B_T) \subseteq B_T$.

Proof. • For egg:

$$\begin{aligned}
 |\Phi_E(U)(t, x) - E_0(x)| &\leq \left| \alpha_m \int_0^t e^{-(\gamma_{E,L} + \mu_E)(t-s)} (S_m(t, x) + I_m(t, x)) ds \right. \\
 &\quad \left. + e^{-(\gamma_{E,L} + \mu_E)t} E_0(x) - E_0(x) \right| \\
 &\leq \left| \alpha_m \int_0^t e^{-(\gamma_{E,L} + \mu_E)(t-s)} (S_m(t, x) + I_m(t, x)) ds \right. \\
 &\quad \left. + (e^{-(\gamma_{E,L} + \mu_E)t} - 1) E_0(x) \right|.
 \end{aligned}$$

Applying triangle inequality we get

$$\begin{aligned}
 |\Phi_E(U)(t, x) - E_0(x)| &\leq \alpha_m \left| \int_0^t e^{-(\gamma_{E,L} + \mu_E)(t-s)} (S_m(t, x) + I_m(t, x)) ds \right| \\
 &\quad + \left| e^{-(\gamma_{E,L} + \mu_E)t} - 1 \right| |E_0(x)|.
 \end{aligned}$$

Then,

$$\begin{aligned}
 \left| \int_0^t e^{-(\gamma_{E,L} + \mu_E)(t-s)} (S_m(t, x) + I_m(t, x)) ds \right| &\leq \left| \int_0^t \sup_{t \in [0, T]} (e^{-(\gamma_{E,L} + \mu_E)(t-s)} (S_m(t, x) + I_m(t, x))) ds \right| \\
 &\leq \sup_{t \in [0, T]} \left| e^{-(\gamma_{E,L} + \mu_E)(t-s)} (S_m(t, x) + I_m(t, x)) \right| \int_0^T ds \\
 &\leq T \sup_{t \in [0, T]} (|S_m(t, x)| + |I_m(t, x)|) \\
 &\leq T \left(\sup_{t \in [0, T]} |S_m(t, x)| + \sup_{t \in [0, T]} |I_m(t, x)| \right) \\
 &\leq T \left(\sup_{t \in [0, T]} |U(t, x)| + \sup_{t \in [0, T]} |U(t, x)| \right) \\
 &\leq 2T \sup_{t \in [0, T]} |U(t, x)|.
 \end{aligned}$$

Therefore, $|\Phi_E(U)(t, x) - E_0(x)|$ will become

$$\begin{aligned}
 |\Phi_E(U)(t, x) - E_0(x)| &\leq \alpha_m T \sup_{t \in [0, T]} (|S_m(t, x)| + |I_m(t, x)|) + |E_0(x)| \\
 &\leq 2\alpha_m T \sup_{t \in [0, T]} |U(t, x)| + |U_0(x)|
 \end{aligned}$$

Since $U \in B_T$,

$$\begin{aligned}
 \sup_{t \in [0, T]} |U(t, x)| &= \sup_{t \in [0, T]} |U(t, x) - U_0(x) + U_0(x)| \\
 &\leq \sup_{t \in [0, T]} |U(t, x) - U_0(x)| + |U_0(x)| \\
 &\leq r + ||U_0||
 \end{aligned} \tag{6.22}$$

Finally, we obtain

$$|\Phi_E(U)(t, x) - E_0(x)| \leq 2(r + \|U_0\|)\alpha_m T + \|U_0\|.$$

Choose $T \leq \frac{r - \|U_0\|}{2(r + \|U_0\|)\alpha_m}$. Thus,

$$\sup_{t \in [0, T]} \|\Phi_E(U)(t, \cdot) - E_0\|_{L^\infty} \leq r.$$

• For larvae:

$$\begin{aligned} |\Phi_L(U)(t, x) - L_0(x)| &\leq \left| \gamma_{E,L} \int_0^t e^{-(\gamma_{L,P} + \mu_L)(t-s)} E(t, x) ds + e^{-(\gamma_{L,P} + \mu_L)t} L_0(x) - L_0(x) \right| \\ &\leq \left| \gamma_{E,L} \int_0^t e^{-(\gamma_{L,P} + \mu_L)(t-s)} E(t, x) ds \right| + \left| \left(e^{-(\gamma_{L,P} + \mu_L)t} - 1 \right) L_0(x) \right| \\ &\leq \gamma_{E,L} \left| \int_0^t e^{-(\gamma_{L,P} + \mu_L)(t-s)} E(t, x) ds \right| + \left| \left(e^{-(\gamma_{L,P} + \mu_L)t} - 1 \right) |L_0(x)| \right| \end{aligned}$$

As before,

$$\begin{aligned} \left| \int_0^t e^{-(\gamma_{L,P} + \mu_L)(t-s)} E(t, x) ds \right| &\leq \left| \int_0^t \sup_{t \in [0, T]} \left(e^{-(\gamma_{L,P} + \mu_L)(t-s)} E(t, x) \right) ds \right| \\ &\leq T \sup_{t \in [0, T]} |E(t, x)| \\ &\leq T \sup_{t \in [0, T]} |U(t, x)| \end{aligned}$$

Therefore, by equation (6.22),

$$\begin{aligned} |\Phi_L(U)(t, x) - L_0(x)| &\leq \gamma_{E,L} T \sup_{t \in [0, T]} |U(t, x)| + |U_0(x)| \\ &\leq \gamma_{E,L} T(r + \|U_0\|) + \|U_0(x)\|. \end{aligned}$$

Choose $T \leq \frac{r - \|U_0\|}{\gamma_{E,L}(r + \|U_0\|)}$. Then,

$$\sup_{t \in [0, T]} \|\Phi_L(U)(t, \cdot) - L_0\|_{L^\infty} \leq r.$$

• For pupae:

$$\begin{aligned} |\Phi_P(U)(t, x) - P_0(x)| &\leq \left| \gamma_{L,P} \int_0^t e^{-(\gamma_{P,S_m} + \mu_P)(t-s)} L(t, x) ds + e^{-(\gamma_{P,S_m} + \mu_P)t} P_0(x) - P_0(x) \right| \\ &\leq \left| \gamma_{L,P} \int_0^t e^{-(\gamma_{P,S_m} + \mu_P)(t-s)} L(t, x) ds \right| + \left| \left(e^{-(\gamma_{P,S_m} + \mu_P)t} - 1 \right) P_0(x) \right| \\ &\leq \gamma_{L,P} \left| \int_0^t e^{-(\gamma_{P,S_m} + \mu_P)(t-s)} L(t, x) ds \right| + \left| e^{-(\gamma_{P,S_m} + \mu_P)t} - 1 \right| |P_0(x)| \end{aligned}$$

Therefore,

$$\begin{aligned} |\Phi_P(U)(t, x) - P_0(x)| &\leq \gamma_{L,P} T \sup_{t \in [0, T]} |U(t, x)| + |U_0(x)| \\ &\leq \gamma_{L,P} T (r + ||U_0||) + ||U_0(x)||. \end{aligned}$$

Choose $T \leq \frac{r - ||U_0||}{\gamma_{L,P}(r + ||U_0||)}$. Then,

$$\sup_{t \in [0, T]} ||\Phi_P(U)(t, \cdot) - P_0||_{L^\infty} \leq r.$$

- For susceptible human:

$$\begin{aligned} |\Phi_{S_h}(U)(t, x) - S_{h,0}(x)| &\leq \left| \int_0^t (\gamma_h R_h(t, x) - ab_h I_m(t, x) S_h(t, x)) ds \right| \\ &\leq \gamma_h \left| \int_0^t R_h(t, x) ds \right| + ab_h \left| \int_0^t I_m(t, x) S_h(t, x) ds \right| \\ &\leq \gamma_h \left| \int_0^t \sup_{t \in [0, T]} R_h(t, x) ds \right| + ab_h \left| \int_0^t \sup_{t \in [0, T]} I_m(t, x) S_h(t, x) ds \right| \\ &\leq \gamma_h T \sup_{t \in [0, T]} |R_h(t, x)| + ab_h T \sup_{t \in [0, T]} |I_m(t, x)| |S_h(t, x)| \\ &\leq \gamma_h T \sup_{t \in [0, T]} |U(t, x)| + ab_h T \sup_{t \in [0, T]} |U(t, x)|^2 \end{aligned}$$

Therefore, by equation (6.22), for all $x \in \Omega$ and $t \in [0, T]$,

$$|\Phi_{S_h}(U)(t, x) - S_{h,0}(x)| \leq \gamma_h T (r + ||U_0||) + ab_h T (r + ||U_0||)^2.$$

Choose $T \leq \frac{r}{[\gamma_h + ab_h(r + ||U_0||)](r + ||U_0||)}$. Thus,

$$\sup_{t \in [0, T]} ||\Phi_{S_h}(U)(t, \cdot) - S_{h,0}||_{L^\infty} \leq r.$$

- For infected human:

$$\begin{aligned} |\Phi_{I_h}(U)(t, x) - I_{h,0}(x)| &\leq \left| ab_h \int_0^t e^{-\sigma_h(t-s)} I_m(t, x) S_h(t, x) ds + e^{-\sigma_h t} I_{h,0}(x) - I_{h,0}(x) \right| \\ &\leq ab_h \left| \int_0^t e^{-\sigma_h(t-s)} I_m(t, x) S_h(t, x) ds \right| + |e^{-\sigma_h t} - 1| |I_{h,0}(x)| \end{aligned}$$

Note that,

$$\begin{aligned} \left| \int_0^t e^{-\sigma_h(t-s)} I_m(t, x) S_h(t, x) ds \right| &\leq \left| \int_0^t \sup_{t \in [0, T]} \left(e^{-\sigma_h(t-s)} I_m(t, x) S_h(t, x) \right) ds \right| \\ &\leq T \sup_{t \in [0, T]} |I_m(t, x)| |S_h(t, x)| \\ &\leq T \sup_{t \in [0, T]} |U(t, x)|^2 \end{aligned}$$

Therefore, by equation (6.22), $|\Phi_{I_h}(U)(t, x) - I_{h,0}(x)|$ will become

$$\begin{aligned} |\Phi_{I_h}(U)(t, x) - I_{h,0}(x)| &\leq ab_h T \sup_{t \in [0, T]} |U(t, x)|^2 + |U_0(x)| \\ &\leq ab_h T (r + \|U_0\|)^2 + \|U_0(x)\|. \end{aligned}$$

Choose $T \leq \frac{r - \|U_0\|}{ab_h(r + \|U_0\|)^2}$. Then for all x ,

$$\sup_{t \in [0, T]} \|\Phi_{I_h}(U)(t, \cdot) - I_{h,0}\|_{L^\infty} \leq r.$$

- For recovered human:

$$\begin{aligned} |\Phi_{R_h}(U)(t, x) - R_{h,0}(x)| &\leq \left| \sigma_h \int_0^t e^{-\gamma_h(t-s)} I_h(t, x) ds + e^{-\gamma_h t} R_{h,0}(x) - R_{h,0}(x) \right| \\ &\leq \sigma_h \left| \int_0^t e^{-\gamma_h(t-s)} I_h(t, x) ds \right| + |e^{-\gamma_h t} - 1| |R_{h,0}(x)| \\ &\leq \sigma_h T \sup_{t \in [0, T]} |U(t, x)| + |U_0(x)| \\ &\leq \sigma_h T (r + \|U_0\|) + \|U_0(x)\|. \end{aligned}$$

Choose $T \leq \frac{r - \|U_0\|}{\sigma_h(r + \|U_0\|)}$. Then for all x ,

$$\sup_{t \in [0, T]} \|\Phi_{R_h}(U)(t, \cdot) - R_{h,0}\|_{L^\infty} \leq r.$$

For the terms with diffusion, we have the following

- For susceptible mosquito:

Let $f(U) = \gamma_{P,S_m} P e^{-\beta_m P} - ab_m I_h S_m$. Then $f(U)$ is a Lipschitz function in B_T .

If U_1 and U_2 in B_T , then

$$\begin{aligned} f(U_1) - f(U_2) &= (\gamma_{P,S_m} P_1 e^{-\beta_m P_1} - ab_m I_{h,1} S_{m,1}) - (\gamma_{P,S_m} P_2 e^{-\beta_m P_2} - ab_m I_{h,2} S_{m,2}) \\ &= \gamma_{P,S_m} (P_1 - P_2) e^{-\beta_m P_1} + \gamma_{P,S_m} P_2 (e^{-\beta_m P_1} - e^{-\beta_m P_2}) - ab_m (I_{h,1} S_{m,1} - I_{h,2} S_{m,2}). \end{aligned}$$

Because $I_{h,1}S_{m,1} - I_{h,2}S_{m,2} = (I_{h,1} - I_{h,2})S_{m,1} + (S_{m,1} - S_{m,2})I_{h,2}$, and $e^{-\beta_m P}$ locally 1-Lipschitz, we have

$$\begin{aligned} \|f(U_1) - f(U_2)\| &\leq 2\gamma_{P,S_m}\|P_1 - P_2\| + ab_m(\|I_{h,1} - I_{h,2}\|\|S_{m,1}\| + \|S_{m,1} - S_{m,2}\|\|I_{h,2}\|) \\ &\leq 2\gamma_{P,S_m}\|U_1 - U_2\| + ab_m(\|S_{m,1}\| + \|I_{h,2}\|)\|U_1 - U_2\| \\ &\leq 2(\gamma_{P,S_m} + (r + \|U_0\|)ab_m)\|U_1 - U_2\|. \end{aligned}$$

According to [52], there exists a constant $C_\Omega > 0$, depending only on Ω , such that the kernel satisfies

$$\|K(\cdot, t)\|_{L^\infty(\Omega)} \leq C_\Omega.$$

Thus, for $x \in \Omega$

$$\begin{aligned} |\Phi(S_m)(t, x) - S_{m,0}(x)| &\leq \left| \int_\Omega K(x - y, t) S_{m,0}(y) dy \right| \\ &\quad + \left| \int_0^T \int_{\mathbb{R}^d} K(x - y, t - s) f(U)(s, y) dy ds \right| \\ &\leq C_\Omega \|S_{m,0}\|_{L^\infty(\Omega)} + C_\Omega T \left(\sup_{t \in [0, T]} \|f(U)(t, \cdot)\|_{L^\infty(\Omega)} \right) \\ &\leq C_\Omega \|U_0\| + 2(\gamma_{P,S_m} + (r + \|U_0\|)ab_m)C_\Omega T. \end{aligned}$$

Then

$$\|\Phi(S_m)(t, x) - S_{m,0}(x)\|_{L^\infty(\Omega)} \leq C_\Omega \|U_0\| + 2(\gamma_{P,S_m} + (r + \|U_0\|)ab_m)C_\Omega T.$$

Choose

$$C_\Omega \|U_0\| + 2(\gamma_{P,S_m} + (r + \|U_0\|)ab_m)C_\Omega T \leq r$$

where $T \leq \frac{r - C_\Omega \|U_0\|}{2(\gamma_{P,S_m} + (r + \|U_0\|)ab_m)C_\Omega}$. Then,

$$\sup_{t \in [0, T]} \|\Phi(S_m)(t, \cdot) - S_{m,0}\|_{L^\infty} \leq r.$$

- For infected mosquito:

Let $g(U) = I_h S_m$. Then $g(U)$ is a Lipschitz function in B_T . If U_1 and U_2 in B_T , then

$$\begin{aligned} g(U_1) - g(U_2) &= I_{h,1}S_{m,1} - I_{h,2}S_{m,2} \\ &= I_{h,1}S_{m,1} - I_{h,1}S_{m,2} + I_{h,1}S_{m,2} - I_{h,2}S_{m,2} \\ &= I_{h,1}(S_{m,1} - S_{m,2}) + S_{m,2}(I_{h,1} - I_{h,2}). \end{aligned}$$

Thus,

$$\begin{aligned}
||g(U_1) - g(U_2)|| &\leq \sup_{t \in [0, T]} |I_{h,1}| |S_{m,1} - S_{m,2}| + \sup_{t \in [0, T]} |S_{m,2}| |I_{h,1} - I_{h,2}| \\
&\leq \sup_{t \in [0, T]} |U(t, x)| |U_1(t, x) - U_1(t, x)| + \sup_{t \in [0, T]} |U(t, x)| |U_1(t, x) - U_1(t, x)| \\
&\leq 2 \sup_{t \in [0, T]} |U(t, x)| |U_1(t, x) - U_1(t, x)| \\
&\leq 2(r + ||U_0||) ||U_1 - U_2||.
\end{aligned}$$

- Similar to the susceptible mosquito, we have

$$\begin{aligned}
|\Phi(I_m)(t, \cdot) - I_{m,0}| &\leq C_\Omega ||I_{m,0}(\cdot)||_{L^\infty(\Omega)} + ab_m C_\Omega T \left(\sup_{t \in [0, T]} ||g(U)(t, \cdot)||_{L^\infty(\Omega)} \right) \\
&\leq C_\Omega ||U_0|| + ab_m C_\Omega T (2(r + ||U_0||)).
\end{aligned}$$

Then

$$||\Phi(I_m)(t, \cdot) - I_{m,0}||_{L^\infty(\Omega)} \leq C_\Omega ||U_0|| + ab_m C_\Omega T (2(r + ||U_0||)).$$

Choose

$$T \leq \frac{r - C_\Omega ||U_0||}{ab_m C_\Omega (2(r + ||U_0||))}.$$

Then for all x ,

$$\sup_{t \in [0, T]} ||\Phi(I_m)(t, x) - I_{m,0}(x)||_{L^\infty} \leq r.$$

Finally choosing $r = \max(2||U_0||, 2C_\Omega ||U_0||)$, and T smaller than the minimum between

$$\frac{1}{6\alpha_m}; \frac{1}{3\gamma_{E,L}}; \frac{1}{3\gamma_{L,P}}; \frac{2}{3\gamma_h + 9ab_h ||U_0||}; \frac{1}{9ab_h ||U_0||}; \frac{1}{3\sigma_h}; \frac{||U_0||}{(\gamma_{P,S_m} + 2(2C_\Omega + 1)||U_0||ab_m)}; \frac{1}{2ab_m(2C_\Omega + 1)}$$

implies that $\Phi(B_T) \subset B_T$. \square

Lemma 6.4.3. *There exists a time $T > 0$ such that the map Φ is a contraction map from B_T onto itself.*

Proof. Let U and \tilde{U} be in B_T .

- For the equation for eggs:

$$\begin{aligned}
|\Phi_E(U)(t) - \Phi_E(\tilde{U})(t)| &= \left| \alpha_m \int_0^t e^{-(\gamma_{E,L} + \mu_E)(t-s)} (S_m + I_m) ds \right. \\
&\quad \left. + \alpha_m \int_0^t e^{-(\gamma_{E,L} + \mu_E)(t-s)} (\widetilde{S}_m + \widetilde{I}_m) ds \right| \\
&\leq \alpha_m \left| \int_0^t e^{-(\gamma_{E,L} + \mu_E)(t-s)} \left((S_m - \widetilde{S}_m) + (I_m - \widetilde{I}_m) \right) ds \right|
\end{aligned}$$

Since $\left| e^{-(\gamma_{E,L} + \mu_E)t} \right| \leq 1$ for any time t from 0 to infinity, we have

$$\begin{aligned} |\Phi_E(U)(t) - \Phi_E(\tilde{U})(t)| &\leq \alpha_m T \sup_{t \in [0, T]} \|(S_m - \tilde{S}_m) + (I_m - \tilde{I}_m)\|_{L^\infty} \\ &\leq 2\alpha_m T \sup_{t \in [0, T]} \|U - \tilde{U}\|_{L^\infty}. \end{aligned}$$

Then, $\sup_t |\Phi_E(U)(t) - \Phi_E(\tilde{U})(t)| \leq 2\alpha_m T \sup_{t \in [0, T]} \|U - \tilde{U}\|_{L^\infty}$ which is contraction if $2\alpha_m T < 1$, i.e $T < \frac{1}{2\alpha_m}$.

- For the equation for larvae:

$$\begin{aligned} |\Phi_L(U)(t) - \Phi_L(\tilde{U})(t)| &= \left| \gamma_{E,L} \int_0^t e^{-(\gamma_{L,P} + \mu_L)(t-s)} E \, ds - \gamma_{E,L} \int_0^t e^{-(\gamma_{L,P} + \mu_L)(t-s)} \tilde{E} \, ds \right| \\ &= \gamma_{E,L} \left| \int_0^t e^{-(\gamma_{L,P} + \mu_L)(t-s)} (E - \tilde{E}) \, ds \right| \\ &\leq \gamma_{E,L} T \sup_{t \in [0, T]} \|E - \tilde{E}\|_{L^\infty} \\ &\leq \gamma_{E,L} T \sup_{t \in [0, T]} \|U - \tilde{U}\|_{L^\infty}. \end{aligned}$$

Then, $\sup_t |\Phi_L(U)(t) - \Phi_L(\tilde{U})(t)| \leq \gamma_{E,L} T \sup_{t \in [0, T]} \|U - \tilde{U}\|_{L^\infty}$ which is contraction if $T < \frac{1}{\gamma_{E,L}}$.

- For the equation for pupae:

$$\begin{aligned} |\Phi_P(U)(t) - \Phi_P(\tilde{U})(t)| &= \left| \gamma_{L,P} \int_0^t e^{-(\gamma_{P,S_m} + \mu_P)(t-s)} L \, ds - \gamma_{L,P} \int_0^t e^{-(\gamma_{P,S_m} + \mu_P)(t-s)} \tilde{L} \, ds \right| \\ &= \gamma_{L,P} \left| \int_0^t e^{-(\gamma_{P,S_m} + \mu_P)(t-s)} (L - \tilde{L}) \, ds \right| \\ &\leq \gamma_{L,P} T \sup_{t \in [0, T]} \|L - \tilde{L}\|_{L^\infty} \\ &\leq \gamma_{L,P} T \sup_{t \in [0, T]} \|U - \tilde{U}\|_{L^\infty}. \end{aligned}$$

Then, $\sup_t |\Phi_P(U)(t) - \Phi_P(\tilde{U})(t)| \leq \gamma_{L,P} T \sup_{t \in [0, T]} \|U - \tilde{U}\|_{L^\infty}$ which is contraction if $T < \frac{1}{\gamma_{L,P}}$.

- For the equation for susceptible humans:

$$\begin{aligned}
|\Phi_{S_h}(U)(t) - \Phi_{S_h}(\tilde{U})(t)| &= \left| \int_0^t (\gamma_h R_h - ab_h I_m S_h) ds - \int_0^t (\gamma_h \tilde{R}_h - ab_h \tilde{I}_m \tilde{S}_h) ds \right| \\
&= \left| \int_0^t \gamma_h (R_h - \tilde{R}_h) ds - \int_0^t ab_h (I_m S_h - \tilde{I}_m \tilde{S}_h) ds \right| \\
&\leq \gamma_h T \sup_{t \in [0, T]} \|R_h - \tilde{R}_h\| \\
&\quad + ab_h T \sup_{t \in [0, T]} \|I_m (S_h - \tilde{S}_h) + \tilde{S}_h (I_m - \tilde{I}_m)\| \\
&\leq \gamma_h T \sup_{t \in [0, T]} \|U - \tilde{U}\|_{L^\infty} \\
&\quad + ab_h T \left(\sup_{t \in [0, T]} \|U\|_{L^\infty} \|U - \tilde{U}\|_{L^\infty} + \sup_{t \in [0, T]} \|U\|_{L^\infty} \|U - \tilde{U}\|_{L^\infty} \right) \\
&\leq (\gamma_h T + 2ab_h T(r + \|U_0\|)) \sup_{t \in [0, T]} \|U - \tilde{U}\|_{L^\infty}.
\end{aligned}$$

Then, $\sup_t |\Phi_{S_h}(U)(t) - \Phi_{S_h}(\tilde{U})(t)| \leq (\gamma_h T + 2ab_h T(r + \|U_0\|)) \sup_{t \in [0, T]} \|U - \tilde{U}\|_{L^\infty}$ which is contraction if $T < \frac{1}{\gamma_h + 2ab_h(r + \|U_0\|)}$.

- For the equation for infected humans:

$$\begin{aligned}
|\Phi_{I_h}(U)(t) - \Phi_{I_h}(\tilde{U})(t)| &= \left| ab_h \int_0^t e^{-\sigma_h(t-s)} I_m S_h ds - ab_h \int_0^t e^{-\sigma_h(t-s)} \tilde{I}_m \tilde{S}_h ds \right| \\
&= ab_h \left| \int_0^t e^{-\sigma_h(t-s)} (I_m S_h - \tilde{I}_m \tilde{S}_h) ds \right| \\
&\leq ab_h T \sup_{t \in [0, T]} \|I_m (S_h - \tilde{S}_h) + \tilde{S}_h (I_m - \tilde{I}_m)\| \\
&\leq ab_h T \left(\sup_{t \in [0, T]} \|I_m\| \|S_h - \tilde{S}_h\| + \sup_{t \in [0, T]} \|\tilde{S}_h\| \|I_m - \tilde{I}_m\| \right) \\
&\leq ab_h T \left(\sup_{t \in [0, T]} \|U\|_{L^\infty} \|U - \tilde{U}\|_{L^\infty} + \sup_{t \in [0, T]} \|\tilde{U}\|_{L^\infty} \|U - \tilde{U}\|_{L^\infty} \right) \\
&\leq 2ab_h T \sup_{t \in [0, T]} \|U\|_{L^\infty} \|U - \tilde{U}\|_{L^\infty} \\
&\leq 2ab_h T(r + \|U_0\|) \sup_{t \in [0, T]} \|U - \tilde{U}\|_{L^\infty}.
\end{aligned}$$

Then $\sup_t |\Phi_{I_h}(U)(t) - \Phi_{I_h}(\tilde{U})(t)| \leq 2ab_h T(r + \|U_0\|) \sup_{t \in [0, T]} \|U - \tilde{U}\|_{L^\infty}$ which is contraction if $T < \frac{1}{2ab_h(r + \|U_0\|)}$.

- For the equation for recovered humans:

$$\begin{aligned}
|\Phi_{R_h}(U)(t) - \Phi_{R_h}(\tilde{U})(t)| &= \left| \sigma_h \int_0^t e^{-\gamma_h(t-s)} I_h ds - \sigma_h \int_0^t e^{-\gamma_h(t-s)} \tilde{I}_h ds \right| \\
&= \sigma_h \left| \int_0^t e^{-\gamma_h(t-s)} (I_h - \tilde{I}_h) ds \right| \\
&\leq \sigma_h T \sup_{t \in [0, T]} \|I_h - \tilde{I}_h\| \\
&\leq \sigma_h T \sup_{t \in [0, T]} \|U - \tilde{U}\|_{L^\infty}.
\end{aligned}$$

Then $\sup_t |\Phi_{R_h}(U)(t) - \Phi_{R_h}(\tilde{U})(t)| \leq \sigma_h T \sup_{t \in [0, T]} \|U - \tilde{U}\|_{L^\infty}$ which is contraction if $T < \frac{1}{\sigma_h}$.

- For the equation for susceptible mosquitoes:

$$\begin{aligned}
|\Phi_{S_m}(U)(t) - \Phi_{S_m}(\tilde{U})(t)| &= \left| \int_0^t K f(U) ds - \int_0^t K \star f(\tilde{U}) ds \right| \\
&= \left| \int_0^t K \star (f(U) - f(\tilde{U})) ds \right| \\
&\leq 2C_\Omega(\gamma_{P, S_m} + (r + \|U_0\|)ab_m) \sup_{t \in [0, T]} \|U - \tilde{U}\|_{L^\infty} \\
&\leq T \sup_{t \in [0, T]} \|U - \tilde{U}\|_{L^\infty}.
\end{aligned}$$

where $T < \frac{1}{2C_\Omega(\gamma_{P, S_m} + (r + \|U_0\|)ab_m)}$, which is a contraction mapping.

- For the equation for infected mosquitoes:

$$\begin{aligned}
|\Phi_{I_m}(U)(t) - \Phi_{I_m}(\tilde{U})(t)| &= \left| \int_0^t K \star g(U) ds - \int_0^t K \star g(\tilde{U}) ds \right| \\
&= \left| \int_0^t K \star (g(U) - g(\tilde{U})) ds \right| \\
&\leq C_\Omega(2(r + \|U_0\|)ab_m) \sup_{t \in [0, T]} \|U - \tilde{U}\|_{L^\infty} \\
&\leq T \sup_{t \in [0, T]} \|U - \tilde{U}\|_{L^\infty}.
\end{aligned}$$

where $T < \frac{1}{C_\Omega(2(r + \|U_0\|)ab_m)}$, which is a contraction mapping.

Therefore, $\sup_{t \in [0, T]} \|\Phi(U) - \Phi(\tilde{U})\| \leq K \|U - \tilde{U}\|$ with $K < 1$ if T is strictly smaller than the minimum of

$$\begin{aligned}
&\frac{1}{2\alpha_m}; \frac{1}{\gamma_{E, L}}; \frac{1}{\gamma_{L, P}}; \frac{1}{\gamma_h + 2ab_h(r + \|U_0\|)}; \frac{1}{2ab_h(r + \|U_0\|)}; \\
&\frac{1}{\sigma_h}; \frac{1}{C_\Omega(\gamma_{P, S_m} + 2(r + \|U_0\|)ab_m)}; \frac{1}{C_\Omega(2(r + \|U_0\|)ab_m)}.
\end{aligned}$$

□

Using the lemmas above, we can conclude that our system of equation is globally well-posed. We have the stated the theorem below.

Theorem 6.4.4. *Let $0 \leq S_{h,0}, I_{h,0}, R_{h,0} \leq H_0$ and $0 \leq E_0, L_0, P_0 \leq M_{Y,0}$, $0 \leq S_{m,0}, I_{m,0} \leq M_{A,0}$ where $H_0, M_{Y,0}$ and $M_{A,0}$ are the initial population density for human, young mosquito and adult mosquito population, respectively. Then there exists a unique global in time weak solution $(E, L, P, S_m, I_m, S_h, I_h, R_h) \in L^\infty(\mathbb{R}_+, L^\infty(\Omega))^8$, of the initial boundary value problem. Moreover, the solution is nonnegative, $S_h + I_h \leq H_0$ and $E + L + P \leq M_{Y,0}$, $S_m + I_m \leq M_{A,0}$.*

Proof. Combining Lemmas 6.4.1, 6.4.2 and 6.4.3, one can applied the Picard's fixed point theorem, which provides the local well-posedness. Positivity and boundedness of $E, L, P, S_m, I_m, S_h, I_h, R_h$ follows the one from the model without space (see Lemma 5.3.2). □

6.5 Optimal Control strategies : Copepods, Pesticides & Vaccination

Our aim in this section to minimize the number of infected humans by minimizing the control inputs. We attribute three control inputs, w_Y for the percentage of young mosquitoes exposed to copepods, w_A for the percentage of adult mosquitoes exposed to pesticides, w_H for the percentage of vaccinated susceptible humans. Furthermore, we assume that both control inputs are piece-wise continuous functions that takes its values in a positively bounded set $W = [0, w_{Y,max}] \times [0, w_{A,max}] \times [0, w_{H,max}]$.

Let $U = (E, L, P, S_m, I_m, S_h, I_h, R_h)$ and $w = (w_Y, w_A, w_H)$ be the control inputs. We consider the problem

$$\underset{w}{\text{minimize}} \mathcal{J}(U, w) \text{ where } \mathcal{J}(U, w) = \int_{\Omega} \int_0^T f(U, w, (x, t)) dt dX$$

such that

$$f(U, w, (x, t)) = I_h(x, t) + \frac{1}{2} A_Y w_Y^2(x, t) + \frac{1}{2} A_A w_A^2(x, t) + \frac{1}{2} A_H w_H^2(x, t),$$

subject to

$$\begin{aligned} h(U, \dot{U}, w, (x, t)) &= 0 \\ g(U(0), w) &= (E_0, L_0, P_0, S_{m,0}, I_{m,0}, S_{h,0}, I_{h,0}, R_{h,0}) \end{aligned}$$

where h is defined by

$$\frac{dE(x,t)}{dt} - \alpha_m(S_m(x,t) + I_m(x,t)) + \gamma_{E,L}E(x,t) + \mu_E E(x,t) = 0 \quad (6.23)$$

$$\frac{dL(x,t)}{dt} - \gamma_{E,L}E(x,t) + \gamma_{L,P}L(x,t) + \mu_L L(x,t) + w_Y L(x,t) = 0 \quad (6.24)$$

$$\frac{dP(x,t)}{dt} - \gamma_{L,P}L(x,t) + \gamma_{P,S_m}P(x,t) + \mu_P P(x,t) = 0 \quad (6.25)$$

$$\frac{\partial S_m(x,t)}{\partial t} - D\Delta S_m - \gamma_{P,S_m}P(x,t)e^{-\beta_m P(x,t)} + \mu_A S_m(x,t) + ab_m I_h(x,t)S_m(x,t) + w_A S_m(x,t) = 0 \quad (6.26)$$

$$\frac{\partial I_m(x,t)}{\partial t} - D\Delta I_m - ab_m I_h(x,t)S_m(x,t) + \mu_A I_m(x,t) + w_A I_m(x,t) = 0 \quad (6.27)$$

$$\frac{dS_h(x,t)}{dt} - \gamma_h R_h(x,t) + ab_h I_m(x,t)S_h(x,t) + w_H S_h(x,t) = 0 \quad (6.28)$$

$$\frac{dI_h(x,t)}{dt} - ab_h I_m(x,t)S_h(x,t) + \sigma_h I_h(x,t) = 0 \quad (6.29)$$

$$\frac{dR_h(x,t)}{dt} - \sigma_h I_h(x,t) + \gamma_h R_h(x,t) = 0. \quad (6.30)$$

with $\frac{\partial E}{\partial x} = \frac{\partial L}{\partial x} = \frac{\partial P}{\partial x} = \frac{\partial S_m}{\partial x} = \frac{\partial I_m}{\partial x} = \frac{\partial S_h}{\partial x} = \frac{\partial I_h}{\partial x} = \frac{\partial R_h}{\partial x} = 0$.

6.5.1 Derivation of the Optimal Control

Lemma 6.5.1. *There exists the adjoint variables $\lambda_i, i = 1, 2, \dots, 6$ that satisfy the following backward in time system of partial differential equations*

$$\begin{aligned} -\frac{d\lambda_1(x,t)}{dt} &= \lambda_1(x,t)\mu_E + (\lambda_1(x,t) - \lambda_2(x,t))\gamma_{E,L} \\ -\frac{d\lambda_2(x,t)}{dt} &= \lambda_2(x,t)(\mu_L + w_Y) + (\lambda_2(x,t) - \lambda_3(x,t))\gamma_{L,P} \\ -\frac{d\lambda_3(x,t)}{dt} &= \lambda_3(x,t)\mu_P + (\lambda_3(x,t) - \lambda_4(x,t))(1 - \beta_m P)e^{-\beta_m P}\gamma_{P,S_m} \\ -\frac{\partial \lambda_4(x,t)}{\partial t} - D\Delta \lambda_4 &= -\lambda_1(x,t)\alpha_m + \lambda_4(x,t)(\mu_A + w_A) + (\lambda_4(x,t) - \lambda_5(x,t))ab_m I_h(x,t) \\ -\frac{\partial \lambda_5(x,t)}{\partial t} - D\Delta \lambda_5 &= -\lambda_1(x,t)\alpha_m + \lambda_5(x,t)(\mu_A + w_A) + (\lambda_6(x,t) - \lambda_7(x,t))ab_h S_h(x,t) \\ -\frac{d\lambda_6(x,t)}{dt} &= \lambda_6(x,t)w_H + (\lambda_6(x,t) - \lambda_7(x,t))ab_h I_m(x,t) \\ -\frac{d\lambda_7(x,t)}{dt} &= 1 + (\lambda_7(x,t) - \lambda_8(x,t))\sigma_h + (\lambda_4(x,t) - \lambda_5(x,t))ab_m S_m(x,t) \\ -\frac{d\lambda_8(x,t)}{dt} &= (\lambda_8(x,t) - \lambda_6(x,t))\gamma_h \end{aligned} \quad (6.31)$$

with the transversality condition $\lambda^T(x, T) = 0$ and boundary conditions $\mu^T = \frac{\lambda^T(x, 0)h(U(x, 0))}{g(U(x, 0), w)}$

and $\frac{\partial \lambda(x,t)}{\partial x} \Big|_{\partial \Omega} = \frac{\partial U(x,t)}{\partial x} \Big|_{\partial \Omega} = 0$.

Proof. Consider the Lagrangian corresponding to the optimization problem:

$$\mathcal{L} \equiv \int_{\Omega} \int_0^T [f(U, w, (x, t) + \lambda^T h(U, \dot{U}, w, (x, t)))] dt dX + \int_{\Omega} \mu^T g(U(x, 0), w) dX$$

The vector of Lagrangian multiplier λ is a function of space and time, and μ is another vector of multipliers that are associated with the initial conditions. Then, we

have

$$\begin{aligned}\mathcal{L} = & \mathcal{J} + \int_{\Omega} \mu^T g(U(x,0), w) dX + \int_{\Omega} \int_0^T \left(\lambda_1(x,t)(6.23) + \lambda_2(x,t)(6.24) \right. \\ & + \lambda_3(x,t)(6.25) + \lambda_4(x,t)(6.26) + \lambda_5(x,t)(6.27) \\ & \left. + \lambda_6(x,t)(6.28) + \lambda_7(x,t)(6.29) + \lambda_8(x,t)(6.30) \right) dt dX.\end{aligned}$$

Computing one by one by integration by parts,

For the expression with $\int_{\Omega} \int_0^T \lambda_1(x,t)(6.23) dt dX$ we have

$$\begin{aligned}\int_{\Omega} \int_0^T \lambda_1(x,t)(6.23) dt dX &= \int_{\Omega} \int_0^T \lambda_1(x,t) \left(\frac{\partial E(x,t)}{\partial t} - \alpha_m(S_m(x,t) + I_m(x,t)) \right. \\ &\quad \left. + \gamma_{E,L}E(x,t) + \mu_E E(x,t) \right) dt dX \\ &= \int_{\Omega} \int_0^T \lambda_1(x,t) \left(\frac{\partial E(x,t)}{\partial t} \right) dt dX + \int_{\Omega} \int_0^T \lambda_1(x,t) \left(\mu_E E(x,t) \right. \\ &\quad \left. + \gamma_{E,L}E(x,t) - \alpha_m(S_m(x,t) + I_m(x,t)) \right) dt dX \\ &= \int_{\Omega} \left(\lambda_1(x,t)E(x,t) \Big|_0^T - \int_0^T E(x,t) \frac{\partial \lambda_1(x,t)}{\partial t} dt \right) dX \\ &\quad + \int_{\Omega} \int_0^T \lambda_1(x,t) \left(\mu_E E(x,t) \right. \\ &\quad \left. + \gamma_{E,L}E(x,t) - \alpha_m(S_m(x,t) + I_m(x,t)) \right) dt dX \\ &= \int_{\Omega} \left(\lambda_1(x,T)E(x,T) - \lambda_1(x,0)E(x,0) - \int_0^T E(x,t) \frac{\partial \lambda_1(x,t)}{\partial t} dt \right) dX \\ &\quad + \int_{\Omega} \int_0^T \lambda_1(x,t) \left(\mu_E E(x,t) + \gamma_{E,L}E(x,t) - \alpha_m(S_m(x,t) + I_m(x,t)) \right) dt dX\end{aligned}$$

By transversality condition $\lambda_1(x,T) = 0$, then we can have

$$\begin{aligned}\int_{\Omega} \int_0^T \lambda_1(x,t)(6.23) dt dX &= \int_{\Omega} \left(-\lambda_1(x,0)E(x,0) - \int_0^T E(x,t) \frac{\partial \lambda_1(x,t)}{\partial t} dt \right) dX \\ &\quad + \int_{\Omega} \int_0^T \lambda_1(x,t) \left(\mu_E E(x,t) + \gamma_{E,L}E(x,t) \right. \\ &\quad \left. - \alpha_m(S_m(x,t) + I_m(x,t)) \right) dt dX \\ &= - \int_{\Omega} \lambda_1(x,0)E(x,0) dX - \int_{\Omega} \int_0^T E(x,t) \frac{\partial \lambda_1(x,t)}{\partial t} dt dX \\ &\quad + \int_{\Omega} \int_0^T \lambda_1(x,t) \mu_E E(x,t) dt dX + \int_{\Omega} \int_0^T \lambda_1(x,t) \gamma_{E,L}E(x,t) dt dX \\ &\quad - \int_{\Omega} \int_0^T \lambda_1(x,t) \alpha_m(S_m(x,t) + I_m(x,t)) dt dX\end{aligned}$$

For the expression with $\int_{\Omega} \int_0^T \lambda_2(x, t) (6.24) dt dX$ we have

$$\begin{aligned}
\int_{\Omega} \int_0^T \lambda_2(x, t) (6.24) dt dX &= \int_{\Omega} \int_0^T \lambda_2(x, t) \left(\frac{\partial L(x, t)}{\partial t} - \gamma_{E,L} E(x, t) + \gamma_{L,P} L(x, t) \right. \\
&\quad \left. + \mu_L L(x, t) + w_Y L(x, t) \right) dt dX \\
&= \int_{\Omega} \int_0^T \lambda_2(x, t) \left(\frac{\partial L(x, t)}{\partial t} \right) dt dX - \int_{\Omega} \int_0^T \lambda_2(x, t) \gamma_{E,L} E(x, t) dt dX \\
&\quad + \int_{\Omega} \int_0^T \lambda_2(x, t) \gamma_{L,P} L(x, t) dt dX + \int_{\Omega} \int_0^T \lambda_2(x, t) \mu_L L(x, t) dt dX \\
&\quad + \int_{\Omega} \int_0^T \lambda_2(x, t) w_Y L(x, t) dt dX \\
&= - \int_{\Omega} \lambda_2(x, 0) L(x, 0) dX - \int_{\Omega} \int_0^T L(x, t) \frac{\partial \lambda_2(x, t)}{\partial t} dt dX \\
&\quad - \int_{\Omega} \int_0^T \lambda_2(x, t) \gamma_{E,L} E(x, t) dt dX + \int_{\Omega} \int_0^T \lambda_2(x, t) \gamma_{L,P} L(x, t) dt dX \\
&\quad + \int_{\Omega} \int_0^T \lambda_2(x, t) \mu_L L(x, t) dt dX + \int_{\Omega} \int_0^T \lambda_2(x, t) w_Y L(x, t) dt dX
\end{aligned}$$

For the expression with $\int_{\Omega} \int_0^T \lambda_3(x, t) (6.25) dt dX$ we have

$$\begin{aligned}
\int_{\Omega} \int_0^T \lambda_3(x, t) (6.25) dt dX &= \int_{\Omega} \int_0^T \lambda_3(x, t) \left(\frac{\partial P(x, t)}{\partial t} - \gamma_{L,P} L(x, t) \right. \\
&\quad \left. + \gamma_{P,S_m} P(x, t) + \mu_P P(x, t) \right) dt dX \\
&= \int_{\Omega} \int_0^T \lambda_3(x, t) \left(\frac{\partial P(x, t)}{\partial t} \right) dt dX - \int_{\Omega} \int_0^T \lambda_3(x, t) \gamma_{L,P} L(x, t) dt dX \\
&\quad + \int_{\Omega} \int_0^T \lambda_3(x, t) \gamma_{P,S_m} P(x, t) dt dX + \int_{\Omega} \int_0^T \lambda_3(x, t) \mu_P P(x, t) dt dX \\
&= - \int_{\Omega} \lambda_3(x, 0) P(x, 0) dX - \int_{\Omega} \int_0^T P(x, t) \frac{\partial \lambda_3(x, t)}{\partial t} dt dX \\
&\quad - \int_{\Omega} \int_0^T \lambda_3(x, t) \gamma_{L,P} L(x, t) dt dX \\
&\quad + \int_{\Omega} \int_0^T \lambda_3(x, t) \gamma_{P,S_m} P(x, t) dt dX + \int_{\Omega} \int_0^T \lambda_3(x, t) \mu_P P(x, t) dt dX
\end{aligned}$$

For the expression with $\int_{\Omega} \int_0^T \lambda_4(x, t) (6.26) dt dX$ we have

$$\begin{aligned}
\int_{\Omega} \int_0^T \lambda_4(x, t) (6.26) dt dX &= \int_{\Omega} \int_0^T \lambda_4(x, t) \left(\frac{\partial S_m(x, t)}{\partial t} - D\Delta S_m - \gamma_{P, S_m} P(x, t) e^{-\beta_m P(x, t)} + \mu_A S_m(x, t) \right. \\
&\quad \left. + ab_m I_h(x, t) S_m(x, t) + w_A S_m(x, t) \right) dt dX \\
&= \int_{\Omega} \int_0^T \lambda_4(x, t) \left(\frac{\partial S_m(x, t)}{\partial t} \right) dt dX - \int_{\Omega} \int_0^T \lambda_4(x, t) D\Delta S_m dt dX \\
&\quad - \int_{\Omega} \int_0^T \lambda_4(x, t) \gamma_{P, S_m} P(x, t) e^{-\beta_m P(x, t)} dt dX + \int_{\Omega} \int_0^T \lambda_4(x, t) \mu_A S_m(x, t) dt dX \\
&\quad + \int_{\Omega} \int_0^T \lambda_4(x, t) ab_m I_h(x, t) S_m(x, t) dt dX + \int_{\Omega} \int_0^T \lambda_4(x, t) w_A S_m(x, t) dt dX \\
&= - \int_{\Omega} \lambda_4(x, 0) S_m(x, 0) dX - \int_{\Omega} \int_0^T S_m(x, t) \frac{\partial \lambda_4(x, t)}{\partial t} dt dX \\
&\quad - \int_{\Omega} \int_0^T \lambda_4(x, t) D\Delta S_m dt dX \\
&\quad - \int_{\Omega} \int_0^T \lambda_4(x, t) \gamma_{P, S_m} P(x, t) e^{-\beta_m P(x, t)} dt dX + \int_{\Omega} \int_0^T \lambda_4(x, t) \mu_A S_m(x, t) dt dX \\
&\quad + \int_{\Omega} \int_0^T \lambda_4(x, t) ab_m I_h(x, t) S_m(x, t) dt dX + \int_{\Omega} \int_0^T \lambda_4(x, t) w_A S_m(x, t) dt dX
\end{aligned}$$

For the term with $\int_{\Omega} \int_0^T \lambda_4(x, t) D\Delta S_m dt dX$

$$\begin{aligned}
\int_{\Omega} \int_0^T \lambda_4(x, t) D\Delta S_m dt dX &= \int_{\Omega} \int_0^T \lambda_4(x, t) D \frac{\partial^2}{\partial x^2} S_m dt dX \\
&= \int_0^T \left(\int_{\Omega} \lambda_4(x, t) D \frac{\partial}{\partial x} \left(\frac{\partial S_m}{\partial x} \right) dX \right) dt
\end{aligned}$$

By integration by parts with respect to space, we have

$$\begin{aligned}
\int_{\Omega} \int_0^T \lambda_4(x, t) D\Delta S_m dt dX &= \int_0^T \left(\lambda_4(x, t) D \frac{\partial S_m}{\partial x} \Big|_{\Omega} - \int_{\Omega} \left(\frac{\partial \lambda_4(x, t) D}{\partial x} \right) \frac{\partial S_m}{\partial x} dX \right) dt \\
&= \int_0^T \left(\lambda_4(x, t) D \frac{\partial S_m}{\partial x} \Big|_{\Omega} - \frac{\partial \lambda_4(x, t) D}{\partial x} S_m \Big|_{\Omega} \right. \\
&\quad \left. + \int_{\Omega} S_m \frac{\partial}{\partial x} \left(\frac{\partial \lambda_4(x, t) D}{\partial x} \right) dX \right) dt \\
&= \int_0^T \left(\lambda_4(x, t) \frac{\partial S_m(x, t)}{\partial x} \Big|_{\Omega} - \frac{\partial \lambda_4(x, t)}{\partial x} S_m(x, t) \Big|_{\Omega} \right) D dt \\
&\quad + \int_0^T \int_{\Omega} S_m D \Delta \lambda_4 dX dt
\end{aligned}$$

Since our equation satisfies the Neumann boundary condition, we have

$$\int_{\Omega} \int_0^T \lambda_4(x, t) D\Delta S_m dt dX = \int_0^T \int_{\Omega} S_m D \Delta \lambda_4 dX dt.$$

Therefore, for the expression with $\int_{\Omega} \int_0^T \lambda_4(x, t) (6.26) dt dX$ we have

$$\begin{aligned} \int_{\Omega} \int_0^T \lambda_4(x, t) (6.26) dt dX &= - \int_{\Omega} \lambda_4(x, 0) S_m(x, 0) dX - \int_{\Omega} \int_0^T S_m(x, t) \frac{\partial \lambda_4(x, t)}{\partial t} dt dX \\ &\quad - \int_{\Omega} \int_0^T S_m D \Delta \lambda_4 dt dX - \int_{\Omega} \int_0^T \lambda_4(x, t) \gamma_{P, S_m} P(x, t) e^{-\beta_m P(x, t)} dt dX \\ &\quad + \int_{\Omega} \int_0^T \lambda_4(x, t) \mu_A S_m(x, t) dt dX \\ &\quad + \int_{\Omega} \int_0^T \lambda_4(x, t) ab_m I_h(x, t) S_m(x, t) dt dX \\ &\quad + \int_{\Omega} \int_0^T \lambda_4(x, t) w_A S_m(x, t) dt dX \end{aligned}$$

For the expression with $\int_{\Omega} \int_0^T \lambda_5(x, t) (6.27) dt dX$ we have

$$\begin{aligned} \int_{\Omega} \int_0^T \lambda_5(x, t) (6.27) dt dX &= \int_{\Omega} \int_0^T \lambda_5(x, t) \left(\frac{\partial I_m(x, t)}{\partial t} - D \Delta I_m - ab_m I_h(x, t) S_m(x, t) \right. \\ &\quad \left. + \mu_A I_m(x, t) + w_A I_m(x, t) \right) dt dX \\ &= \int_{\Omega} \int_0^T \lambda_5(x, t) \left(\frac{\partial I_m(x, t)}{\partial t} \right) dt dX - \int_{\Omega} \int_0^T \lambda_5(x, t) D \Delta I_m dt dX \\ &\quad - \int_{\Omega} \int_0^T \lambda_5(x, t) ab_m I_h(x, t) S_m(x, t) dt dX \\ &\quad + \int_{\Omega} \int_0^T \lambda_5(x, t) \mu_A I_m(x, t) dt dX \\ &\quad + \int_{\Omega} \int_0^T \lambda_5(x, t) w_A I_m(x, t) dt dX \\ &= - \int_{\Omega} \lambda_5(x, 0) I_m(x, 0) dX - \int_{\Omega} \int_0^T I_m(x, t) \frac{\partial \lambda_5(x, t)}{\partial t} dt dX \\ &\quad - \int_{\Omega} \int_0^T I_m D \Delta \lambda_5 dt dX \\ &\quad - \int_{\Omega} \int_0^T \lambda_5(x, t) ab_m I_h(x, t) S_m(x, t) dt dX \\ &\quad + \int_{\Omega} \int_0^T \lambda_5(x, t) \mu_A I_m(x, t) dt dX \\ &\quad + \int_{\Omega} \int_0^T \lambda_5(x, t) w_A I_m(x, t) dt dX \end{aligned}$$

For the expression with $\int_{\Omega} \int_0^T \lambda_6(x, t) (6.28) dt dX$ we have

$$\begin{aligned}
 \int_{\Omega} \int_0^T \lambda_6(x, t) (6.28) dt dX &= \int_{\Omega} \int_0^T \lambda_6(x, t) \left(\frac{\partial S_h(x, t)}{\partial t} - \gamma_h R_h(x, t) + ab_h I_m(x, t) S_h(x, t) \right. \\
 &\quad \left. + w_H S_h(x, t) \right) dt dX \\
 &= \int_{\Omega} \int_0^T \lambda_6(x, t) \left(\frac{\partial S_h(x, t)}{\partial t} \right) dt dX - \int_{\Omega} \int_0^T \lambda_6(x, t) \gamma_h R_h(x, t) dt dX \\
 &\quad + \int_{\Omega} \int_0^T \lambda_6(x, t) ab_h I_m(x, t) S_h(x, t) dt dX \\
 &\quad + \int_{\Omega} \int_0^T \lambda_6(x, t) w_H S_h(x, t) dt dX \\
 &= - \int_{\Omega} \lambda_6(x, 0) S_h(x, 0) dX - \int_{\Omega} \int_0^T S_h(x, t) \frac{\partial \lambda_6(x, t)}{\partial t} dt dX \\
 &\quad - \int_{\Omega} \int_0^T \lambda_6(x, t) \gamma_h R_h(x, t) dt dX \\
 &\quad + \int_{\Omega} \int_0^T \lambda_6(x, t) ab_h I_m(x, t) S_h(x, t) dt dX \\
 &\quad + \int_{\Omega} \int_0^T \lambda_6(x, t) w_H S_h(x, t) dt dX
 \end{aligned}$$

For the expression with $\int_{\Omega} \int_0^T \lambda_7(x, t) (6.29) dt dX$ we have

$$\begin{aligned}
 \int_{\Omega} \int_0^T \lambda_7(x, t) (6.29) dt dX &= \int_{\Omega} \int_0^T \lambda_7(x, t) \left(\frac{\partial I_h(x, t)}{\partial t} - ab_h I_m(x, t) S_h(x, t) + \sigma_h I_h(x, t) \right) dt dX \\
 &= \int_{\Omega} \int_0^T \lambda_7(x, t) \left(\frac{\partial I_h(x, t)}{\partial t} \right) dt dX \\
 &\quad - \int_{\Omega} \int_0^T \lambda_7(x, t) ab_h I_m(x, t) S_h(x, t) dt dX \\
 &\quad + \int_{\Omega} \int_0^T \lambda_7(x, t) \sigma_h I_h(x, t) dt dX \\
 &= - \int_{\Omega} \lambda_7(x, 0) I_h(x, 0) dX - \int_{\Omega} \int_0^T I_h(x, t) \frac{\partial \lambda_7(x, t)}{\partial t} dt dX \\
 &\quad - \int_{\Omega} \int_0^T \lambda_7(x, t) ab_h I_m(x, t) S_h(x, t) dt dX \\
 &\quad + \int_{\Omega} \int_0^T \lambda_7(x, t) \sigma_h I_h(x, t) dt dX
 \end{aligned}$$

For the expression with $\int_{\Omega} \int_0^T \lambda_8(x, t) (6.30) dt dX$ we have

$$\begin{aligned}
 \int_{\Omega} \int_0^T \lambda_8(x, t) (6.30) dt dX &= \int_{\Omega} \int_0^T \lambda_8(x, t) \left(\frac{\partial R_h(x, t)}{\partial t} - \sigma_h I_h(x, t) + \gamma_h R_h(x, t) \right) dt dX \\
 &= \int_{\Omega} \int_0^T \lambda_8(x, t) \left(\frac{\partial R_h(x, t)}{\partial t} \right) dt dX - \int_{\Omega} \int_0^T \lambda_8(x, t) \sigma_h I_h(x, t) dt dX \\
 &\quad + \int_{\Omega} \int_0^T \lambda_8(x, t) \gamma_h R_h(x, t) dt dX \\
 &= - \int_{\Omega} \lambda_8(x, 0) R_h(x, 0) dX - \int_{\Omega} \int_0^T R_h(x, t) \frac{\partial \lambda_8(x, t)}{\partial t} dt dX \\
 &\quad - \int_{\Omega} \int_0^T \lambda_8(x, t) \sigma_h I_h(x, t) dt dX \\
 &\quad + \int_{\Omega} \int_0^T \lambda_8(x, t) \gamma_h R_h(x, t) dt dX
 \end{aligned}$$

Therefore, combining the results gives us

$$\begin{aligned}
\mathcal{L} &= \mathcal{J} + \int_{\Omega} \mu^T g(U(x,0), w) dX + \int_{\Omega} \int_0^T \left(\lambda_1(x,t)(6.23) + \lambda_2(x,t)(6.24) \right. \\
&\quad + \lambda_3(x,t)(6.25) + \lambda_4(x,t)(6.26) + \lambda_5(x,t)(6.27) \\
&\quad \left. + \lambda_6(x,t)(6.28) + \lambda_7(x,t)(6.29) + \lambda_8(x,t)(6.30) \right) dt dX \\
&= \mathcal{J} + \int_{\Omega} \mu^T g(U(0), w) dX \\
&\quad - \int_{\Omega} \lambda_1(x,0) E(x,0) dX - \int_{\Omega} \int_0^T E(x,t) \frac{\partial \lambda_1(x,t)}{\partial t} dt dX \\
&\quad + \int_{\Omega} \int_0^T \lambda_1(x,t) \mu_E E(x,t) dt dX + \int_{\Omega} \int_0^T \lambda_1(x,t) \gamma_{E,L} E(x,t) dt dX \\
&\quad - \int_{\Omega} \int_0^T \lambda_1(x,t) \alpha_m (S_m(x,t) + I_m(x,t)) dt dX \\
&\quad - \int_{\Omega} \lambda_2(x,0) L(x,0) dX - \int_{\Omega} \int_0^T L(x,t) \frac{\partial \lambda_2(x,t)}{\partial t} dt dX \\
&\quad - \int_{\Omega} \int_0^T \lambda_2(x,t) \gamma_{E,L} E(x,t) dt dX + \int_{\Omega} \int_0^T \lambda_2(x,t) \gamma_{L,P} L(x,t) dt dX \\
&\quad + \int_{\Omega} \int_0^T \lambda_2(x,t) \mu_L L(x,t) dt dX + \int_{\Omega} \int_0^T \lambda_2(x,t) w_Y L(x,t) dt dX \\
&\quad - \int_{\Omega} \lambda_3(x,0) P(x,0) dX - \int_{\Omega} \int_0^T P(x,t) \frac{\partial \lambda_3(x,t)}{\partial t} dt dX - \int_{\Omega} \int_0^T \lambda_3(x,t) \gamma_{L,P} L(x,t) dt dX \\
&\quad + \int_{\Omega} \int_0^T \lambda_3(x,t) \gamma_{P,S_m} P(x,t) dt dX + \int_{\Omega} \int_0^T \lambda_3(x,t) \mu_P P(x,t) dt dX \\
&\quad - \int_{\Omega} \lambda_4(x,0) S_m(x,0) dX - \int_{\Omega} \int_0^T S_m(x,t) \frac{\partial \lambda_4(x,t)}{\partial t} dt dX - \int_{\Omega} \int_0^T S_m D \Delta \lambda_4 dt dX \\
&\quad - \int_{\Omega} \int_0^T \lambda_4(x,t) \gamma_{P,S_m} P(x,t) e^{-\beta_m P(x,t)} dt dX + \int_{\Omega} \int_0^T \lambda_4(x,t) \mu_A S_m(x,t) dt dX \\
&\quad + \int_{\Omega} \int_0^T \lambda_4(x,t) ab_m I_h(x,t) S_m(x,t) dt dX + \int_{\Omega} \int_0^T \lambda_4(x,t) w_A S_m(x,t) dt dX \\
&\quad - \int_{\Omega} \lambda_5(x,0) I_m(x,0) dX - \int_{\Omega} \int_0^T I_m(x,t) \frac{\partial \lambda_5(x,t)}{\partial t} dt dX - \int_{\Omega} \int_0^T I_m D \Delta \lambda_5 dt dX \\
&\quad - \int_{\Omega} \int_0^T \lambda_5(x,t) ab_m I_h(x,t) S_m(x,t) dt dX + \int_{\Omega} \int_0^T \lambda_5(x,t) \mu_A I_m(x,t) dt dX \\
&\quad + \int_{\Omega} \int_0^T \lambda_5(x,t) w_A I_m(x,t) dt dX \\
&\quad - \int_{\Omega} \lambda_6(x,0) S_h(x,0) dX - \int_{\Omega} \int_0^T S_h(x,t) \frac{\partial \lambda_6(x,t)}{\partial t} dt dX - \int_{\Omega} \int_0^T \lambda_6(x,t) \gamma_h R_h(x,t) dt dX \\
&\quad + \int_{\Omega} \int_0^T \lambda_6(x,t) ab_h I_m(x,t) S_h(x,t) dt dX + \int_{\Omega} \int_0^T \lambda_6(x,t) w_H S_h(x,t) dt dX \\
&\quad - \int_{\Omega} \lambda_7(x,0) I_h(x,0) dX - \int_{\Omega} \int_0^T I_h(x,t) \frac{\partial \lambda_7(x,t)}{\partial t} dt dX \\
&\quad - \int_{\Omega} \int_0^T \lambda_7(x,t) ab_h I_m(x,t) S_h(x,t) dt dX + \int_{\Omega} \int_0^T \lambda_7(x,t) \sigma_h I_h(x,t) dt dX \\
&\quad - \int_{\Omega} \lambda_8(x,0) R_h(x,0) dX - \int_{\Omega} \int_0^T R_h(x,t) \frac{\partial \lambda_8(x,t)}{\partial t} dt dX - \int_{\Omega} \int_0^T \lambda_8(x,t) \sigma_h I_h(x,t) dt dX \\
&\quad + \int_{\Omega} \int_0^T \lambda_8(x,t) \gamma_h R_h(x,t) dt dX
\end{aligned}$$

Now, combining like terms, we have

$$\begin{aligned}
\mathcal{L} = & \int_{\Omega} \int_0^T \left(I_h(x, t) + \frac{1}{2} A_Y w_Y^2(x, t) + \frac{1}{2} A_A w_A^2(x, t) + \frac{1}{2} A_H w_H^2(x, t) \right) dt dX + \int_{\Omega} \mu^T g(U(x, 0), w) dX \\
& - \int_{\Omega} \lambda_1(x, 0) E(x, 0) dX - \int_{\Omega} \lambda_2(x, 0) L(x, 0) dX - \int_{\Omega} \lambda_3(x, 0) P(x, 0) dX - \int_{\Omega} \lambda_4(x, 0) S_m(x, 0) dX \\
& - \int_{\Omega} \lambda_5(x, 0) I_m(x, 0) dX - \int_{\Omega} \lambda_6(x, 0) S_h(x, 0) dX - \int_{\Omega} \lambda_7(x, 0) I_h(x, 0) dX - \int_{\Omega} \lambda_8(x, 0) R_h(x, 0) dX \\
& - \int_{\Omega} \int_0^T E(x, t) \frac{\partial \lambda_1(x, t)}{\partial t} dt dX + \int_{\Omega} \int_0^T \lambda_1(x, t) \mu_E E(x, t) dt dX \\
& + \int_{\Omega} \int_0^T \lambda_1(x, t) \gamma_{E,L} E(x, t) dt dX - \int_{\Omega} \int_0^T \lambda_2(x, t) \gamma_{E,L} E(x, t) dt dX \\
& - \int_{\Omega} \int_0^T L(x, t) \frac{\partial \lambda_2(x, t)}{\partial t} dt dX + \int_{\Omega} \int_0^T \lambda_2(x, t) \mu_L L(x, t) dt dX + \int_{\Omega} \int_0^T \lambda_2(x, t) w_Y L(x, t) dt dX \\
& + \int_{\Omega} \int_0^T \lambda_2(x, t) \gamma_{L,P} L(x, t) dt dX - \int_{\Omega} \int_0^T \lambda_3(x, t) \gamma_{L,P} L(x, t) dt dX \\
& - \int_{\Omega} \int_0^T P(x, t) \frac{\partial \lambda_3(x, t)}{\partial t} dt dX + \int_{\Omega} \int_0^T \lambda_3(x, t) \mu_P P(x, t) dt dX \\
& + \int_{\Omega} \int_0^T \lambda_3(x, t) \gamma_{P,S_m} P(x, t) dt dX - \int_{\Omega} \int_0^T \lambda_4(x, t) \gamma_{P,S_m} P(x, t) e^{-\beta_m P(x,t)} dt dX \\
& - \int_{\Omega} \int_0^T S_m(x, t) \frac{\partial \lambda_4(x, t)}{\partial t} dt dX - \int_{\Omega} \int_0^T S_m D \Delta \lambda_4 dt dX \\
& - \int_{\Omega} \int_0^T \lambda_1(x, t) \alpha_m S_m(x, t) dt dX + \int_{\Omega} \int_0^T \lambda_4(x, t) \mu_A S_m(x, t) dt dX + \int_{\Omega} \int_0^T \lambda_4(x, t) w_A S_m(x, t) dt dX \\
& + \int_{\Omega} \int_0^T \lambda_4(x, t) ab_m I_h(x, t) S_m(x, t) dt dX - \int_{\Omega} \int_0^T \lambda_5(x, t) ab_m I_h(x, t) S_m(x, t) dt dX \\
& - \int_{\Omega} \int_0^T I_m(x, t) \frac{\partial \lambda_5(x, t)}{\partial t} dt dX - \int_{\Omega} \int_0^T I_m D \Delta \lambda_5 dt dX \\
& - \int_{\Omega} \int_0^T \lambda_1(x, t) \alpha_m I_m(x, t) dt dX + \int_{\Omega} \int_0^T \lambda_5(x, t) \mu_A I_m(x, t) dt dX + \int_{\Omega} \int_0^T \lambda_5(x, t) w_A I_m(x, t) dt dX \\
& + \int_{\Omega} \int_0^T \lambda_6(x, t) ab_h I_m(x, t) S_h(x, t) dt dX - \int_{\Omega} \int_0^T \lambda_7(x, t) ab_h I_m(x, t) S_h(x, t) dt dX \\
& - \int_{\Omega} \int_0^T S_h(x, t) \frac{\partial \lambda_6(x, t)}{\partial t} dt dX + \int_{\Omega} \int_0^T \lambda_6(x, t) w_H S_h(x, t) dt dX \\
& - \int_{\Omega} \int_0^T I_h(x, t) \frac{\partial \lambda_7(x, t)}{\partial t} dt dX + \int_{\Omega} \int_0^T \lambda_7(x, t) \sigma_h I_h(x, t) dt dX - \int_{\Omega} \int_0^T \lambda_8(x, t) \sigma_h I_h(x, t) dt dX \\
& - \int_{\Omega} \int_0^T R_h(x, t) \frac{\partial \lambda_8(x, t)}{\partial t} dt dX + \int_{\Omega} \int_0^T \lambda_8(x, t) \gamma_h R_h(x, t) dt dX - \int_{\Omega} \int_0^T \lambda_6(x, t) \gamma_h R_h(x, t) dt dX
\end{aligned}$$

Factoring out the common terms give us

$$\begin{aligned}
\mathcal{L} = & \int_{\Omega} \int_0^T \left(\frac{1}{2} A_Y w_Y^2(x, t) + \frac{1}{2} A_A w_A^2(x, t) + \frac{1}{2} A_H w_H^2(x, t) \right) dt dX + \int_{\Omega} \mu^T g(U(x, 0), w) dX - \int_{\Omega} \lambda(x, 0) U(x, 0) dX \\
& + \int_{\Omega} \int_0^T \left(-\frac{\partial \lambda_1(x, t)}{\partial t} + \lambda_1(x, t) \mu_E + (\lambda_1(x, t) - \lambda_2(x, t)) \gamma_{E,L} \right) E(x, t) dt dX \\
& + \int_{\Omega} \int_0^T \left(-\frac{\partial \lambda_2(x, t)}{\partial t} + \lambda_2(x, t) (\mu_L + w_Y) + (\lambda_2(x, t) - \lambda_3(x, t)) \gamma_{L,P} \right) L(x, t) dt dX \\
& + \int_{\Omega} \int_0^T \left(-\frac{\partial \lambda_3(x, t)}{\partial t} + \lambda_3(x, t) \mu_P + (\lambda_3(x, t) - \lambda_4(x, t)) e^{-\beta_m P(x, t)} \gamma_{P,S_m} \right) P(x, t) dt dX \\
& + \int_{\Omega} \int_0^T \left(-\frac{\partial \lambda_4(x, t)}{\partial t} - D \Delta \lambda_4 - \lambda_1(x, t) \alpha_m + \lambda_4(x, t) (\mu_A + w_A) \right) S_m(x, t) dt dX \\
& + \int_{\Omega} \int_0^T \lambda_4(x, t) a b_m I_h(x, t) S_m(x, t) dt dX - \int_{\Omega} \int_0^T \lambda_5(x, t) a b_m I_h(x, t) S_m(x, t) dt dX \\
& + \int_{\Omega} \int_0^T \left(-\frac{\partial \lambda_5(x, t)}{\partial t} - D \Delta \lambda_5 - \lambda_1(x, t) \alpha_m + \lambda_5(x, t) (\mu_A + w_A) \right) I_m(x, t) dt dX \\
& + \int_{\Omega} \int_0^T \lambda_6(x, t) a b_h I_m(x, t) S_h(x, t) dt dX - \int_{\Omega} \int_0^T \lambda_7(x, t) a b_h I_m(x, t) S_h(x, t) dt dX \\
& + \int_{\Omega} \int_0^T \left(-\frac{\partial \lambda_6(x, t)}{\partial t} + \lambda_6(x, t) w_H \right) S_h(x, t) dt dX \\
& + \int_{\Omega} \int_0^T \left(-\frac{\partial \lambda_7(x, t)}{\partial t} + 1 + (\lambda_7(x, t) - \lambda_8(x, t)) \sigma_h \right) I_h(x, t) dt dX \\
& + \int_{\Omega} \int_0^T \left(-\frac{\partial \lambda_8(x, t)}{\partial t} + (\lambda_8(x, t) - \lambda_6(x, t)) \gamma_h \right) R_h(x, t) dt dX.
\end{aligned}$$

Since the total derivative of \mathcal{L} is equal to zero at the minimum, i.e.,

$$d\mathcal{L} = \frac{\partial \mathcal{L}}{\partial w} \cdot \partial w + \frac{\partial \mathcal{L}}{\partial U} \cdot \partial U = 0$$

we have the partial derivative of \mathcal{L} with respect to U ,

$$\begin{aligned}
\frac{\partial \mathcal{L}}{\partial E} &= -\frac{\partial \lambda_1(x, t)}{\partial t} + \lambda_1(x, t) \mu_E + (\lambda_1(x, t) - \lambda_2(x, t)) \gamma_{E,L} \\
\frac{\partial \mathcal{L}}{\partial L} &= -\frac{\partial \lambda_2(x, t)}{\partial t} + \lambda_2(x, t) (\mu_L + w_Y) + (\lambda_2(x, t) - \lambda_3(x, t)) \gamma_{L,P} \\
\frac{\partial \mathcal{L}}{\partial P} &= -\frac{\partial \lambda_3(x, t)}{\partial t} + \lambda_3(x, t) \mu_P + (\lambda_3(x, t) - \lambda_4(x, t)) (1 - \beta_m P(x, t)) e^{-\beta_m P} \gamma_{P,S_m} \\
\frac{\partial \mathcal{L}}{\partial S_m} &= -\frac{\partial \lambda_4(x, t)}{\partial t} - D \Delta \lambda_5 - \lambda_1(x, t) \alpha_m + \lambda_4(x, t) (\mu_A + w_A) + (\lambda_4(x, t) - \lambda_5(x, t)) a b_m I_h(x, t) \\
\frac{\partial \mathcal{L}}{\partial I_m} &= -\frac{\partial \lambda_5(x, t)}{\partial t} - D \Delta \lambda_5 - \lambda_1(x, t) \alpha_m + \lambda_5(x, t) (\mu_A + w_A) + (\lambda_6(x, t) - \lambda_7(x, t)) a b_h S_h(x, t) \\
\frac{\partial \mathcal{L}}{\partial S_h} &= -\frac{\partial \lambda_6(x, t)}{\partial t} + \lambda_6(x, t) w_H + (\lambda_6(x, t) - \lambda_7(x, t)) a b_h I_m(x, t) \\
\frac{\partial \mathcal{L}}{\partial I_h} &= -\frac{\partial \lambda_7(x, t)}{\partial t} + 1 + (\lambda_7(x, t) - \lambda_8(x, t)) \sigma_h + (\lambda_4(x, t) - \lambda_5(x, t)) a b_m S_m(x, t) \\
\frac{\partial \mathcal{L}}{\partial R_h} &= -\frac{\partial \lambda_8(x, t)}{\partial t} + (\lambda_8(x, t) - \lambda_6(x, t)) \gamma_h
\end{aligned}$$

Therefore, the adjoint system is defined by

$$\begin{aligned}
\frac{\partial \lambda_1(x, t)}{\partial t} &= \lambda_1(x, t)\mu_E + (\lambda_1(x, t) - \lambda_2(x, t))\gamma_{E,L} \\
\frac{\partial \lambda_2(x, t)}{\partial t} &= \lambda_2(x, t)(\mu_L + w_Y) + (\lambda_2(x, t) - \lambda_3(x, t))\gamma_{L,P} \\
\frac{\partial \lambda_3(x, t)}{\partial t} &= \lambda_3(x, t)\mu_P + (\lambda_3(x, t) - \lambda_4(x, t)(1 - \beta_m P(x, t))e^{-\beta_m P(x, t)})\gamma_{P,S_m} \\
\frac{\partial \lambda_4(x, t)}{\partial t} - D\Delta\lambda_4 &= -\lambda_1(x, t)\alpha_m + \lambda_4(x, t)(\mu_A + w_A) + (\lambda_4(x, t) - \lambda_5(x, t))ab_m I_h(x, t) \\
\frac{\partial \lambda_5(x, t)}{\partial t} - D\Delta\lambda_5 &= -\lambda_1(x, t)\alpha_m + \lambda_5(x, t)(\mu_A + w_A) + (\lambda_6(x, t) - \lambda_7(x, t))ab_h S_h(x, t) \\
\frac{\partial \lambda_6(x, t)}{\partial t} &= \lambda_6(x, t)w_H + (\lambda_6(x, t) - \lambda_7(x, t))ab_h I_m(x, t) \\
\frac{\partial \lambda_7(x, t)}{\partial t} &= 1 + (\lambda_7(x, t) - \lambda_8(x, t))\sigma_h + (\lambda_4(x, t) - \lambda_5(x, t))ab_m S_m(x, t) \\
\frac{\partial \lambda_8(x, t)}{\partial t} &= (\lambda_8(x, t) - \lambda_6(x, t))\gamma_h.
\end{aligned}$$

□

Theorem 6.5.2. *The optimal control variable w^* is defined as*

$$\begin{aligned}
w_Y^*(t) &= \max\left(0, \min\left(\frac{\lambda_2 L}{-A_Y}, w_{Y,max}\right)\right) \\
w_A^*(t) &= \max\left(0, \min\left(\frac{(\lambda_4 I_h + \lambda_5 S_h)}{-A_A}, w_{A,max}\right)\right) \\
w_H^*(t) &= \max\left(0, \min\left(\frac{\lambda_6 S_h}{-A_H}, w_{H,max}\right)\right).
\end{aligned}$$

Proof. The partial derivative of \mathcal{L} with respect to w is written

$$\begin{aligned}
\frac{\partial \mathcal{L}}{\partial w_Y} &= A_Y w_Y(x, t) + \lambda_2(x, t)L(x, t) \\
\frac{\partial \mathcal{L}}{\partial w_A} &= A_A w_A(x, t) + \lambda_4(x, t)S_m(x, t) + \lambda_5(x, t)I_m(x, t) \\
\frac{\partial \mathcal{L}}{\partial w_H} &= A_H w_H(x, t) + \lambda_6(x, t)S_h(x, t).
\end{aligned}$$

Furthermore, almost everywhere in Ω , we have

$$\begin{aligned}
A_Y w_Y + \lambda_2 L &= 0 & A_A w_A + \lambda_4 S_m + \lambda_5 I_m &= 0 & A_H w_H + \lambda_6 S_h &= 0 \\
w_Y &= \frac{\lambda_2 L}{-A_Y} & w_A &= \frac{\lambda_4 S_m + \lambda_5 I_m}{-A_A} & w_H &= \frac{\lambda_6 S_h}{-A_H}.
\end{aligned}$$

Finally,

$$\begin{aligned} w_Y^*(t) &= \max \left(0, \min \left(\frac{\lambda_2 L}{-A_Y}, w_{Y,max} \right) \right) \\ w_A^*(t) &= \max \left(0, \min \left(\frac{\lambda_4 S_m + \lambda_5 I_m}{-A_A}, w_{A,max} \right) \right) \\ w_H^*(t) &= \max \left(0, \min \left(\frac{\lambda_6 S_h}{-A_H}, w_{H,max} \right) \right). \end{aligned}$$

□

6.5.2 Numerical Simulation of the Model with one laying site

This section shows the numerical simulations of the model above in minimizing the infected human by applying three control strategies: vector control by copepode and pesticide and vaccination for human.

The control weights A_Y and A_A are the efforts in insecticide administration for mosquito population while A_H is the effort to vaccinate susceptible humans. Since adult mosquitoes are readily available in the population, the efforts used in controlling them would be simpler than the effort exerted for controlling young mosquitoes and vaccinating the susceptible humans. Thus, A_Y, A_H are set smaller than A_M . Hence, we initially set the control weights as $A_M = 10$, $A_Y = 1$ and $A_H = 1$. Note that the values of A_M, A_Y, A_H do not change the convergence of optimal control.

The optimality of the system is numerically solved using Algorithm 3 with $\epsilon = 0.01$.

Algorithm 3 Computation of optimal control of dengue model with spatial distribution

Given $U_0 = (10000, 500, 100, 10000, 1000, 1000, 10, 0)$ as initial datum, a final time $T = 50$, a domain $[-200, 200]$ and a tolerance $\epsilon > 0$.

Let $w_{Y,0}, w_{A,0}, w_{H,0}$ randomly chosen following $\mathcal{N}(0, 1)$.

while $||\nabla \mathcal{L}(w, U, \lambda)|| > \epsilon$ **do**,

 solve the forward system U ,

 solve the backward system λ ,

 update w

 solve the gradient $\nabla \mathcal{L}(w, U, \lambda)$

$w^* = w^n$.

Explicit Euler finite differences are used to numerically solve the direct and the adjoint system of ordinary differential equations and partial differential equations.

The simulations were carried out using $D_{min} = 0.1$, $\alpha = 0.01$ and $\beta = 0.1$ the as values for the diffusion coefficients. Parameters are summarized in the table below.

Parameters	Description	Value	Source
α_m	Oviposition	1 day^{-1}	[13]
$\gamma_{E,L}$	Transformation from egg to larva	$0.330000 \text{ day}^{-1}$	[13]
$\gamma_{L,P}$	Transformation from larvae to pupa	$0.140000 \text{ day}^{-1}$	[13]
γ_{P,S_m}	Transformation from pupa to adult mosquito	$0.346000 \text{ day}^{-1}$	[13]
μ_E	Mortality rates of egg	$0.050000 \text{ day}^{-1}$	[13]
μ_L	Mortality rates of larva	$0.050000 \text{ day}^{-1}$	[13]
μ_P	Mortality rates of pupa	$0.016700 \text{ day}^{-1}$	[13]
μ_A	Mortality rates of mosquito	$0.042000 \text{ day}^{-1}$	[13]
γ_h	Rate of decline in human immunity to disease	$0.575000 \text{ day}^{-1}$	[43]
σ_h	Rate of cure for disease	$0.328833 \text{ day}^{-1}$	[43]
ab_m	Probability of susceptible mosquitoes to be infectious	$0.375000 \text{ day}^{-1}$	[43]
ab_h	Probability of susceptible humans to be infected	$0.750000 \text{ day}^{-1}$	[43]
$w_{Y,max}$	upper bound of young mosquitoes exposed to copepods	23.96	[53]
$w_{A,max}$	upper bound of adult mosquitoes exposed to fogging	0.65	[47]
$w_{H,max}$	upper bound of vaccinated susceptible humans	0.8	[35, 64]

TABLE 6.2: Value of the Parameters used for the simulations.

The initial configuration follows Figure 6.2. The spatial domain is $[-200, 200]$. The laying site is located at the center with a width of 20. Adult mosquitoes are initially located between -100 and 100 . Humans are everywhere except on the laying site.

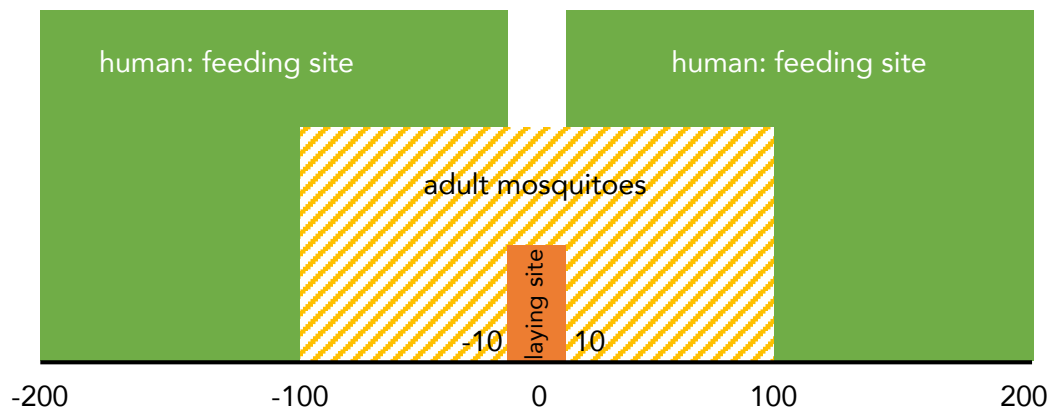


FIGURE 6.2: Initial configuration made of one laying site.

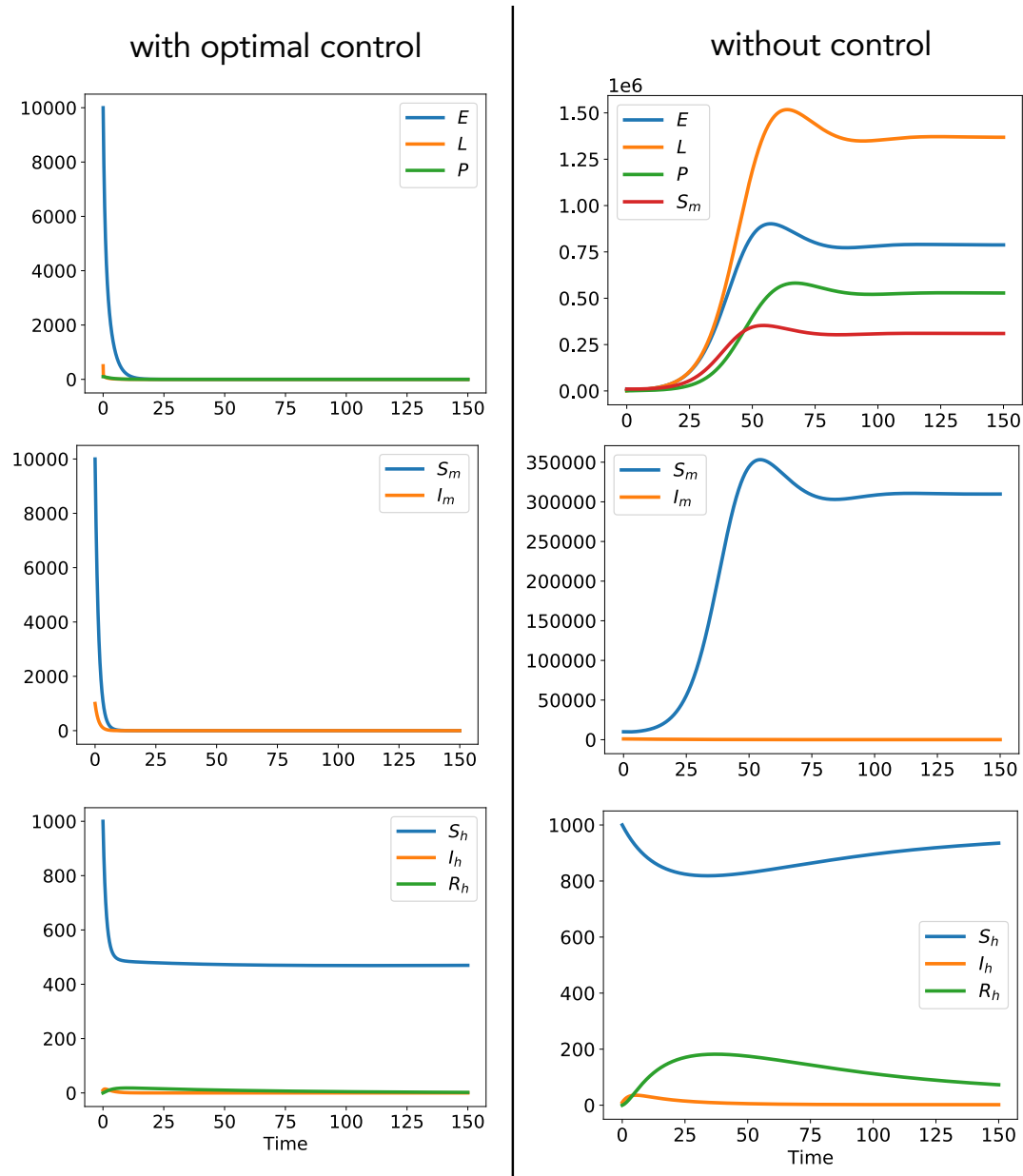


FIGURE 6.3: Behavior of each variables in the model with spatial distribution with three control inputs (left) and without control inputs (right).

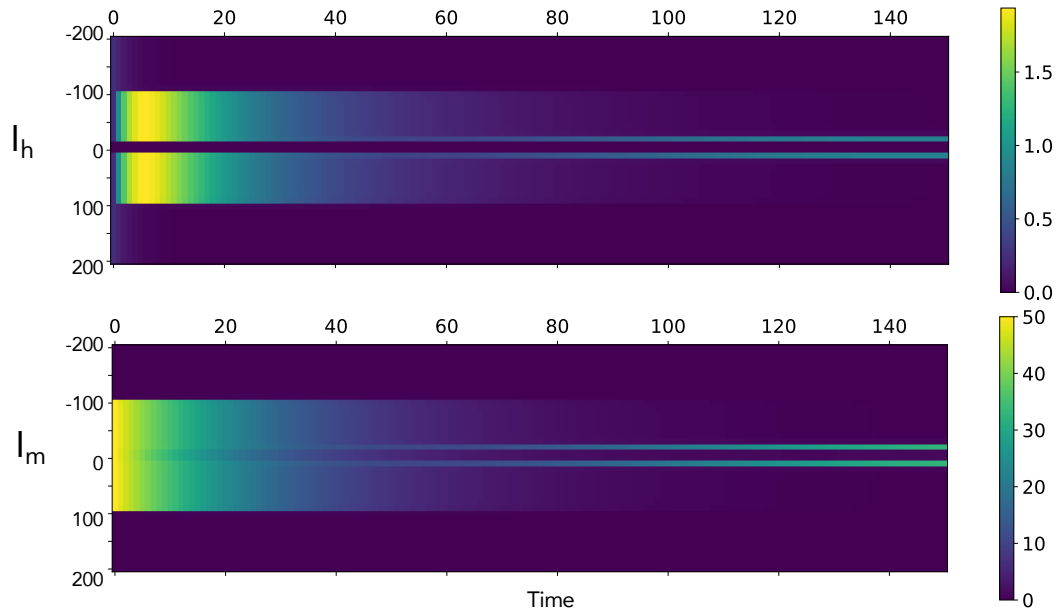
Figure 6.3 shows the comparison of the behavior of each variables in the model with diffusion using 3 control inputs and without control input. It clearly shows that having control strategy is better than no control at all.

For the young mosquito compartments (upper figures of Figure 6.3), we can see that with the control inputs, specifically the copepod application w_Y^* , there is a rapid decrease in each population for a short time towards equilibrium. Whereas without control, each population increases faster and shows no sign of decrease. With no predator for larvae, the figure shows that larvae increase faster than egg and pupae. Similarly, for adult mosquito compartments (middle figures of Figure 6.3), since pesticide administration affects both susceptible and infected mosquitoes, the figure shows that with the control inputs, both populations decrease exponentially over a short period.

The human compartment (bottom figure of Figure 6.3) shows that the application of control strategies effectively minimizes infected humans. It increases for at least ten days and then decreases exponentially towards zero.

Figure 6.4 shows the spatiotemporal evolution of infectious humans and mosquitoes with and without control. The figure shows that without control inputs, we need to apply the control strategy for a long time and then decrease it. However, decreasing the control strategy's efforts does not mean stopping its application. The figure shows that we must continuously apply the control strategy near the laying sites. Consequently, with the three control inputs, we only need to apply the control strategy for a short period and eventually stop it in more or less 20 days.

without control



with optimal control

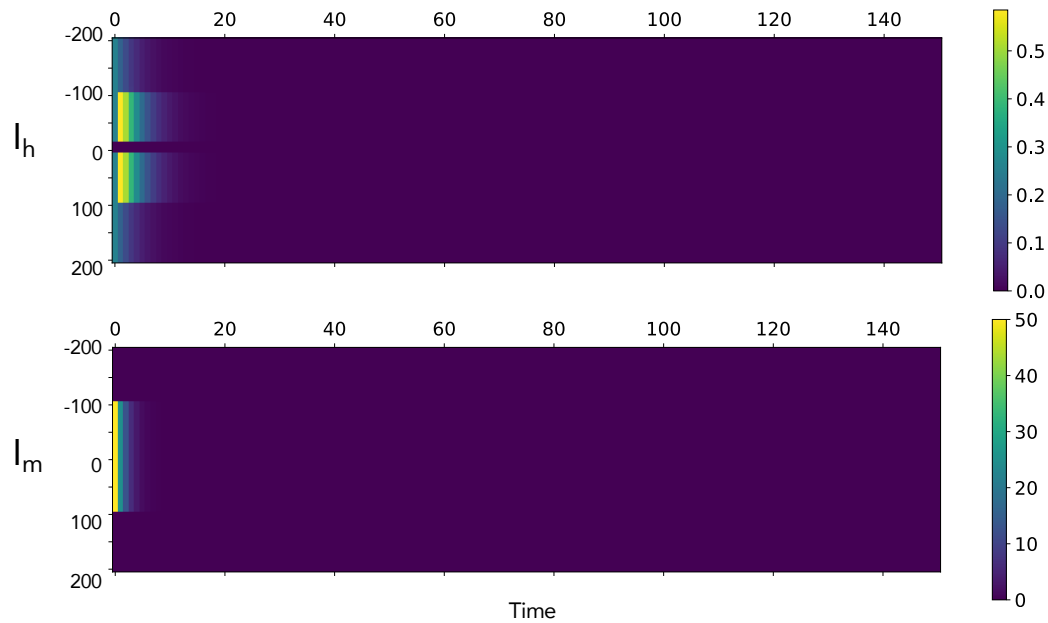


FIGURE 6.4: Spatiotemporal evolution of the infected human I_h and infectious mosquitoes I_m without control (top) and with optimal control (down).

Figure 6.5 shows the spatiotemporal evolution of each optimal control variable of the model with three control inputs. It shows that we need to administer copepod continuously for 45 days while lowering pesticide application and vaccination over time. However, the figure shows that we need to continuously apply the pesticide and vaccination near the laying sites unfadingly.

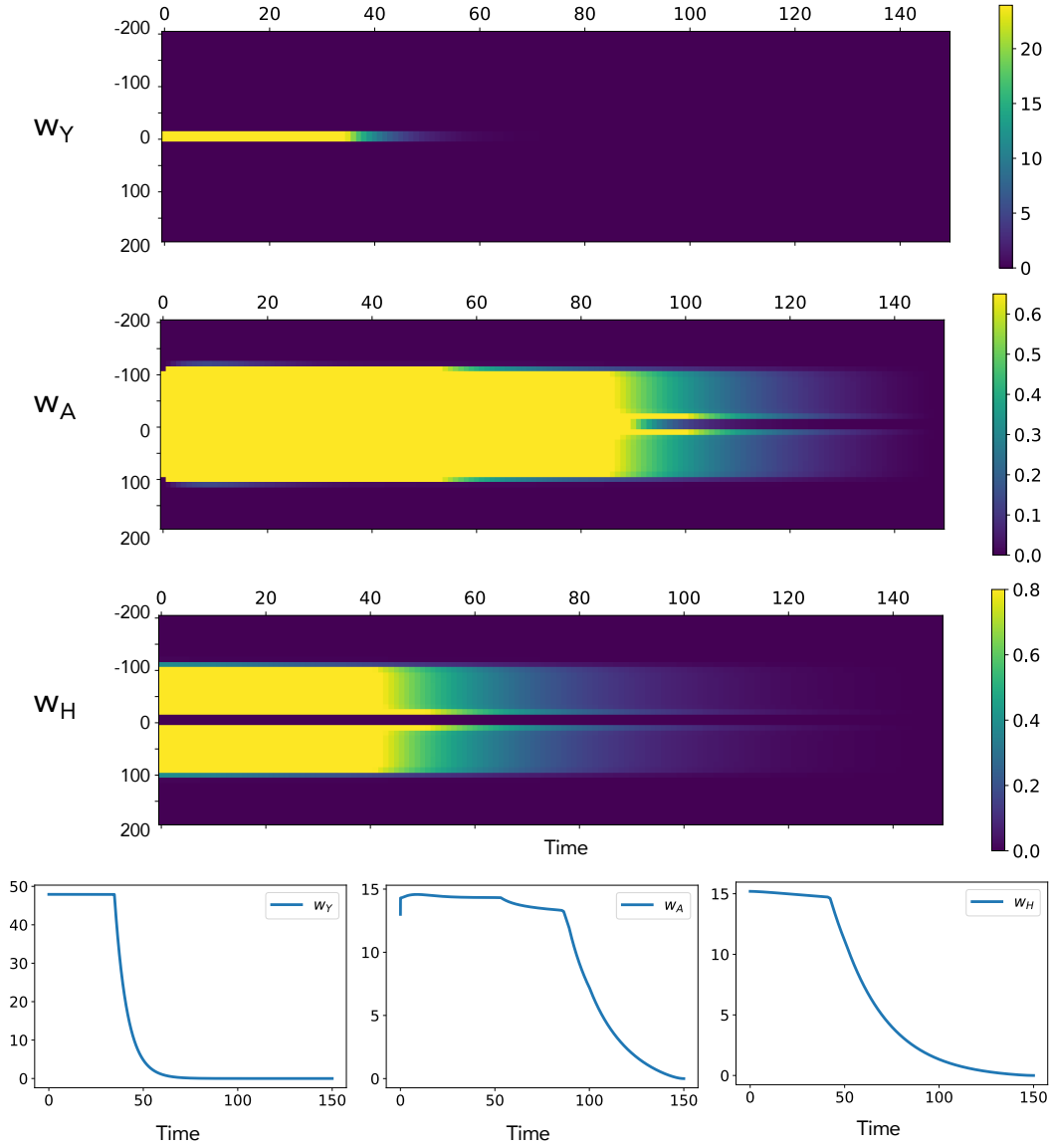


FIGURE 6.5: Spatiotemporal evolution of the optimal control variables w_Y, w_A, w_H of the model (top) and its sum in space (down).

6.5.3 Numerical Simulation of the Model with Spatial Distribution having Two Laying Sites

In this section, we consider a numerical simulation with 2 laying sites. We assumed that mosquitoes would prefer the nearest laying site to its position. The initial configuration follows Figure 6.6. The spatial domain is $[-200, 200]$. The laying sites are located between $[-50, -30]$ and $[30, 50]$. Adult mosquitoes are initially located between -100 and 100 . Humans are everywhere except on the laying site.

Using Algorithm 3, we get the following behavior of each variables in the system.

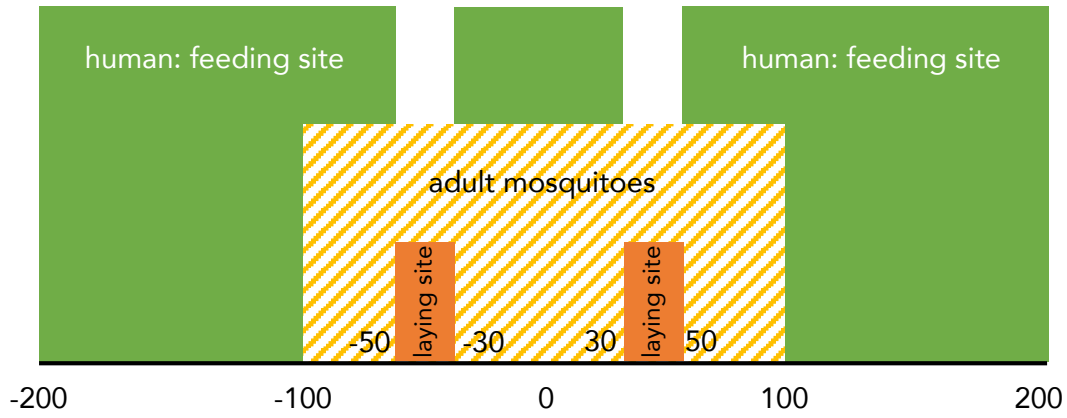


FIGURE 6.6: Initial configuration made of two laying sites.

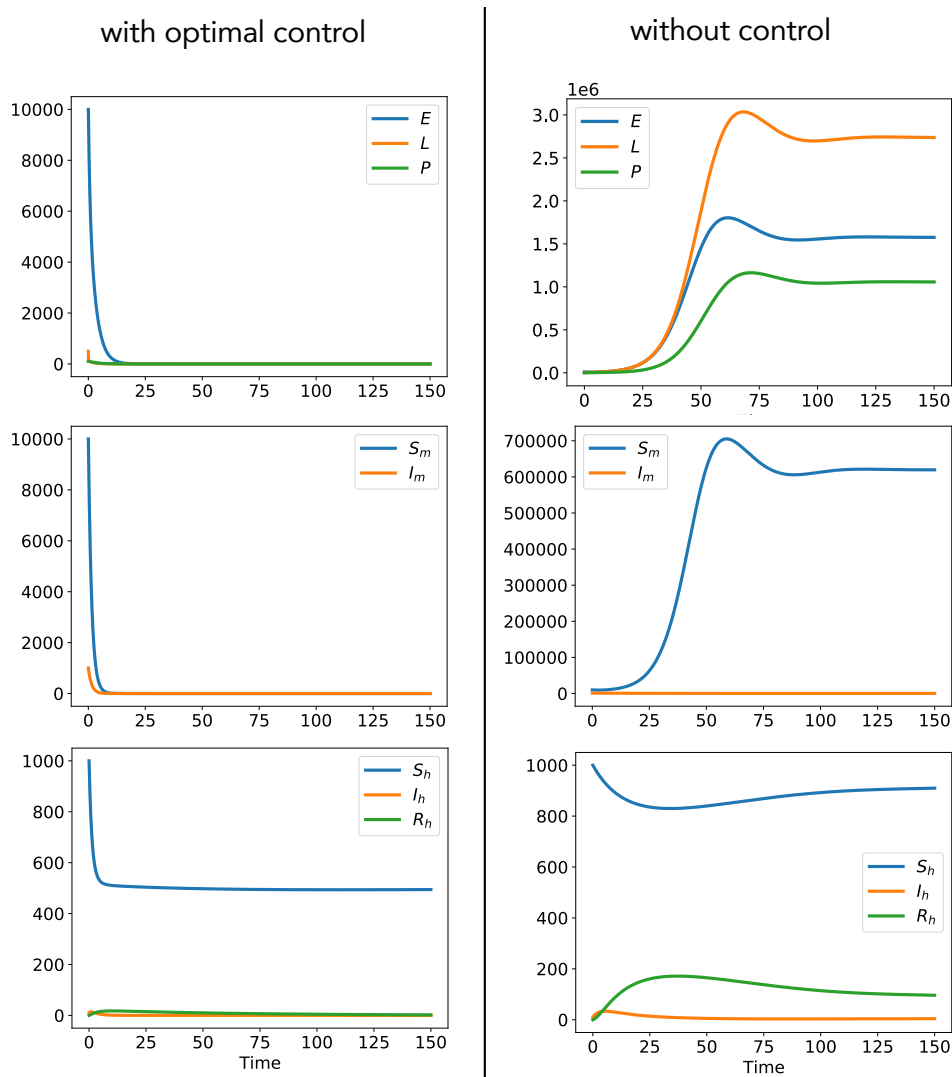
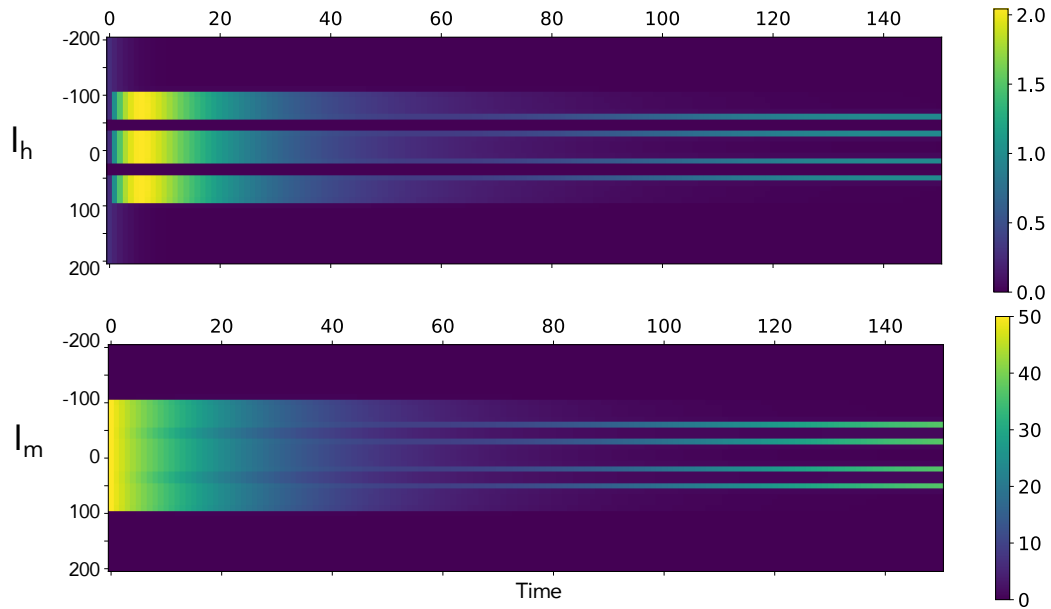


FIGURE 6.7: Behavior of each variables in the model with spatial distribution with three control inputs (left) and without control inputs (right).

Figure 6.7 shows that we get a relatively similar graph as the left Figure 6.3. As observed, due to the increase of carrying capacity of mosquitoes laying site, the

susceptible mosquitoes increases after the tenth day. But due to the application of the three control strategy, an increase in susceptible mosquitoes does not affect the infected mosquitoes.

without control



with optimal control

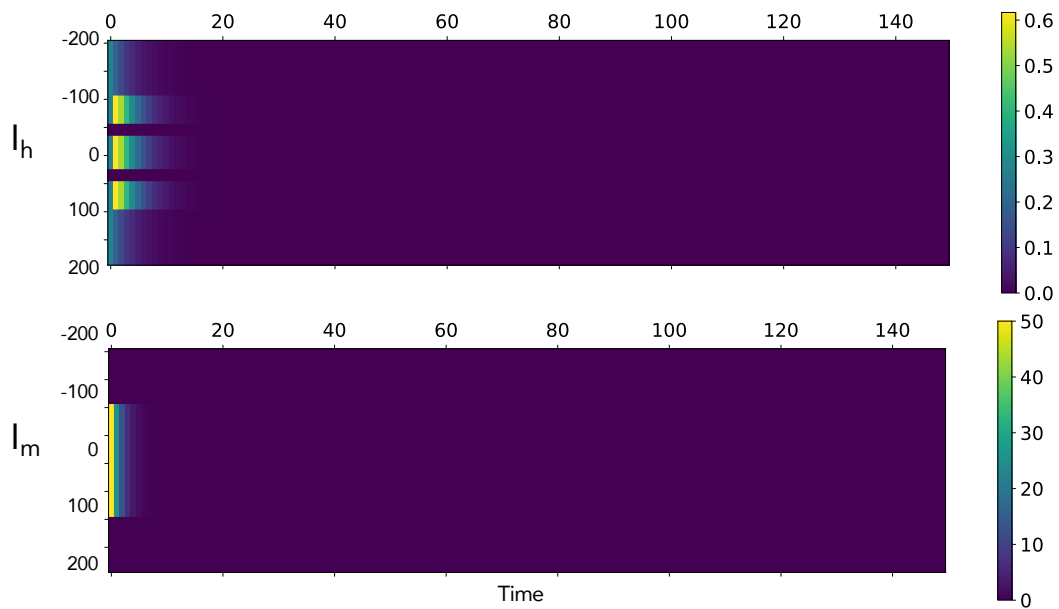


FIGURE 6.8: Spatiotemporal evolution of the infected human I_h and infectious mosquitoes I_m without control (top) and with optimal control (down).

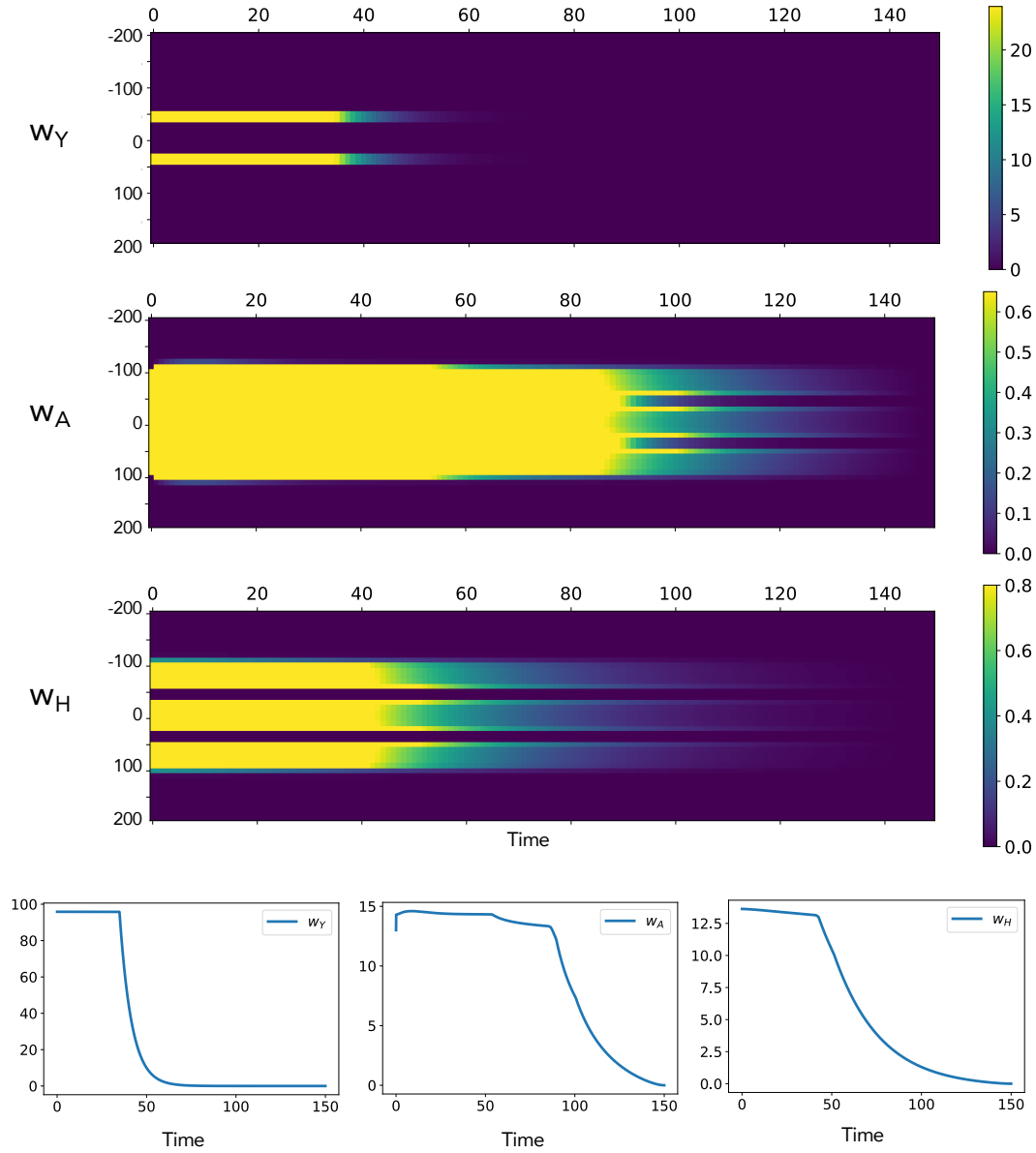


FIGURE 6.9: Spatiotemporal evolution of the optimal control variables w_Y, w_A, w_H of the model (top) and its sum in space (down).

Figure 6.9, shows the progression of the optimal control w_Y^*, w_A^* and w_H^* , respectively. It shows that a near zero optimal control does not mean a termination of applying the control strategies. Instead, it shows that we need to continue applying the control strategy near the laying sites at maximum capacity for an interval of time.

6.6 Behavior with respect to capacity and diffusion parameters

6.6.1 Influence of the Carrying Capacity of pupae

We denote the carrying capacity of pupae $k_{pup} = \frac{1}{\beta_m}$.

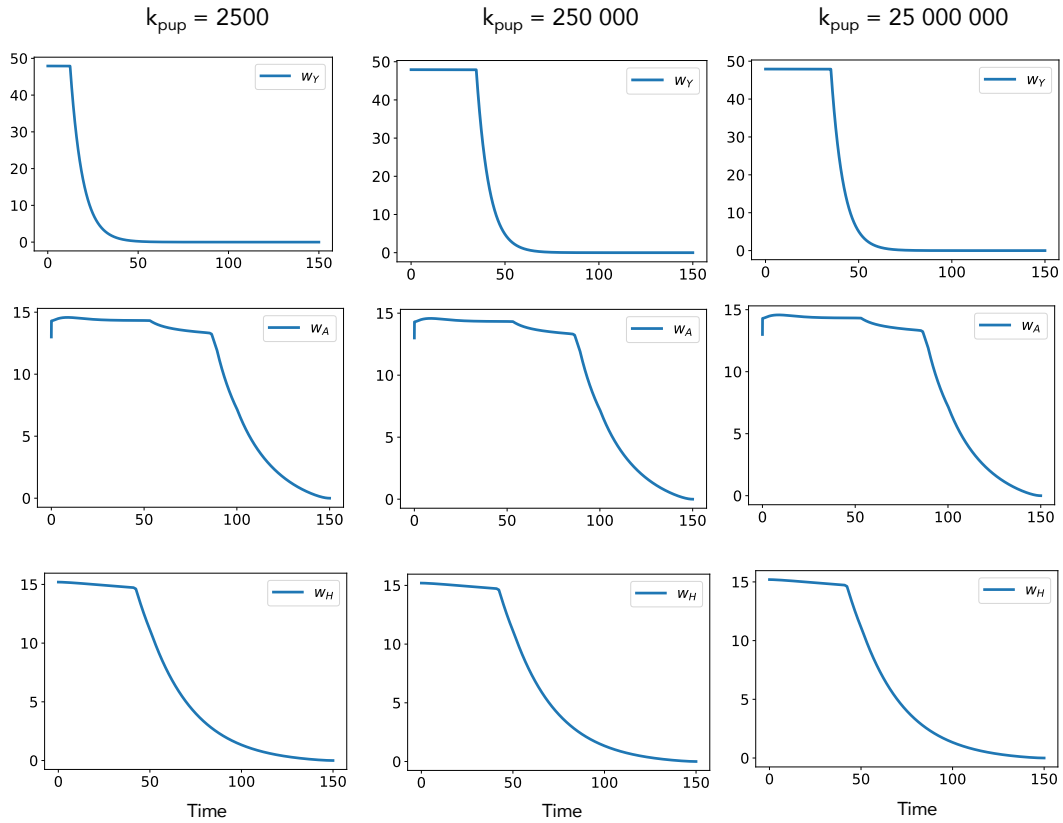


FIGURE 6.10: Behavior of eggs, larvae, and pupae in different capacities of pupae.

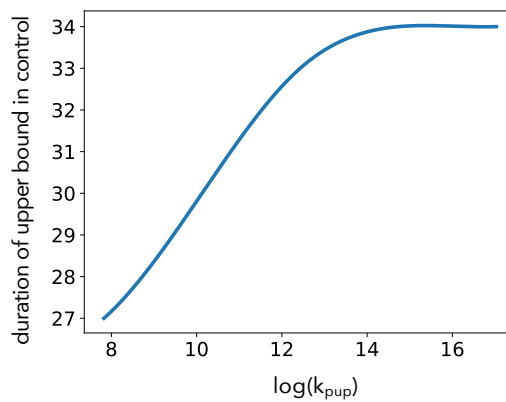


FIGURE 6.11: Duration of the upper bound in the optimal control w_Y with respect to the carrying capacity of pupae.

6.6.2 Influence of the Laying Sites Capacity

In this section, we consider changing the capacity of the laying sites. The equation for eggs E is modified to take into account the laying capacity as

$$E' = \alpha_m(S_m + I_m) \left(1 - \frac{E}{k_{lay}}\right) - \gamma_{E,L}E - \mu_E E$$

where k_{lay} represents the capacity of the laying sites. The adjoint problem is then modified as follows

$$\begin{aligned} \frac{\partial \lambda_1(x, t)}{\partial t} &= \lambda_1(x, t) \left(\mu_E - \frac{\alpha_m}{k_{lay}}(S_m + I_m) \right) + (\lambda_1(x, t) - \lambda_2(x, t))\gamma_{E,L} \\ \frac{\partial \lambda_4(x, t)}{\partial t} - D\Delta \lambda_4 &= -\lambda_1(x, t)\alpha_m \left(1 - \frac{E}{k_{lay}}\right) \\ &\quad + \lambda_4(x, t)(\mu_A + w_A) + (\lambda_4(x, t) - \lambda_5(x, t))ab_m I_h(x, t) \\ \frac{\partial \lambda_5(x, t)}{\partial t} - D\Delta \lambda_5 &= -\lambda_1(x, t)\alpha_m \left(1 - \frac{E}{k_{lay}}\right) \\ &\quad + \lambda_5(x, t)(\mu_A + w_A) + (\lambda_6(x, t) - \lambda_7(x, t))ab_h S_h(x, t). \end{aligned}$$

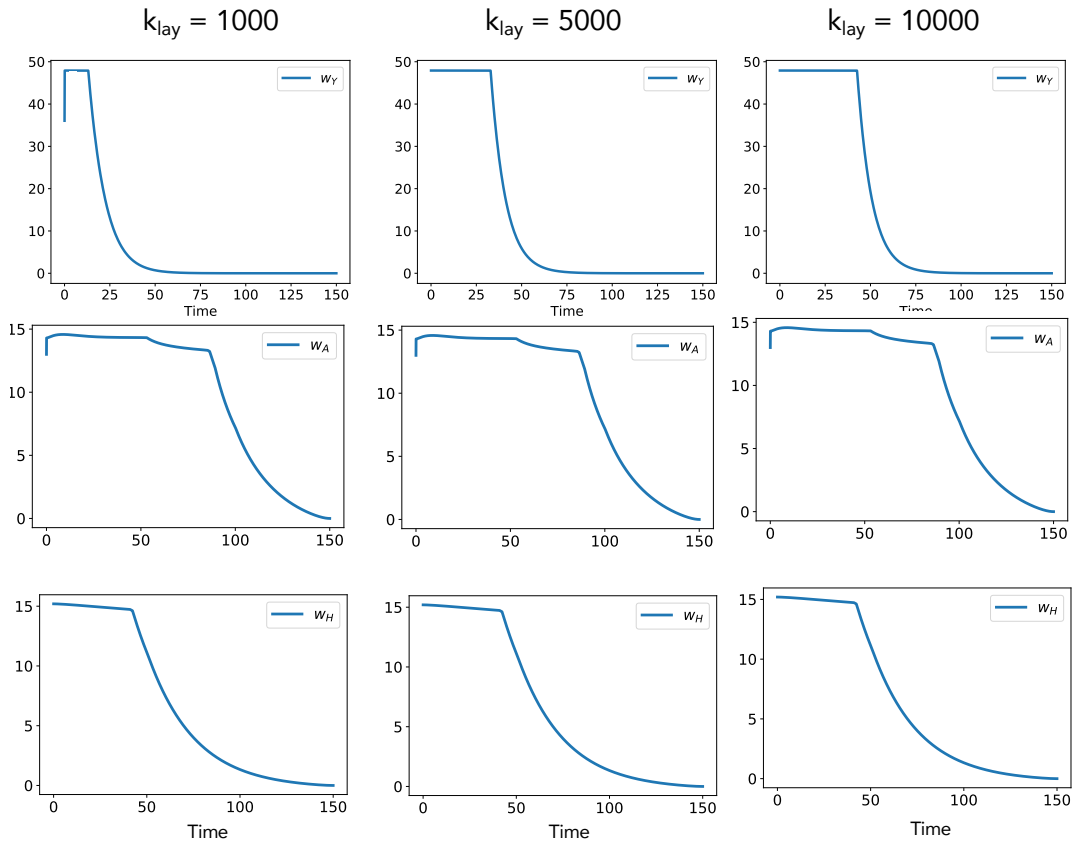


FIGURE 6.12: Behavior of eggs, larvae, and pupae in different capacities of the laying sites.

Figure 6.12 show that controls of adult mosquitoes and the human population do not depend on the carrying capacity k_{lay} . On the contrary, the control of larvae changes with k_{lay} . As shown in Figure 6.13, the greater the carrying capacity k_{lay} , the longer the application optimal control w_y . It is explained because more eggs can be accommodated, and thus more larvae.

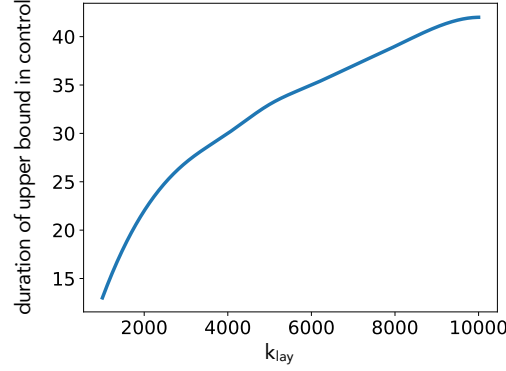


FIGURE 6.13: Duration of the upper bound in the optimal control w_y with respect to the laying capacity.

6.6.3 Sensitivity Analysis with respect to the diffusion

In this section, we study the effect of different parameter values on the number of infected humans since measuring the spatial spread of mosquitoes is a difficult task. So we compute the maximum number of infected humans by varying D_{min} between 0.1 to 1, c_f , c_l , α and β between 10^{-4} to 10^{-3} . The numerical simulations presented in Section 6.5 use an insensitive parameter.

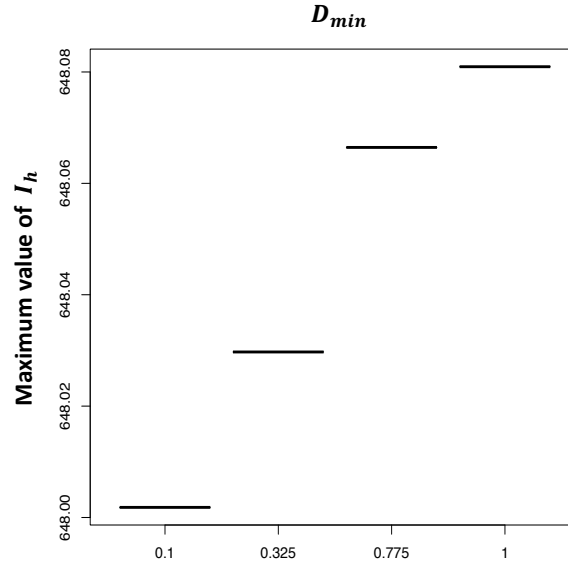
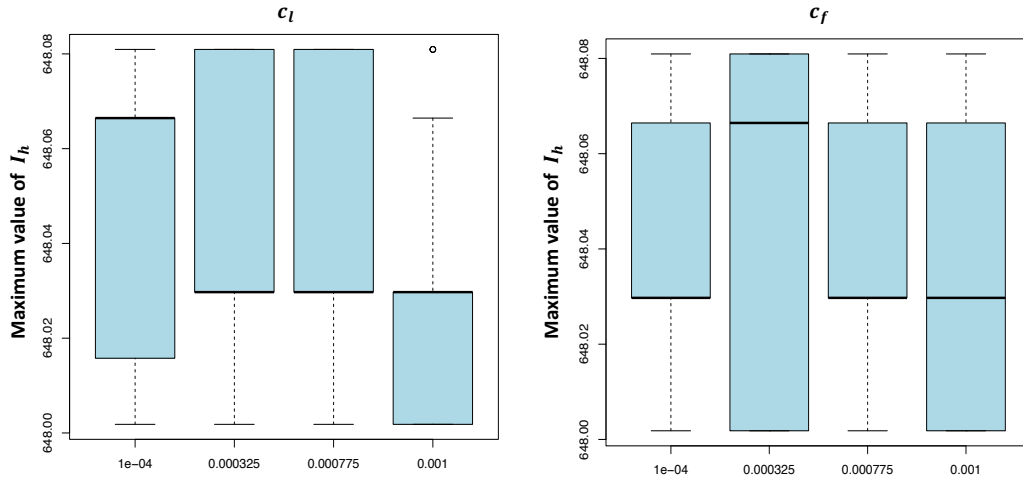
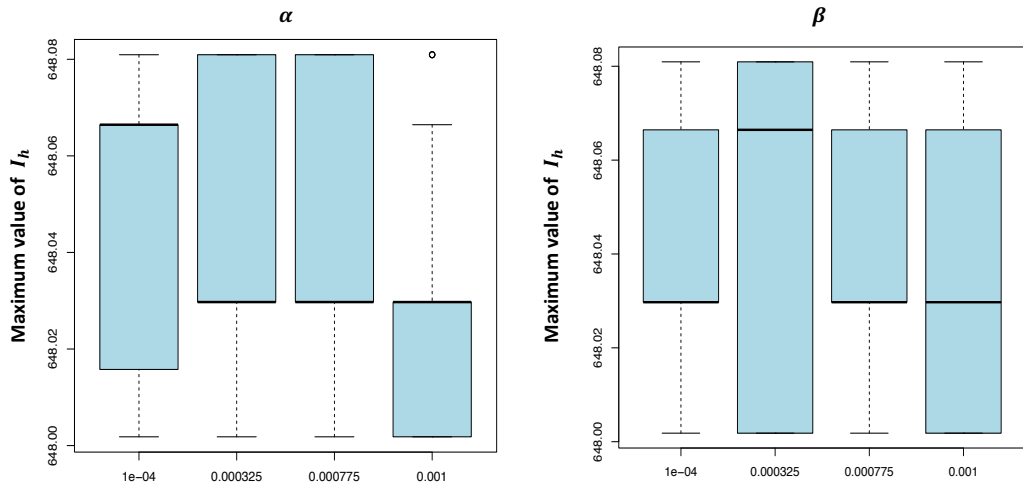


FIGURE 6.14: Effect on the maximum of infected humans I_h from the variations of D_{min} .

Figure 6.14 and 6.15 shows the maximum values of the infected humans in varying values of D_{min} , c_l , c_f , α , and β . It shows that the varying values give no significant difference in the maximum values of an infected human. There is only a 0.08 difference in the human population. This is due to the fact that the perception is exponentially decreasing.



(A) Effect on the maximum of infected humans I_h from the variations of c_l and c_f .



(B) Effect on the maximum of infected humans I_h from the variations of α and β .

FIGURE 6.15: Maximum value of an infected human in varying parameter values involved in diffusion coefficients.

Bibliography

- [1] Maíra Aguiar, Sebastien Ballesteros, Bob Kooi, and Nico Stollenwerk. The role of seasonality and import in a minimalistic multi-strain dengue model capturing differences between primary and secondary infections: Complex dynamics and its implications for data analysis. *Journal of theoretical biology*, 289:181–96, 09 2011. doi:[10.1016/j.jtbi.2011.08.043](https://doi.org/10.1016/j.jtbi.2011.08.043).
- [2] Maíra Aguiar and Nico Stollenwerk. Mathematical models of dengue fever epidemiology: multi-strain dynamics, immunological aspects associated to disease severity and vaccines. *Communication in Biomathematical Sciences*, 1:1–12, 12 2017. doi:[10.5614/cbms.2017.1.1.1](https://doi.org/10.5614/cbms.2017.1.1.1).
- [3] Maíra Aguiar, Nico Stollenwerk, and Scott Halstead. The impact of the newly licensed dengue vaccine in endemic countries. *PLoS Neglected Tropical Diseases*, 10, 2016. URL: <https://doi.org/10.1371/journal.pntd.0005179>.
- [4] Luis Almeida, Michel Duprez, Yannick Privat, and Nicolas Vauchelet. Mosquito population control strategies for fighting against arboviruses. *Mathematical Biosciences and Engineering*, 16(6):6274–6297, 2019. URL: <https://www.aimspress.com/article/doi/10.3934/mbe.2019313>, doi:[10.3934/mbe.2019313](https://doi.org/10.3934/mbe.2019313).
- [5] Bruce Anderson, Jeffrey Jackson, and Meera Sitharam. Descartes’ rule of signs revisited. *The American Mathematical Monthly*, 105(5):447–451, 1998. URL: <http://www.jstor.org/stable/3109807>.
- [6] Iurri Bakach and James Braselton. A survey of mathematical models of dengue fever. *Journal of Computer Science & Systems Biology*, 08, 01 2015. URL: <https://doi.org/10.4172/jcsb.1000198>.
- [7] Elina Barredo and Matthew DeGennaro. Not just from blood: Mosquito nutrient acquisition from nectar sources. *Trends in Parasitology*, 36:473–484, 2020. URL: <https://doi.org/10.1016/j.pt.2020.02.003>.
- [8] Norbert Becker, Dušan Petrić, Marija Zgomba, Clive Boase, Minoo Madon, Christine Dahl, and Achim Kaiser. Mosquitoes, identification, ecology and control. 01 2020. doi:[10.1007/978-3-030-11623-1](https://doi.org/10.1007/978-3-030-11623-1).
- [9] P-A Bliman, D. Cardona-Salgado, Y. Dumont, and O. Vasilieva. Implementation of control strategies for sterile insect techniques. *Mathematical Biosciences*, 314:43–60, 2019. URL: <https://doi.org/10.1016/j.mbs.2019.06.002>.

- [10] Yoann Bourhis, Sylvain Poggi, Youcef Mammeri, Anne-Marie Cortesero, Anne Le Ralec, and Nicolas Parisey. Perception-based foraging for competing resources: Assessing pest population dynamics at the landscape from heterogeneous resource distribution. *Ecological Modelling*, 312:211–221, 2005. URL: <https://doi.org/10.1016/j.ecolmodel.2015.05.029>.
- [11] P. Cailly, A. Tran, T. Balenghien, G. L’Ambert, C. Toty, and P. Ezanno. Climate-driven abundance model to assess mosquito control strategies. *Ecological Modelling*, pages 7–17, 2012. URL: <https://doi.org/10.1016/j.ecolmodel.2011.10.027>.
- [12] Aureliano Sylvestre Carvalho, Stella Silva, and I. Charret. Mathematical modeling of dengue epidemic: Control methods and vaccination strategies. *Theory in Biosciences*, 138, 2015. URL: <https://doi.org/10.1007/s12064-019-00273-7>.
- [13] Sylvestre Aureliano Carvalho, Stella Olivia da Silva, and Iraziet da Cunha Charret. Mathematical modeling of dengue epidemic: control methods and vaccination strategies. *Theory in Biosciences*, 138(2):223–239, 2019. doi:10.1007/s12064-019-00273-7.
- [14] CDC. Mosquitoes with wolbachia for reducing numbers of aedes aegypti mosquitoess, 17 September 2020. URL: <https://www.cdc.gov/mosquitoes/mosquito-control/community/sit/wolbachia.html>.
- [15] CDC. Dengue: Symptoms and treatments, 20 September 2021. URL: <https://www.cdc.gov/dengue/symptoms/index.html>.
- [16] CDC. Where mosquitoes live. *U.S. Department of Health & Human Services*, 2021. URL: <https://www.cdc.gov/mosquitoes/about/where-mosquitoes-live.html>.
- [17] CDC. Mosquitoes image library. *U.S. Department of Health & Human Services*, 22 October 2021. URL: <https://www.cdc.gov/dengue/transmission/index.html>.
- [18] CDC. Dengue transmission. *U.S. Department of Health & Human Services*, 26 September 2019. URL: <https://www.cdc.gov/dengue/transmission/index.html>.
- [19] CDC. *Mosquitoes: Mosquito Life Cycles*, 5 March 2015. URL: <https://www.cdc.gov/mosquitoes/about/life-cycles/aedes.html>.
- [20] CDC. *Life Cycle of Aedes aegypti and Ae. albopictus Mosquitoes*, 5 March 2020. URL: <https://www.cdc.gov/mosquitoes/about/life-cycles/aedes.html>.
- [21] Bill Chappell. 5 stars: A mosquito’s idea of a delicious human. *NPR.org*, 12 July 2013. URL: <https://www.npr.org/sections/thetwo-way/2013/>

- 07/12/201521175/5-stars-a-mosquitos-idea-of-a-delicious-human?t=1620814216339.
- [22] Edward Codling, Michael Plank, and Simon Benhamou. Random walks in biology. *Journal of the Royal Society, Interface / the Royal Society*, 5:813–34, 09 2008. URL: <https://doi.org/10.1098/rsif.2008.0014>.
- [23] Ph.D. Craig Freudenrich. How mosquitoes work. *HowStuffWorks.com*, 5 July 2001. URL: <https://animals.howstuffworks.com/insects/mosquito.htm>.
- [24] Shroyer DA. Vertical maintenance of dengue-1 virus in sequential generations of aedes albopictus. *Journal of the American Mosquito Control Association*, 6:312–314, 1990. URL: <https://www.biodiversitylibrary.org/part/126188>.
- [25] Kaur Dapinder, Dapinder Bakshi, Devinder Kocher, Shreya Kocher, Shreya Jamwal, and Ashwani Kumar. Mosquito larvae specific predation by native cyclopoid copepod species, mesocyclops aspericornis (daday, 1906), 01 2018. doi:10.13140/RG.2.2.17529.16483.
- [26] Lilianne Denis-Vidal, Ghislaine Joly-Blanchard, and Céline Noiret. Some effective approaches to check the identifiability of uncontrolled nonlinear systems. *Mathematics and Computers in Simulation*, 57(1):35–44, 2001. URL: <https://www.sciencedirect.com/science/article/pii/S0378475401002749>, doi: [https://doi.org/10.1016/S0378-4754\(01\)00274-9](https://doi.org/10.1016/S0378-4754(01)00274-9).
- [27] Mohamed Derouich, Abdesslam Boutayeb, and E Twizell. A model of dengue fever. *Biomedical Engineering Online*, 2, 2003. URL: <https://doi.org/10.1186/1475-925X-2-4>.
- [28] DOH Department of Health. *Report 8: Monthly dengue report: January 1 - August 31, 2019 (MW 1-35)*, Accessed April 22, 2020 2019. URL: <https://www.doh.gov.ph/sites/default/files/statistics/2019%20Dengue%20Monthly%20Report%20No.%208.pdf>.
- [29] G. Fernández-Grandon, Salvador Gezan, John Armour, John Pickett, and James Logan. Heritability of attractiveness to mosquitoes. *PloS one*, 10:e0122716, 04 2015. URL: <https://doi.org/10.1371/journal.pone.0122716>.
- [30] Victor Henrique Ferreira-de Lima and Tamara Lima-Camara. Natural vertical transmission of dengue virus in aedes aegypti and aedes albopictus: A systematic review. *Parasites & Vectors*, 11, 02 2018. doi:10.1186/s13071-018-2643-9.
- [31] Environment Directorate Organisation for Economic Cooperation and Developments. *Consensus Document on the Biology of Mosquito Aedes*, 13 July 2018. URL: [https://www.oecd.org/officialdocuments/publicdisplaydocumentpdf/?cote=3DENV%2FJM%2FMONO\(2018\)23%26docLanguage=3DEn&clen=2735825](https://www.oecd.org/officialdocuments/publicdisplaydocumentpdf/?cote=3DENV%2FJM%2FMONO(2018)23%26docLanguage=3DEn&clen=2735825).

- [32] Regional Office for the Americas of the World Health Organization. PAHO statement on zika virus transmission and prevention. *Pan American Health Organization*, 24 January 2016. URL: https://web.archive.org/web/20160126055104/http://www.paho.org/hq/index.php?option=com_content&view=article&id=11605&Itemid=0&lang=en.
- [33] WHO. Regional Office for the Western Pacific. *Guidelines for dengue surveillance and mosquito control*. 2nd ed. WHO Regional Office for the Western Pacific, 2003.
- [34] Justin George, Simon Blanford, Matthew Thomas, and Thomas Baker. Malaria mosquitoes host-locate and feed upon caterpillars. *PLoS ONE*, 9(11):1–6, 11 2014. URL: <https://doi.org/10.1371/journal.pone.0108894>.
- [35] S.R Hadinegoro, J.L Arredondo-García, Capeding M.R, and et al. Efficacy and long-term safety of a dengue vaccine in regions of endemic disease. *N. Engl. J. Med.*, 373:1195–1206, 2015.
- [36] Chelsea Harvey. Mosquito-borne disease could threaten half the globe by 2050, 7 March 2019. URL: <https://www.scientificamerican.com/article/mosquito-borne-disease-could-threaten-half-the-globe-by-2050/>.
- [37] Barry D. Hughes. *Random Walks and Random Environments: Volume 1: Random Walks*. Oxford University Press, USA, 1995.
- [38] Enahoro Iboi and Abba Gumel. Mathematical assessment of the role of dengvaxia vaccine on the transmission dynamics of dengue serotypes. *Mathematical Biosciences*, 304, 2018. URL: <https://doi.org/10.1016/j.mbs.2018.07.003>.
- [39] John Staughton. Do animals get mosquito bites? *ScienceABC.com*, 19 Jan 2022. [Online; accessed 10-June-2022]. URL: <https://www.scienceabc.com/eyeopeners/do-animals-get-mosquito-bites.html>.
- [40] Girish Khera. 10 solid links between the zika virus and neurological defects, 26 April 2016. URL: <https://www.scientificanimations.com/neurological-defects-caused-by-zika-virus/>.
- [41] M. J. Lehane. *The Biology of Blood-Sucking in Insects*. Cambridge University Press, 2 edition, 2005. URL: <https://doi.org/10.1017/CB09780511610493>.
- [42] Suzanne Lenhart and John Workman. *Optimal Control Applied to Biological Models*. 01 2007.
- [43] Yansheng Liu, Wahidah Sanusi, Nasiah Badwi, Ahmad Zaki, Sahlan Sidjara, Nurwahidah Sari, Muhammad Isbar Pratama, and Syafruddin Side. Analysis and simulation of sirs model for dengue fever transmission in south sulawesi, indonesia. *Journal of Applied Mathematics*, 2021:2918080, 2021. doi:10.1155/2021/2918080.

- [44] Gerald G. Marten and Janet W. Reid. Cyclopoid copepods. *Journal of the American Mosquito Control Association*, 23:65–92, 2007. URL: [https://doi.org/10.2987/8756-971X\(2007\)23\[65:CC\]2.0.CO;2](https://doi.org/10.2987/8756-971X(2007)23[65:CC]2.0.CO;2).
- [45] Hongyu Miao, Xiaohua Xia, Alan S Perelson, and Hulin Wu. On identifiability of nonlinear ode models and applications in viral dynamics. *SIAM review. Society for Industrial and Applied Mathematics*, 53(1):3–39, 01 2011. URL: <https://pubmed.ncbi.nlm.nih.gov/21785515>, doi:10.1137/090757009.
- [46] Ministry of Heath Nutrition and Indigenous Medicine. Potential breeding sites. URL: <http://www.dengue.health.gov.lk/web/index.php/en/information/potential-breeding-sites>.
- [47] M.S Mistica, L.A de las Llagas, and A.G Bertuso. Dengue mosquito ovitrapping and preventive fogging trials in the philippines. *Philippine Entomologist*, 21:136–145, 2007.
- [48] Jagriti Narang and Manika Khanujan. *Small Bite, Big Threat: Deadly Infections Transmitted by Aedes Mosquitoes*. Jenny Stanford Publishing, Singapore, 2020.
- [49] Robert Nau. Notes on the random walk model. *Fuqua School of Business, Duke University*, (2014). Last Updated: 11/4/2014.
- [50] Dennis Normile. Surprising new dengue virus throws a spanner in disease control efforts. *Science (New York, N.Y.)*, 342:415, 10 2013. URL: <https://doi.org/10.1126/science.342.6157.415>.
- [51] Nuning Nuraini, Edy Soewono, and Kuntjoro Sidarto. Mathematical model of dengue disease transmission with severe dhf compartment. *Bull. Malays. Math. Sci. Soc*, 30:143–157, 2007. URL: <http://emis.dsd.sztaki.hu/journals/BMMSS/pdf/v30n2/v30n2p7.pdf>.
- [52] El Maati Ouhabaz. *Analysis of Heat Equations on Domains*. (LMS-31). Princeton University Press, 2005. URL: <http://www.jstor.org/stable/j.ctt7s45z>.
- [53] Cecilia Mejica Panogadia-Reyes, Estrella Iriandez Cruz, and Soledad Lopez Bautista. Philippine species of mesocyclops (crustacea: Copepoda) as a biological control agent of aedes aegypti (linnaeus). *Dengue Bulletin*, 28:174–178, 2004.
- [54] Puntani Pongsumpun, I.-Ming Tang, and Napasool Wongvanich. Optimal control of the dengue dynamical transmission with vertical transmission. *Advances in Difference Equations*, 2019, 05 2019. doi:10.1186/s13662-019-2120-6.
- [55] World Mosquito Program. How it works. URL: <https://www.worldmosquitoprogram.org/en/work/wolbachia-method/how-it-works>.

- [56] Izabela Rodenhuis-Zybert, Jan Wilschut, and Jolanda Smit. Dengue virus life cycle: Viral and host factors modulating infectivity. *Cellular and molecular life sciences : CMLS*, 67:2773–86, 04 2010. URL: <https://doi.org/10.1007/s00018-010-0357-z>.
- [57] Nur Afrida Rosvita, Nia Kania, Eko Suhartono, Adi Nugroho, and Erida Wydiamala. Spatial-temporal distribution of dengue in banjarmasin, indonesia from 2016 to 2020. *International Journal of Public Health Science (IJPHS)*, 11:1167–1175, 2022. doi:10.11591/ijphs.v11i4.21780.
- [58] Leopoldo Rueda. Pictorial keys for the identification of mosquitoes (diptera: Culicidae) associated with dengue virus transmission. *Zootaxa*, 589, 08 2004. doi:10.11646/zootaxa.589.1.1.
- [59] Chris A. Schmidt, Genevieve Comeau, Andrew J. Monaghan, Daniel J. Williamson, and Kacey C. Ernst. Effects of desiccation stress on adult female longevity in *Aedes aegypti* and *Ae. albopictus* (Diptera: Culicidae): results of a systematic review and pooled survival analysis. *Parasit & Vectors*, 11(1):167, 2018. URL: <https://doi.org/10.1186/s13071-018-2808-6>.
- [60] P. SHarris and D. Cooke. Survival and fecundity of mosquitoes fed on insect haemolymph. *Nature*, 222(5200):1264–1265, 1969. URL: <https://doi.org/10.1038/2221264a0>.
- [61] Yoshikazu Shirai, Hisashi Funada, Hisao Takizawa, Taisuke Seki, Masaaki Morohashi, and Kiyoshi Kamimura. Landing preference of aedes albopictus (diptera: Culicidae) on human skin among abo blood groups, secretors or non-secretors, and abh antigens. *Journal of Medical Entomology*, 41(4):796–799, 07 2004. URL: <https://doi.org/10.1603/0022-2585-41.4.796>.
- [62] Syafruddin Side and M Noorani. SEIR model for transmission of dengue fever. *International Journal on Advance Science, Engineering & Information Technology*, 2(5), 2012. URL: <https://doi.org/10.18517/ijaseit.2.5.217>.
- [63] R. Slooff and E. N. Marks. Mosquitoes (culicidae) biting a fish (periophthalmidae). *Journal of Medical Entomology*, 2(1):16–16, 04 1965. URL: <https://doi.org/10.1093/jmedent/2.1.16>.
- [64] S Sridhar, A Luedtke, E Langevin, and et al. Effect of dengue serostatus on dengue vaccine safety and efficacy. *N. Engl. J. Med.*, 379:327–340, 2018.
- [65] The Philippine Star. Senate invites aquino to vaccine probe. *PhilStar.com*, 12 December 2017. Accessed: April 7, 2020. URL: <https://www.philstar.com/headlines/2017/12/12/1767890/senate-invites-aquino-vaccine-probe>.
- [66] Adi Utarini, Citra Indriani, Riris A. Ahmad, Warsito Tantowijoyo, Eggi Arguni, M. Ridwan Ansari, Endah Supriyati, D. Satria Wardana, Yeti Meitika, Inggrid

- Ernesia, Indah Nurhayati, Equatori Prabowo, Bkti Andari, Benjamin R. Green, Lauren Hodgson, Zoe Cutcher, Edwige Rancès, Peter A. Ryan, Scott L. O'Neill, Suzanne M. Dufault, Stephanie K. Tanamas, Nicholas P. Jewell, Katherine L. Anders, and Cameron P. Simmons. Efficacy of wolbachia-infected mosquito deployments for the control of dengue. *New England Journal of Medicine*, 384(23):2177–2186, 2021. PMID: 34107180. [arXiv:https://doi.org/10.1056/NEJMoa2030243](https://doi.org/10.1056/NEJMoa2030243), doi:10.1056/NEJMoa2030243.
- [67] P Van den Driessche and J. Watmough. Reproduction numbers and sub-threshold endemic equilibria for compartmental models of disease transmission. *Mathematical Biosciences*, 180(1-2):29–48, 2000. URL: [https://doi.org/10.1016/S0025-5564\(02\)00108-6](https://doi.org/10.1016/S0025-5564(02)00108-6).
- [68] WHO. Dengue and severe dengue. *World Health Organization*, 19 May 2021. URL: <https://www.who.int/news-room/fact-sheets/detail/dengue-and-severe-dengue>.
- [69] Wikipedia contributors. Aedes — Wikipedia, the free encyclopedia, 2022. [Online; accessed 10-June-2022]. URL: <https://en.wikipedia.org/w/index.php?title=Aedes&oldid=1076960311>.
- [70] Gabriella H. Wolff and Jeffrey A. Riffell. Olfaction, experience and neural mechanisms underlying mosquito host preference. *Journal of Experimental Biology*, 221(4), 02 2018. URL: <https://doi.org/10.1242/jeb.157131>.
- [71] World Health Organization. *Dengue vaccine: WHO position paper*, weekly epidemiological record edition, September 2018. URL: <https://apps.who.int/iris/handle/10665/274316>.
- [72] Hyun Yang and Claudia Ferreira. Assessing the effects of vector control on dengue transmission. *Applied Mathematics and Computation*, 198:401–413, 2008. URL: <https://doi.org/10.1016/j.amc.2007.08.046>.
- [73] Bao-Ting Yu, Yin Hu, Yan-Mei Ding, Jia-Xin Tian, and Jian-Chu Mo. Feeding on different attractive flowering plants affects the energy reserves of culex pipiens pallens adults. *Parasitology Research*, 117(1):67–73, 2018. URL: <https://doi.org/10.1007/s00436-017-5664-y>.

Appendix A

Accounting for Symptomatic and Asymptomatic in a SEIR-type model of COVID-19

During my Ph.D., I was involved in a project related to Covid-19. This appendix contains the published paper *Jayrold P. Arcede, Randy L. Caga-anan, Cheryl Q. Mentuda and Youcef Mammeri, Accounting for Symptomatic and Asymptomatic in a SEIR-type model of COVID-19, Math. Model. Nat. Phenom. 15 (2020) 34.*

A.1 Introduction

In late 2019, a disease outbreak emerged in a city of Wuhan, China. The culprit was a certain strain called Coronavirus Disease 2019 or COVID-19 in brief [Wor20b]. This virus has been identified to cause fever, cough, shortness of breath, muscle ache, confusion, headache, sore throat, rhinorrhoea, chest pain, diarrhea, and nausea and vomiting [HAM⁺20, CZD⁺20]. COVID-19 belongs to the *Coronaviridae* family. A family of coronaviruses that cause diseases in humans and animals, ranging from the common cold to more severe diseases. Although only seven coronaviruses are known to cause disease in humans, three of these, COVID-19 included, can cause a much severe infection, and sometimes fatal to humans. The other two to complete the list were the severe acute respiratory syndrome (SARS) identified in 2002 in China, and the Middle East respiratory syndrome (MERS) originated decade after in Saudi Arabia.

Like MERS and SARS, COVID-19 is a zoonotic virus and believed to be originated from bats transmitted to humans [ZYWea20]. In comparison with SARS, MERS, the COVID-19 appears to be less deadly. However, the World Health Organization (WHO) reported that it has already infected and killed more people than its predecessors combined. Also, COVID-19 spreads much faster than SARS and MERS. It only took over a month before it surpassed the number of cases recorded by the SARS outbreak in 2012. According to WHO, it only took 67 days from the beginning of the outbreak in China last December 2019 for the virus to infect the

first 100,000 people worldwide [Wor20a]. As of the 25th of March 2020, a cumulative total of 372,757 confirmed cases, while 16,231 deaths have been recorded for COVID-19 by World Health Organization [Wor20c].

Last 30th of January, WHO characterized COVID-19 as Public Health Emergency of International Concern (PHEI) and urge countries to put in place strong measures to detect disease early, isolate and treat cases, trace contacts, and promote social distancing measures commensurate with the risk [Wor20d]. In response, the world implemented its actions to reduce the spread of the virus. Limitations on mobility, social distancing, and self-quarantine have been applied. Moreover, health institutions advise people to practice good hygiene to keep from being infected. All these efforts have been made to reduce the transmission rate of the virus.

For the time being, COVID-19 infection is still on the rise. Government and research institutions scramble to seek antiviral treatment and vaccines to combat the disease. Several reports list possible drugs combination to apply, yet it is still unclear which drugs could combat the viral disease and which won't.

Several mathematical models have been proposed from various epidemiological groups. These models help governments as an early warning device about the size of the outbreak, how quickly it will spread, and how effective control measures may be. However, due to the limited emerging understanding of the new virus and its transmission mechanisms, the results are largely inconsistent across studies.

In this paper, we will mention a few models and, in the end, to propose one. Gardner and his team [Gar20] at Center for Systems Science and Engineering, Johns Hopkins University, implemented on a previously published model applied for COVID-19. It is a metapopulation network model represented by a graph with each nodes follows a discrete-time Susceptible-Exposed-Infected-Recovered (SEIR) compartmental model. The model gives an estimate of the expected number of cases in mainland China at the end of January 2020, as well as the global distribution of infected travelers. They believe that the outbreak began in November 2019 with hundreds of infected already present in Wuhan last early December 2019. Wu et al. [WLL20] from WHO Collaborating Centre for Infectious Disease Epidemiology and Control at the University of Hong Kong presented a modeling study on the nowcast and forecast of the 2019-nCoV outbreak at Wuhan. The group used an SEIR metapopulation model to simulate epidemic and found reproductive number R_0 around 2.68 (with 95% credible interval 2.47-2.86). Imai et al. [IDC+20] estimates R_0 around 2.6 with uncertainty range of 1.5-3.5. Zhao et al. [ZLR+20, ZML+20] found R_0 to range from 2.24 to 5.71 based on the reporting rate of cases. If the reporting rate increase 2-fold, $R_0 = 3.58$, if it increase 8-fold, $R_0 = 2.24$. If there is no change in the reporting rate, the estimated R_0 is 5.71. Similar to the above authors, Wang et al. [WWDDea20] employed an infectious disease dynamics model (SEIR model) for modeling and predicting the number of COVID-19 cases in Wuhan. They opined that to reduce R_0 significantly, the government should continue implementing strict measures on containment and public health issues. In the same tune as the latter, the model of

Danchin et al. [DNT20] also suggests continuing to implement effective quarantine measures to avoid a resurgence of infection. The model consists of five (5) compartments: susceptible, infected, alternative infection, detected, and removed.

Here, we proposed an extension from the classical SEIR model by adding a compartment of asymptomatic infected. We address the challenge of predicting the spread of COVID-19 by giving our estimates for the basic reproductive numbers \mathcal{R}_0 and its effective reproductive number \mathcal{R}_{eff} . Afterward, we also assess risks and interventions via containment strategy or treatments of exposed and symptomatic infected.

The rest of the paper is organized as follows. Section 2, outlines our methodology. Here the model was explained, where the data was taken, and its parameter estimates. Section 3 contained the qualitative analysis for the model. Here, we give the closed-form equation of reproductive number \mathcal{R}_0 , then tackling the best strategy to reduce transmission rates. Finally, section 4 outlines our brief discussion on some measures to limit the outbreak.

A.2 Materials and methods

A.2.1 Confirmed and death data

In this study, we used the publicly available dataset of COVID-19 provided by the Johns Hopkins University [DDG20]. This dataset includes many countries' daily count of confirmed cases, recovered cases, and deaths. Data can be downloaded from https://github.com/CSSEGISandData/COVID-19/tree/master/csse_covid_19_data. These data are collected through public health authorities' announcements and are directly reported public and unidentified patient data, so ethical approval is not required.

A.2.2 Mathematical model

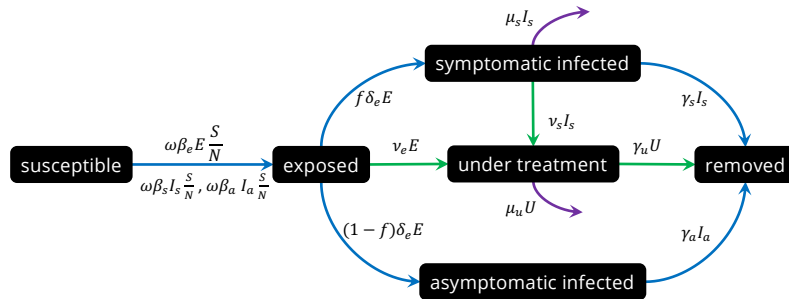


FIGURE A.1: Compartmental representation of the $SEI_a I_s UR$ -model. Blue arrows represent the infection flow. Green arrows denote for the treatments. Purple arrow is the death.

We focus our study on six components of the epidemic flow (Figure A.1), *i.e.* Susceptible individual (S), Exposed individual (E), Symptomatic Infected individual (I_s), Asymptomatic Infected individual (I_a), Under treatment individual (U), and Removed individual (R). To build the mathematical model, we followed the standard strategy developed in the literature concerning SIR model [DH00, BCC12]. We assumed that susceptible can be infected by exposed, symptomatic infected as well as asymptomatic infected individuals. While exposed individuals are generally quarantined, symptomatics are hospitalized. Due to the lack of serological tests to evaluate asymptomatic patients, no treatment is applied to them. To lighten the model, quarantine or hospitalization are not distinguished.

The dynamics is governed by a system of six ordinary differential equations (ODE) as follows

$$\begin{aligned} S'(t) &= -\omega (\beta_e E + \beta_s I_s + \beta_a I_a) \frac{S}{N} \\ E'(t) &= \omega (\beta_e E + \beta_s I_s + \beta_a I_a) \frac{S}{N} - (\delta_e + \nu_e) E \\ I'_s(t) &= f \delta_e E - (\gamma_s + \mu_s + \nu_s) I_s \\ I'_a(t) &= (1 - f) \delta_e E - \gamma_a I_a \\ U'(t) &= \nu_e E + \nu_s I_s - (\gamma_u + \mu_u) U \\ R'(t) &= \gamma_s I_s + \gamma_a I_a + \gamma_u U \end{aligned}$$

Note that the total living population follows $N'(t) = -\mu_s I_s - \mu_u U$, while death is computed by $D'(t) = \mu_s I_s + \mu_u U$. We assume that there is no new recruit. The parameters are described in Table A of Figure A.2.

A.2.3 Parameters estimation

Calibration is made before intervention. Thus it is set $\nu_e = \nu_s = 0$. The model is made up of eleven parameters $\theta = (\omega, \beta_e, \beta_s, \beta_a, \delta_e, f, \gamma_s, \mu_s, \gamma_a, \gamma_u, \mu_u)$ that need to be determined. Given, for n days, the observations $I_{s,obs}(t_i)$ and $D_{obs}(t_i)$, the cost function consists of a nonlinear least square function

$$J(\theta) = \sum_{i=1}^n (I_{s,obs}(t_i) - I_s(t_i, \theta))^2 + (D_{obs}(t_i) - D(t_i, \theta))^2,$$

with constraints $\theta \geq 0$, and $0 \leq f \leq 1$. Here $I_s(t_i, \theta)$ and $D(t_i, \theta)$ denote output of the mathematical model at time t_i computed with the parameters θ . The optimization problem is solved using Approximate Bayesian Computation combined with a quasi-Newton method [CBGF10].

A.3 Results

A.3.1 Basic and effective reproduction numbers

It is standard to check that the domain

$$\Omega = \{(S, E, I_s, I_a, U, R) \in \mathbb{R}_+^6; 0 \leq S + E + I_s + I_a + U + R \leq N(0)\}$$

is positively invariant. In particular, there exists a unique global in time solution (S, E, I_s, I_a, U, R) in $\mathcal{C}(\mathbb{R}_+; \Omega)$ as soon as the initial condition lives in Ω .

Since the infected individuals are in E, I_a and I_s , the rate of new infections in each compartment (\mathcal{F}) and the rate of other transitions between compartments (\mathcal{V}) can be rewritten as

$$\mathcal{F} = \begin{pmatrix} \omega(\beta_e E + \beta_s I_s + \beta_a I_a) \frac{S}{N} \\ 0 \\ 0 \end{pmatrix}, \quad \mathcal{V} = \begin{pmatrix} (\delta_e + \nu_e)E \\ (\gamma_s + \mu_s + \nu_s)I_s - f\delta_e E \\ \gamma_a I_a - (1-f)\delta_e E \end{pmatrix}.$$

Thus,

$$F = \begin{pmatrix} \frac{\omega\beta_e S}{N} & \frac{\omega\beta_s S}{N} & \frac{\omega\beta_a S}{N} \\ 0 & 0 & 0 \\ 0 & 0 & 0 \end{pmatrix},$$

and

$$V = \begin{pmatrix} (\delta_e + \nu_e) & 0 & 0 \\ -f\delta_e & \gamma_s + \mu_s + \nu_s & 0 \\ -(1-f)\delta_e & 0 & \gamma_a \end{pmatrix}, \quad V^{-1} = \begin{pmatrix} \frac{1}{\delta_e + \nu_e} & 0 & 0 \\ \frac{f}{\gamma_s + \mu_s + \nu_s} & \frac{1}{\gamma_s + \mu_s + \nu_s} & 0 \\ \frac{1-f}{\gamma_a} & 0 & \frac{1}{\gamma_a} \end{pmatrix}.$$

Therefore, the next generation matrix is

$$FV^{-1} = \begin{pmatrix} \frac{\omega\beta_e S}{(\delta_e + \nu_e)N} + \frac{f\omega\beta_s S}{(\gamma_s + \mu_s + \nu_s)N} + \frac{(1-f)\omega\beta_a S}{\gamma_a N} & \frac{\omega\beta_s S}{(\gamma_s + \mu_s + \nu_s)N} & \frac{\omega\beta_a S}{\gamma_a N} \\ 0 & 0 & 0 \\ 0 & 0 & 0 \end{pmatrix}.$$

We deduce as in [vdDW00] that the basic reproduction number \mathcal{R}_0 for the Disease Free Equilibrium $(S^*, 0, 0, 0, R^*)$, with $N^* = S^* + R^*$, is

$$\mathcal{R}_0 := \omega \left(\frac{\beta_e}{\delta_e + \nu_e} + \frac{f\beta_s}{\gamma_s + \mu_s + \nu_s} + \frac{(1-f)\beta_a}{\gamma_a} \right) \frac{S^*}{N^*} =: \mathcal{R} \frac{S^*}{N^*}.$$

This number has an epidemiological meaning. The term $\frac{\omega\beta_e}{\delta_e + \nu_e}$ represents the contact rate with exposed during the average latency period $1/(\delta_e + \nu_e)$. The term $\frac{\omega f\beta_s}{\gamma_s + \mu_s + \nu_s}$ is the contact rate with symptomatic during the average infection period, and the last one is the part of asymptomatic.

In the subsequent, we write *DFE* when we mean by Disease Free Equilibrium.

Theorem A.3.1. *The DFE $(S^*, 0, 0, 0, R^*)$ is the unique positive equilibrium. Moreover it is globally asymptotically stable.*

Proof. By computing the eigenvalues of the Jacobian matrix, we deduce that if $\mathcal{R}_0 < 1$, then DFE is locally asymptotically stable.

Here we will prove that global asymptotic stability is independent that of \mathcal{R}_0 . Indeed, from the last differential equation in our system of ODE, we can deduce that R is an increasing function bounded by $N(0)$. Thus $R(t)$ converges to R^* as t goes to $+\infty$. Then integrating over time this equation provides

$$R(t) - R(0) = \int_0^t \gamma_s I_s(s) + \gamma_a I_a(s) + \gamma_u U(s) ds$$

and

$$R^* - R(0) = \int_0^{+\infty} \gamma_s I_s(s) + \gamma_a I_a(s) + \gamma_u U(s) ds,$$

which is finite. Furthermore, $\gamma_s I_s + \gamma_a I_a + \gamma_u U$ goes to 0 as $t \rightarrow +\infty$, and each term of this sum does thanks to the positivity of the solution. Adding the two first equations implies that

$$(S + E)' = -(\delta_e + \nu_e)E$$

and $S + E$ is a nonnegative decreasing function whose derivative tends to zero. Then $E(t) \rightarrow_{t \rightarrow +\infty} 0$ and $S(t) \rightarrow_{t \rightarrow +\infty} S^*$. \square

This theorem means that the asymptotic behavior does not depend on \mathcal{R}_0 . For all initial data in Ω , the solution converges to the DFE when time goes to infinity. Nevertheless, to observe initial exponential growth, $\mathcal{R}_0 > 1$ is necessary. Indeed, S is initially close to N such that infected states are given by the linear system of differential equations

$$\begin{pmatrix} E \\ I_s \\ I_a \end{pmatrix}'(t) = \begin{pmatrix} \omega\beta_e - \delta_e - \nu_s & \omega\beta_s & \omega\beta_a \\ f\delta_e & -(\gamma_s + \mu_s + \nu_s) & 0 \\ (1-f)\delta_e & 0 & -\gamma_a \end{pmatrix} \begin{pmatrix} E \\ I_s \\ I_a \end{pmatrix}.$$

The characteristic polynomial is $P(x) = x^3 + a_2x^2 + a_1x + a_0$, with $a_0 = (\gamma_s + \mu_s + \nu_s)\gamma_a(\delta_e + \nu_s)(1 - \mathcal{R})$. If $\mathcal{R} > 1$, there is at least one positive eigenvalue that coincides with an initial exponential growth rate of solutions.

To better reflect the time dynamic of the disease, the effective reproduction number

$$\mathcal{R}_{\text{eff}}(t) = \omega \left(\frac{\beta_e}{\delta_e + \nu_s} + \frac{f\beta_s}{\gamma_s + \mu_s + \nu_s} + \frac{(1-f)\beta_a}{\gamma_a} \right) \frac{S(t)}{N(t)}.$$

is represented in Figure A.2D and values of \mathcal{R} are computed in Table A of Figure A.2.

A.3.2 Model resolution

To calibrate the model, our simulations start the day of first confirmed infection and finish before interventions to reduce the disease. Therefore ν_e and ν_s are assumed to be equal to 0. We assume that the whole population of the country is susceptible to the infection. Seven states with comparable populations are chosen. The objective function J is computed to provide a relative error of order less than 10^{-2} . In Figure A.2, Table A. shows estimated parameters. The rest of the Figure presents the solution and data. Note that the product $\omega\beta_i$ ($i = e, s, a$) is uniquely identifiable but not ω and β_i separately. Figure A.3 represents the effective reproduction number, the fitted symptomatic infected and death of the posterior distribution.

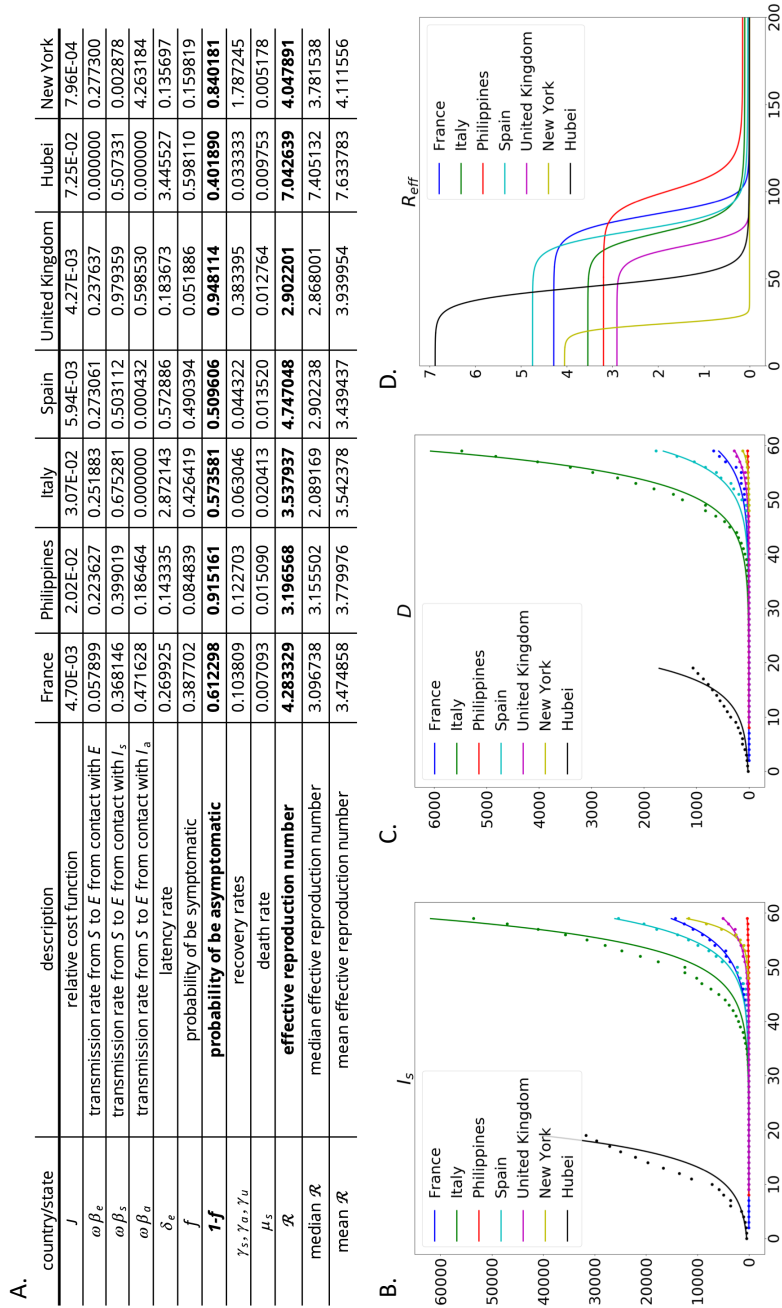


FIGURE A.2: A. Parameters calibrated according to data from France, Philippines, Italy, Spain, United Kingdom, Hubei, and New York. B. and C. Calibrated solution (straight line) and data (dots) with respect to day for France, Philippines, Italy, Spain, United Kingdom, Hubei and New York. First is the infected I_s (B.), and the second one is the death D (C.). D. Effective reproduction number with respect to day.

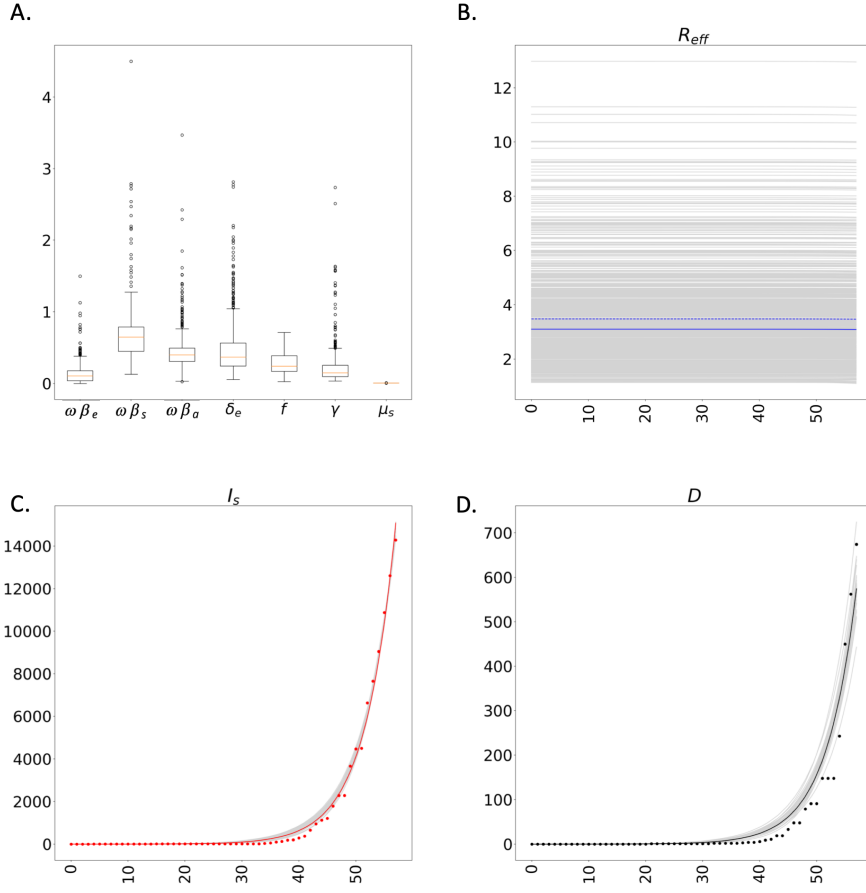


FIGURE A.3: A. Boxplot of the posterior distribution computed from France data. B. Effective reproduction number in grey of the posterior distribution, median (= 3.096738) in blue straight line, mean (= 3.474858) is dotted line. C. Fitted symptomatic infected in grey of the posterior distribution, median in red straight line, mean is dotted line. D. Fitted death in grey of the posterior distribution, median in black straight line, mean is dotted line.

A.3.3 Strategy to reduce disease to a given threshold

To temporarily reduce the value of \mathcal{R}_{eff} , three strategies regarding different interventions are being compared. The first one consists in reducing the number of contacts ω . Full containment is translated by $\omega = 0$, and no containment by $\omega = 1$. The second strategy is expressed by treatment of symptomatic infected. It is translated by modifying the value of ν_s . The treatment of exposed is the third one. Parameters ω , ν_e , and ν_s vary such that intervention is carried out from 0 to 100% of susceptible, exposed, and symptomatic respectively. Given a critical infection threshold \mathcal{T}_c , the model runs until the time t_c such that

$$E(t_c) + I_s(t_c) + I_a(t_c) \leq \mathcal{T}_c.$$

To juxtapose the benefit of the intervention, we assume that interventions start 53 days after the first confirmed infection. We remind that the first infection in France

was confirmed on January 24th, 2020, and containment begins on March 17th, 2020. Comparison between three strategies can be found in Table A.1 and Figures A.4-A.5. Without intervention to control the disease, the maximum number of symptomatic infecteds varies from 3.49×10^5 to 2.02×10^7 . The maximum number of deaths totals from 8.85×10^3 to 7.92×10^6 . We observe that any intervention strongly reduces the number of dead. Concerning France, Philippines, Italy, Spain, and the United Kingdom, when containment is fully respected and when the sum of infecteds is reduced to 1, the maximum number of symptomatic infecteds and deaths has been cut sharply, of order 10^3 . It varies now from 5.75×10^2 to 7.04×10^4 and 1.94×10^2 to 2.52×10^4 respectively. To wait from 104 to 407 days is the price to pay. On the contrary, for the states of Hubei and New York, 53 days to intervene seems to be already too late. We can also see in Table A.1 that treating only the symptomatic does not reduce the duration

Note that when the intervention ends at time t_c , the number of susceptible $S(t_c)$ is large so that the effective reproduction number \mathcal{R}_{eff} is larger than 1.

Figure A.6 compares the maximum number of dead and symptomatic but infected individuals, as well as the intervention duration, to reach $\mathcal{T}_c = 1000$ varying from 0 to 100%. Containment is the most efficient when it is respected by more than 76% in France, 63% in the Philippines. Beyond that, treating the exposed is the best choice. We also observe that the intervention duration becomes long below 89% in France, 82% in the Philippines. This can be understood by too little susceptibility to achieve recovery but enough for the disease to persist.

country/state	France	Philippines	Italy	Spain	United Kingdom	Hubei	New York
population	6.67E+07	1.03E+08	6.03E+07	4.63E+07	6.49E+07	5.84E+07	1.95E+07
maximum number of symptomatic infected without control	7.74E+06	1.75E+06	9.43E+06	1.05E+07	3.49E+05	2.02E+07	9.25E+04
maximum number of dead without control	1.64E+06	9.15E+05	6.15E+06	5.29E+06	1.02E+05	7.92E+06	8.85E+03
intervention duration if $\mathcal{T}_c = 1$ and full containment starting 53 days after the first confirmed infection	104	93	194	262	78	407	119
maximum number of symptomatic infected with full containment	8.78E+03	5.75E+02	1.19E+05	7.40E+04	1.16E+04	2.00E+07	9.22E+04
maximum number of dead with full containment	1.24E+03	1.94E+02	4.24E+04	2.52E+04	1.96E+03	6.53E+06	6.82E+03
intervention duration if $\mathcal{T}_c = 1000$ and full containment starting 53 days after the first confirmed infection	39	33	86	110	40	292	68
intervention duration if $\mathcal{T}_c = 1000$ and 100% of exposed under treatment starting 53 days after the first confirmed infection	44	39	87	118	44	342	82
intervention duration if $\mathcal{T}_c = 1000$ and 100% of symptomatic under treatment starting 53 days after the first confirmed infection	163	188	202	263	103	408	122

TABLE A.1: Comparison between the maximum number of symptomatic infected and death without control and the solution reducing contact rate to 0, 100% of exposed under treatment, and 100% of symptomatic infected under treatment to reach $\mathcal{T}_c = 1$ and $\mathcal{T}_c = 1000$. Interventions are assumed to being 53 days after the first confirmed infection.

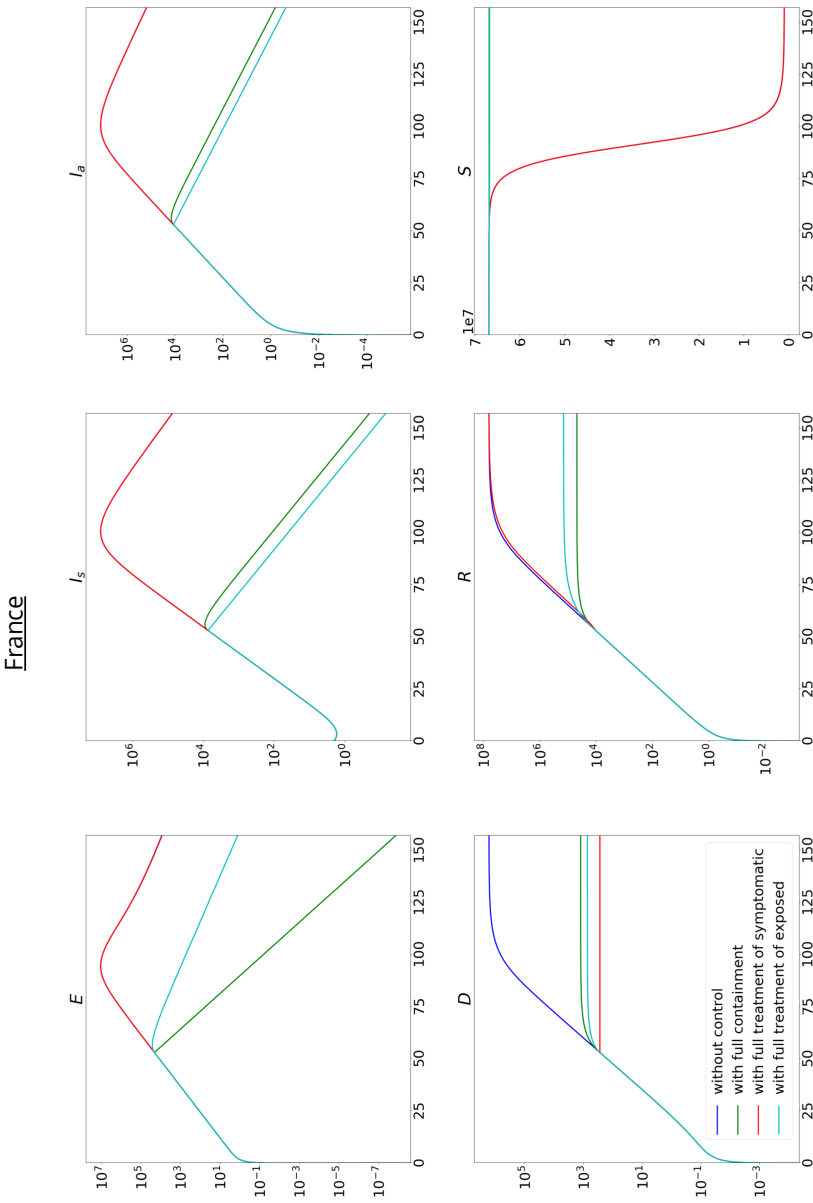


FIGURE A.4: Comparison of solutions S, E, I_s, I_a, R, D without control in blue, full containment in green, full treatment of symptomatic in red, and full treatment of exposed in cyan for France. Ordinate axis is expressed in log.

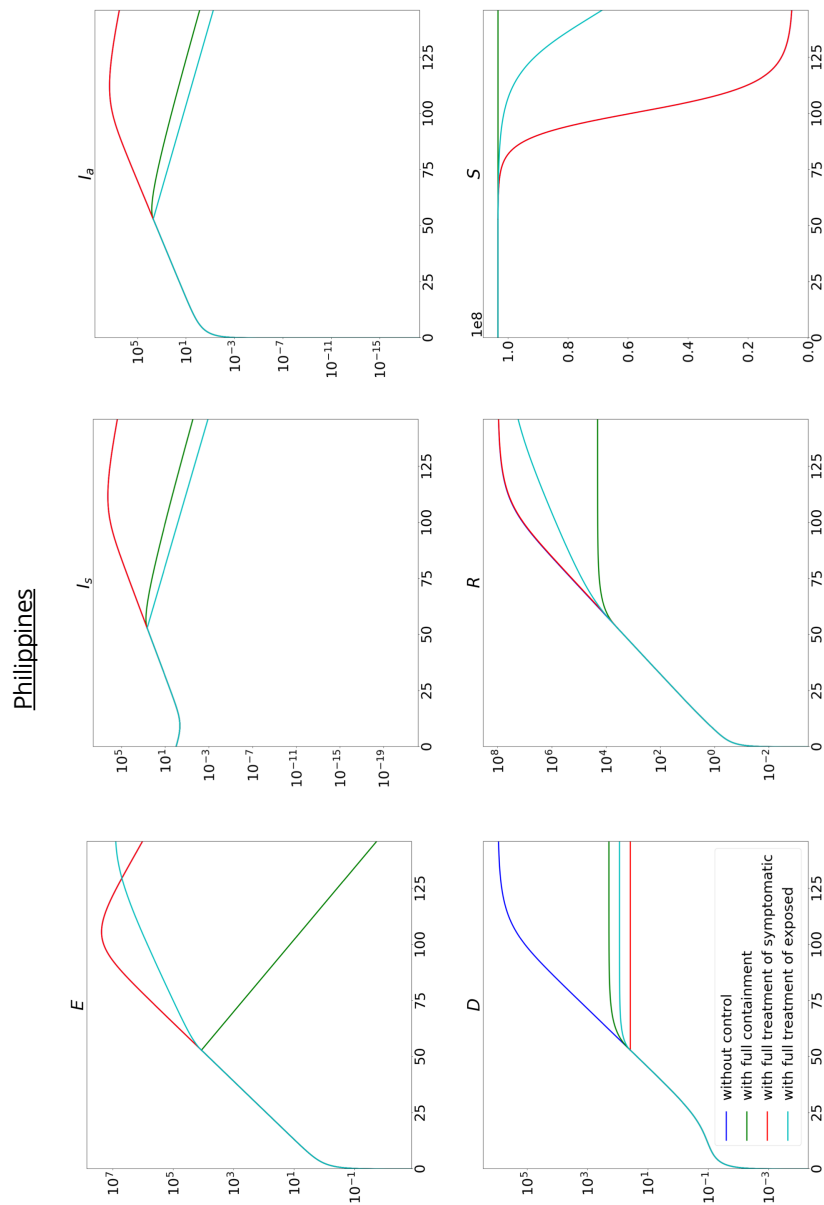


FIGURE A.5: Comparison of solutions S, E, I_s, I_a, R, D without control in blue, full containment in green, full treatment of symptomatic in red, and full treatment of exposed in cyan for the Philippines. Ordinate axis is expressed in log.

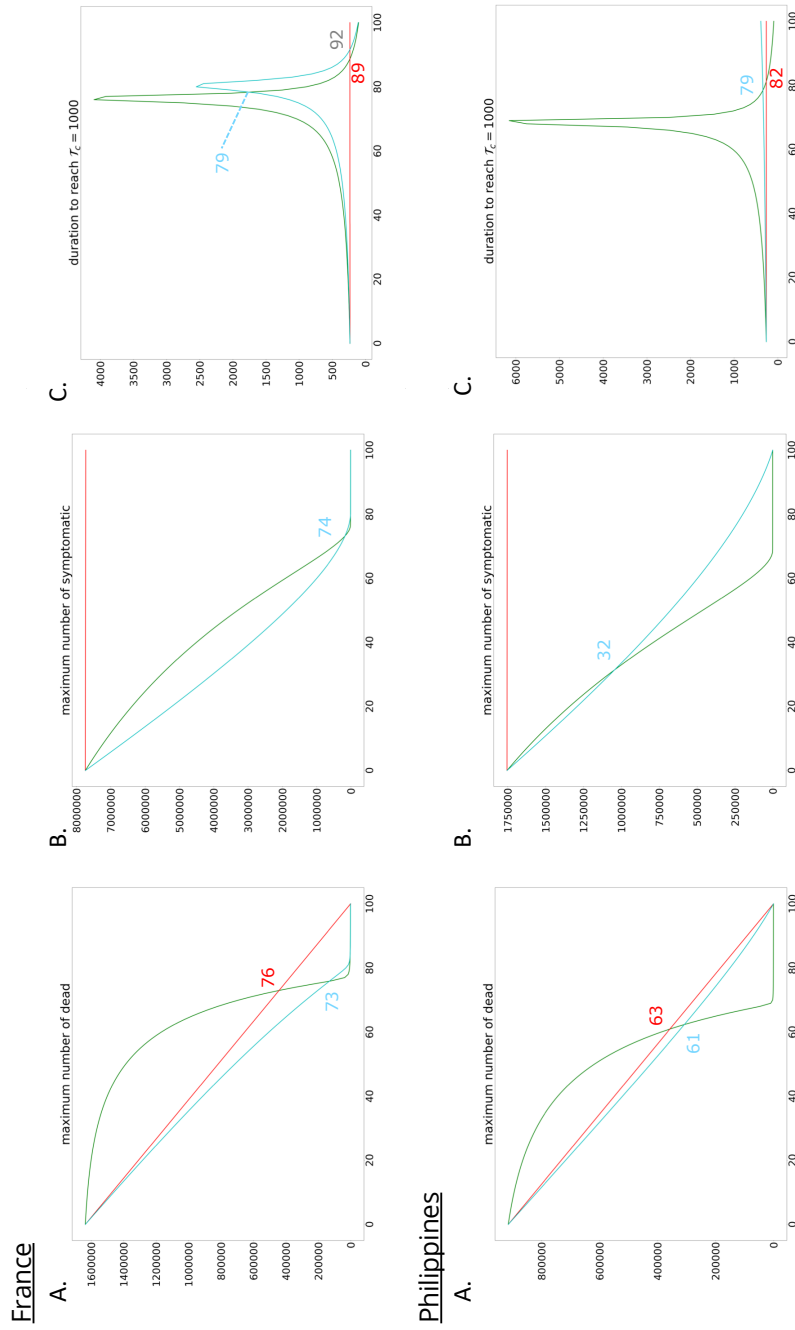


FIGURE A.6: A. Comparison of the maximum number of dead. B. Comparison of the maximum number of symptomatic infected. C. Comparison of the intervention duration to reach $T_c = 1000$ with respect to percentage of containment (green), treatment of symptomatic (red), and treatment of exposed (cyan) for France and Philippines.

A.4 Discussion

Without intervention, we observe in Figures A.4-A.5 that the number of susceptible S is decreasing; most of the individuals are recovering, which generates population immunity. It translates that the disease free equilibrium is globally asymptotically stable. Nevertheless, the price to pay is high, the number of deaths being excessive. As presented in Figure A.2, the effective reproduction is decreasing and points out that control has to be done as fast as possible.

The other important information is that, as discovered by Danchin et al. [DNT20], an alternative transmission way may occur. Here, it is due to the proportion of asymptomatic infected individuals that is not negligible, as shown in Table A.1.

Finally, with the little knowledge about COVID-19 nowadays, decreasing transmission, *i.e.* $\beta_e, \beta_s, \beta_a$, is the preferred option. The simplest choice consists in reducing contact between individuals. Table A.1 and Figures A.4-A.5-A.6 show that total and partial containment do indeed drastically reduce the disease. However, the duration of containment may be too long and then impracticable especially if we aim at totally eradicating the infection ($\mathcal{T}_c = 1$). Instead, to stop the containment as soon as the capacity of the hospitals has been reached could be privileged. When this criterion is set to 1000 patients ($\mathcal{T}_c = 1000$), the duration goes from 104 to 39 days for France. A similar reduction in duration is also obtained for other countries. Again, we see that the earlier the intervention, the more effective it is. Due to the high number of susceptible, it is worth noting that the effective reproduction number remains large after containment. Screening tests, especially to carry out exposed individuals, are then necessary to be carried out, and the positive individuals are quarantined.

Bibliography

- [BCC12] F. Brauer and C. Castillo-Chavez. *Mathematical Models in Population Biology and Epidemiology*. Springer, New York, NY, 2012.
- [CBGF10] K. Csilléry, M. G. Blum, O. E. Gaggiotti, and O. François. Approximate bayesian computation (abc) in practice. *Trends in ecology & evolution*, 25(7):410–418, 2010.
- [CZD⁺20] N. Chen, M. Zhou, X. Dong, J. Qu, F. Gong, Y. Han, Y. Qiu, J. Wang, Y. Liu, Y. Wei, J. Xia, T. Yu, X. Zhang, and L. Zhang. Epidemiological and clinical characteristics of 99 cases of 2019 novel coronavirus pneumonia in wuhan, china: A descriptive study. *The Lancet*, 395(10223):507–513, 2020.
- [DDG20] E. Dong, H. Du, and L. Gardner. An interactive web-based dashboard to track covid-19 in real time. *The Lancet Infectious Diseases*, 2020.
- [DH00] O. Diekmann and J.A.P. Heesterbeek. *Mathematical Epidemiology of Infectious Diseases: Model Building, Analysis and Interpretation*. Chichester: John Wiley, 2000.
- [DNT20] A. Danchin, T. W. P. Ng, and G. Turinici. A new transmission route for the propagation of the sars-cov-2 coronavirus. *medRxiv*, 2020.
- [Gar20] L. Gardner. Modeling the spreading risk of 2019-ncov. 31 january 2020. retrieved 25 march 2020. Technical report, Center for Systems Science and Engineering, Johns Hopkins University, 2020.
- [HAM⁺20] D. S. Hui, E. I. Azhar, T. A. Madani, F. Ntoumi, R. Kock, O. Dar, G. Ippolito, T. D. Mchugh, Z. A. Memish, C. Drosten, A. Zumla, and E. Petersen. The continuing 2019-ncov epidemic threat of novel coronaviruses to global health - the latest 2019 novel coronavirus outbreak in wuhan, china. *International Journal of Infectious Diseases*, 91:264–266, 2020.
- [IDC⁺20] N. Imai, I. Dorigatti, A. Cori, C. Donnelly, S. Riley, and N. M. Ferguson. Report 2: Estimating the potential total number of novel coronavirus cases in wuhan city, china. retrieved 25 march 2020. Technical report, Imperial College London, 2020.

- [vdDW00] P van den Driessche and J. Watmough. Reproduction numbers and sub-threshold endemic equilibria for compartmental models of disease transmission. *Mathematical Biosciences*, 180(1-2):29–48, 2000.
- [WLL20] J. T. Wu, K. Leung, and G. M. Leung. Nowcasting and forecasting the potential domestic and international spread of the 2019-ncov outbreak originating in wuhan, china: A modelling study. *The Lancet*, 395(10225):689–697, 2020.
- [Wor20a] World Health Organization. *COVID-19*, Accessed March 25, 2020 2020.
- [Wor20b] World Health Organization. *Naming the coronavirus disease (COVID-19) and the virus that causes it*, Accessed March 21, 2020 2020.
- [Wor20c] World Health Organization. *Novel Coronavirus(2019-nCoV) Situation Report 64*. Accessed March 25, 2020, 2020.
- [Wor20d] World Health Organization. *Statement on the Second Meeting of the International Health Regulations. (2005). Emergency Committee Regarding the Outbreak of Novel Coronavirus (2019-nCoV)*, 2020.
- [WWDea20] H. Wang, Z. Wang, Y. Dong, and et al. Phase-adjusted estimation of the number of coronavirus disease 2019 cases in wuhan, china. *Cell Discovery*, 6(10), 2020.
- [ZLR⁺20] S. Zhao, Q. Lin, Musa Ran, J., Yang S. S., Wang G., Lou W., D. Y., Gao, L. Yang, D. He, and M. H. Wang. Preliminary estimation of the basic reproduction number of novel coronavirus (2019-ncov) in china, from 2019 to 2020: A data-driven analysis in the early phase of the outbreak. *International Journal of Infectious Diseases*, 92:214–217, 2020.
- [ZML⁺20] S. Zhao, S. S. Musa, Q. Lin, J. Ran, G. Yang, W. Wang, Y. Lou, and et al. Estimating the unreported number of novel coronavirus (2019-ncov) cases in china in the first half of january 2020: A data-driven modelling analysis of the early outbreak. *Journal of Clinical Medicine*, 9(2):388, 2020.
- [ZYWea20] P. Zhou, X. Yang, X. Wang, and et al. A pneumonia outbreak associated with a new coronavirus of probable bat origin. *Nature*, 579:270–273, 2020.

Modélisation mathématique de l'invasion des ravageurs et application à la lutte contre les maladies transmises par les ravageurs aux Philippines

Résumé. La dengue est une infection virale transmise par les moustiques dans les régions tropicales et subtropicales du monde entier. Il s'agit d'une infection virale causée par quatre types de virus (DENV-1, DENV-2, DENV-3, DENV-4), qui se transmettent par la piqûre de moustiques femelles infectés (*Aedes aegypti*) et (*Aedes albopictus*) pendant la journée. Le premier vaccin à être utilisé commercialement est le CYD-TDV, commercialisé sous le nom de dengvaxia par Sanofi Pasteur. Dengvaxia est un vaccin vivant des sérotypes 1, 2, 3 et 4. Il doit être administré en trois doses de 0,5 ml par voie sous-cutanée (SC) à six mois d'intervalle. Sanofi Pasteur recommande que le vaccin ne soit utilisé que chez les personnes âgées de 9 à 45 ans et chez les personnes déjà infectées par un type de virus.

Cette thèse présente un modèle épidémique de type Ross pour décrire l'interaction entre les humains et les moustiques. Après avoir établi le nombre de reproduction de base \mathcal{R}_0 et la stabilité des équilibres, nous présentons trois stratégies de contrôle : la vaccination, le contrôle des vecteurs par l'application de pesticides, et l'introduction de copépodes comme contrôle vectoriel pour les larves. Le principe du maximum de Pontryagin est utilisé pour caractériser le contrôle optimal, et des simulations numériques sont appliquées pour déterminer les stratégies les mieux adaptées à la population.

Dans le dernier chapitre, nous avons défini un nouveau modèle décrivant explicitement la distribution spatiale des moustiques adultes. Dans ce modèle d'équations aux dérivées partielles, nous avons montré qu'en appliquant le théorème du point fixe de Picard, l'existence et l'unicité d'une solution faible globale en temps. Nous déterminons la stratégie de contrôle optimale en appliquant trois contrôles : l'exposition au copépode w_Y pour les jeunes moustiques dans les zones de pontes, le pesticide w_A pour les moustiques adultes, et l'application de la vaccination w_H pour les humains.

Nos résultats montrent que la vaccination des humains sensibles secondaires uniquement n'est pas idéale. Cela demande un effort constant et prend beaucoup de temps pour les vacciner. Par ailleurs, les copépodes et les pesticides constituent une stratégie efficace pour éliminer la maladie et les populations de moustiques. Cependant, le retour à l'équilibre est lent. La combinaison des pesticides et de la vaccination semble moins efficace que la combinaison des copépodes et des pesticides. Il faut moins de temps pour réduire le nombre de moustiques infectieux avec une durée d'application de la lutte réduite.

Mots-clés. Dengvaxia, Vaccination, \mathcal{R}_0 , Contrôle optimal, Principe du maximum de Pontryagin

Mathematical modeling of pest invasion and application to pest-borne disease control in the Philippines

Abstract. Dengue is a mosquito-borne viral infection found in tropical and subtropical regions worldwide. It is a viral infection caused by four types of viruses (DENV-1, DENV-2, DENV-3, DENV-4), which transmit through the bite of infected *Aedes aegypti* and *Aedes albopictus* female mosquitoes during the daytime. The first vaccine to be used commercially is CYD-TDV, marketed as dengvaxia by Sanofi Pasteur. Dengvaxia is a live vaccine of serotypes 1, 2, 3, and 4. It should be administered in three doses of 0.5 mL subcutaneous (SC) six months apart. Sanofi Pasteur recommended that the vaccine only be used in people between the age of 9 to 45 and people already infected by one type of virus.

This thesis presents a Ross-type epidemic model to describe the vaccine interaction between humans and mosquitoes using different population growth models. After establishing the basic reproduction number \mathcal{R}_0 and the stability of the equilibrium, we present three control strategies: vaccination, vector control through pesticide application, and the introduction of copepods as a vector control for larvae. Pontryagin's maximum principle is used to characterize optimal control, and numerical simulations are applied to determine which strategies best suit the population.

In the last chapter, we defined a new model with an explicit spatial distribution of adult mosquitoes. In this model made of partial differential equations, we have shown that by applying Picard's fixed point theorem, the existence and uniqueness of global in time weak solution. We determine the optimal control strategy by applying three control: exposure to copepod w_Y for the young mosquitoes in the laying sites, pesticide w_A for the adult mosquitoes, and application of vaccination w_H for the humans.

Our results show that vaccinating secondary susceptible humans only is not ideal. It requires constant effort and takes a long time to vaccinate them. Also, copepods and pesticides are a good strategy for eliminating the disease and mosquito populations. However, the recovery of infected humans is slow. The combination of pesticide and vaccination seems less efficient than the combination of copepods and pesticides. It takes a shorter time to reduce the number of mosquitoes with a reduced duration of the control application.

Keywords. Dengvaxia, Vaccination, \mathcal{R}_0 , Optimal Control, Pontryagin maximum principle